TECHNICAL REPORT STANDARD TITLE PAGE

| 1. Report No. | 2. Government Accession No. | 3. Recipient's Catalog No. |
|---|---|---|
| FHWA/TX-82/55+301-1F | | |

| 4. Title and Subtitle | 5. Report Date |
|---|---|
| HYDRAULIC PERFORMANCE OF CULVERTS WITH SAFETY GRATES | March 1983 |
| | 6. Performing Organization Code |

| 7. Author(s) | 8. Performing Organization Report No. |
|---|---|
| Larry W. Mays, Morey E. Walker, Michael S. Bennett, and Randal P. Arbuckle | Research Report 301-1F |

| 9. Performing Organization Name and Address | 10. Work Unit No. |
|---|---|
| Center for Transportation Research<br>The University of Texas at Austin<br>Austin, Texas 78712-1075 | 11. Contract or Grant No.<br>Research Study 3-5-80-301 |
| | 13. Type of Report and Period Covered |
| 12. Sponsoring Agency Name and Address<br>Texas State Department of Highways and Public Transportation; Transportation Planning Division<br>P. O. Box 5051<br>Austin, Texas 78763 | Final |
| | 14. Sponsoring Agency Code |

15. Supplementary Notes

Study conducted in cooperation with the U. S. Department of Transportation, Federal Highway Administration.

Research Study Title: "Hydraulic Performance of Culverts with Safety Grates"

16. Abstract

The purpose of this research was to establish through an experimental study, the hydraulic characteristics of culvert end treatments (safety grates) on both box and pipe culverts. A significant amount of work has been performed in the past to establish the hydraulic characteristics of culverts, but there has been very little effort to study the hydraulics of culverts with grates. A 1:4 scale model was built to simulate flow conditions in a 5 × 8-ft box culvert. Investigators also tested a 1:4 scale model simulating flow in a 60-in. helical corrugated metal pipe culvert. The slopes of the culverts, the flowrates and the elevations of the tailwater were varied to simulate the various types of flow conditions which can exist in a highway culvert. The box culvert was tested with no safety grates, pipe safety grates and bar safety grates. The pipe culvert was tested with no safety grates and pipe safety grates. A regression analysis of the experimental data was performed so as to relate (1) for outlet control, the various hydraulic parameters to the entrance headloss coefficient, and (2) for inlet control, the headwater depth to the discharge.

| 17. Key Words | 18. Distribution Statement |
|---|---|
| culverts, box, pipe, safety grates, hydraulic, model, regression analysis | No restrictions. This document is available to the public through the National Technical Information Service, Springfield, Virginia 22161. |

| 19. Security Classif. (of this report) | 20. Security Classif. (of this page) | 21. No. of Pages | 22. Price |
|---|---|---|---|
| Unclassified | Unclassified | 342 | |

Form DOT F 1700.7 (8-69)

# HYDRAULIC PERFORMANCE OF CULVERTS WITH SAFETY GRATES

by

Larry W. Mays
Morey E. Walker
Michael S. Bennett
Randal P. Arbuckle

Research Report Number 301-1F

Hydraulic Performance of Culverts with Safety Grates
Research Project 3-5-80-301

conducted for

Texas
State Department of Highways and Public Transportation

in cooperation with the
U. S. Department of Transportation
Federal Highway Administration

by the

CENTER FOR TRANSPORTATION RESEARCH
BUREAU OF ENGINEERING RESEARCH
THE UNIVERSITY OF TEXAS AT AUSTIN

March 1983

The contents of this report reflect the views of the authors, who are responsible for the facts and the accuracy of the data presented herein. The contents do not necessarily reflect the official views or policies of the Federal Highway Administration. This report does not constitute a standard, specification, or regulation.

There was no invention or discovery conceived or first actually reduced to practice in the course of or under this contract, including any art, method, process, machine, manufacture, design or composition of matter, or any new and useful improvement thereof, or any variety of plant which is or may be patentable under the patent laws of the United States of America or any foreign country.

# PREFACE

The research reported herein is a study of the performance of culverts with and without safety grate end treatments. The experimental work was carried out on 1) a 2-ft x 1.25-ft box culvert and 2) a 15-inch diameter helical corrugated metal pipe culvert. Experiments were conducted to determine the effect of safety grate end treatments on culvert hydraulics.

The study was initiated under an agreement between the State Department of Highways and Public Transportation, the State of Texas, the Federal Highway Administration and the Center for Highway Research of the University of Texas, Austin. Special acknowledgment is made to Messrs. Dwight Reagan and Sam Fox of the Texas Highway Department and Messrs. Sterling Jones and Dan O'Conner of the Federal Highway Administration for their valuable suggestions and comments during the investigation.

Special thanks are also due to the Armco Metal Pipe Corp. for providing the 15-in diameter helical corrugated metal pipe used in this study. The authors also wish to thank Messrs. Red Worley, J. Pritchard, Delbert Stark, Michael Pepe and J. Paul Hendrix for their assistance in construction of the models and the collection of the data. The assistance of Messrs. Nisai Wanakule and Yeou Koung Tung in carrying out the statistical analysis, was highly appreciated. Finally the authors wish to thank Ms. Nickla Tayarani for typing the manuscript, and the administrative staff at the Center for Research in Water Resources for their efforts and support towards completing this project.

## ABSTRACT

The purpose of this research was to establish through an experimental study, the hydraulic characteristics of culvert end treatments (safety grates) on both box and pipe culverts. A significant amount of work has been performed in the past to establish the hydraulic characteristics of culverts, but there has been very little effort to study the hydraulics of culverts with grates. A 1:4 scale model was built to simulate flow conditions in a 5 x 8-ft box culvert. Investigators also tested a 1:4 scale model simulating flow in a 60-in helical corrugated metal pipe culvert. The slopes of the culverts, the flowrates and the elevations of the tailwater were varied to simulate the various types of flow conditions which can exist in a highway culvert. The box culvert was tested with no safety grates, pipe safety grates and bar safety grates. The pipe culvert was tested with no safety grates and pipe safety grates. A regression analysis of the experimental data was performed so as to relate (1) for outlet control, the various hydraulic parameters to the entrance headloss coefficient, and (2) for inlet control, the headwater depth to the discharge.

TABLE OF CONTENTS

TABLE OF CONTENTS (continued)

TABLE OF CONTENTS (continued)

TABLE OF CONTENTS (continued)

LIST OF TABLES

LIST OF TABLES (continued)

LIST OF FIGURES

LIST OF FIGURES (continued)

LIST OF FIGURES (continued)

APPENDIX A

## APPENDIX B

APPENDIX B (continued)

## APPENDIX C

APPENDIX D

APPENDIX D (continued)

APPENDIX E

APPENDIX F

## APPENDIX G

# CHAPTER I INTRODUCTION

## 1.1 Statement of Problem

Culverts are designed to convey flow of stream water both along and across highway right of ways. If not properly designed, culverts could become dangerous obstructions to vehicles accidentally driven off a highway. To minimize the hazard, culverts could be designed so that the inlet and outlet structures are outside the highway right of way. Another safety feature would be the installation of guard rails. However, in some instances, the least costly and most practical safety design could be to install safety grates at the culvert ends (inlet and outlet structures).

Hydraulic engineers are concerned about the effect that safety grates have on the hydraulic performance of the culvert. Safety grates can cause an increase in entrance head losses affecting the culvert hydraulics and susceptibility to clogging. During flooding conditions, a large amount of debris (tree branches, trash, etc.) is usually present in the flow. If the debris clogs the entrance, then the culvert could become hydraulically ineffective and the possibility of overtopping the highway may exist. This can result in flood damages to adjacent property, damage to the highway embankment and structure, and increase traffic delays.

The purpose of this experimental study was to determine the effect of safety grates on the hydraulic performance of both box culverts and corrugated metal pipe culverts. Specifically studied were the changes in the entrance head losses for various flow regimes and the effect of clogging on the

culvert performance. The results are presented for use in the future design of highway culverts.

## 1.2 Safety Grate Design

The design of the safety grates is based on two constraints. First, the grates must have enough structural integrity to support an automobile. Second, the safety grates should have a minimum amount of materials for least possible interference of the natural flow. The Texas Transportation Institute (TTI) at Texas A & M University conducted a series of tests to determine a safety grate design considering automobile safety. Essentially, automobiles were driven at varying speeds over safety grates constructed of steel pipes. The result of the TTI study was a safety grate design constructed of 3-in diameter pipes placed on 30-in centers. These grates are referred to as "pipe safety grates" in this study and are illustrated in Fig. 1.1.

These grates are to be installed on highway embankments such that there are no protrusions above the highway embankments. For a complete discussion of the TTI study, refer to Texas Highway and Transportation Project Study No. 2-5-79-280 "Safe End Treatment for Roadside Culverts."

The experimental study described herein performed hydraulic model studies of the TTI design using a 1:4 scale model of an 8-ft x 5-ft box culvert. Also a bar type safety grate was tested using the 1:4 scale box culvert. Prototype dimensions of the bar grates are 1/2-in x 2-in placed on 5-in centers (Figure 1.2). Clogging tests using the box culvert were also performed. Safety grates for a pipe culvert (Figure 1.3) which had prototype dimensions of 3-in pipes placed on 24-in centers were also tested. The safety grates are discussed in detail in Section 2.7. Each of the grates are placed parallel with the highway embankments so that there are no vertical protrusions above the embankments.

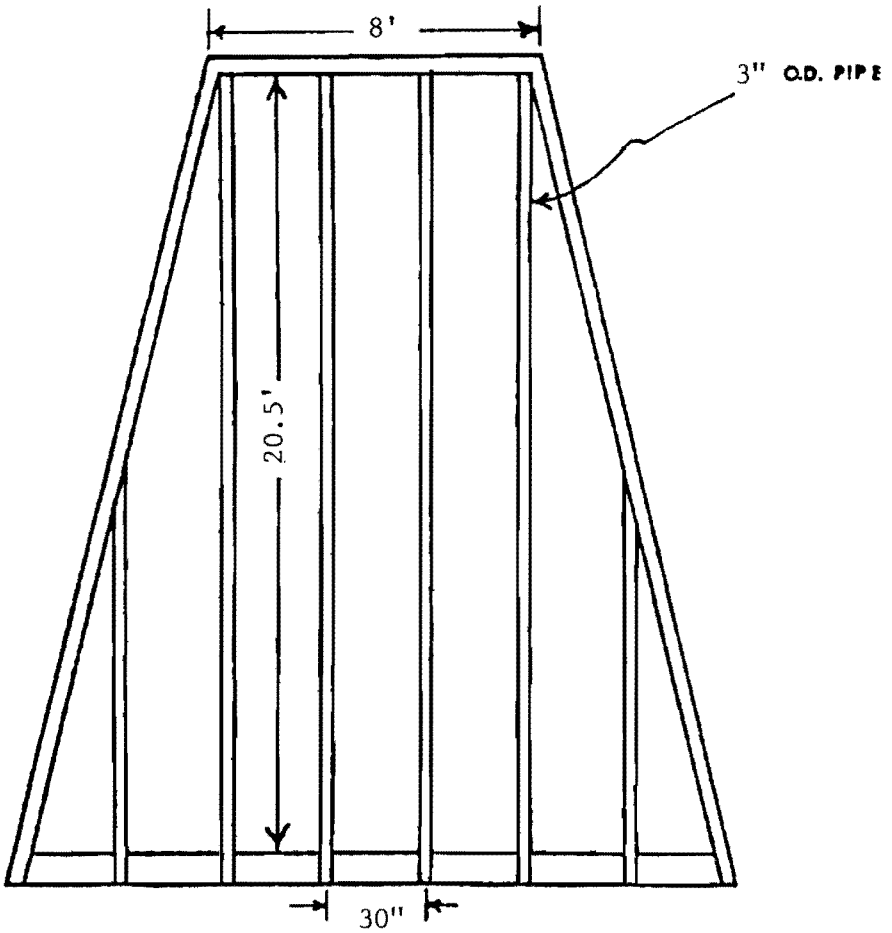


Figure 1.1 Pipe Safety Grate, Prototype

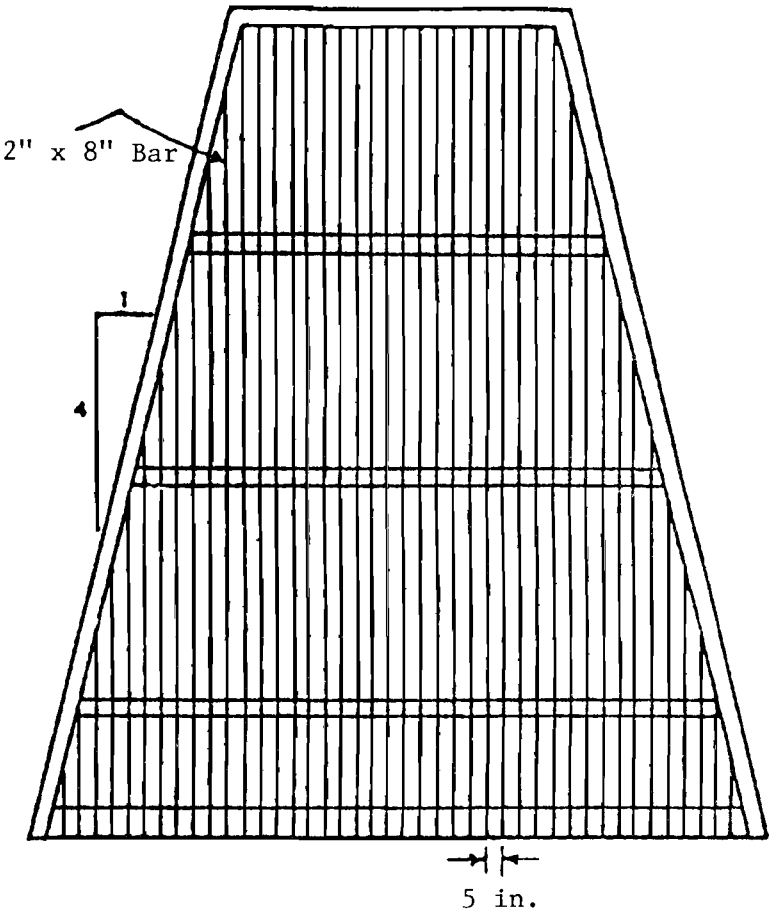


Figure 1.2 Bar Safety Grate, Prototype

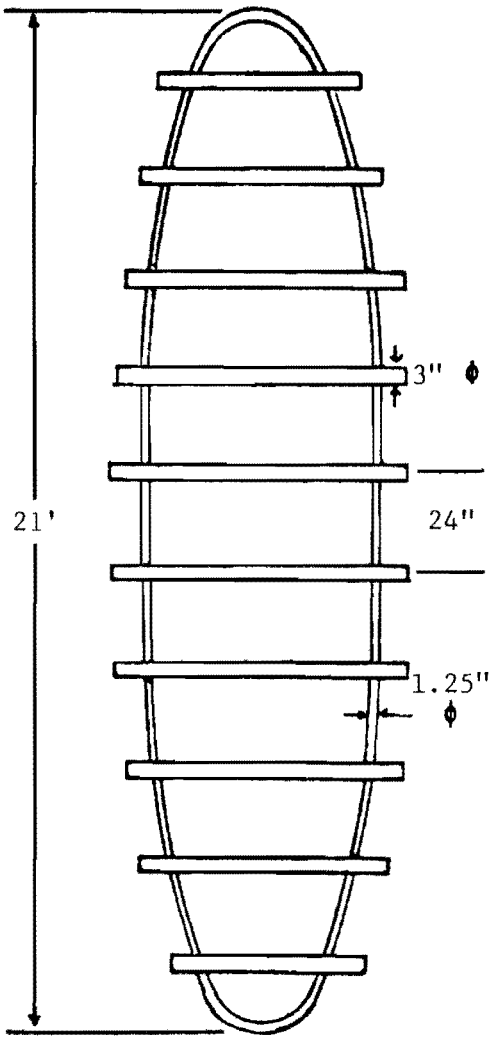


Figure 1.3 Pipe Grate for Pipe Culvert, Prototype

A 4:1 slope of a highway embankment was used in all the experiments presented in this report. Results generally can be safely extrapolated to other embankment slopes.

## 1.3 Review of Previous Studies

Numerous investigators have researched the hydraulic controls and flow types of culverts. The primary controls of culverts have long been identified. However, the hydraulic performance of a new culvert design cannot be theoretically modeled with accuracy, and must be experimentally determined. A review of previous experiments contributes an understanding of culvert hydraulic controls and experimental techniques.

Mavis (1942) conducted one of the most comprehensive studies performed on culvert hydraulics. The culverts tested were 3-in, 4-in, 6-in, and 12-in diameter pipes. These pipes represented "conduits of intermediate lengths" which most field culverts are classified. Short length culverts have been defined as having negligible frictional resistance, and the discharge depends upon the geometry of the inlet and on headwater depth (Mavis, 1942). Hydraulically long culverts have headlosses which are a function of conduit geometry, frictional forces, flow rate, and Reynold's Number. Mavis determined that intermediate-length culverts operate under five sets of conditions which are:

1. Part-full free outfall
2. Part-full with outfall partially submerged
3. Full with outfall completely submerged
4. Full with outfall partially submerged
5. Full with free outfall.

The study results were charts and nomographs that have been used in a substantial number of design manuals.

Shoemaker and Clayton (1953) performed a series of model studies of box culverts on steep grades. Objectives of this study were to determine culvert hydraulics and to improve effectiveness of the Oregon State Highway Standard inlet. Three inlet types were tested: (1) an inlet with no flare or taper; (2) an inlet with tapered sides; and (3) an inlet designed to operate under entrance control. The investigators observed that a submerged standard inlet operates as a sluice gate while a tapered inlet allows flow full with no sluice gate contraction. The increase in culvert capacity due to the tapered inlet resulted from an increase in flow area by elimination of the sluice gate contraction.

Schiller (1955) conducted a series of tests on circular pipe culvert inlets. The purpose of the study was to determine efficient inlet designs based on hydraulic controls. Two inlet designs were compared; (1) a square-edged flush inlets with flared, straight, and parallel wingwalls; and (2) a mitered sharp-edged inlet. The square-edged flush inlet performed more efficiently than the mitered, sharp-edged inlet.

French (1955) presented a discussion of Schiller's works. He noted that the upstream approach channel characteristics greatly influenced the efficiency of the inlet. The greater the turbulence in the approach channel, the larger the amount of separation occurring at the inlet boundary surface. The ability of the upstream approach channel to control the full capacity was experimentally shown for culverts placed on steep slopes. French also noted that the effects of the approach channel would be smaller on larger scale models.

French (1957) also studied the effect of approach channel characteristics on pipe culvert operations. He concluded that general reproducibility of experimental results to field conditions involves considerable awareness of approach flow conditions.

Bossey (1961) presented an unpublished paper outlining the hydraulics of conventional highway culverts. He observed that two primary factors controlled culvert capacity - (1) the cross-sectional area of the barrel and (2) the headwater depth. Secondary factors were: (1) shape of barrel; (2) inlet geometry; (3) resistance characteristics; (4) length; and (5) slope. The secondary factors generated an increase in headwater depth as flow contracts into the culvert.

French (1966) also conducted an experimental study to determine the hydraulics of tapered box culvert inlets. Since the box culvert was placed on a steep slope, the experimental work involved only inlet control conditions. Again, the hydraulic performance of a highway box culvert on super-critical slopes could be substantially increased by tapering the inlet. Also, the hydraulic efficiency could be increased by not allowing subatmospheric pressure regions to form.

Blaisdell (1966) further categorized culvert flow into four regimes: (1) weir control; (2) orifice control; (3) slug and mixture control; and (4) pipe control. Weir control was defined for either an unsubmerged entrance geometry control on steep slopes or barrel geometry control on mild slopes. Orifice control represents submerged entrance geometry control. Slug and mixture control describes barrel geometry controlling a flow of water and entrained air. Pipe control was determined for a full flowing culvert controlled by barrel characteristics and/or tailwater depth. A graphical representation of the different flow types can be expressed in a headwater versus discharge plot (Figure 1.4).

Numerous design manuals exist for step by step selection of a culvert. Some of the most widely used manuals are listed in the references. In

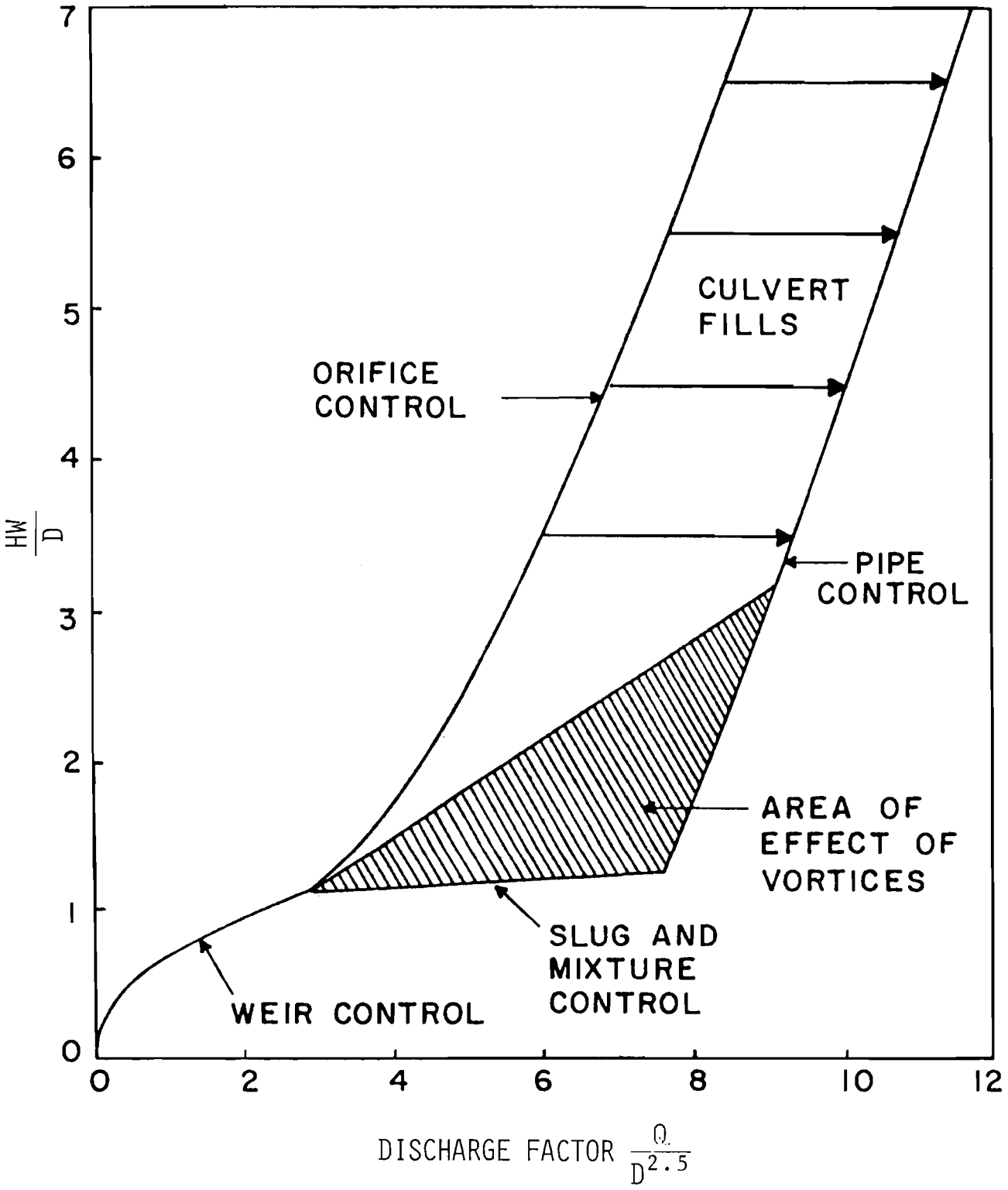


Figure 1.4 Head-Discharge Relationship {after Blaisdell (1966)}

addition, computer programs have been written to aid in the culvert selection process. The State Department of Highways and Public Transportation in Texas uses the Texas Hydraulics System (THYSYS) in culvert design. THYSYS uses inputted values of the design discharge, the estimated tailwater, the culvert dimension parameters and slope, and determines the appropriate flow regime, headwater depth, and outlet velocity. THYSYS generally distinguishes between steep and mild slope regimes and specifically determines other parameters.

## 1.4 Study Objectives

As illustrated by the previous review, numerous experimental studies have been performed on the hydraulics of culverts, but none have been reported in the literature on culverts with safety grates. Several objectives included:

1. Perform studies using a box culvert model to make a direct comparison of culvert performance with and without safety grates. This included hydraulic tests varying the culvert slope, discharge, headwater depth, and tailwater depth. For each variation of these parameters experimental data were collected without grates, with pipe grates installed, and with bar grates installed. The results of these tests are summarized in Chapter 3.

2. A second major objective was to determine the hydraulic effects of various levels of clogging of the safety grates. The problem of clogging is not addressed in current culvert design as culverts are presently designed without regard to clogging. Culverts without safety grates are usually large enough for trash or debris to pass through. However, from informal field

observations, safety grates can retain a significant amount of debris and can effectively clog the culvert. The effect of clogging on the entrance headloss coefficient was determined using various percentages of clogging ranging from 15 to 90 percent. Since the amount of debris collected on a grate cannot be predicted it would be difficult to develop guidelines for future culvert design taking into the effect of clogging. The results of the clogging tests are summarized in Chapter 4.

3. Perform studies using a corrugated metal pipe culvert to make a direct comparison of culvert performance with grates installed and without safety grates. This included hydraulic tests varying the culvert slope, dishcarge, headwater depth, and tailwater depth. For each variation of these parameters, experimental data were collected with and without safety grates installed. The results of these tests are summarized in Chapter 5.

4. For inlet control conditions, headwater-discharge relationships were developed. Regression equations were derived using the box culvert results for the situations: (1) no grates; (2) pipe grates installed; and (3) bar grates installed. Regression equations were devised using the pipe culvert results for the situations: (1) no grates; and (2) pipe grates installed.

   The results for the box culvert are summarized in Section 3.2 and for the pipe culvert are summarized in Section 5.2.

5. The box culvert results for outlet control were used to derive regression equations to define the entrance head loss coeffi-

cient as a function of the various hydraulic parameters. Several relationships were derived for each of the following conditions:

(a) Each flow regime separately

(b) Submerged conditions of the inlet

(c) Unsubmerged conditions of the inlet

(d) Submerged and unsubmerged conditions combined.

Because either inlet or outlet control in general is considered in design, the regression equations considering each flow regime separately may not be of practical use. The results of the above regression analysis are described in Chapter 3.

6. The pipe culvert results for outlet control were used to derive regressions to define the entrance head loss coefficient as a function of the various hydraulic parameters. Several relationships were derived for each of the following conditions:

   (a) Submerged conditions of the inlet

   (b) Submerged and unsubmerged combined.

7. Another major objective was to put the regression results of the entrance headloss coefficient (outlet control) for the box culvert and pipe culvert, with and without grates, in a graphical form for easy use by the designer.

## 1.5 Review of Culvert Hydraulics for Design

Designing culverts involves many factors including estimating flood peaks, hydraulic performance, structural adequacy, and costs. The design of culverts, based on the interrelationship of numerous controlling factors is not an exact scientific procedure. Some of the many factors which control flow

through culverts are: (1) discharge; (2) inlet and barrel geometries; (3) frictional resistance; (4) headwater depth; (5) tailwater depth; and (6) slope. Generally, only two or three primary factors determine the flow regime through a particular culvert. For example, the size and shape of the inlet may determine the capacity of a certain culvert. On the other hand, frictional resistance and tailwater depth might control the flow in another case. However, the primary factors are not always identifiable before a design is made. Iterative design procedures identify the controlling factors for given design parameters.

According to Blaisdell (1966), thirty-eight factors influence the hydraulic performance of a culvert (Table 1.1). The primary controlling factors can be divided into two main groups: (1) flow with inlet control (steep-slope regime - $S_o \geq S_c$); and (2) flow with outlet control (mild slope regime - $S_o < S_c$). The inlet control group determines the capacity of the culvert based on inlet conditions, while the outlet control group determines the capacity based on the barrel and outlet conditions. The outlet control group is a combination of the outlet control and barrel control groups as defined by Blaisdell.

There have been many reported laboratory tests and field observations that show the two major types of culvert flow. For each type of control, different factors and formulas are used to compute the hydraulic capacity of a culvert. Under inlet control, the cross-section area of the culvert barrel, the inlet geometry and the amount of headwater or ponding at the entrance are of primary importance. Outlet control involves the additional consideration of the elevation of the tailwater in the outlet channel and the slope, roughness and length of the culvert barrel.

Hydraulic computations can be used to determine the probable type of flow under which a culvert will operate for a given set of conditions. The

Table 1.1 CLASSIFICATION OF CULVERT HYDRAULIC CONTROLS

(after Blaisdell (1966))

I. Inlet
- A. Unsubmerged
  - 1. Weir
  - 2. Surface profile
- B. Submerged
  - 1. Orifice
  - 2. Vortex
  - 3. Full

II. Barrel
- A. Length
  - 1. Short
  - 2. Long
- B. Slope
  - 1. Mild
    - a. Barrel slope less than critical slope
      - i. Part full, normal depth greater than critical depth
      - ii. Full, not applicable
    - b. Barrel slope less than friction slope
      - i. Part full, depth increases along barrel
      - ii. Full, barrel under pressure
  - 2. Steep
    - a. Barrel slope steeper than critical slope
      - i. Part full, normal depth less than critical depth
      - ii. Full, not applicable
    - b. Barrel slope steeper than friction slope
      - i. Part full, depth decreases along barrel (increases if the inlet causes the depth inside the inlet to be less than the normal depth)
      - ii. Full, barrel under suction
- C. Flow
  - 1. Part full
  - 2. Slug and mixture
  - 3. Full

III. Outlet
- A. Part full
  - 1. Critical depth
  - 2. Tailwater
- B. Full
  - 1. Free
  - 2. Submerged

Federal Highway Administration (FHWA) in their Hydraulic Engineering Circular (HEC) No. 5 provide charts for computing headwater depths for both inlet control and outlet control and then use the higher value to indicate the type of control and to determine the headwater depth.

### 1.5.1 Inlet Control

Inlet control means that the discharge capacity of a culvert is controlled at the culvert entrance by the depth of headwater (HW) and the entrance geometry, including the barrel shape and cross-sectional area, and the type of inlet edge. For inlet control the roughness and length of the culvert barrel and the outlet conditions (including depth of tailwater) are not factors in determining culvert capacity. An increase in barrel slope reduces headwater to a small degree and any correction for slope can be neglected for conventional or commonly used culverts flowing with inlet control.

In all culvert design, headwater or depth of ponding at the entrance to a culvert is an important factor in culvert capacity. The headwater depth (or headwater HW) is the vertical distance from the culvert invert at the entrance to the energy line of the headwater pool (depth + velocity head). Because of the low velocities in most entrance pools and the difficulty in determining the velocity head for all flows, the water surface and the energy line at the entrance are assumed to be coincident thus the headwater depths given by the inlet control charts (in HEC 5) can be higher than may occur in some installations. For the purposes of measuring headwater, the culvert invert at the entrance is the low point in the culvert opening at the beginning of the full cross-section of the culvert barrel.

### 1.5.2 Outlet Control

For outlet control, the conditions downstream of the entrance are the controlling factors in the culvert hydraulic performance. Either or both the frictional forces or the tailwater depth directly control the flow through the culvert. The barrel friction predominates if critical depth occurs at the outlet. Tailwater controls the flow if the tailwater depth is large enough to effect the headwater depth. Outlet control conditions usually exist in areas of low topographical relief.

Culverts flowing with outlet control can flow with the culvert barrel full or part full for part or all of the barrel length. If the entire cross section of the barrel is filled with water for the total length of the barrel, the culvert is said to be in full flow or flowing full. The procedures given in HEC 5 provide methods for the accurate determination of headwater depth for the full flow conditions. The method given in HEC 5 for the part full flow condition, gives a solution for headwater depth that decreases in accuracy as the headwater decreases.

The head, H, or energy required to pass a given quantity of water through a culvert flowing in outlet control with the barrel flowing full throughout its length is made up of three major parts (Figure 1.5). This energy is obtained from ponding of water at the entrance and is expressed as

$$H = H_v + H_e + H_f \qquad (1.1)$$

where $H_v$ is the velocity head, $H_e$ is the entrance headloss and $H_f$ is the friction loss. A more usable form of the above equation is expressed as

$$HW = d + \frac{V^2}{2g} + C_e \frac{V^2}{2g} + H_f - S_o L \qquad (1.2)$$

where HW is headwater depth, d is depth of flow, V is the mean flow velocity, $C_e$ is the entrance headloss coefficient, g is acceleration of gravity, $H_f$ is frictional

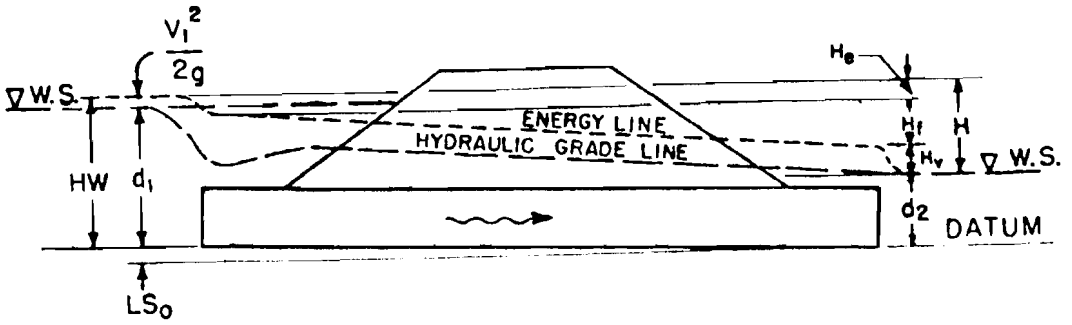


Figure 1.5 Definition Sketch (from H.E.C. 5)

losses expressed as $H_f = S_f \cdot L$, $S_f$ is the friction slope, $S_o$ is the culvert slope, and L is culvert length; the datum is the elevation of the culvert invert at the exit.

The FHWA manual (HEC 5) and state highway design manuals specify that the entrance loss, $H_e$ depends upon the geometry of the inlet edge. This loss is expressed as a coefficient, $C_e$, times the barrel velocity head or $H_e = C_e \frac{V^2}{2g}$. The entrance loss coefficients $C_e$ for various types of entrances when the flow is in outlet control are listed in Table 1.2 which is from HEC 5.

## 1.6 Flow Regimes

The Federal Highway Administration (FHWA) and the State Department of Highways and Public Transportation in Texas (DHT) distinguishes between inlet and outlet control for design purposes. DHT (1970) also categorizes flow into six different regimes (Figures 1.6 and 1.7) which will be used throughout this report. Four of the flow regimes (1, 2, 4A, and 4B) are considered outlet control (Fig. 1.6). The other two flow regimes (3A and 3B) are considered inlet control (Fig. 1.7).

### 1.6.1 Outlet Control Regimes

Type 1 flow conditions (Fig. 1.6) occur when the culvert slope is less than the critical slope ($S_o < S_c$), the headwater is less than 1.2 times the culvert height ($HW < 1.2D$), and the tailwater depth is less than the critical depth ($TW < d_c$). The energy equation is written between the entrance and outlet as

$$HW = d_c + \frac{V_c^2}{2g} + C_e \frac{V_c^2}{2g} + H_f - S_o L \qquad (1.3)$$

Table 1.2 - ENTRANCE LOSS COEFFICIENTS

Outlet Control, Full or Partly Full

Entrance head loss $H_e = C_e \frac{V^2}{2g}$

| Type of Structure and Design of Entrance | Coefficient $C_e$ |
|---|---|
| **Pipe, Concrete** | |
| Projecting from fill, socket end (groove-end) | 0.2 |
| Projecting from fill, sq. cut end | 0.5 |
| Headwall or headwall and wingwalls | |
| Socket end of pipe (groove-end) | 0.2 |
| Square-edge | 0.5 |
| Rounded (radius = 1/12D) | 0.2 |
| Mitered to conform to fill slope | 0.7 |
| *End-Section conforming to fill slope | 0.5 |
| Beveled edges, 33.7° or 45° bevels | 0.2 |
| Side-or slope-tapered inlet | 0.2 |
| **Pipe, or Pipe-Arch, Corrugated Metal** | |
| Projecting from fill (no headwall) | 0.9 |
| Headwall or headwall and wingwalls square-edge | 0.5 |
| Mitered to conform to fill slope, paved or unpaved slope | 0.7 |
| *End-Section conforming to fill slope | 0.5 |
| Beveled edges, 33.7° or 45° bevels | 0.2 |
| Side-or slope-tapered inlet | 0.2 |
| **Box, Reinforced Concrete** | |
| Headwall parallel to embankment (no wingwalls) | |
| Square-edged on 3 edges | 0.5 |
| Rounded on 3 edges to radius of 1/12 barrel dimension, or beveled edges on 3 sides | 0.2 |
| Wingwalls at 30° to 75° to barrel | |
| Square-edged at crown | 0.4 |
| Crown edge rounded to radius of 1/12 barrel dimension, or beveled top edge | 0.2 |
| Wingwall at 10° to 25° to barrel | |
| Square-edged at crown | 0.5 |
| Wingwalls parallel (extension of sides) | |
| Square-edged at crown | 0.7 |
| Side-or slope-tapered inlet | 0.2 |

*Note: "End Section conforming to fill slope," made of either metal or concrete, are the sections commonly available from manufacturers. From limited hydraulic tests they are equivalent in operation to a headwall in both inlet and outlet control. Some end sections, incorporating a closed taper in their design have a superior hydraulic performance.

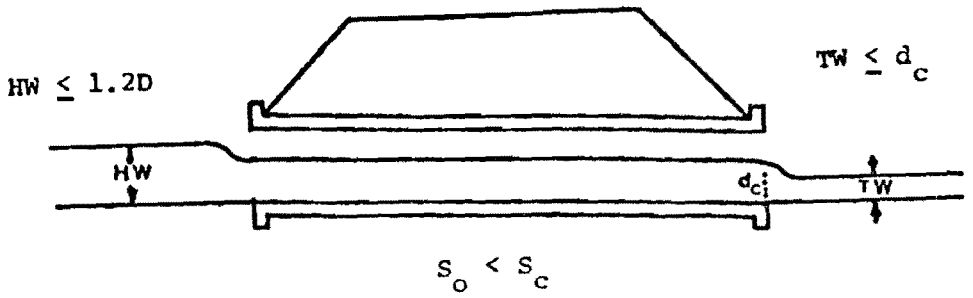


TYPE 1: Free Surface, Outlet Control

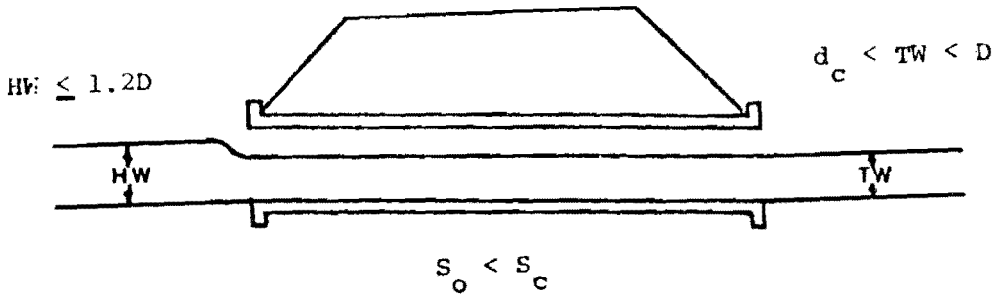


TYPE 2: Free Surface, Outlet Control

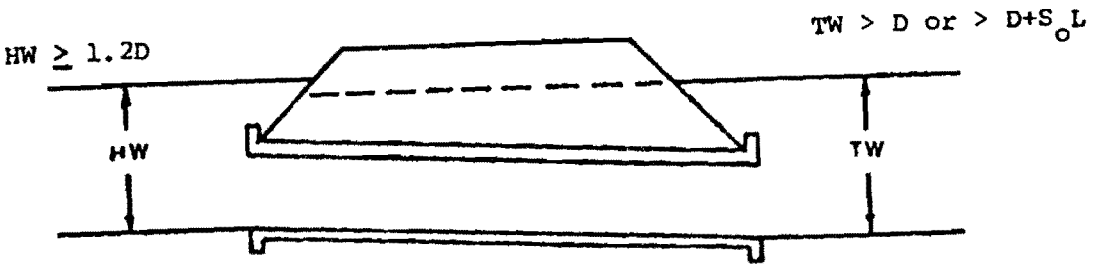


TYPE 4A: Pressure Flow Throughout, Outlet Control

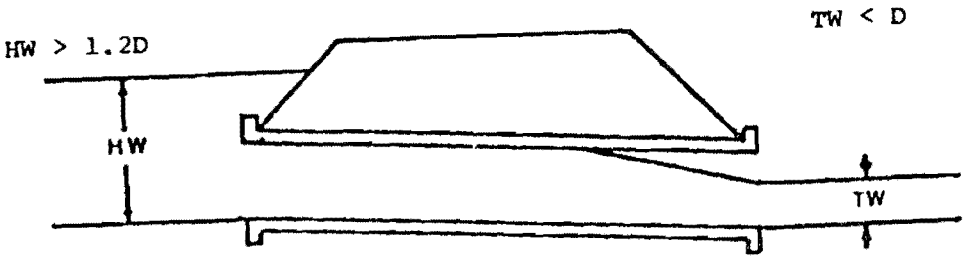


TYPE 4B: Submerged Inlet, Outlet Control

Figure 1.6 Flow Regimes (Outlet Control)

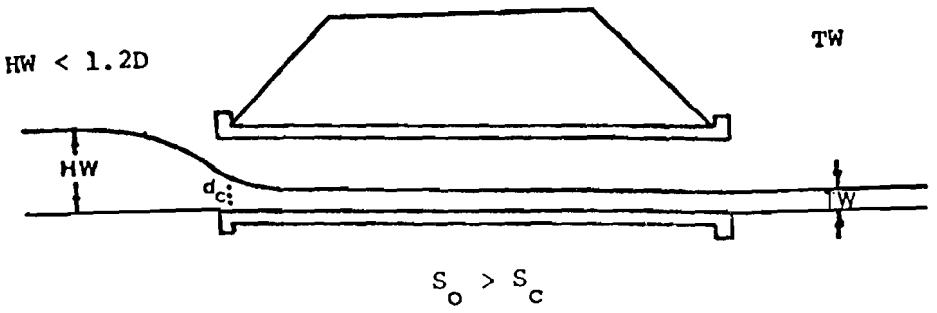


TYPE 3A: Free Inlet, Inlet Control

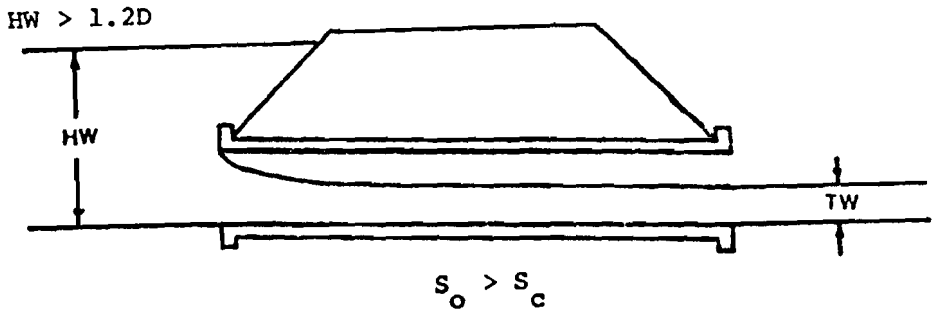


TYPE 3A: Inlet Submerged, Inlet Control

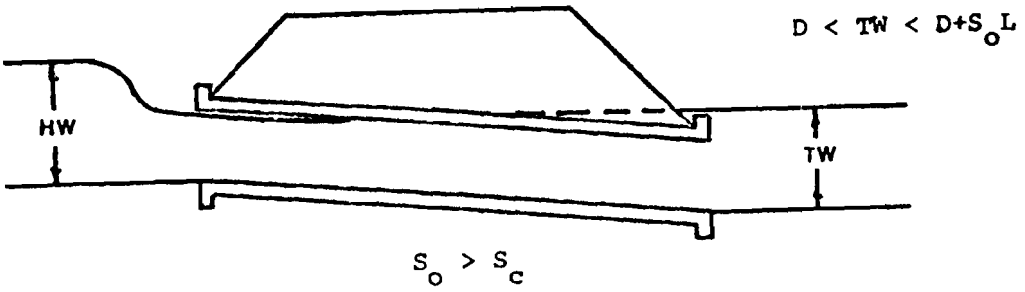


TYPE 3B: Outlet Submerged, Inlet Control

Figure 1.7 Flow Regimes (Inlet Control)

where $d_c$ is the critical depth, $V_c$ is the critical velocity, and $H_f$ is the friction loss. For Type 1 flow conditions, there is a transition from subcritical flow in the culvert to supercritical tailwater flow. This situation requires the development of an estimate for $S_f$. In the DHT solution to the energy equation, $S_f$ is estimated by assuming uniform flow at a constant depth of $1.1 \cdot d_c$.

Type 2 Flow Regime

Type 2 flow conditions (Figure 1.6) occur when the entrance is unsubmerged ($HW \leq 1.2D$), the slope is less than critical ($S_o < S_c$), and the tailwater depth is between the critical depth and the culvert height ($d_c < TW < D$). The energy equation is expressed as

$$HW = TW + \frac{V_{tw}^2}{2g} + C_e \frac{V_{tw}^2}{2g} + H_f - S_o L \qquad (1.4)$$

where TW is the tailwater depth, and $V_{tw}$ is the outlet velocity. For Type 2 flow conditions $S_f$ is estimated by assuming uniform flow at a depth equal to TW.

Type 4A Flow Regime

Type 4A flow conditions (Figure 1.6) occur when either the slope is less than critical ($S_o < S_c$) and the tailwater depth is greater than D ($TW > D$), or the slope is greater than critical ($S_o > S_c$) and the tailwater depth is greater than slope times length plus D ($TW > S_o \cdot L + D$). This type of flow is controlled by tailwater conditions. The energy equation is expressed as

$$HW = \frac{V^2}{2g} + C_e \frac{V^2}{2g} + H_f + TW - S_o L \qquad (1.5)$$

where V is based on full culvert flow, and $H_f$ is the full pipe flow frictional losses.

Type 4B Flow Regime

Type 4B flow conditions (Fig. 1.6) occur when the entrance is submerged (HW > 1.2D), tailwater is less than D, (TW < D), and the culvert flows full for part of its length. This type of flow is controlled by the barrel and tailwater conditions. The culvert hydraulic performance is approximated by

$$HW = \frac{V^2_{tw}}{2g} + C_e \frac{V^2}{2g} + H_f + P - S_o L \qquad (1.6)$$

where V is based on full culvert flow, P is estimated as $(d_c + D)/2$ when $TW < d_c$ or is TW when $TW > d_c$ and $V_{tw}$ is based on $d_c$ for $TW < d_c$ or is based on TW for $TW > d_c$.

1.6.2 Inlet Control Regimes

Type 3A Flow Regime

Type 3A flow conditions (Fig 1.7) occur when the slope is greater than or equal to critical ($S_o \geq S_c$) and tailwater depth is less than the slope times the length ($TW < S_o L$). Critical depth controls at the entrance when the entrance is unsubmerged and entrance geometry controls when the entrance is submerged. The culvert hydraulic performance is determined by empirical curves based on experimental measurements (HEC 5).

Type 3B Flow Regimes

Type 3B flow conditions (Figure 1.7) are similar to the Type 3A flow conditions, except $S_o L < TW < S_o L + D$. The inlet is either submerged or unsubmerged. Control may be at either the entrance, or the outlet, or may transfer back and forth as slug flow. Hydraulic performance is predicted from empirical nomographs or by type 4A and 4B hydraulic characteristics.

# CHAPTER 2 EXPERIMENTAL CONSIDERATIONS

The planning, construction, and hydraulic testing of the model culvert with safety grates were divided into several stages. First, the physical parameters effecting the hydraulic performance of a culvert were determined by examining the energy equation. After identification of the controlling physical parameters, hydraulic similitude was utilized to express the relationship between the scale model culvert properties and the full size culvert performance. The model culvert was then designed and constructed to simulate possible field conditions. Finally, numerous hydraulic studies were performed on the culvert and the resulting experimental data was reduced for analysis.

## 2.1 Energy Equation

The primary objective of this study was to determine the effect that safety grates have on the entrance headloss coefficient. Naturally, the entrance headloss coefficient could not be physically measured, but was determined using experimentally collected data to solve the energy equation for $C_e$. Referring to Fig. 2-1, the energy equation written between points A and C is expressed as:

$$HW + \frac{V_A^2}{2g} = \frac{V^2}{2g} + C_e \frac{V_e^2}{2g} + H_f + d \qquad (2.1)$$

where HW is the headwater depth, $V_A$ is the mean approach velocity, V is the mean velocity in the culvert, $C_e$ is the entrance headloss coefficient, $H_f$ is the frictional headloss in the culvert, d is the value of the hydraulic grade line at the entrance, and $V_e$ is the mean entrance velocity measured at the entrance, point B in Fig. 2.1.

This general form of the energy equation could be solved for the entrance headloss coefficient if all other terms were physically measured. To

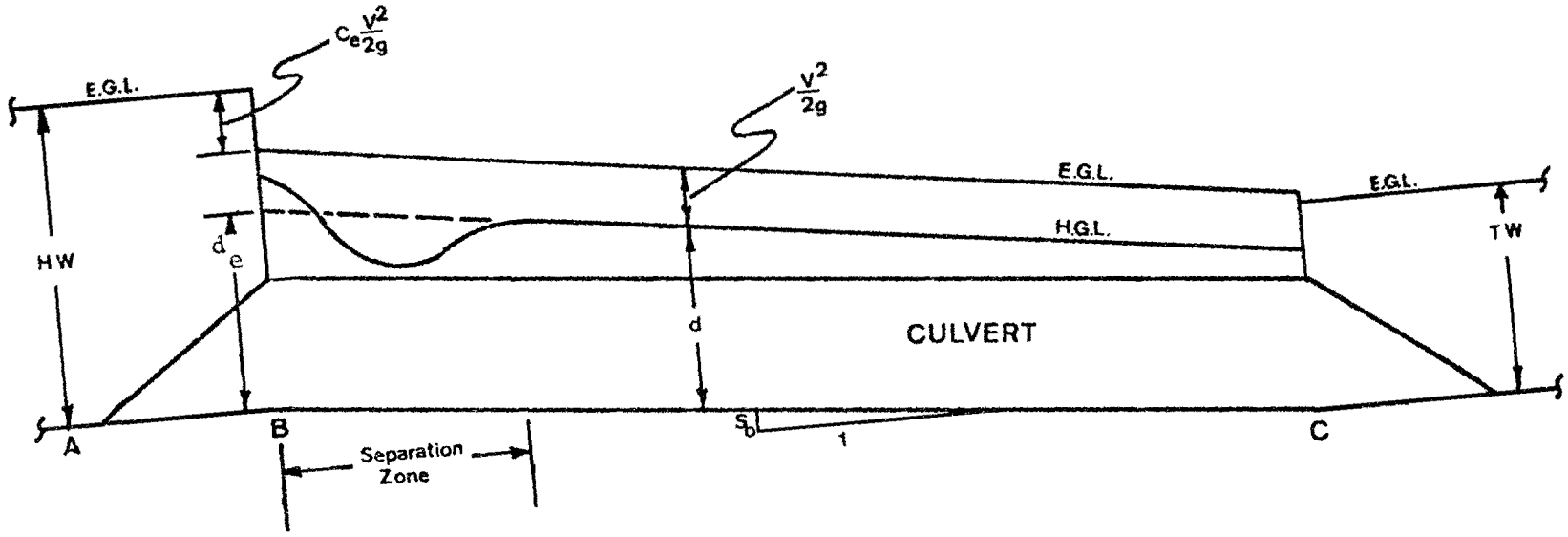


Figure 2.1 Energy and Hydraulic Gradelines

minimize the number of terms to be measured, the energy equation was simplified. First, the model culvert approach channel was designed wider than the model culvert cross-section (velocity assumed to be zero). The approach velocity head term, $V_A/2g$, was then neglected in the energy equation. Most culvert design procedures do consider a zero approach velocity. However, referring to Fig. 2.1, the energy equation between A and B is expressed as:

$$HW = \frac{V^2}{2g} + d_e + C_e \frac{V_e^2}{2g} \qquad (2.2)$$

where $d_e$ is the value of the hydraulic gradeline at the entrance and V is the mean velocity at the entrance. The entrance headloss coefficient* can be expressed as:

$$C_e = \frac{(HW - (d_e + V_e^2/2g))}{V^2/2g} \qquad (2.3)$$

A major problem was encountered in measuring the depth of flow at the entrance because of a large amount of turbulence generated at the entrance. A separation zone forms along the culvert sides (Fig. 2.1) in which the streamlines have substantial curvature and, thus, an acceleration component of flow. The hydrostatic law of pressure distribution cannot be applied to a flow with a large acceleration component in the cross-sectional plane. In order to circumvent this problem, piezometers were used in the experimental program to measure the hydraulic head at intervals along the culvert. From the piezometer readings and elevation data, the depth of flow and the area of flow were calculated for each location. The velocity at each piezometer location was determined from the area of flow and the flowrate; V = Q/A. The total energy head at each location equals the velocity head plus the piezometer reading (adjusted to datum). A least squares, linear fit, of the adjusted piezometer readings downstream of the separation zone, was utilized to define the hydraulic

*All $C_e$ values were determined using the mean entrance velocity.

gradeline. The total energy heads at these locations were similarly linearly extrapolated to yield the energy gradeline. The calculated hydraulic and energy gradelines together with the elevation data were used to determine the depth of flow at the entrance and the entrance velocity.

## 2.2 Hydraulic Similitude

Hydraulic model studies are based on the application of the laws of hydraulic similitude. These laws are derived from the basic relations of fluid mechanics and express the interrelationship of the various fluid flow parameters, such as velocity, pressure, and shear, under similar boundary conditions. Similitude requires geometric, kinematic, and dynamic similarity be maintained between the model culvert and the prototype culvert.

The first condition of geometric similarity is satisfied if the ratio of all corresponding lengths in the model and prototype are equal. This scale ratio ($L_R$) can be expressed as

$$L_R = \frac{L_m}{L_p} \tag{2.4}$$

where $L_m$ and $L_p$ are corresponding lengths in the model and prototype, respectively. Geometric similarity does not depend on fluid motion or force.

The second condition of kinematic similarity is satisfied when the ratio of all corresponding components of velocity and acceleration are equal. Since the ratio of the components of motion can be written in terms of the scale ratio, the flow lines will be geometrically similar. The resulting velocity ratio, $V_R$, is

$$V_R = \frac{V_m}{V_p} \tag{2.5}$$

where $V_m$ and $V_p$ are velocities in model and prototype, respectively. Once the geometric and kinematic similarities are satisfied, dynamic similarity is also satisfied.

In this culvert model study, gravitational forces are the dominant factors describing flow condition. The inertial, gravitational, and pressure forces are the major controlling factors affecting the flow in the culvert. Viscous and surface tension forces do affect the flow, but these effects are insignificant compared to the magnitude of the inertial, gravitational, and pressure forces and thus can be neglected.

## 2.3 Laboratory Facilities

All experimental tests for this study were performed at the Center for Research in Water Resources (CRWR) hydraulics laboratory at the Balcones Research Center of the University of Texas at Austin.

Permanent equipment such as pumps, a pipe system, and a return channel provide a system of recirculating water flow through the model. A schematic layout of the CRWR hydraulics lab is shown in Fig 2.2. The outdoor storage reservoir has a diameter of 100-ft and a storage capacity of approximately 550,000 gallons. Two pumps supplied a range of flows up to a maximum of approximately 12 cfs through model culverts. Regulating valves are located between the pumps and the indoor hydraulics laboratory. The supply piping system consists of 12-in diameter overhead pipes housed in a 97-ft by 100-ft room. The 4-ft x 4-ft return channel is located below the floor level of the laboratory. A sharp crested weir and a Lory Point gage were used to measure the discharge in the return channel.

A general schematic of the model setup is shown in Fig 2.3. Water from the supply pipe system enters an 8-ft x 8-ft x 6-ft high head box. This head box was constructed from 3/4-in thick A-C plywood and set in a metal frame. All plywood surfaces exposed to water were impregnated with polyester resin and all joints were reinforced with fiberglass tape. Two sets of baffles

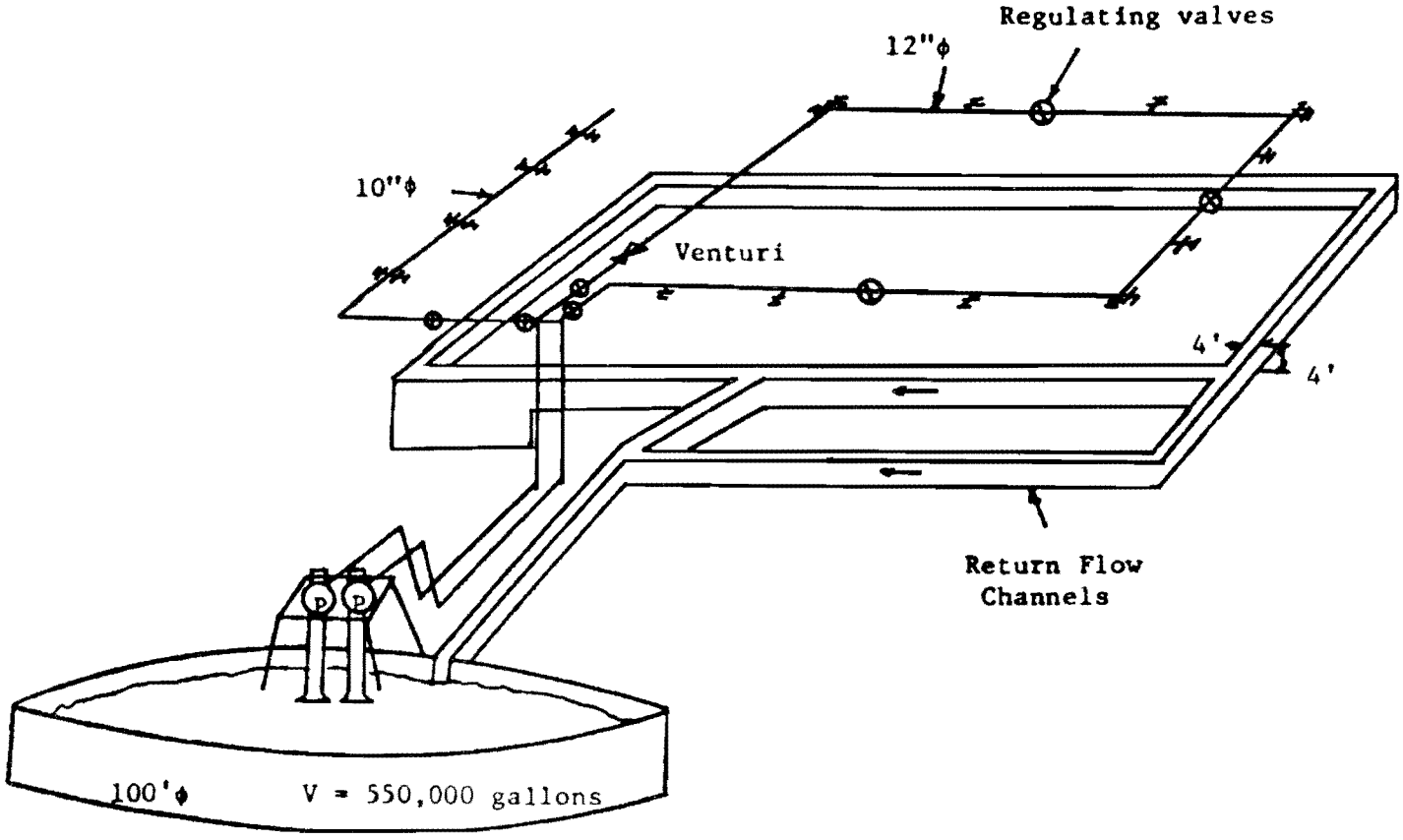


Figure 2.2 Schematic of Hydraulics Laboratory

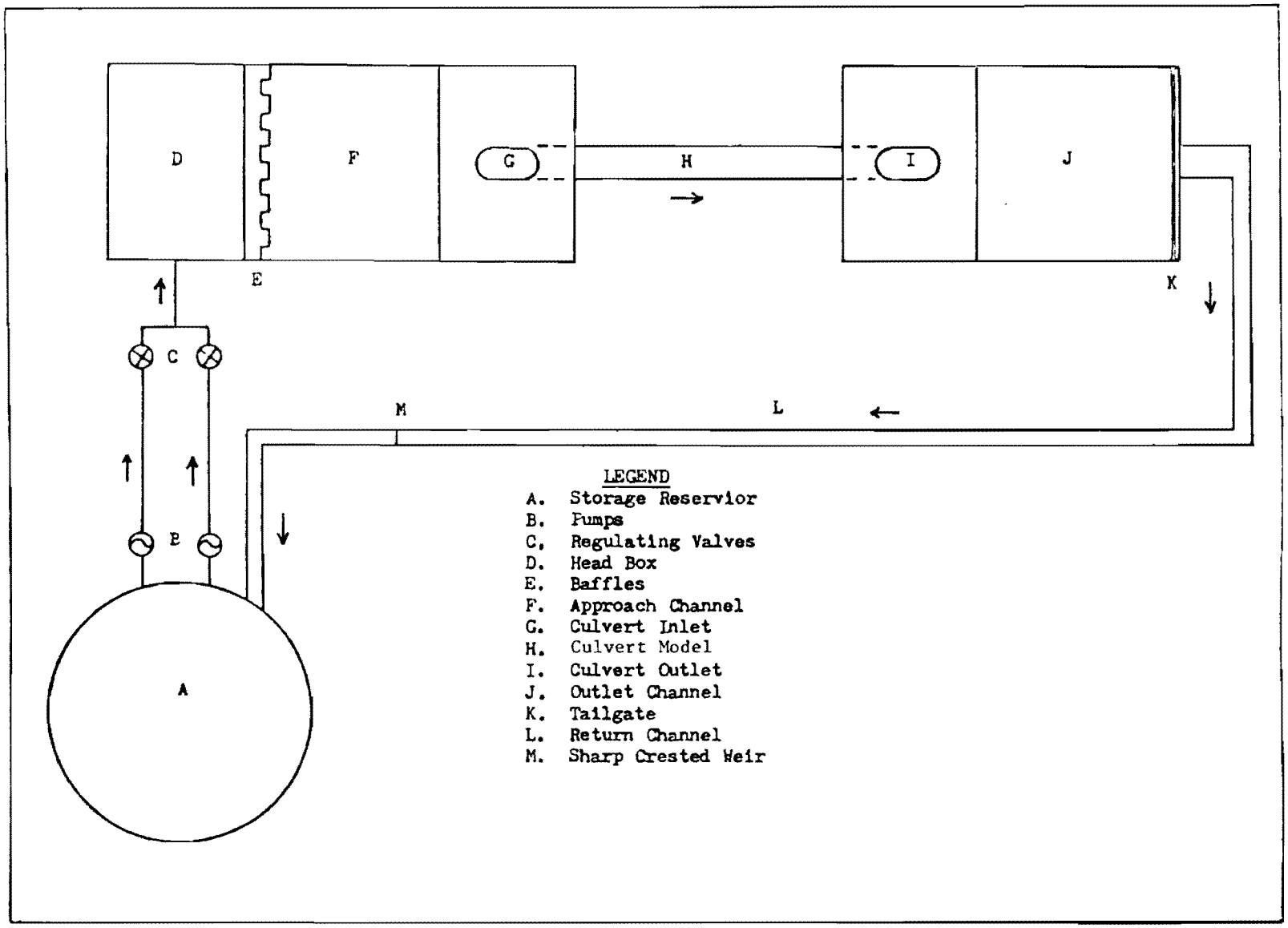


Figure 2.3 Overview of Test Facilities

were used to reduce the amount of turbulence and were located at the approach channel entrance. The baffles were constructed of 1-in by 2-in vertical slats placed on alternating sides of a wooden frame. Two large styrofoam pads were used to decrease the amount of surface turbulence. From the head box the water flows into an 8-ft wide by 4-ft deep by 20-ft long horizontal approach channel. The channel was also constructed of 3/4-inch thick A-C plywood and was placed on a 2-ft high wooden frame. The measurements of headwater depth were made by two Lory Point gages located in the approach channel. Figure 2.4 shows the head box and approach channel. The water flows from the culvert model into a discharge channel (Fig. 2.5), also constructed of plywood.

The 8-ft wide by 4-ft high by 9-ft 4-in long outlet or discharge channel was supported on two stiffened W 10-ft x 12-ft steel beams. Six 5-ton screw jacks were used to vary outlet channel elevation and culvert slope. An 8-ft wide by 4-ft 5-in high by 3/16-in thick sliding steel tailgate was mounted at the downstream end of the outlet channel in an 8-ft by 7-ft 8-in frame made of 2-in x 2-in angle iron. Tailwater depth was varied by two pulley mechanisms to raise and lower the tailgate. After passing the tailgate, water flows through a 12-ft wide by 4-ft long by 3-ft 10-in deep outfall box made of 3/4-in A-C plywood. The outfall box was supported by 2-in x 2-in angle iron and stiffened with 3/8-in diameter reinforcing steel bars.

## 2.4 Experimental Set up for Box Culvert Tests

Schematics (side view and plan view) of the experimental set up for the box culvert tests are shown in Fig. 2.6. The box culvert was constructed of 3/4-in plywood with 1/2-in plexiglass installed on one side (Fig. 2.7). The plexiglass enabled visual observation of the different flow regimes. The dimension of the culvert were 2-ft wide by 1.25-ft high by 27-ft long. The

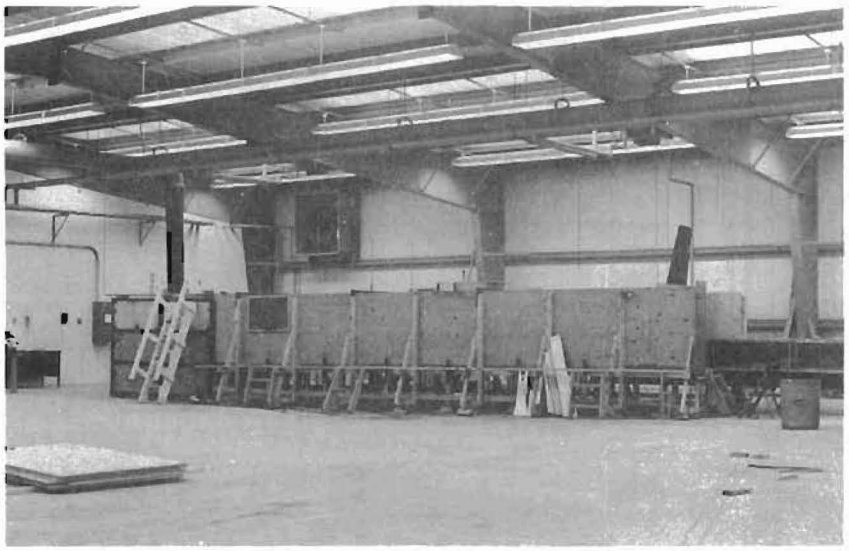

a. Headbox and Approach Channel

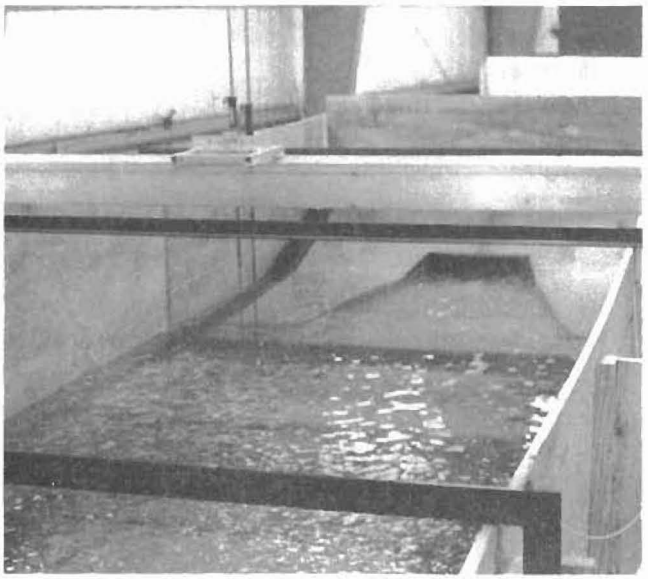

b. Entrance to the Culvert

Figure 2.4 Experimental Set-Up

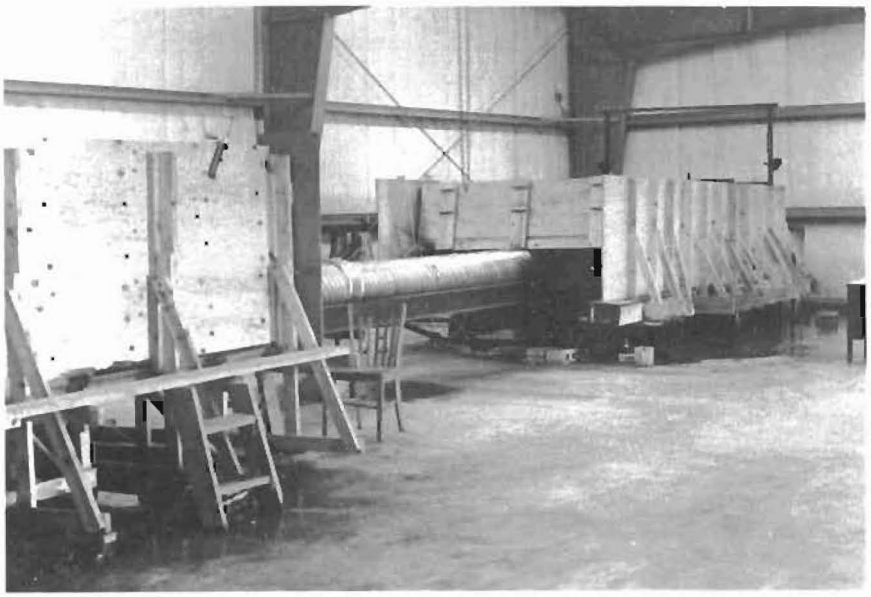

Figure 2.5 Outlet Channel

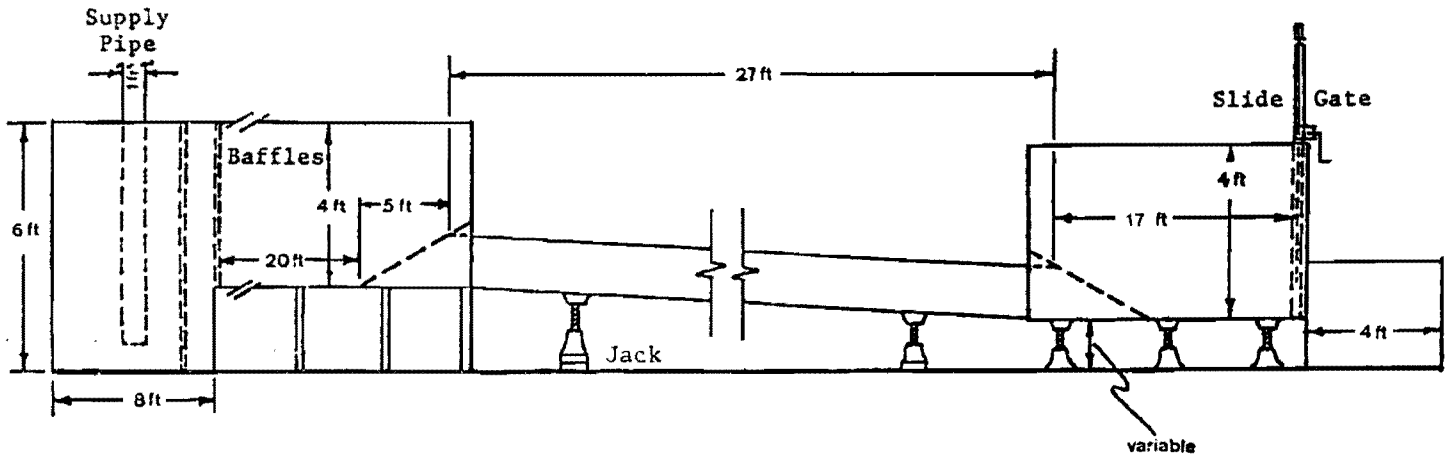


(a) SIDE VIEW

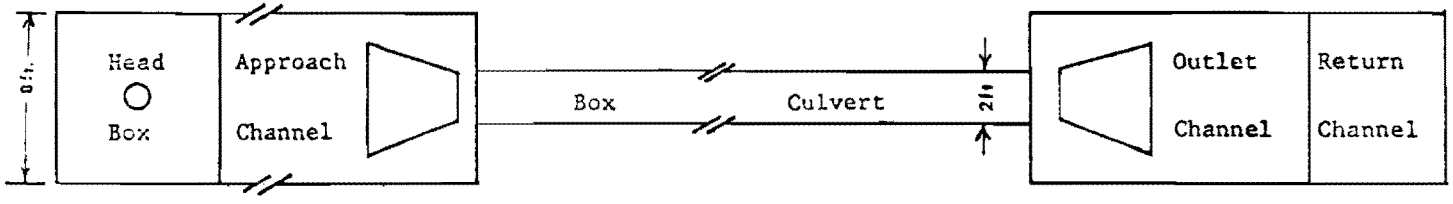


(b) PLAN VIEW

Figure 2.6 Schematics of Experimental Setup

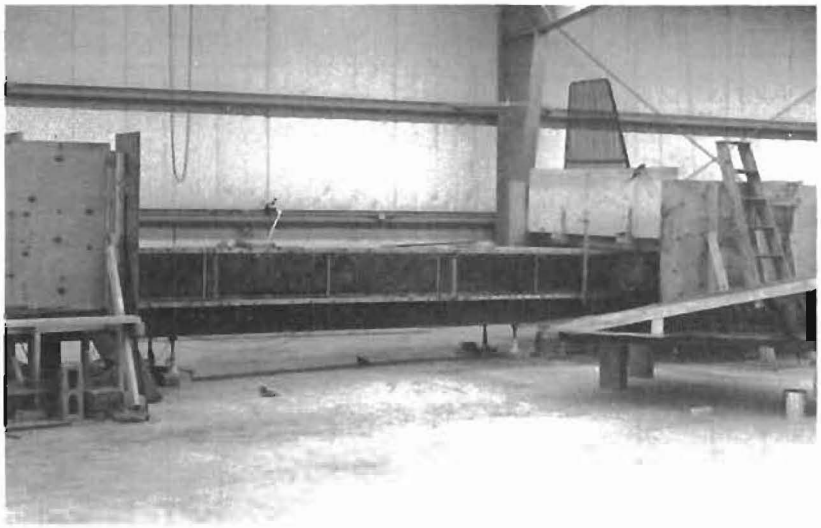

Figure 2.7 Box Culvert

culvert was supported on two W 12 x 22 steel beams to keep deflections in the culvert to a minimum. Four 5-ton screw jacks were used to change the culvert slope and support the culvert. The slope of the culvert was set by the use of a Dumpy level. The headwalls to the box culvert were constructed of plywood on a 4 to 1 slope with a wingwall flare of 4 to 1. Figure 2.8 is a schematic of the box culvert headwalls. Figure 2.4 (b) shows water entering the box culvert.

## 2.5 Experimental Set Up for Pipe Culvert Tests

Schematics (side view and plan view of the pipe culvert model) are shown in Fig. 2.9. The pipe culvert is a 15-in diameter, ½-in by 2-3/4-in helical corrugated metal pipe* (Fig. 2.10). Two sections of pipe were connected by a bolt lock collar. The pipe was mounted on two stiffened W 10 x 12 steel beams. Five 5-ton screw jacks provided culvert support and slope variability.

The headwalls of the pipe culvert were constructed of 3/4-in A-C plywood (Fig. 2.11). The headwalls were mounted on a 4:1 sloping 2-in by 4-in wood frame. Polyester resin sealant, fiberglass tape, rubber stripping, metal plates, and sheet metal screws were used to waterproof the headwall.

## 2.6 Instrumentation

Discharge was measured with a sharp crested weir and depths were measured using Lory point gages, stagnation tubes, an open air manometer, and piezometers. The discharge was measured with a Lory point gage and a sharp crested weir, located in the return channel. Headwater depth was measured in the approach channel 10-ft upstream of the culvert entrance with two Lory point gages. The tailwater depths were measured with a piezometer, located in the outlet channel floor. The piezometers were connected by "Tygon" tubing to its separate, graduated, open air manometer. The slope of the culvert was measured with a Dumpy level.

---

*Donated to the project by Armco, Inc., Middletown, Ohio.

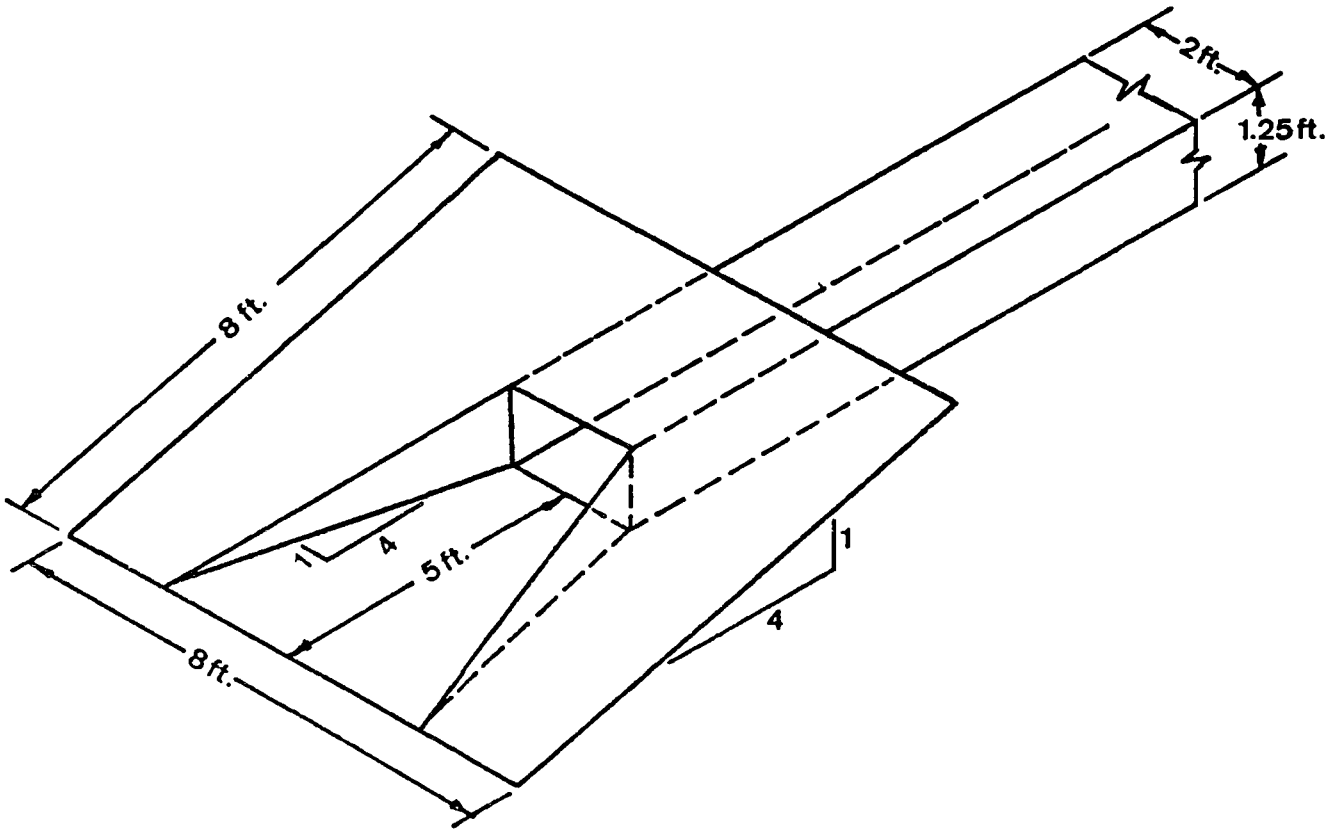


Figure 2.8 Headwall Design and Dimensions

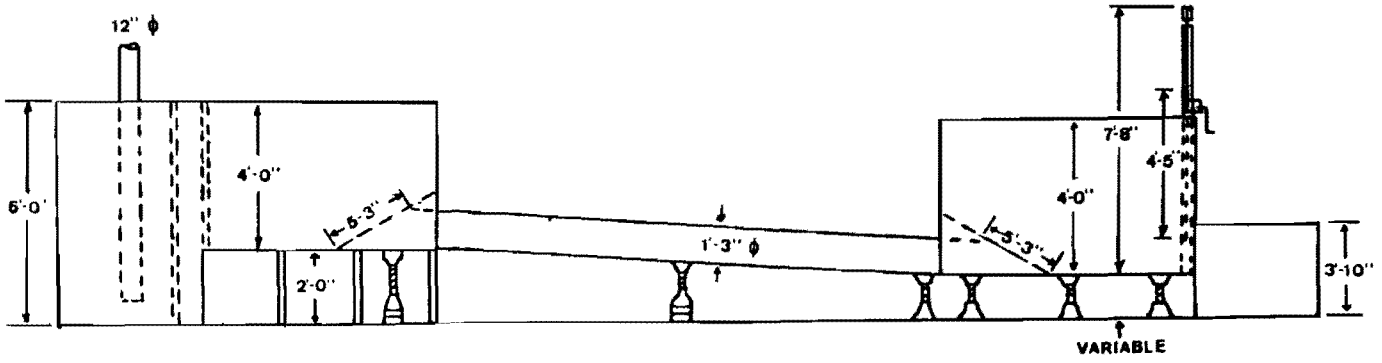


Side View

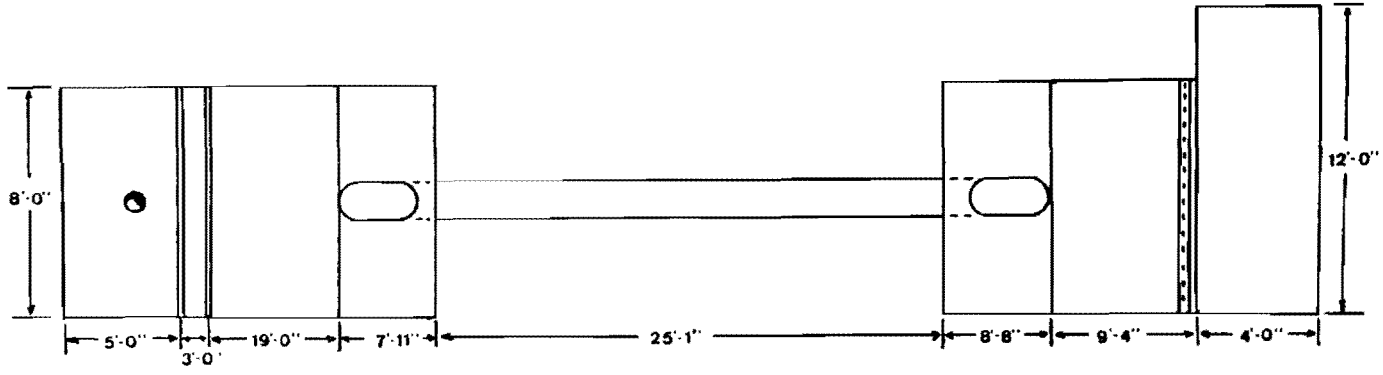


Plan View

Figure 2.9 Pipe Culvert Model - Side and Plan Views

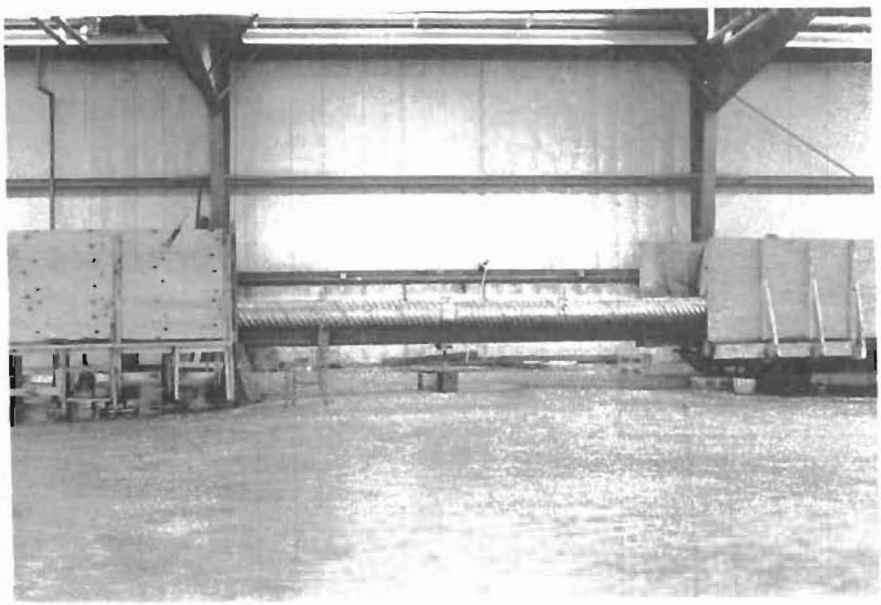

Figure 2.10 Pipe Culvert

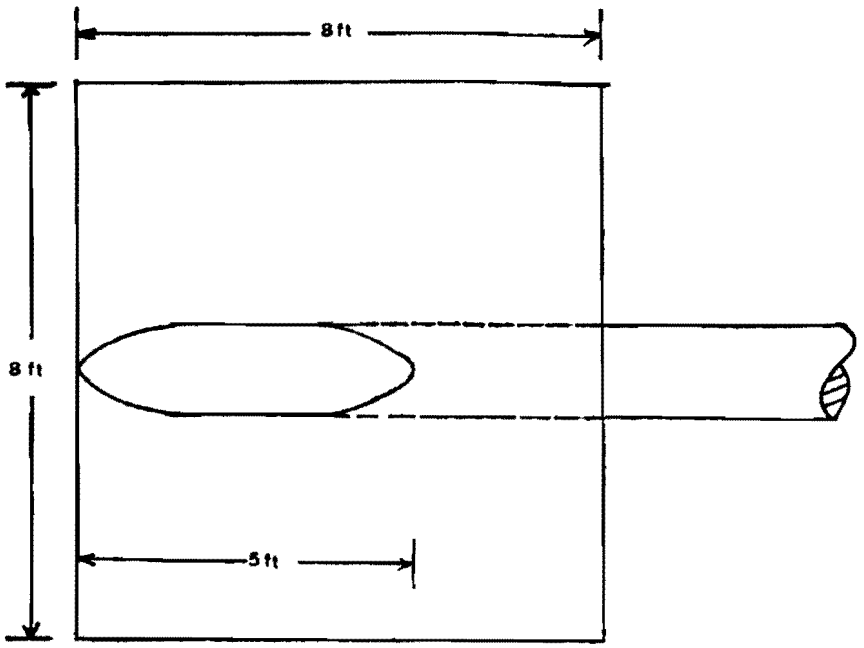


TOP VIEW

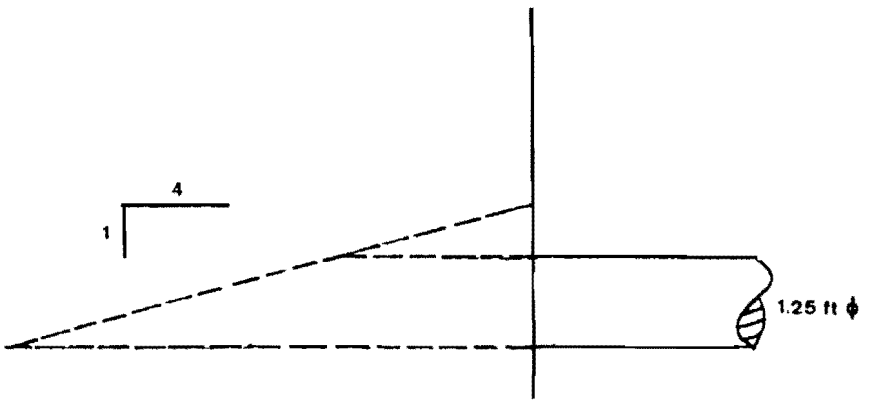


SIDE VIEW

Figure 2.11 Pipe Culvert Headwall Dimensions

For the box culvert model the piezometric depths were measured by twelve piezometers located along the culvert centerline. The piezometers were connected by Tygon tubing to 1/2-in diameter open air manometers shown in Fig 2.12. Another manometer tube was placed at the downstream end of the box culvert for the 12th piezometer.

For the pipe culvert, hydraulic depths were measured by eight stagnation tubes and open air manometers. Eight 1-1/8-in diameter holes were drilled at approximately 3-1/2-ft intervals along the pipe. The stagnation tubes (Fig. 2.13) were set in rubber stoppers and mounted in the holes with silicon sealant, rubber gaskets, steel plates, and sheet metal screws. The stagnation tubes were connected by "Tygon" tubing to the 1/2-in diameter open air manometers (Fig. 2.12).

## 2.7 Model Safety Grates

Safety grates for the box culvert model included 1:4 scale model grates of the prototype grates (3-in diameter on 30-in centers) determined by the Texas Transportation Institute (TTI) study (1979). The model safety grate of the TTI design is shown in Fig. 2.14(a). These grates are referred to as the pipe safety grates for the purpose of this report. These model pipe grates were constructed of 3/4-in O.D. pipe conduit and were placed on 7.5-in centers as illustrated in Fig. 2.14(a).

In addition to using the model pipe grates, tests were also performed for prototype grates that have been used in the field. These prototype grates are constructed of 1/2-in x 2-in flat iron bars and are placed on 5-in centers: These grates are referred to as "bar grates" for the purpose of this report. The model bar grates are shown in Fig. 2.14(b). These model grates which are also a 1:4 scale model are 1/8-in x 1/2-in flat iron bars placed on 1.25-in centers. Figures

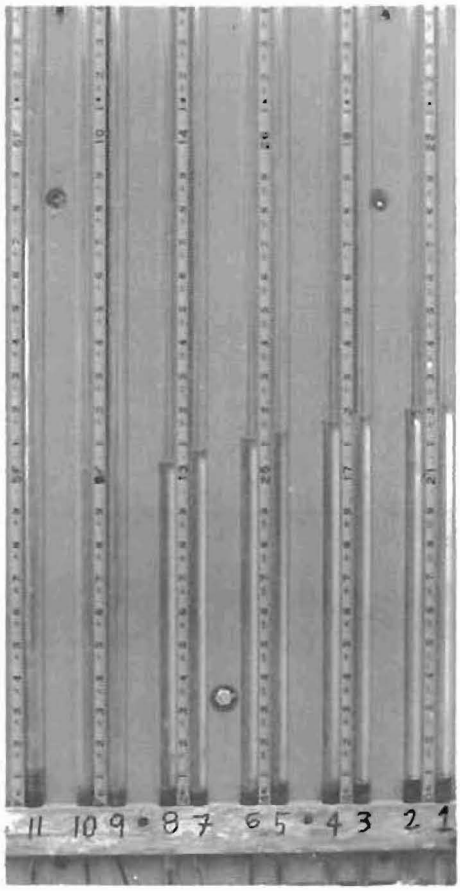


Figure 2.12 Manometers

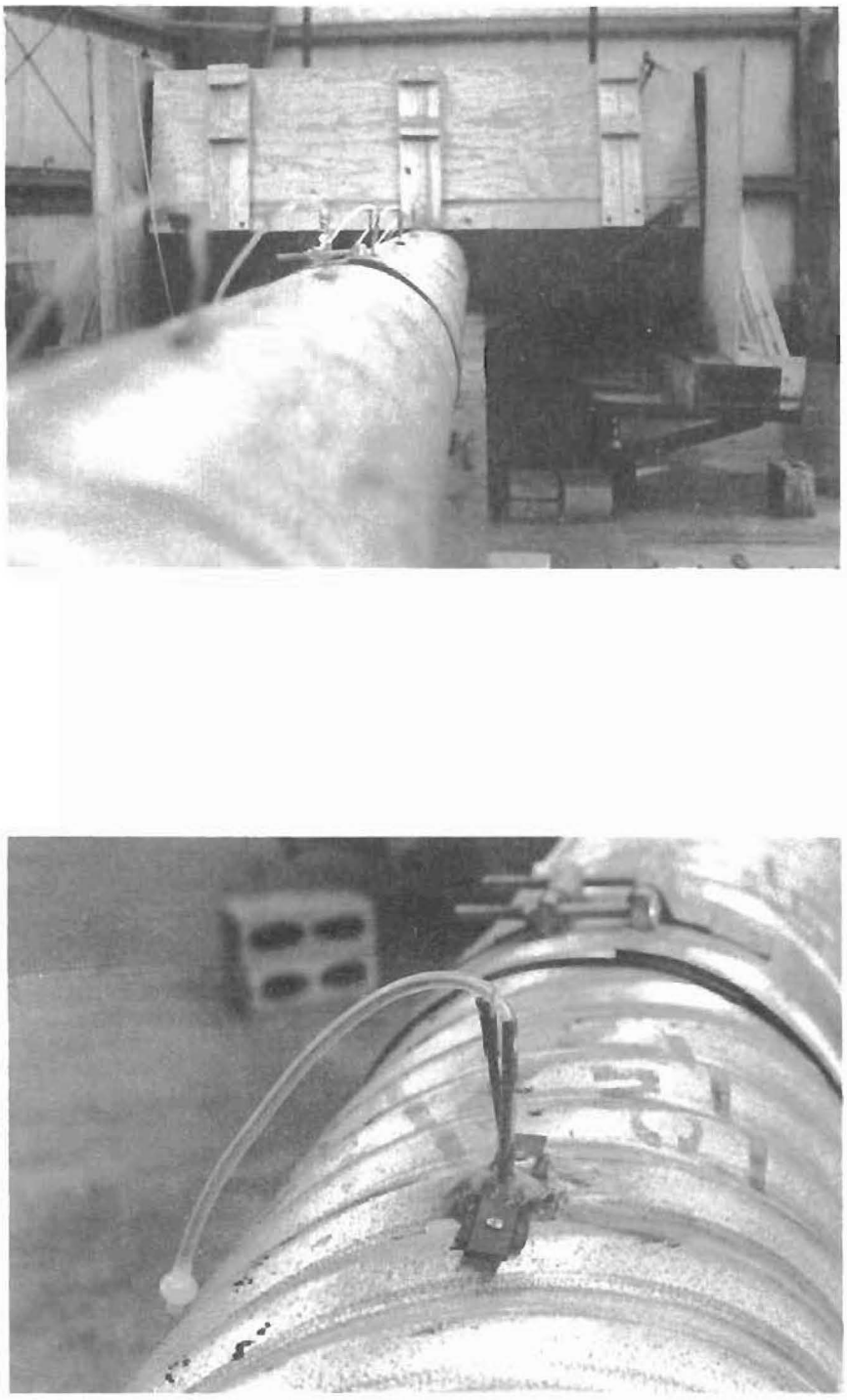

Figure 2.13 Stagnation Tubes For Pipe Culvert

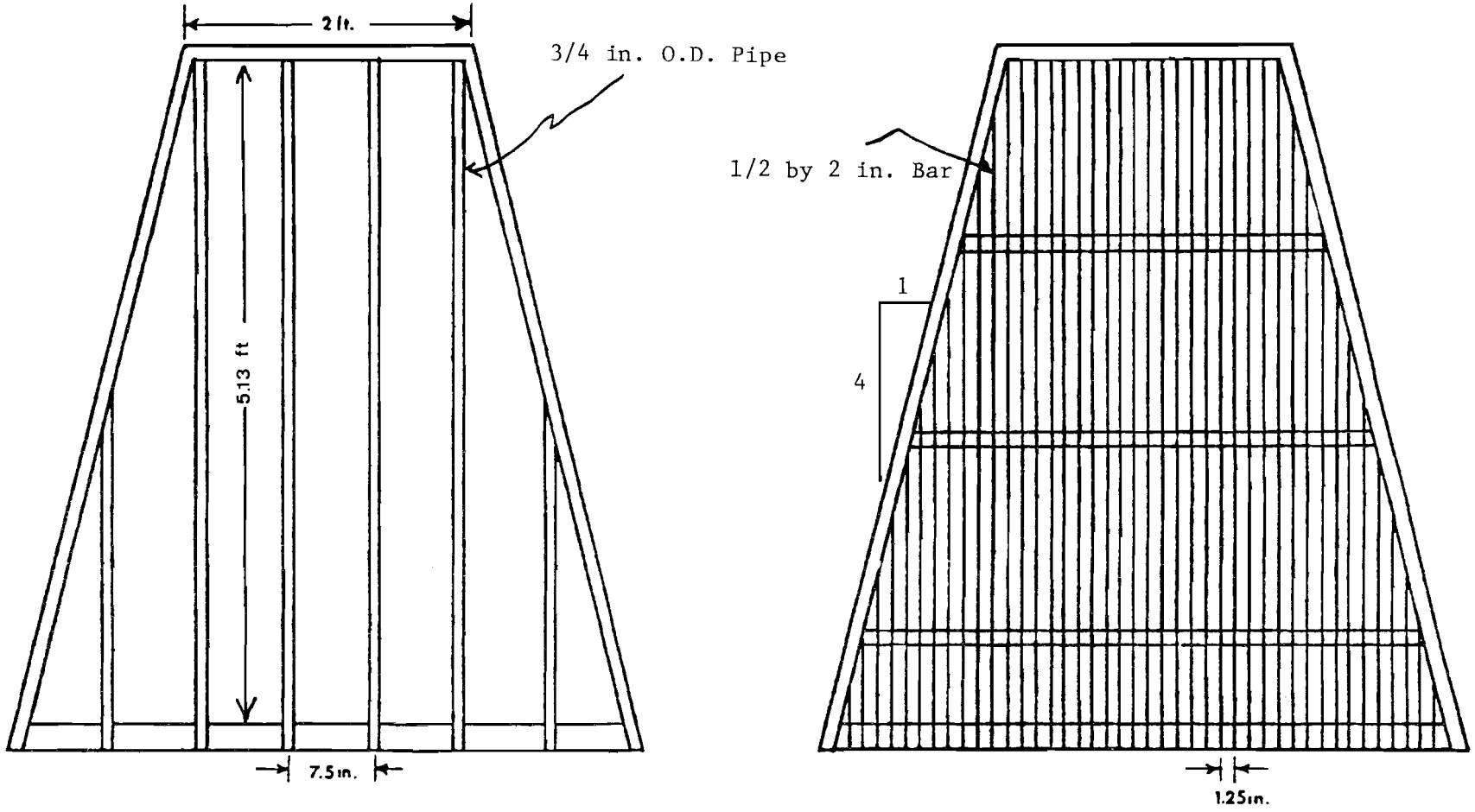


(a) Pipe Safety Grate

(b) Bar Safety Grate

Figure 2.14 Model Safety Grates For Box Culvert

2.15(a) and (b) show the pipe and bar safety grates installed on the headwalls of the box culvert model.

The safety grates for the corrugated metal pipe culvert are shown in Fig. 2.16. these grates have a somewhat different design than either of the two box culvert grates. These grates were constructed of 3/4-in diameter conduits placed on 6-in centers; they simulate 3-in diameter conduits placed on 24-in centers and are shown in Fig. 2.16. Figure 2.17 shows the pipe grates installed at the pipe culvert inlet and Fig. 2.18 shows the grates installed at the outlet.

## 2.8 Measurements For Entrance Headloss

Several flow parameters were measured in both free outfall and tailwater tests: (1) slope; (2) discharge; (3) headwater depth; (4) tailwater depth; and (5) hydraulic depths. Measurements were taken for three different situations: (1) no safety grate at the inlet or outlet; (2) a safety grate at the inlet only; and (3) safety grates at both the inlet and the outlet. A range of discharges were considered. This testing procedure enabled a direct comparison of the effect of safety grates on the entrance headloss coefficient.

For the pipe culvert tests, free outfall and tailwater test trials were performed for only two situations: (1) no safety grate treatment of inlet or outlet; and (2) safety grate installation on both inlet and outlet.

### Free Outfall Tests

Free outfall conditions occur when the tail water depth is less than the critical depth at the outlet. The general procedure to take free outfall test measurements was as follows:

1. The discharge was determined from the weir reading once the flow was stabilized (generally, a period of 10 minutes).
2. The headwater depth was measured with the two Lory Point gages in the approach channel.

(a) Pipe Safety Grates Installed

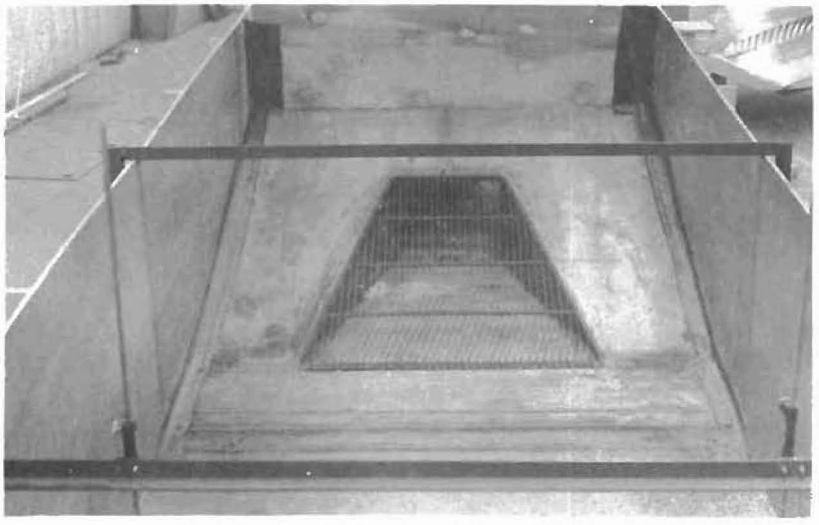

(b) Bar Safety Grates Installed

Figure 2.15 Safety Grates

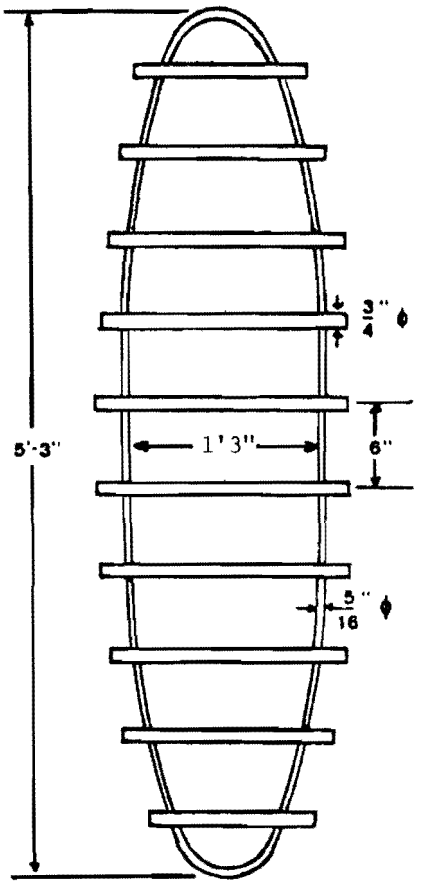


Scale: 1"= 1'

Figure 2.16 Pipe Model Safety Grate

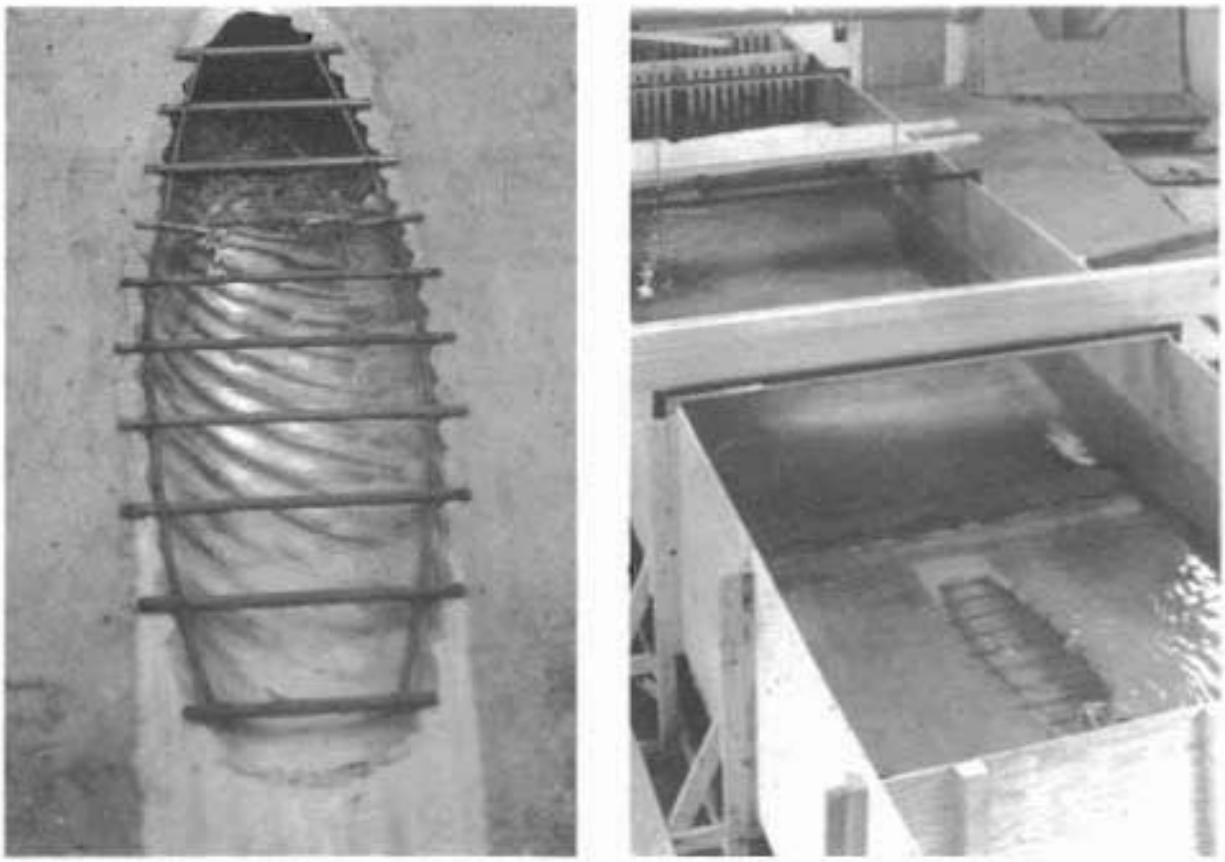

Figure 2.17 Pipe Grates At Inlet

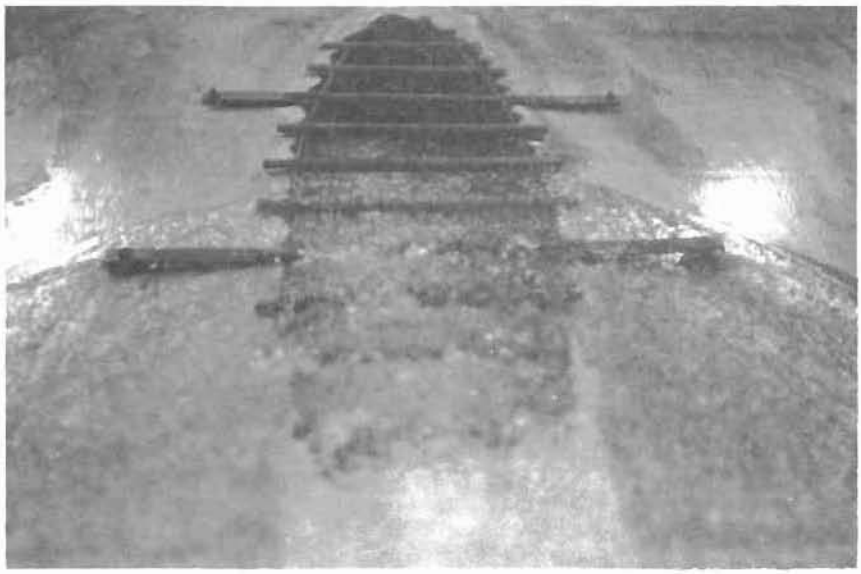

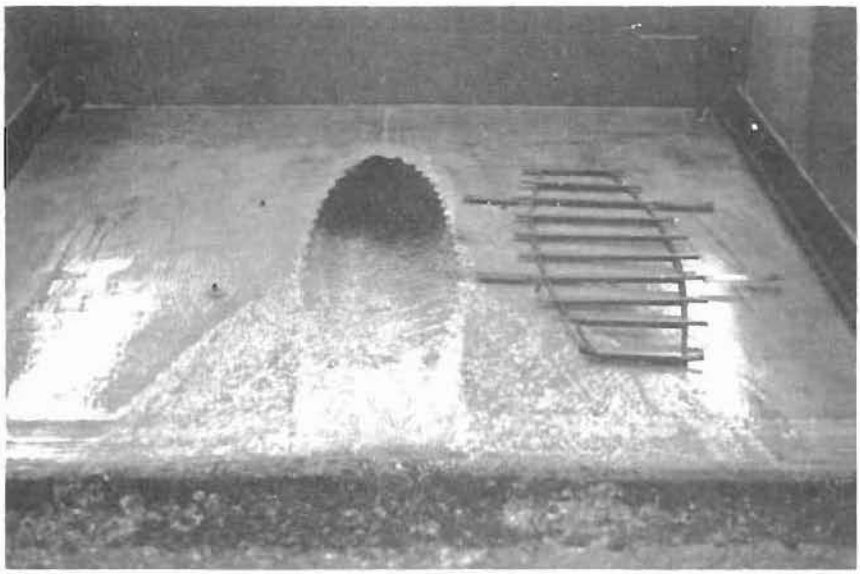

Figure 2.18 Pipe Grates At Outlet

3. The hydraulic grade line in the culvert was measured.

4. Steps 2 and 3 were repeated.
   (a) No grates in place.
   (b) Grate at the inlet only. (Box culvert only)
   (c) Grates at both the inlet and outlet.

5. Steps 1, 2, 3 and 4 were repeated for different discharges.

Tailwater Test

The general procedure for taking measurements for the tailwater tests (when tailwater is greater than critical depth at the outlet) were as follows:

1. A constant flow rate was established in the culvert and weir readings were taken for determining the discharge.

2. A free outfall test ($TW < d_c$) was run for the constant discharge.

3. An initial tail water depth was established by lowering the discharge channel gate.

4. After the flow stabilized, the two upstream point gages, the culvert piezometers, and the discharge channel piezometer were read and the values recorded.

5. The tailwater depth was increased in increments of $\frac{TW}{D} = 0.1$ and Step 4 was repeated. The tailwater depth was limited to $\frac{TW}{D} = 1.8$.

## 2.9 Data Reduction

The experimental data from the test measurements were converted into actual values of headwater depths, tailwater depths, entrance flow depths, and entrance velocity head. The data reduction was accomplished by using computer programs developed only for this purpose.

The computer program, CULVERT, was developed by the authors. A Fortran listing of the program and a user's manual is provided in Appendix A.

CULVERT was used to reduce raw data into flow parameters and the

entrance coefficient. Routines within the program computed the following quantities:

1. headwater depth,
2. tailwater depth,
3. hydraulic and energy grade lines,
4. velocity head at the culvert entrance,
5. entrance loss coefficient, $C_e$ (based on Eq. 2.3),
6. tailwater depth divided by culvert diameter $\frac{TW}{D}$,
7. headwater depth divided by culvert diameter $\frac{HW}{D}$,
8. discharge factors $\frac{Q}{BD^{1.5}}$ for the box culvert and $\frac{Q}{D^{2.5}}$ for the pipe culvert.
9. culvert slope.

Headwater Depth Determination

The headwater depth was measured by two Lory point gages 10-ft upstream from the culvert entrance. The gages were placed far enough upstream to minimize effects of the entrance turbulence but close enough to the entrance to keep frictional losses at a minimum. The difference in elevation between the culvert entrance invert and the pointer tip at the zero mark was added to the Lory gage readings to determine the headwater depth.

Hydraulic Head and Velocity Head at Entrance

The determination of the hydraulic head and velocity head at the entrance involves several steps:

a. The piezometer readings (or the stagnation tube readings for the pipe) were converted into elevations above the inlet invert. The conversion is the difference in elevation between the inlet invert and the manometer zero point. A linear extrapolation of the converted instrument readings gives the approximate hydraulic grade line, from which the hydraulic head at the

entrance is obtained.

b. The velocity head (using average velocities) at each piezometer (stagnation tube) location was added to the hydraulic head to obtain the energy head. The velocities were determined by dividing the discharge by the corresponding flow area at each piezometer location. The approximate energy grade line was determined by linear extrapolation of the energy head values at each instrument location.

c. The velocity head ($V^2/2g$) at the entrance is obtained by subtracting the value at this location of the hydraulic grade line from the value of the energy grade line.

Tailwater Depth Determination

The tailwater depth was measured by a piezometer located in the middle of the outlet channel. An open air manometer was used to determine the hydrostatic pressure measured by the piezometer. To calibrate the piezometer to measure tailwater depth, the difference in elevation between the culvert outlet invert and the zero mark on the manometer was added to the manometer readings.

## 2.10 Summary of Box Culvert Tests

### 2.10.1 Safety Grate Tests

The tests were designed to provide adequate data for evaluating the hydraulic effects, of pipe or bar safety grates, for both entrance and outlet control, so as to include the six basic flow regimes of culvert flow. A summary of the tests are given in Table 2.1. The box culvert was tested for each of five slopes, ranging from 0.008 to 0.0128. A series of flowrates were run, either with no safety grates in place or with pipe safety grates on both upstream and downstream ends. The tailwater depth was increased for four specified values of flowrate, at each of three slopes. The tailwater gate was lowered such that the value of $\frac{TW}{D}$ was increased, in increments of approximately 0.1, for each flowrate up to 1.8. The bar safety grates were similiarly tested for three slopes.

Table 2.1 Summary of Box Culvert Tests

| | Tests for $TW < d_c$ | | Tailwater Tests. $TW > d_c$ | | |
|---|---|---|---|---|---|
| Slopes | Grates Tested | Range of Discharges. (cfs) | Grates Tested | Range of Discharges | $\frac{TW}{D}$ |
| 0.0008 | No Grates<br>Pipe<br>Bar | 3.3 to 11.7 cfs<br>in 0.8 increments | No Grates<br>Pipe<br>Bar | 6.14, 8.12, 10.4, 11.8<br>same as for no grates<br>4.0, 6.5, 8.1, 11.0 | 0.4 to 1.8<br>increments of 0.1 |
| 0.0013 | No Grates<br>Pipe | 5.0 to 11.7 cfs<br>in 0.7 increments | None | | |
| 0.0063 | No Grates<br>Pipe<br>Bar | 3.0 to 11.7 cfs<br>in 0.8 increments | No Grates<br>Pipe<br>Bar | 6.14, 8.12, 9.66, 11.8 | 0.5 to 1.8<br>increments of 0.1 |
| 0.0108 | No Grates<br>Pipe<br>Bar | 3.0 to 11.7 cfs<br>in 0.8 increments | No Grates<br>Pipe<br>Bar | 6.14, 8.12, 9.66, 11.8 | 0.4 to 1.8<br>increments of 0.1 |
| 0.0128 | No Grates<br>Pipe | 3.0 to 11.7 cfs<br>in 0.8 increments | None | | |

### 2.10.2 Clogging Tests

Clogging tests were performed in order to evaluate the hydraulic effects of various degrees of debris blockage as could be caused by the safety grates. The pipe grates were tested using 3 slopes and 4 discharge for each slope. The bar grates were tested at one slope using 5 different discharges. In each case, the percentage of the entrance that was blocked, was increased from bottom to top in increments of 15% of the total available from 0 to 90 percent blockage. The tests were then repeated, beginning at the top of the entrance and increasing toward the bottom, until 90% blockage was achieved. A summary of the tests are given in Table 2.2.

## 2.11 Summary of Pipe Culvert Tests

The tests as summarized in Table 2.3, were designed to provide adequate data for evaluating the hydraulic effects of pipe grates on culvert flow, for both entrance and outlet control, so as to include the six basic flow regimes. For each of three slopes (0.0007, 0.008, and 0.05), a series of flowrates, in increments of approximately 0.3 cfs were run. Tailwater tests were made for $S_o$ = 0.0007 and $S_o$ = 0.008, at flowrates of 3.5, 4.5 and 5.5 cfs, and a range of $\frac{TW}{D}$ up to 1.9 in increments 0.1. All tests were performed with no safety grates and then with pipe safety grates at both upstream and downstream ends. Clogging tests were not performed on the pipe culvert.

Table 2.2 Summary of Clogging Tests for Box Culvert

| Slopes | Grates Tested | Range of Discharges. (cfs) | Percent Clogging |
|---|---|---|---|
| 0.0008 | Pipe | 9, 9.6, 10.0, 11.2 | All tests for clogging 0% to 90% in increments of 15% |
| 0.0063 | Pipe | 8.04, 9.11, 10.04, 11.17 | |
| | Bar | 8.12, 9.09, 10.1, 11.05, 11.91 | |
| 0.028 | Pipe | 9.0, 10.0 | |

Table 2.3 Summary of Pipe Culvert Tests

| | Tests for $TW < d_c$ | Tailwater Tests. $TW > d_c$ | |
|---|---|---|---|
| Slopes | Range of Discharges | $\frac{TW}{D}$ | Range of Discharges |
| 0.0007 | 2.0 to 8.0 cfs | 0.0 to 1.9 | 3.5 |
| 0.008 | in increments of 0.3 cfs. | in increments of 0.1 | 4.5<br>5.5 |
| 0.05 | 2.3 to 9.6 cfs<br>in increments of 0.3 cfs | No Tests | No tests |

# CHAPTER 3 BOX CULVERT RESULTS

The experimental tests using the pipe and bar safety grates for the box culvert model are presented and analyzed in this chapter. Figures are presented to compare the hydraulic effect with and without the pipe and bar safety grates under different combinations of slopes, discharges, headwater depths, and tailwater depths. For comparison, the experimental tests without safety grates are also included on selected figures. Discussion of the tests are presented describing the change in the hydraulics due to the safety grates. In addition, regression equations are presented for predicting entrance headloss coefficients for different conditions for outlet control. Also, regression equations are presented for determining headwater-discharge relationships for inlet control.

## 3.1 Entrance Headloss Coefficients With and Without Safety Grates (Mild Slopes)

The box culvert was tested under numerous possible conditions including low to high flow rates, mild to steep slopes, and free outfall to high tailwater. The effect of the pipe and bar safety grates on the entrance headloss coefficient, $C_e$, is illustrated by graphs of $C_e$ for the safety grates installed versus $C_e$ without the safety grates installed.

Figures B.1 through B.6 (Appendix B) show the entrance headloss coefficients with pipe safety grates installed versus the entrance headloss coefficients without safety grates installed. The entrance headloss coefficients with the bar safety grates installed versus the entrance headloss coefficients without safety grates installed are shown in Figures B.7 through B.9.

On Figs. B.1 through B.9, a line intersecting the origin was drawn at a 45 degree angle with the abscissa. If either the safety grates increased the entrance headloss coefficient then the corresponding data points would plot above this line. If the entrance headloss coefficient decreased with the safety grates then the data points would plot below this line.

Types 1 and 2 flow regimes had a slight increase in the entrance headloss coefficient with pipe safety grates for slopes .0008 and .0063 (Fig. B. 1 and B.3) and a slight decrease for slope .0013 (Fig. B.2). These two flow regimes had the lowest entrance headloss coefficients for outlet control conditions.

The Type 4A flow regime (Figs. B.1 through B.5) had the highest entrance headloss coefficients for both inlet and outlet control conditions. For this flow regime, the $C_e$ values with and without pipe safety grates had a large amount of variability. For Type 4A flow regime, very general conclusions are that the pipe safety grates had little or no effect on the entrance headloss coefficient for slopes .0008 and . 0063 (Figs. B.1 and B.3) and slightly decreased the $C_e$ values on slopes .0013, .0108, and .0128 (Figs. B.2, B.4, and B.5). Again it should be noted, for Type 4A flow regime, the change in the entrance headloss coefficients with the pipe safety grates were not consistent and the conclusions should be viewed judiciously.

For the Type 4B flow regime, the entrance headloss coefficients increased with the pipe safety grates for slopes .0008 and .0063 (Figs. B.1 and B.3) and decreased for the slope .0013 (Fig. B.2).

The entrance headloss coefficients with the bar safety grates were generally higher than without safety grates (Fig. B.6 through B.8). For slopes .0008 and .0108 (Fig. B.6 and B.8), the increase in $C_e$ with the bar safety grate was obvious for all flow regimes. For slope .0063 (Fig. B.7), the increase in the

entrance headloss coefficient was evident for flow regimes 2 and 4B. For flow regime 1, the $C_e$ with and without the bar safety grates were similar for slope .0063. Similar to the pipe safety grates, the Type 4A flow regime for slope .0063 (Fig. B.7) had a large variability in the entrance coefficient with and without the bar safety grates and the effect of the bar safety grates on the entrance headloss coeficient was not clearly evident.

For each slope, linear regression analyses were performed for each flow regime using collected data points. The linear regression analysis determined the coefficients for the following equation:

$$C_e(\text{with grates}) = A\ C_e(\text{without grates}) + B \qquad (3.1)$$

where A and B are the slope and y-intercept, respectively. Tables 3.1 and 3.2 are the linear regression analysis results performed for each slope and flow regime for the pipe and bar safety grates, respectively.

## 3.2 Headwater-Discharge Relationships (Inlet Control)

A unique relationship exists between the headwater and the discharge for inlet control. Inlet control should have only one headwater value for each discharge. Figures B.10 through B.17 are the relationships of $\frac{HW}{D}$ vs $\frac{Q}{BD^{1.5}}$ for inlet control. For each discharge, the headwater depth was measured with and without the safety grates. Figures B.10 through B.14 are results for the pipe safety grate tests and Fig. B.15 through B.17 are results for the bar safety grate tests.

For the pipe safety grate testing program (Fig. B.10 through B.14), the pipe safety grates had no effect on the headwater depth. Noting that the plots are for hydraulic tests with "clear" water (debris free), the test data with and without the pipe safety grates were identical. No noticeable increases in

Table 3.1 Regression Equations for Comparing $C_e$
(With and Without Pipe Safety Grates)

| | $S_o$ = .0008 | | | $S_o$ = .0013 | | | $S_o$ = .0063 | | |
|---|---|---|---|---|---|---|---|---|---|
| Flow Regime | A* | B* | R** | A | B | R | A | B | R |
| 1 | 1.348 | -.062 | .869 | 1.036 | -.022 | .832 | .983 | .140 | .993 |
| 2 | | | | 1.285 | -.066 | .992 | 2.416 | -.203 | .802 |
| 4A | 2.36 | -.981 | .423 | | | | 1.138 | -.109 | .87 |
| 4B | | | | .957 | .001 | .961 | -3.704 | -1.06 | -.115 |
| All | 1.086 | -.045 | .915 | .978 | -.025 | .952 | .961 | .0185 | .967 |

*A and B are defined in Eq. (3.1)
**Coefficient of determination of the regression equation

Table 3.2 Regression Equations for Comparing $C_e$
(With and Without Bar Safety Grates)

| | $S_o$ = .0008 | | | $S_o$ = .0063 | | | $S_o$ = .1080 | | |
|---|---|---|---|---|---|---|---|---|---|
| Flow Regime | A | B | R | A | B | R | A | B | R |
| 1 | 1.059 | .063 | .988 | .041 | .844 | .904 | | | |
| 2 | 1.351 | -.030 | .396 | .192 | .176 | .225 | | | |
| 4A | .914 | .904 | .819 | .696 | .198 | .731 | .095 | .718 | .174 |
| 4B | | | | 2.525 | -.204 | .303 | | | |
| All | 1.029 | -.065 | .981 | .834 | .103 | .859 | .972 | .065 | .935 |

headwater depth due to the pipe safety grates were indicated for either outlet control conditions (Fig. B.10 through B.12) or inlet control conditions (Fig. B.13 and B.14). Referring to Figs. B.12 and B.13, differences in headwater depths with and without safety grates were noted at the higher discharges. Not enough data was taken at these higher discharges to determine if the differences were due to the safety grates or were due to uncertainties in the measuring devices.

For the bar safety grate tests (Fig. B.15 and B.17), the headwater depth did increase with the bar safety grates. The bar safety grate test data plotted slightly above the test data without the safety grates. The increase in headwater was not constant but varied with discharge.

Headwater-discharge equations were determined by using all data points for inlet control conditions. Type 3A flow regime is inlet controlled, and the hydraulic capacity of a culvert depends upon the entrance geometry. Empirical curves which determine the culvert hydraulic performance are in the form

$$\frac{HW}{D} = a_o + a_1 \frac{Q}{BD^{1.5}} + a_2 \left(\frac{Q}{BD^{1.5}}\right)^2 + \ldots + a_n \left(\frac{Q}{BD^{1.5}}\right)^n \quad (3.2)$$

where $a_o$, $a_1$, ..., $a_n$ are the regression coefficients. The equations used $\frac{HW}{D}$ as the dependent variable and $\frac{Q}{BD^{1.5}}$ as the independent variable. The results of the regression analysis are summarized in Table 3.3. Because the pipe grates made no significant hydraulic effect, the results are presented as with and without pipe safety grates in Table 3.3a. The regression results for the bar grates are presented in Table 3.3b.

## 3.3 Entrance Headloss Coefficient - Headwater Relationship

Figures B.18 through B.25 are plots of the entrance headloss coefficients versus measured headwater depth. Each figure was for a constant slope

Table 3.3 Headwater Discharge Relationships For Inlet Control

(a) With And Without Pipe Safety Grates

| | $a_o$ | $a_1$ | $a_2$ | $a_3$ | $a_4$ | $a_5$ | R |
|---|---|---|---|---|---|---|---|
| 1 | .1395 | .3141 | | | | | .98 |
| 2 | .3624 | .1270 | .0349 | | | | .99 |
| 3 | -.0587 | .6814 | -.1897 | .0281 | | | .99 |
| 4 | -.0934 | .7534 | -.2349 | .4000 | -.0011 | | .99 |
| 5 | 1.8880 | -3.7450 | 3.6310 | -1.5390 | .3071 | -.0231 | .99 |

(b) Bar Safety Grates

| | $a_o$ | $a_1$ | $a_2$ | $a_3$ | $a_4$ | $a_5$ | R |
|---|---|---|---|---|---|---|---|
| 1 | .1190 | .3291 | | | | | .98 |
| 2 | .3827 | .1090 | .0403 | | | | .99 |
| 3 | .0433 | .5655 | -.1450 | .0231 | | | .99 |
| 4 | -.5938 | 1.7280 | -.8811 | .2170 | -.0181 | | .99 |
| 5. | 1.3236 | -2.661 | 2.9070 | -1.3330 | .2843 | -.0226 | .99 |

where the discharge and tailwater were varied. The corresponding flow regime was identified for each data point. The pipe safety grate tests are shown in Figs. B.18 through B.25 and the bar safety grates are shown in Figs. B. 23 and B. 25.

For outlet control conditions (Figs. B. 18 through B.20) and Type 4A flow regime (Figs. B.21 through B.22), the pipe safety grate tests data points are approximately grouped together according to the appropriate flow regime. The lowest average entrance headloss coefficients were measured for the Type 1 flow regime. Type 4A flow regime had the highest average entrance headloss coefficients. As a general trend, the entrance headloss coefficient increased with an increase in headwater. The $C_e$ values did appear to reach a limit at HW/D greater than 1.5.

For the inlet control conditions (Figs. B.21 and B.22), the entrance headloss coefficients also increased with an increase in the headwater depth. The increase in the $C_e$ value was very obvious for Type 3B flow regime for a slope .0108 (Fig. B.21). The maximum entrance headloss coefficient occurred at HW/D greater than 1.5.

Similarly, the bar safety grates data tended to group together according to flow regime (Figs. B.23 through B.25). For outlet control, the lowest and highest average entrance coefficients were for Types 1 and 4A flow regimes, respectively. For inlet control, Type 3A flow regime had the lowest average entrance coefficients. The entrance headloss coefficient had an obvious increase with an increase in headwater for slopes .0008 and .0063 (Fig B. 23 and B.24). The $C_e$ values reached a maximum at HW/D greater than 1.5.

No direct evidence as to the effect of either pipe or bar safety grates can be inferred from the entrance headloss coefficient versus headwater relationships (Figs. B.18 through B.25). The changes in the entrance headloss

coefficient were not necessarily caused only by the pipe or bar safety grates. The entrance headloss coefficient actually depended upon the headwater which was in turn affected by the discharge, slope, tailwater, etc.

3.4 Entrance Headloss Coefficient - Discharge Relationship

Figures B.26 through B.24 are plots of entrance headloss coefficient versus the discharge factor $(\frac{Q}{BD^{1.5}})$. Each data point was identified as to the corresponding flow regime. For each plot, the slope remained constant while the discharge and tailwater were varied. Figures B.26 through B.30 are for the pipe safety grates. Figures B.31 through B.34 are for the bar safety grates. For Figs. B.26 through B.28, and B.30 through B.32, designated discharges were held constant and the tailwater depth was varied. The different $C_e$ values for the same discharge resulted from changes in tailwater depth.

For the pipe safety grates (Figs. B.26 through B.30), the lower entrance headloss coefficients were for Type 1 and 3A flow regimes and the higher $C_e$ values were generally for Type 4A flow regime. From the figures, the entrance headloss coefficients varied with discharge and different flow regimes. Types 1 and 3A flow regimes had the lowest variability of entrance headloss coefficients with discharge.

For the bar safety grates (Fig. B.26 through B.30), the lower entrance headloss coefficients were for Types 1 and 3A flow regimes and the higher $C_e$ values were generally for Type 4A flow regime. From the figures,the entrance headloss coefficients varied with discharge and different flow regimes. Type 1 and 3A flow regime had the lowest variability of entrance headloss coefficients with discharge.

For the bar safety grates (Figs. B.31 through B.33), the entrance headloss coefficients also varied with discharge and flow regime. Types 1 and

3A flow regimes had the lowest $C_e$ values and the smallest range in values. Again, Type 4A flow regime had the largest entrance headloss coefficients.

## 3.5 Headwater - Tailwater Relationships

For the tailwater tests, the tailwater was increased from free outfall conditions to full flow. The measured headwater versus the measured tailwater for pipe, bar, and no safety grates are shown in Figs. B.37 through B.48. On each plot, the calculated discharges were identified for the tested slopes. For Figs. B.36, B.39 through 41, and B.45 through 48, the measured data for the pipe, bar, and no safety grates were presented on the same plots. For these plots, using the same discharge, the headwaters with the pipe and bar safety grates were compared to the headwater without safety grates.

The plots of headwater versus tailwater have two distinct parts. In the first part, the headwater was not affected by the tailwater and the data points plotted horizontal. In the second part, the headwater increased with an increase in tailwater depth. For outlet control conditions, the tailwater did not affect the headwater until the tailwater depth was greater than critical depth. For inlet control conditions, the tailwater was greater than the slope times the length plus the critical depth when the tailwater affected the headwater.

For slopes of .0063 and .0108, seven different tests were run using four different discharges (Fig. B.38 through B.49). As evident, the data points from the pipe safety grates tests were approximately identical with the data for no safety grates tests. The effect of the pipe safety grates was less than the accuracy at which the tests were run. The bar safety grate tests did indicate an increase in the headwater depth for the lower tailwater (Figs. B.40 through B.41 and B.45 through B.48) but indicated little increase for the higher tailwater.

Large deviations in headwater depths between the pipe, bar, and no safety grate tests were noted for a slope of .0063 and a discharge of 11.81 cfs in Fig. B.42.

## 3.6 Regression Equations Considering Flow Regimes

### 3.6.1 Development of Regression Equations

Present engineering practice normally has a single entrance headloss coefficient for each culvert entrance design. However, based upon this experimental study, the entrance headloss coefficient varies with different flow conditions. Using a constant $C_e$ value, the culvert could be under-designed for a given flow regime. To aid in the design of culverts with and without safety grates, several regression equations were determined which can be used to predict the entrance headloss coefficient based on (combinations of) design discharge, headwater, tailwater and/or slope. In this study, equations were derived for each of the four flow regimes under outlet control.

The regression equations for outlet control can be expressed in the general form

$$Y = B_o + B_1 x_1 + B_2 x_2 + \ldots + B_n X_n \qquad (3.3)$$

where Y is the dependent variable to be estimated, $X_{1,\ 2,\ \ldots n}$ are the independent variables, and $B_o$, $B_1$, $\ldots B_n$ are the regression coefficients. For this study, the dependent variable was the entrance headloss coefficient, $C_e$.

### 3.6.2 Regression Equations for $C_e$

The different equations used for the theoretical models and the general models are listed in Table C.1. Equations 1 through 7 in Table C.1 are theoretical regression models, and Eqs. 8 through 19 are the general models. The regression results (best fit models) for the pipe grates, no grates and bar grates are listed in Tables 3.4, 3.5, and 3.6, respectively. The equations are presented

Table 3.4 Regression Coefficients (Pipe Safety Grates)

| Regime | Equation | $B_o$ | $B_1$ | $B_2$ | $B_3$ | $B_4$ | R |
|---|---|---|---|---|---|---|---|
| 1 | 13 | .203 | 2.258 | -.651 | -.084 | 34.185 | .918 |
| 2 | 8 | .387 | 1.450 | -.321 | | | .944 |
| 3A | 6 | .205 | -.472 | | | | .655 |
| 4A | 9 | .365 | .688 | -.036 | -.498 | | .591 |
| 4B | 11 | -.610 | 2.321 | -.479 | -105.65 | | .945 |

Table 3.5 Regression Coefficients (No Grates)

| Regime | Equation | $B_o$ | $B_1$ | $B_2$ | $B_3$ | $B_4$ | R |
|---|---|---|---|---|---|---|---|
| 1 | 13 | .210 | 2.956 | -.842 | -.112 | 42.682 | .884 |
| 2 | 8 | -.333 | 1.367 | -.309 | | | .958 |
| 3A | 1 | .344 | -2.823 | 1.154 | | | .586 |
| 4A | 9 | .003 | .525 | .014 | -.153 | | .653 |
| 4B | 11 | -.354 | -1.664 | .827 | -41.657 | | .779 |

Table 3.6 Regression Coefficients (Bar Safety Grates)

| Regime | Equation | $B_0$ | $B_1$ | $B_2$ | $B_3$ | $B_4$ | R |
|---|---|---|---|---|---|---|---|
| 1 | 13 | -.091 | 1.581 | -.196 | -.108 | 16.073 | .919 |
| 2 | 8 | -.269 | 1.782 | -.4702 | | | .941 |
| 3A | 6* | .543 | -.608 | | | | .818 |
| 4A | 2 | .747 | 5.091 | -3.648 | -3.081 | | .700 |
| 4B | 13 | -8.193 | -.689 | 4.210 | -.421 | -12.012 | .980 |

* $(C_e)^{1/2}$

in Tables 3.7 through 3.9. The information presented on the best fit models includes the appropriate regime, the model equation, the regression coefficients, and the coefficient of determination. A complete listing of each regression equation analyzed is presented in Appendix C.

Equations 13 and 8 (Table C.1) were the best fit equations for Type 1 and 2 flow regimes, respectively. For the pipe safety grates, and no safety grates, the best regression equations for flow regimes 4A and 4B are Eqs. 9 and 11, respectively (Table C.1). For the bar safety grates, Eq. 2 (Table C.1) for flow regime 4A and Eq. 13 (Table C.1) for flow regime 4B had the lowest coefficients of determination. The highest coefficients of determination were for the pipe and bar safety grate regression equations for flow regime 4B.

## 3.7 Regression Equations for Submerged Conditions

The regression equations developed for submerged inlet, unsubmerged inlet and combined submerged and unsubmerged inlet conditions, all with outlet control are developed for use in design. From the viewpoint of design considerations, regression equations should be in the simplest form with the least number of independent variables. The suggested or recommended equations may not necessarily be the best fit (largest coefficient of determination) because of the number of independent variables considered.

For submerged inlet conditions, $\frac{HW}{D} \leq 1.2$, (flow regimes 4A and 4B), regression equations were developed using the data for all slopes and discharges in these regimes. A summary of the regression equations and the results are presented in Table 3.10. One set of best fit regressions are as follows (Eq. 8, Table C.1):

No Grates

$$C_e = -0.061 + 0.519 \left(\frac{HW}{D}\right) - 0.049 \left(\frac{Q}{BD^{1.5}}\right) \qquad (3.4)$$

Table 3.7 Regression Equations for $C_e$ (No Grates)

Regime 1

$$C_e = 0.210 + 2.956 \left(\frac{HW}{D}\right)^2 - 0.842 \left(\frac{Q}{BD^{1.5}}\right) - 0.112 \left(\frac{Q}{BD^{1.5}}\right)^2 + 42.682\, S_o$$

Regime 2

$$C_e = -0.333 + 1.367 \left(\frac{HW}{D}\right) - 0.309 \left(\frac{Q}{BD^{1.5}}\right)$$

Regime 4A

$$C_e = 0.003 + 0.525 \left(\frac{HW}{D}\right) + 0.014 \left(\frac{Q}{BD^{1.5}}\right) - 0.153 \left(\frac{TW}{D}\right)$$

Regime 4B

$$C_e = -0.354 - 1.664 \left(\frac{HW}{D}\right) + 0.827 \left(\frac{Q}{BD^{1.5}}\right) - 41.657\, S_o$$

TABLE 3.8 Regression Equations for $C_e$ (Pipe Safety Grates)

Regime 1

$$C_e = 0.203 + 2.258 \left(\frac{HW}{D}\right)^2 - 0.651 \left(\frac{Q}{BD^{1.5}}\right) - 0.084 \left(\frac{Q}{BD^{1.5}}\right)^2 + 34.185\, S_o$$

Regime 2

$$C_e = -0.387 + 1.450 \left(\frac{HW}{D}\right) - 0.321 \left(\frac{Q}{BD^{1.5}}\right)$$

Regime 4A

$$C_e = 0.365 + 0.688 \left(\frac{HW}{D}\right) - 0.036 \left(\frac{Q}{BD^{1.5}}\right) - 0.498 \left(\frac{TW}{D}\right)$$

Regime 4B

$$C_e = 0.610 + 2.321 \left(\frac{HW}{D}\right) - 0.479 \left(\frac{Q}{BD^{1.5}}\right) - 105.650\, S_o$$

Table 3.9 Regression Equations for $C_e$ (Bar Safety Grates)

Regime 1

$$C_e = -0.091 + 1.581 \left(\frac{HW}{D}\right)^2 - 0.196 \left(\frac{Q}{BD^{1.5}}\right) - 0.108 \left(\frac{Q}{BD^{1.5}}\right)^2 + 16.073\, S_o$$

Regime 2

$$C_e = -0.269 + 1.782 \left(\frac{HW}{D}\right) - 0.470 \left(\frac{Q}{BD^{1.5}}\right)$$

Regime 4A

$$C_e = +0.747 + 5.091 \left(\frac{HW}{D}\right)\left(\frac{Q}{BD^{1.5}}\right)^{-2} - 3.648 \left(\frac{Q}{BD^{1.5}}\right)^{-2} - 3.081 \left(\frac{TW}{D}\right)\left(\frac{Q}{BD^{1.5}}\right)^{-2}$$

Regime 4B

$$C_e = 8.193 - 0.689 \left(\frac{HW}{D}\right)^2 + 4.210 \left(\frac{Q}{BD^{1.5}}\right) - 0.421 \left(\frac{Q}{BD^{1.5}}\right)^2 - 12.012\, S_o$$

Table 3.10 Summary of Regression Results for Submerged Condition

| Equation Number | Type Of Grates | $B_o$ | $B_1$ | $B_2$ | $B_3$ | $B_4$ | R |
|---|---|---|---|---|---|---|---|
| | No | | | | | | |
| 2 | Grates | 0.820 | -1.838 | -4.279 | 3.932 | | 0.64 |
| 8 | | -0.061 | 0.519 | -0.049 | | | 0.56 |
| 9 | | -0.055 | 0.073 | 0.072 | 0.260 | | 0.70 |
| 11 | | -0.067 | 0.519 | -0.048 | 0.759 | | 0.56 |
| 13 | | -0.163 | 0.162 | 0.292 | -0.054 | 1.755 | 0.57 |
| 16 | | 0.670 | -0.270 | 1.740 | | | 0.10 |
| 21 | | 0.421 | 0.102 | -0.348 | | | 0.65 |
| | Bar | | | | | | |
| 2 | Grates | 0.814 | -1.421 | -6.070 | 5.032 | | 0.71 |
| 8 | | -0.023 | 0.595 | -0.086 | | | 0.63 |
| 9 | | -0.064 | 0.130 | 0.032 | 0.318 | | 0.76 |
| 11 | | -0.061 | 0.600 | -0.086 | 4.900 | | 0.64 |
| 13 | | -0.118 | 0.180 | 0.258 | -0.052 | 6.28 | 0.64 |
| 16 | | 0.920 | -0.088 | 6.800 | | | 0.25 |
| 21 | | 0.616 | 0.063 | -0.433 | | | 0.67 |
| | Pipe | | | | | | |
| 2 | Grates | 0.785 | -1.379 | -2.896 | 2.779 | | 0.45 |
| 8 | | -0.023 | 0.595 | -0.086 | | | 0.38 |
| 9 | | 0.216 | -0.029 | 0.067 | 0.199 | | 0.50 |
| 11 | | 0.241 | 0.267 | -0.005 | -5.730 | | 0.40 |
| 13 | | 0.223 | 0.075 | 0.157 | -0.025 | -5.410 | 0.38 |
| 16 | | 0.660 | 0.000 | -7.530 | | | 0.14 |
| 21 | | 0.470 | .080 | -0.250 | | | 0.47 |

Pipe Safety Grates

$$C_e = 0.21 + 0.269 \left(\frac{HW}{D}\right) - 0.003 \left(\frac{Q}{BD^{1.5}}\right) \quad (3.5)$$

Bar Safety Grates

$$C_e = -0.023 + 0.595 \left(\frac{HW}{D}\right) - 0.086 \left(\frac{Q}{BD^{1.5}}\right) \quad (3.6)$$

The coefficients of determination for Eqs. 3.4, 3.5, and 3.6 are 0.56, 0.38 and 0.63, respectively. Figures 3.1, 3.2, and 3.3 are the respective graphs of Eqs. 3.4, 3.5 and 3.6.

Another set of best fit regression equations for submerged conditions are as follows (Eq. 21, Table C.1):

No Grates

$$C_e = 0.421 + 0.102 \left(\frac{Q}{BD^{1.5}}\right) - 0.348 \left(\frac{HW-TW}{D}\right) \quad (3.7)$$

Pipe Safety Grates

$$C_e = 0.474 + 0.080 \left(\frac{Q}{BD^{1.5}}\right) - 0.254 \left(\frac{HW-TW}{D}\right) \quad (3.8)$$

Bar Safety Grates

$$C_e = 0.616 + 0.063 \left(\frac{Q}{BD^{1.5}}\right) - 0.433 \left(\frac{HW-TW}{D}\right) \quad (3.9)$$

The coefficients of determination for Eqs. 3.7, 3.8, and 3.9 are 0.65, 0.47 and 0.67, respectively. Figures 3.4, 3.5 and 3.6 are the respective graphs of Eqs. 3.4, 3.5, and 3.6.

## 3.8 Regression Equations for Unsubmerged Conditions

For unsubmerged inlet conditions, $\frac{HW}{D} \leq 1.2$, (flow regimes 1 and 2) regression equations were developed using the data for all slopes and discharges

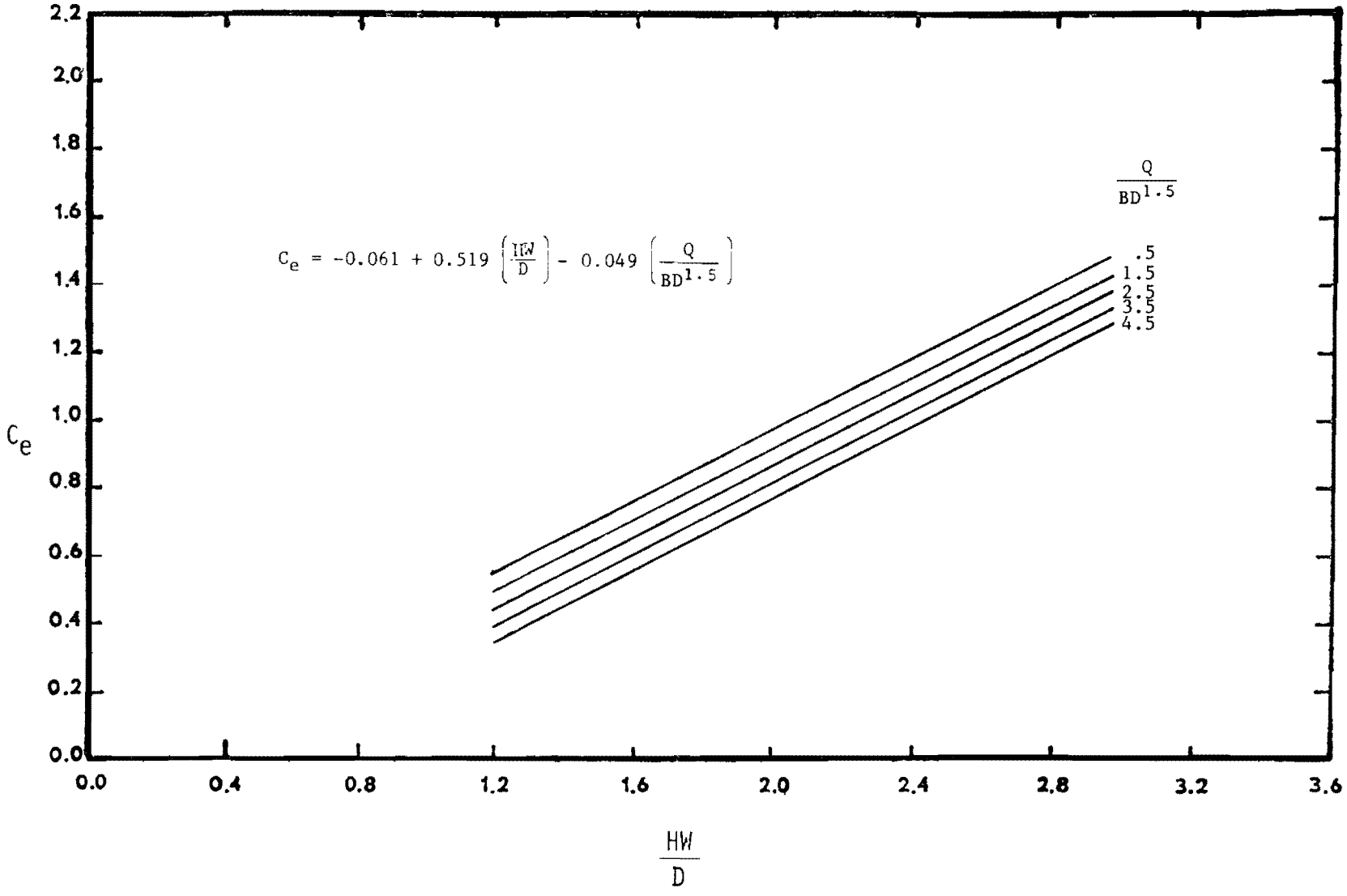


Figure 3.1 Entrance Headloss Coefficient for Submerged Conditions, No Grates (Eq. 3.4)

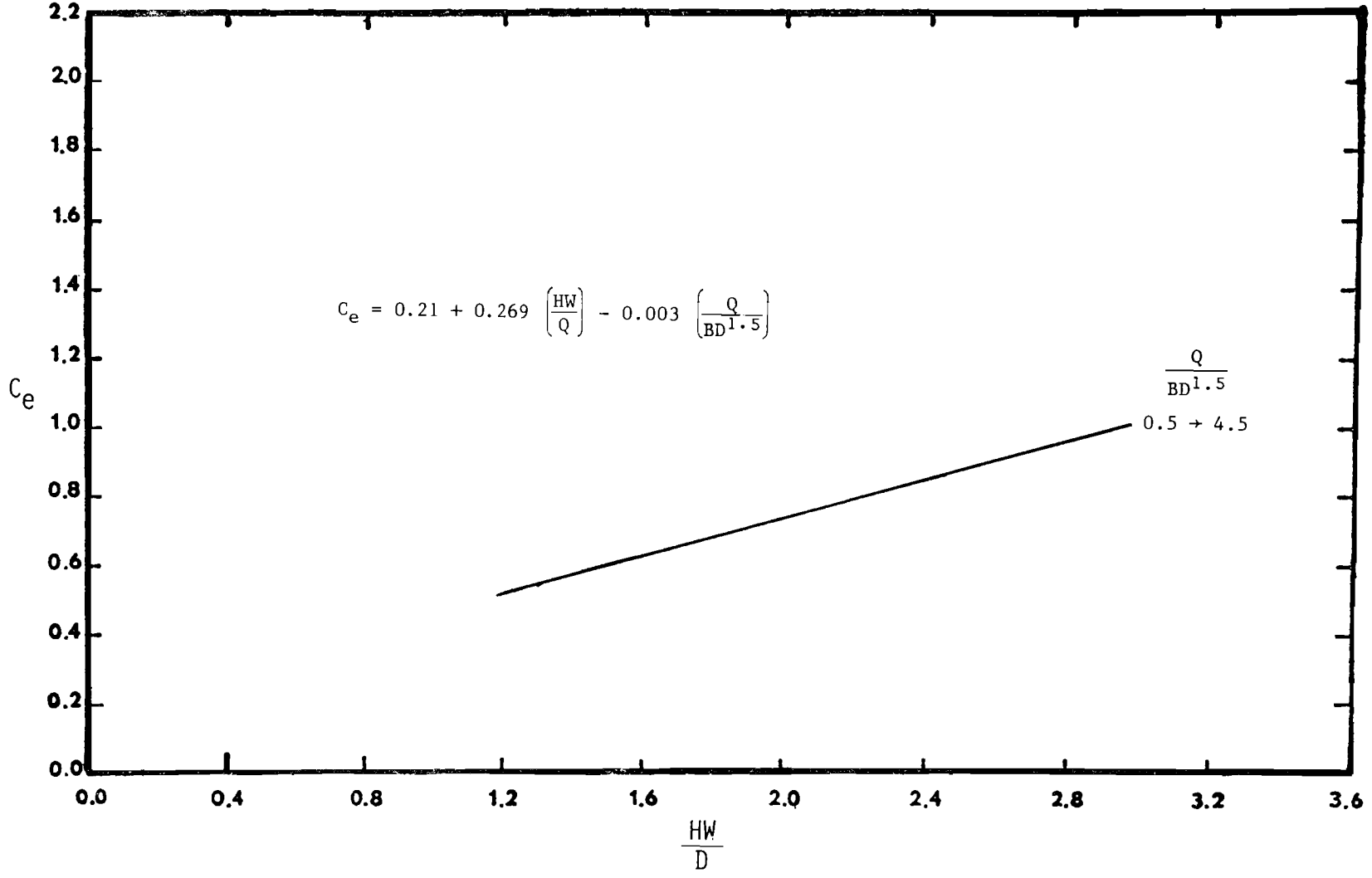


Figure 3.2 Entrance Headloss Coefficient for Submerged Conditions, Pipe Grates (Eq. 3.5 )

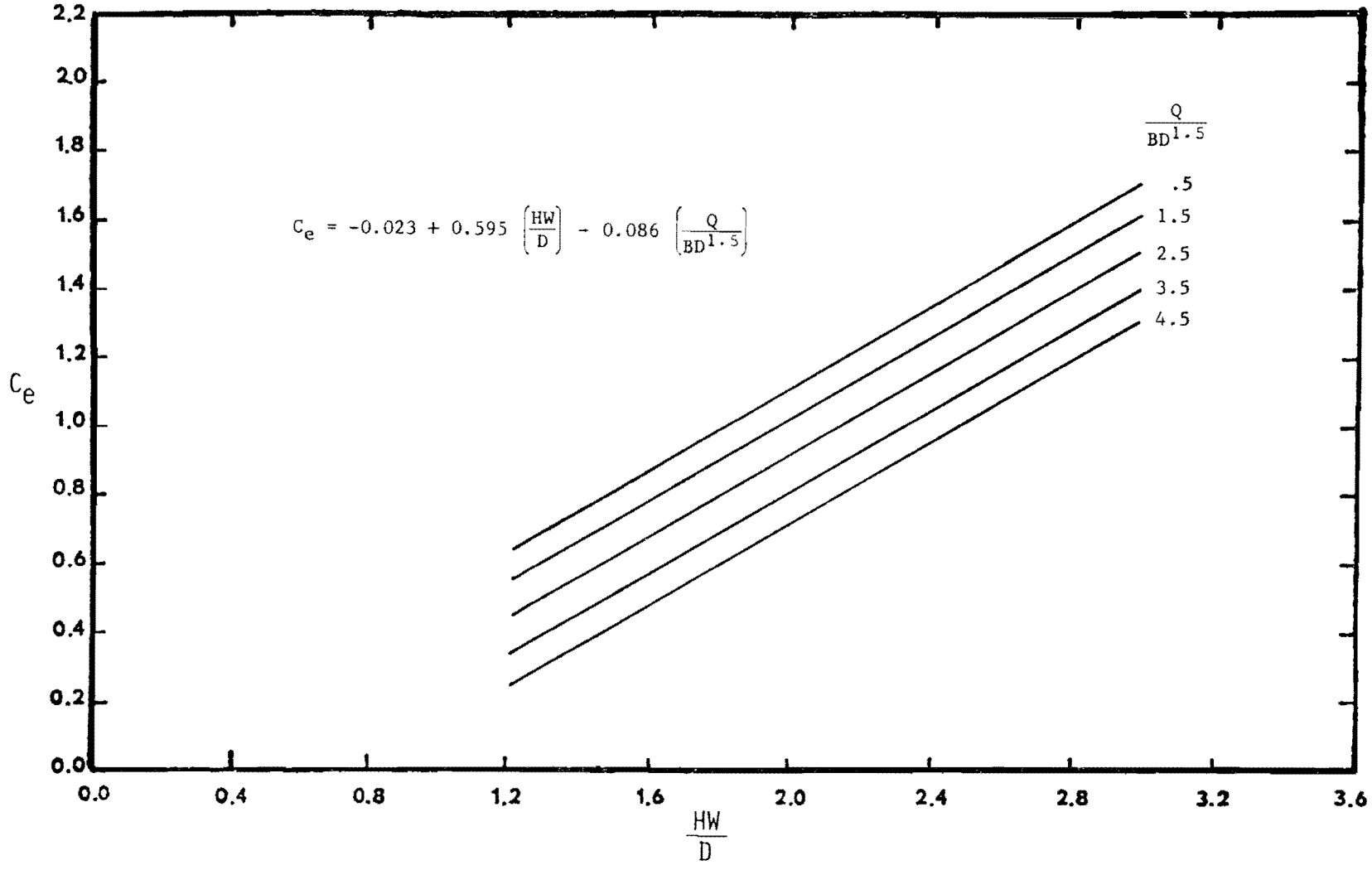


Figure 3.3 Entrance Headloss Coefficient for Submerged Conditions, Bar Grates (Eq. 3.6)

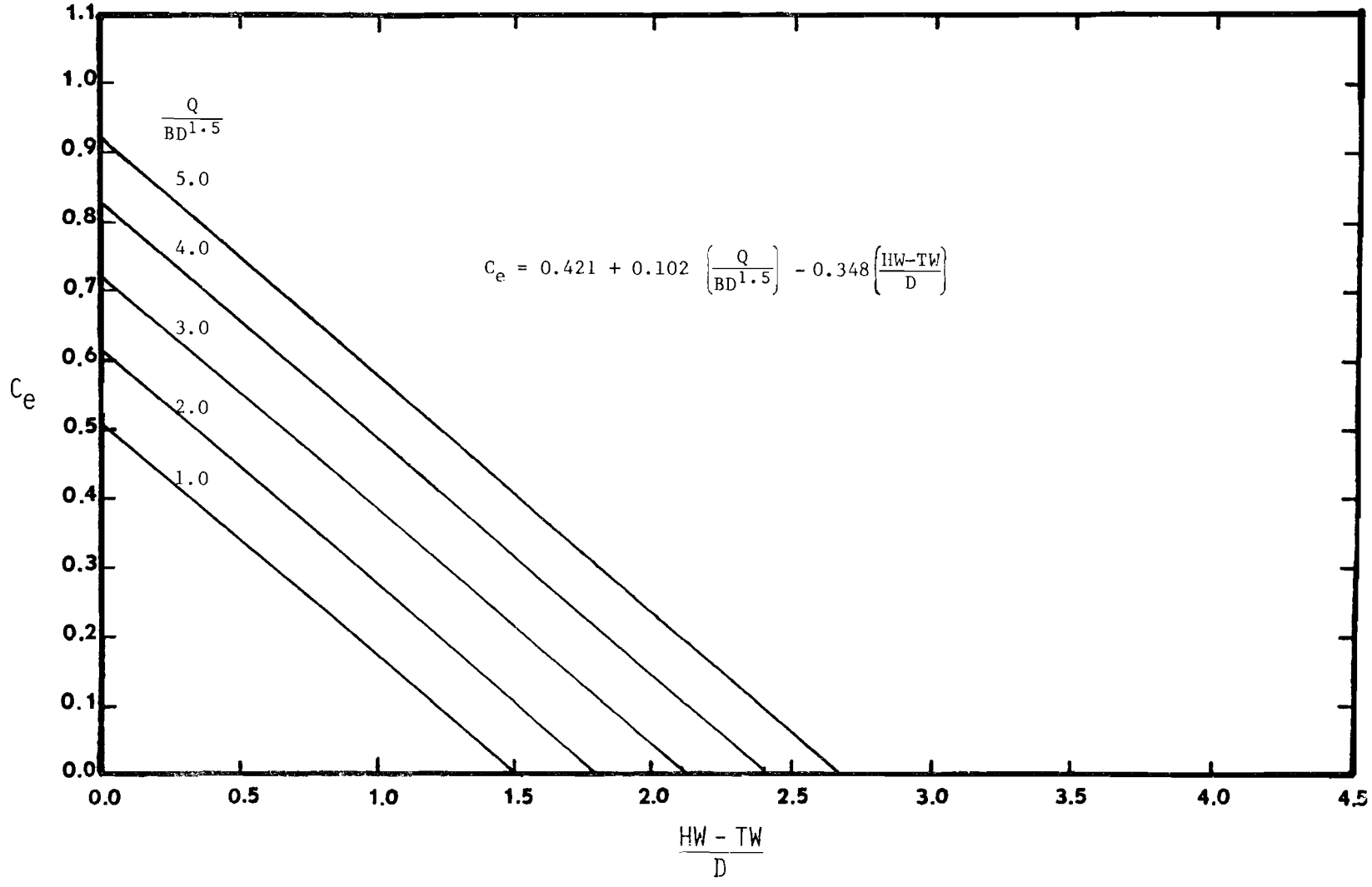


Figure 3.4 Entrance Headloss Coefficient for Submerged Conditions, No Grates (Eq. 3.7 )

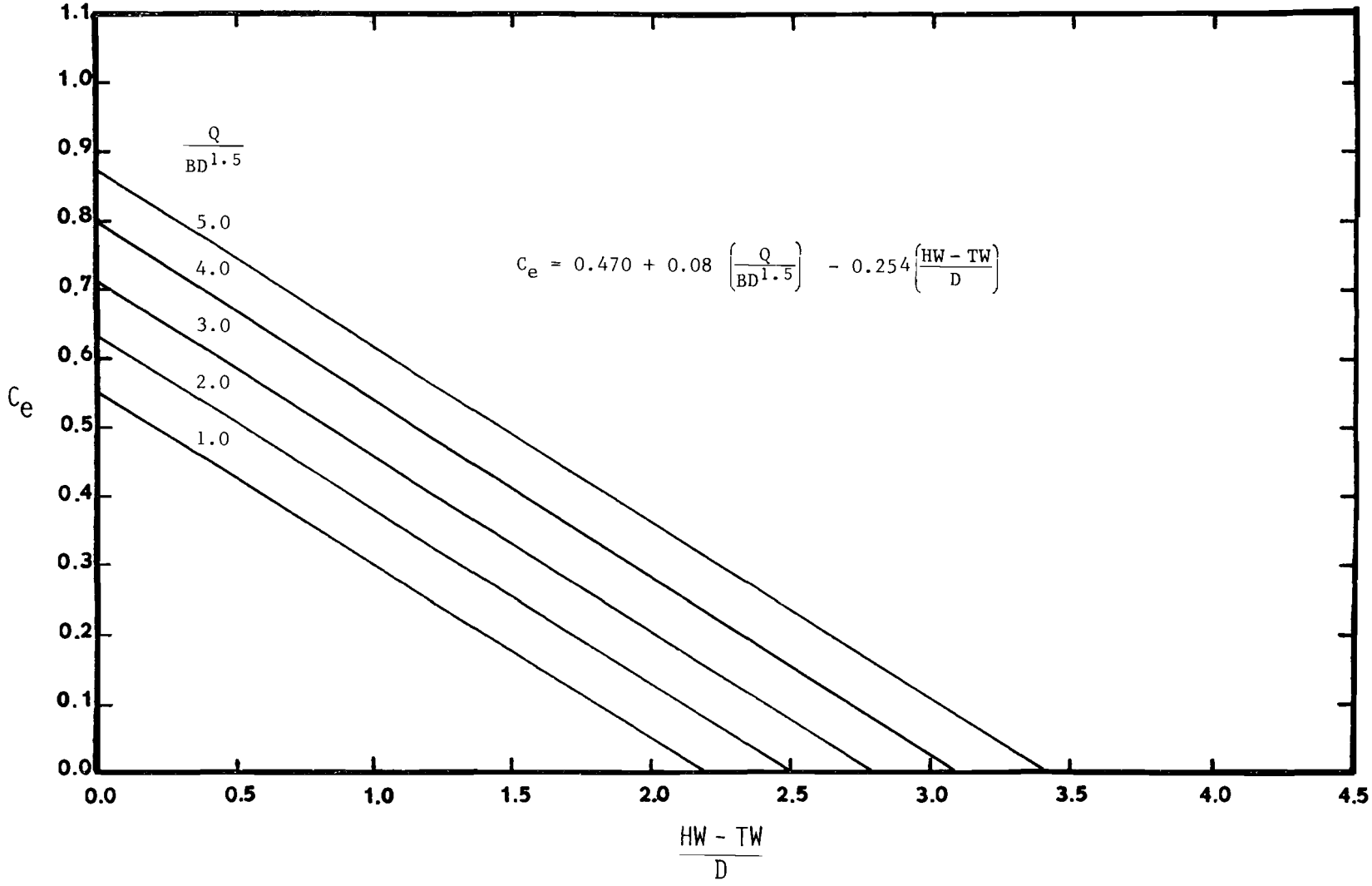


Figure 3.5 Entrance Headloss Coefficient for Submerged Conditions, Pipe Grates (Eq. 3.8)

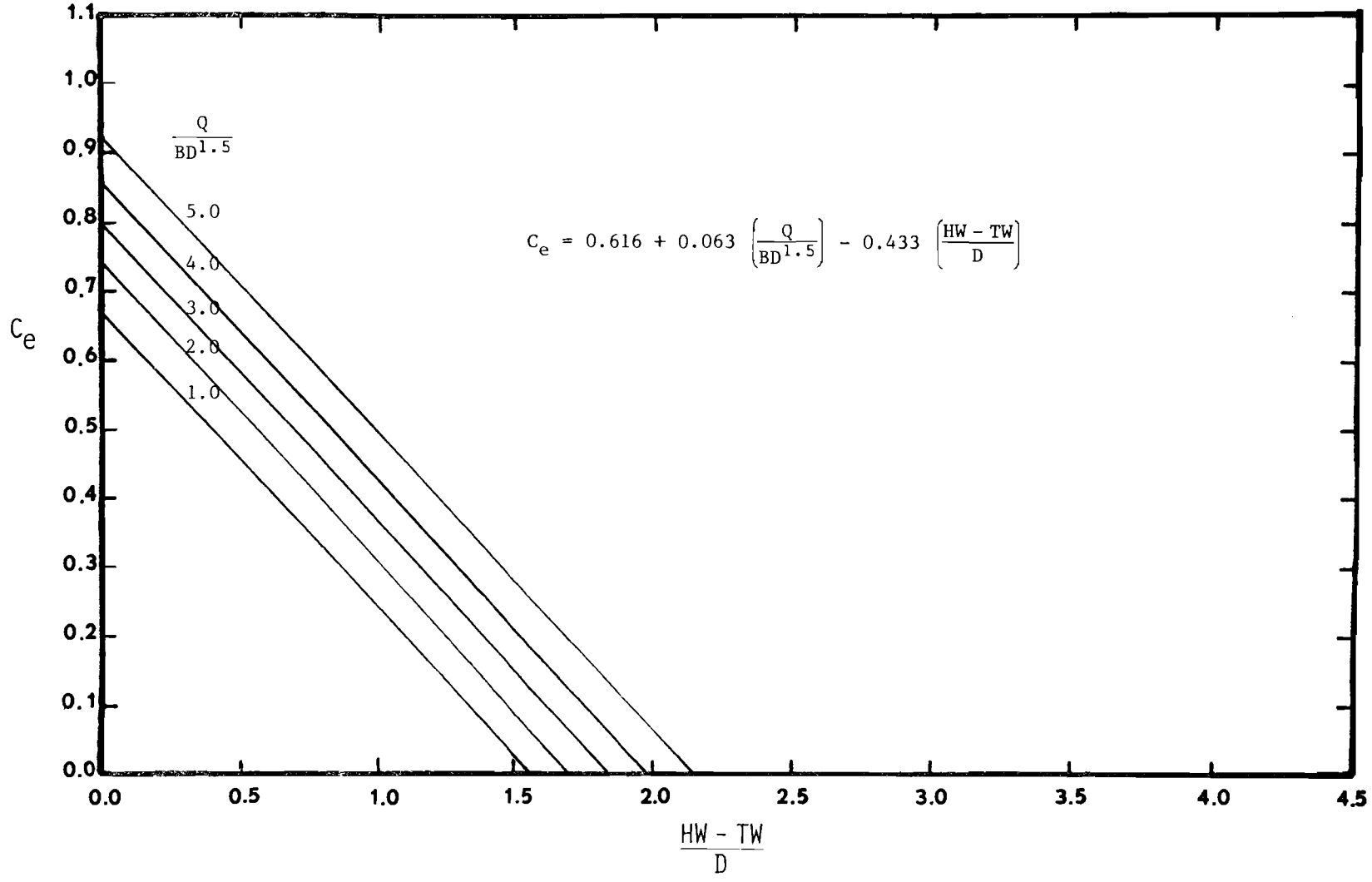


Figure 3.6 Entrance Headloss Coefficient for Submerged Conditions, Bar Grates (Eq. 3.9 )

in these regimes. A summary of the regression equations and results are presented in Table 3.11. The best fit regressions are as follows (Eq. 8, Table C.1):

No Grates

$$C_e = -0.040 + 1.000 \left(\frac{HW}{D}\right) - 0.276 \left(\frac{Q}{BD^{1.5}}\right) \quad (3.10)$$

Pipe Safety Grates

$$C_e = -0.122 + 1.046 \left(\frac{HW}{D}\right) - 0.262 \left(\frac{Q}{BD^{1.5}}\right) \quad (3.11)$$

Bar Safety Grates

$$C_e = -0.213 + 1.448 \left(\frac{HW}{D}\right) - 0.366 \left(\frac{Q}{BD^{1.5}}\right) \quad (3.12)$$

The coefficients of determination for Eqs. 3.10, 3.11, and 3.12 are 0.81, 0.79, and 0.82, respectively. Figures 3.7, 3.8, and 3.9 are the respective graphs of Eqs. 3.10, 3.11, 3.12.

## 3.9 Regression Equations for Submerged and Unsubmerged Combined

For the combined submerged and unsubmerged inlet conditions, regresssion equations were developed using the data for all slopes and discharges for the outlet control regimes. A summary of the regression equations and results are presented in Table 3.12. The best fit regressions are as follows (Eq. 8, Table C.1):

No Grates

$$C_e = -0.187 + 0.614 \left(\frac{HW}{D}\right) - 0.060 \left(\frac{Q}{BD^{1.5}}\right) \quad (3.13)$$

Pipe Safety Grates

$$C_e = -0.172 + 0.479 \left(\frac{HW}{D}\right) + 0.001 \left(\frac{Q}{BD^{1.5}}\right) \quad (3.14)$$

Table 3.11 Summary of Regression Results for Unsubmerged Conditions

| Equation Number | Type Of Grates | $B_o$ | $B_1$ | $B_2$ | $B_3$ | $B_4$ | R |
|---|---|---|---|---|---|---|---|
| | No | | | | | | |
| 2 | Grates | -0.053 | 4.070 | -2.039 | -0.152 | | 0.71 |
| 8 | | -0.040 | 1.00 | -0.276 | | | 0.81 |
| 9 | | -0.074 | 1.096 | -0.294 | -0.030 | | 0.82 |
| 11 | | 0.004 | 0.921 | -0.258 | -3.618 | | 0.82 |
| 13 | | 0.800 | 0.535 | -0.585 | 0.062 | -3.974 | 0.88 |
| 16 | | 0.400 | -0.046 | -13.00 | | | 0.53 |
| | | 0.355 | -0.045 | | | | 0.29 |
| | Bar | | | | | | |
| 2 | Grates | 0.035 | 3.881 | -2.288 | 0.090 | | 0.85 |
| 8 | | -0.213 | 1.448 | -0.366 | | | 0.82 |
| 9 | | -0.232 | 1.538 | -0.388 | -0.033 | | 0.83 |
| 11 | | -0.127 | 1.285 | -0.318 | -12.818 | | 0.85 |
| 13 | | 0.980 | 0.639 | -0.797 | 0.110 | -10.352 | 0.87 |
| 16 | | 0.470 | -0.033 | -27.00 | | | 0.55 |
| 20 | | 0.446 | -0.062 | | | | 0.24 |
| | Pipe | | | | | | |
| 2 | Grates | 0.022 | 3.933 | -2.111 | -0.092 | | 0.65 |
| 8 | | -0.122 | 1.046 | -0.262 | | | 0.79 |
| 9 | | -0.153 | 1.125 | -0.274 | -0.028 | | |
| 11 | | -0.159 | 1.12 | -0.282 | 4.554 | | 0.80 |
| 13 | | 0.464 | 0.605 | -0.377 | 0.018 | 3.95 | 0.89 |
| 16 | | 0.320 | -0.017 | -9.19 | | | 0.28 |
| 20 | | 0.300 | -0.023 | | | | 0.13 |

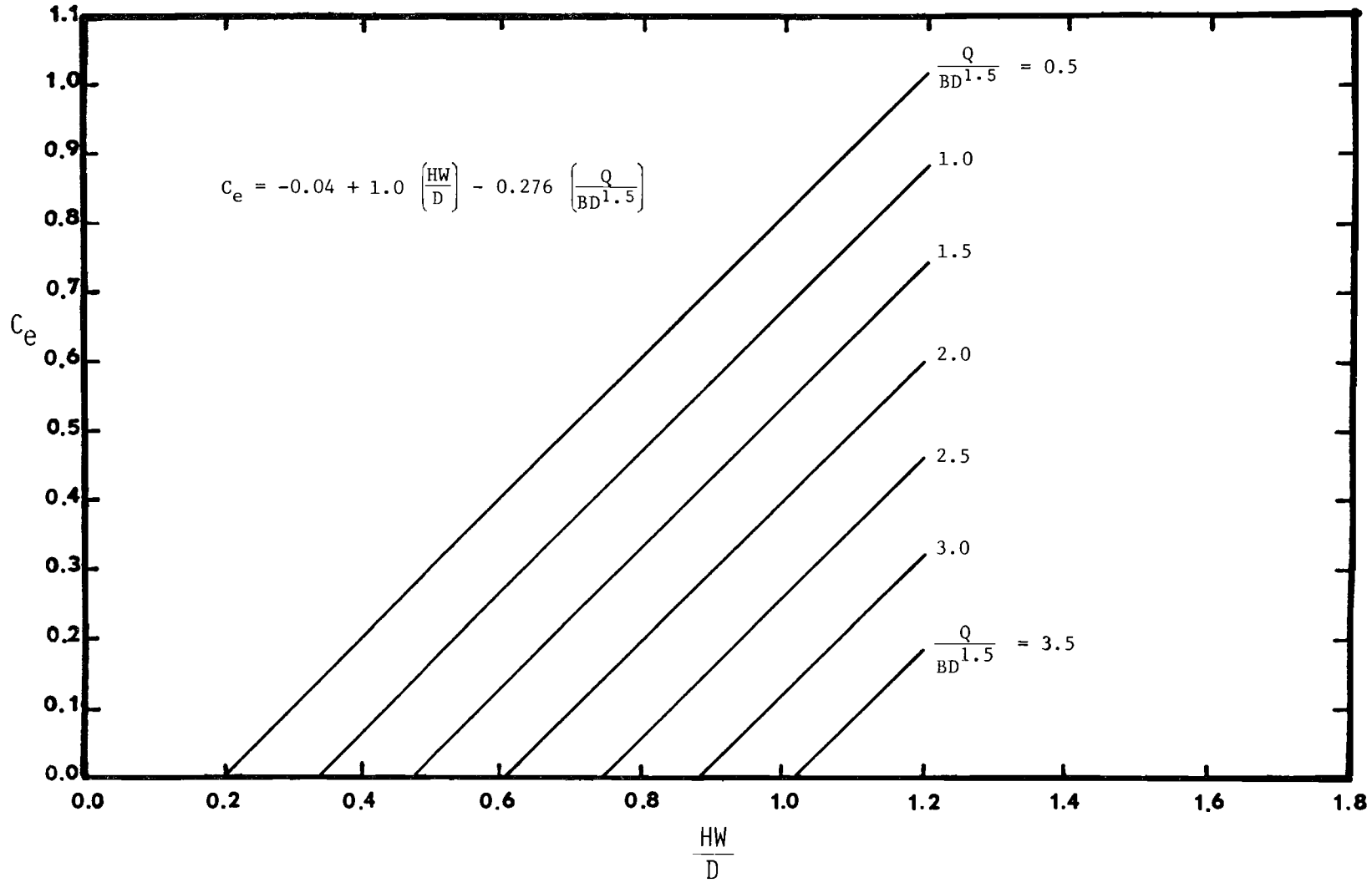


Figure 3.7 Entrance Headloss Coefficient for Unsubmerged Conditions, No Grates (Eq. 3.10)

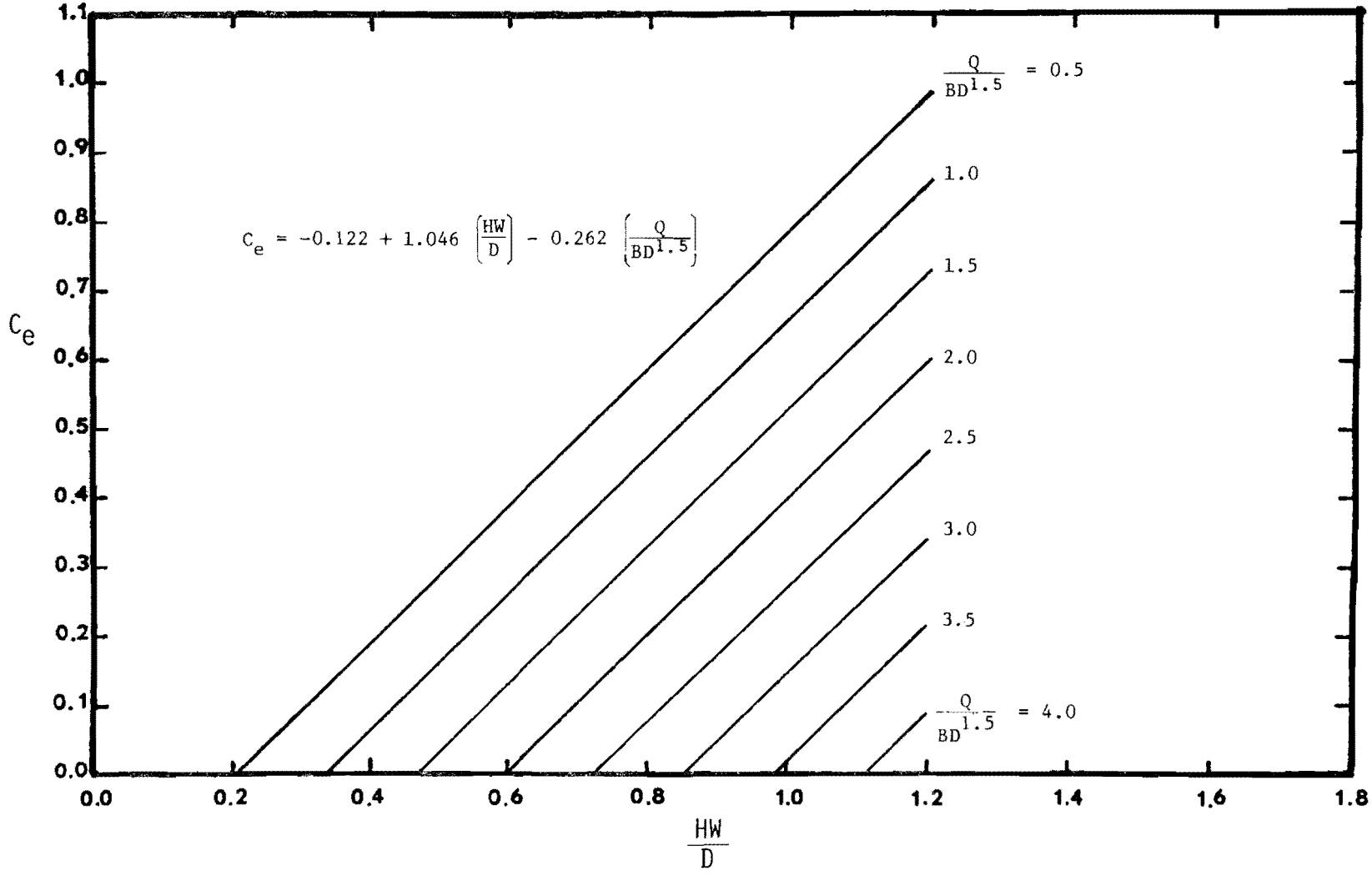


Figure 3.8 Entrance Headloss Coefficient for Unsubmerged Conditions, Pipe Grates (Eq. 3.11)

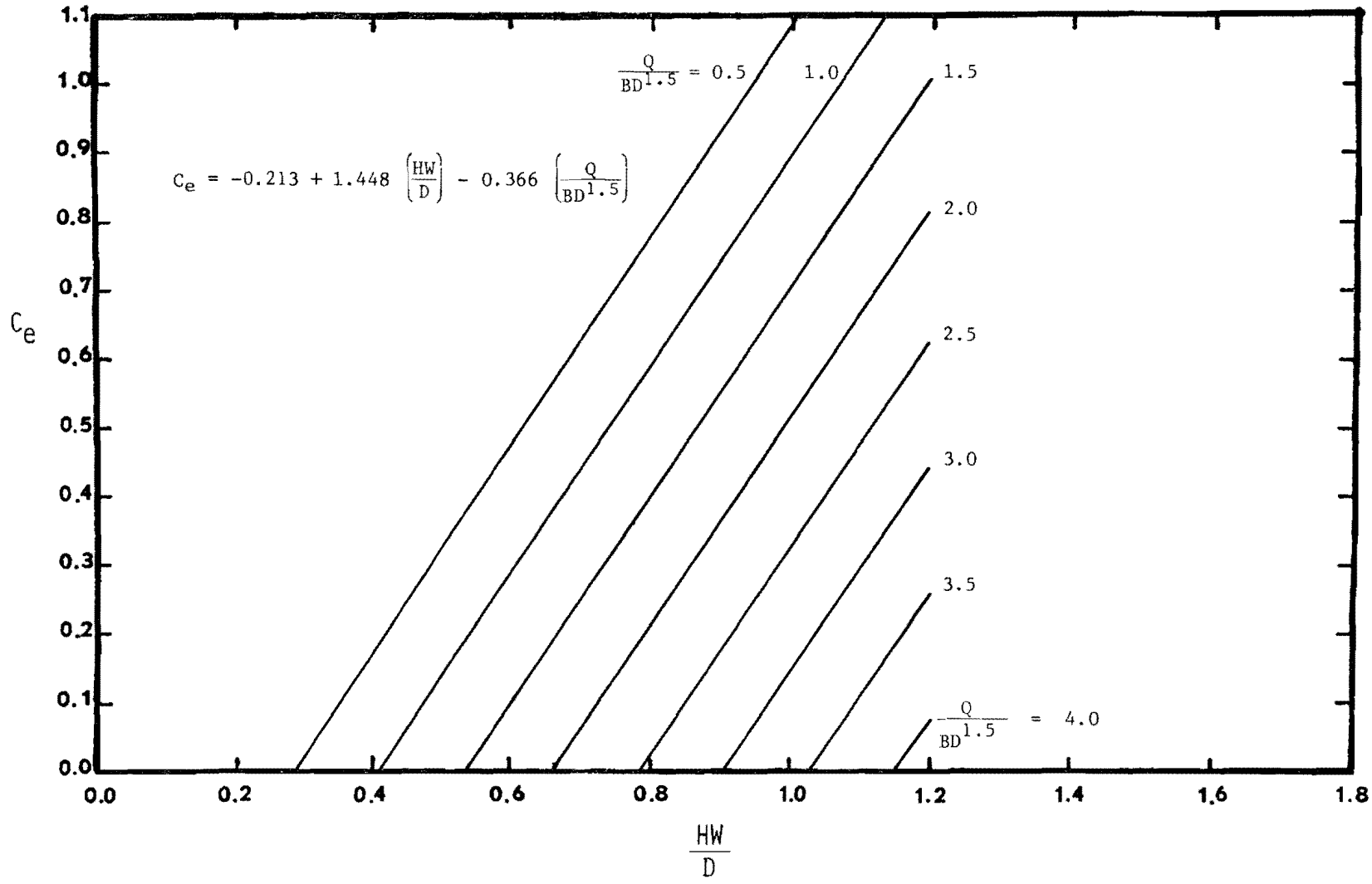


Figure 3.9 Entrance Headloss Coefficient for Unsubmerged Conditions, Bar Grates (Eq. 3.12)

Table 3.12 Summary of Regression Results for Submerged and Unsubmerged Conditions Combined

| Equation Number | Type Of Grates | $B_o$ | $B_1$ | $B_2$ | $B_3$ | $B_4$ | R |
|---|---|---|---|---|---|---|---|
| 1 | No Grates | 0.452 | 2.279 | -2.734 | | | 0.55 |
| 2 | | 0.485 | 1.365 | -2.291 | 0.524 | | 0.55 |
| 6 | | 0.417 | 0.387 | | | | 0.16 |
| 8 | | -0.187 | 0.614 | -0.060 | | | 0.76 |
| 9 | | -0.174 | 0.362 | 0.005 | 0.146 | | 0.80 |
| 11 | | -0.188 | 0.614 | -0.060 | 0.159 | | 0.76 |
| 13 | | 0.131 | 0.206 | -0.005 | -0.006 | 1.340 | 0.75 |
| 16 | | 0.211 | 0.073 | 9.200 | | | 0.26 |
| | Bar Grates | | | | | | |
| 8 | | -0.025 | 0.643 | -0.111 | | | 0.78 |
| 9 | | -0.004 | 0.301 | -0.029 | 0.211 | | 0.82 |
| 11 | | -0.024 | 0.644 | -0.110 | -0.538 | | 0.78 |
| 13 | | 0.370 | 0.216 | -0.123 | 0.008 | 2.369 | 0.77 |
| | | 0.290 | 0.070 | 7.580 | | | 0.28 |
| | Pipe Grates | | | | | | |
| 8 | | -0.172 | 0.479 | 0.001 | | | 0.73 |
| 9 | | -0.004 | 0.311 | 0.036 | 0.110 | | 0.74 |
| 11 | | -0.143 | 0.477 | 0.000 | -6.193 | | 0.74 |
| 13 | | 0.274 | 0.149 | -0.064 | 0.013 | -5.715 | 0.70 |
| 16 | | 0.230 | 0.100 | -7.900 | | | 0.36 |

Bar Safety Grates

$$C_e = -0.025 + 0.643\left(\frac{HW}{D}\right) - 0.111\left(\frac{Q}{BD^{1.5}}\right) \qquad (3.15)$$

The coefficients of determination for Eqs. 3.13, 3.14, and 3.15 are 0.76, 0.73, and 0.78, respectively. Figures 3.10, 3.11, and 3.12 are the respective graphs of Eqs. 3.13, 3.14, and 3.15.

Figures 3.10 - 3.13 present a comparison of equations of the form $C_e = f\left(\frac{HW}{D}, \frac{Q}{BD^{1.5}}\right)$ considering submerged conditions, unsubmerged conditions, and combined submerged and unsubmerged conditions. Figure 3.13 shows graphs of Eq. (3.4) for submerged conditions, Eq. (3.10) for unsubmerged conditions, and Eq. (3.13) for submerged and unsubmerged combined. Each of these curves in Figure 3.13 are for $\frac{Q}{BD^{1.5}} = 1.0$ and no grates. Similar graphs of Eqs. (3.4, 3.10, and 3.13) for $\frac{Q}{BD^{1.5}} = 3.0$ and no grates are shown in Fig. 3.14.

Figure 3.15 shows graphs of Eq. (3.6) for submerged conditions (bar grates), Eq. (3.15) for unsubmerged conditions (bar grates), and Eq. (3.15) for submerged and unsubmerged combined (bar grates). These graphs are for $\frac{Q}{BD^{1.5}} = 1.0$. The same set of graphs for $\frac{Q}{BD^{1.5}} = 3.0$ are presented in Fig. 3.16.

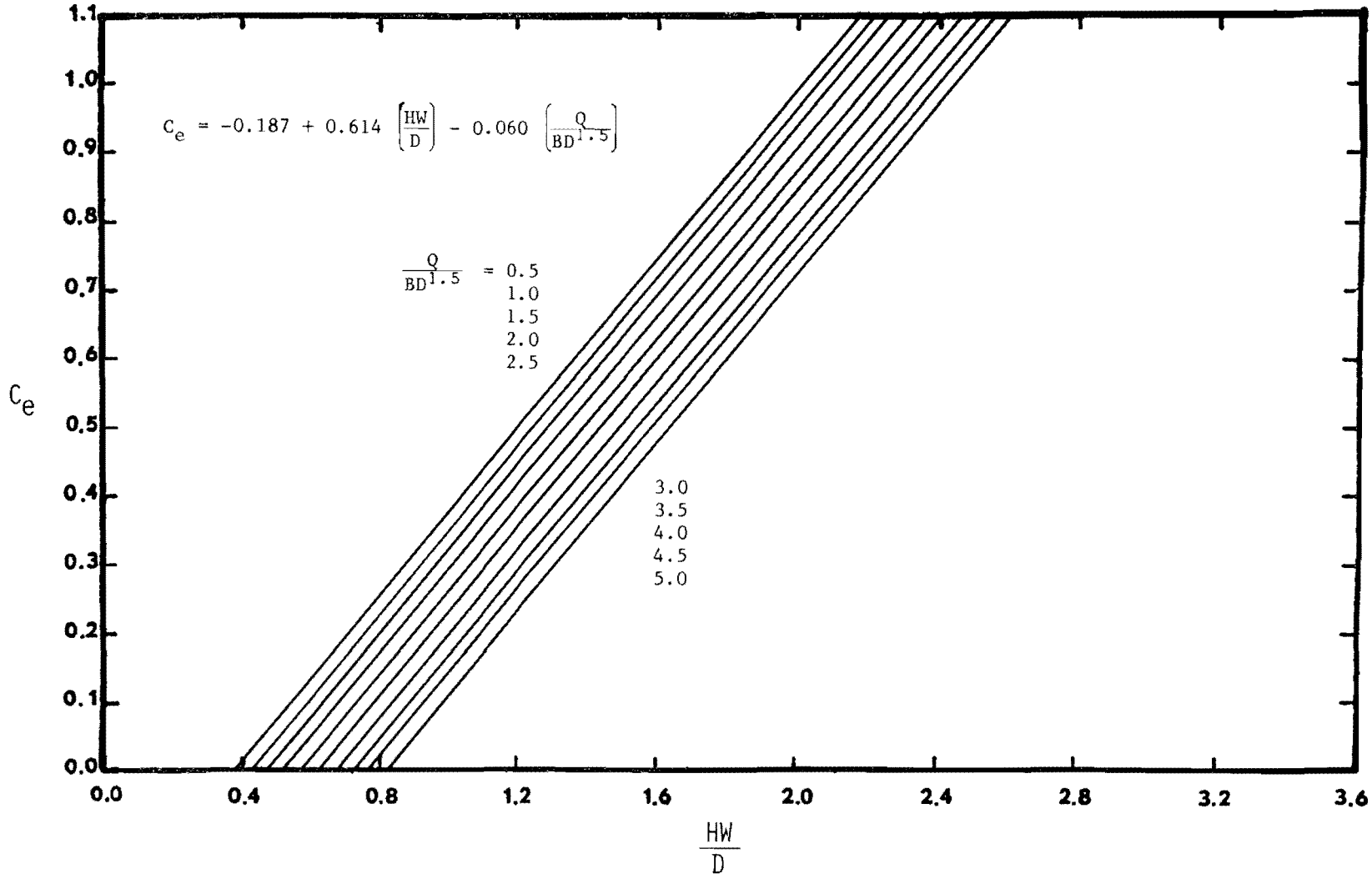


Figure 3.10 Entrance Headloss Coefficient for Submerged and Unsubmerged Conditions Combined, No Grates (Eq. 3.13)

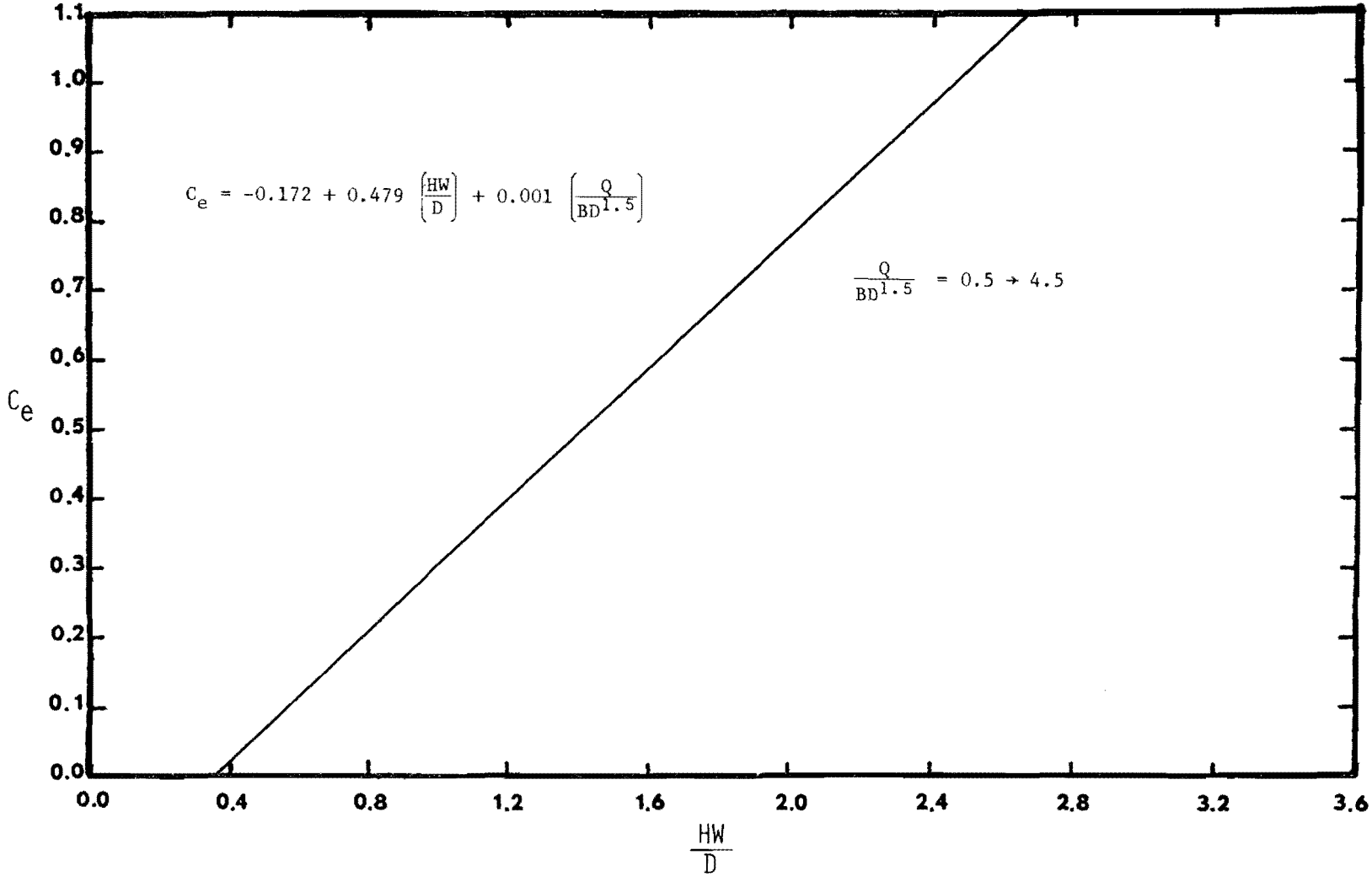


Figure 3.11 Entrance Headloss Coefficient for Submerged and Unsubmerged Conditions Combined, Pipe Grates (Eq. 3.14)

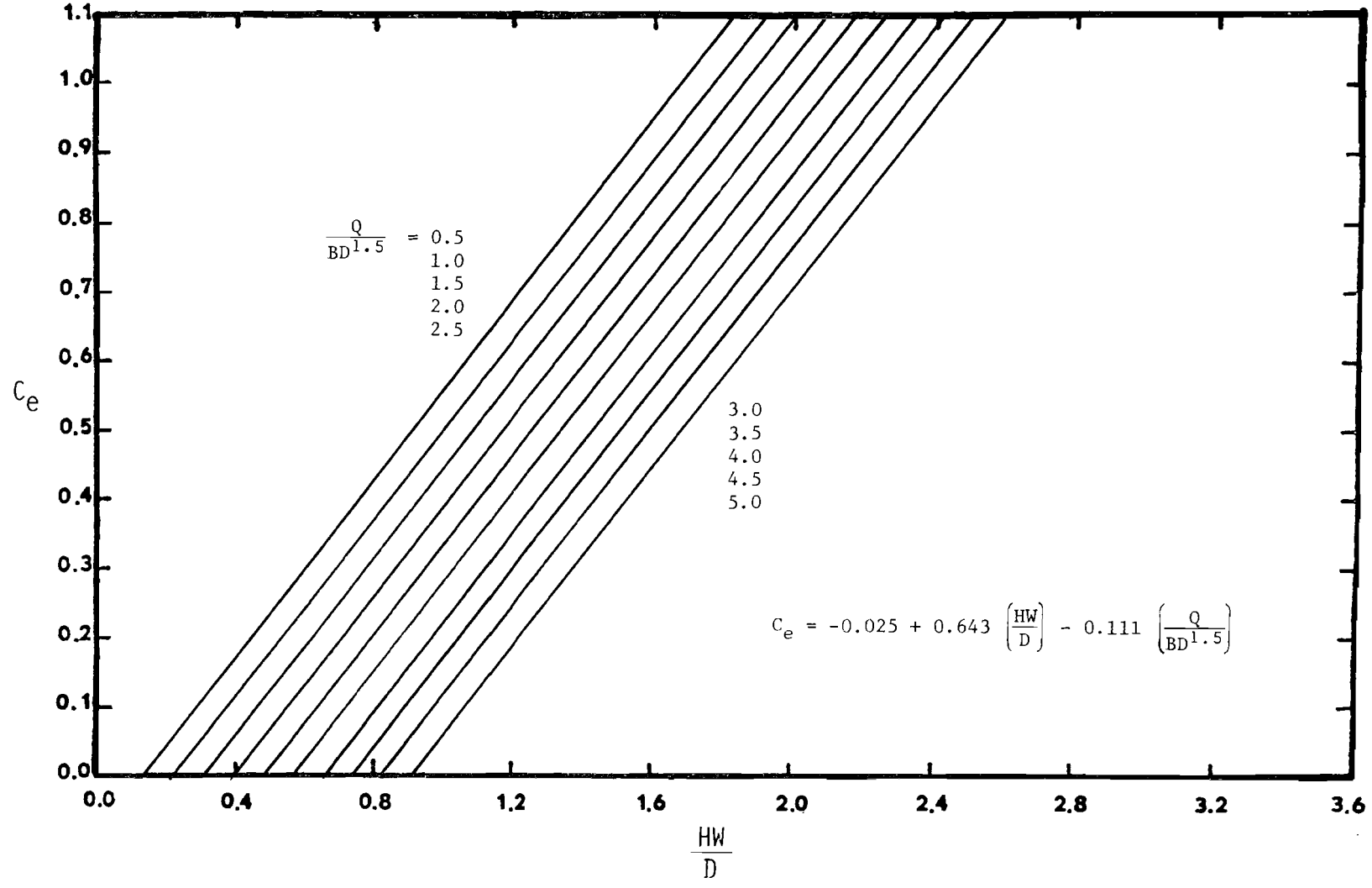


Figure 3.12 Entrance Headloss Coefficient for Submerged and Unsubmerged Conditions Combined, Bar Grates (Eq. 3.15)

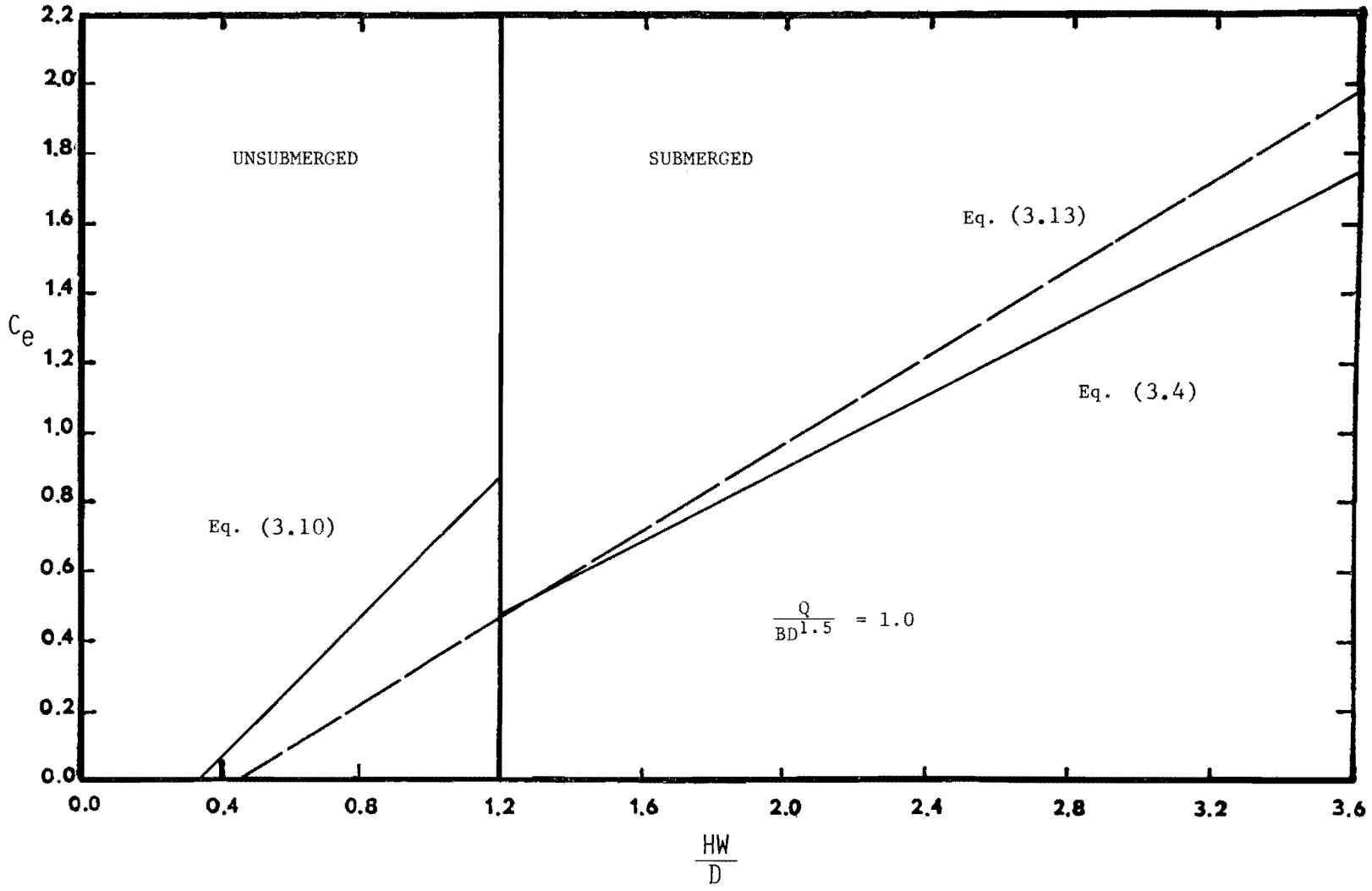


Figure 3.13 Entrance Headloss Coefficient, $\frac{Q}{BD^{1.5}} = 1.0$, for the Outlet Control Conditions, No Grates (Eqs. 3.4, 3.10, 3.13)

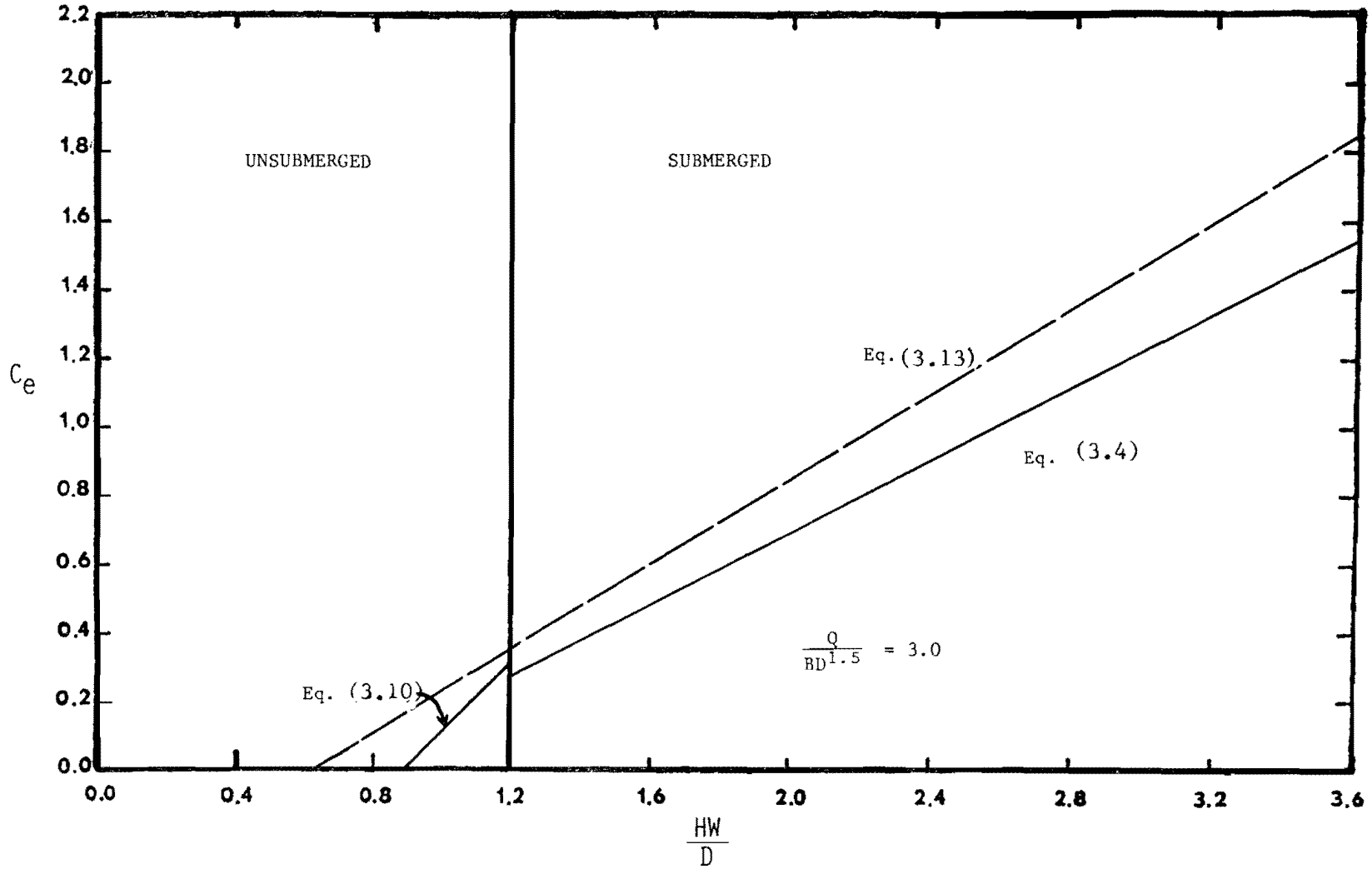


Figure 3.14 Entrance Headloss Coefficient, $\frac{Q}{BD^{1.5}} = 3.0$, for the Outlet Control Conditions, No Grates (Eqs. 3.4, 3.10, 3.13)

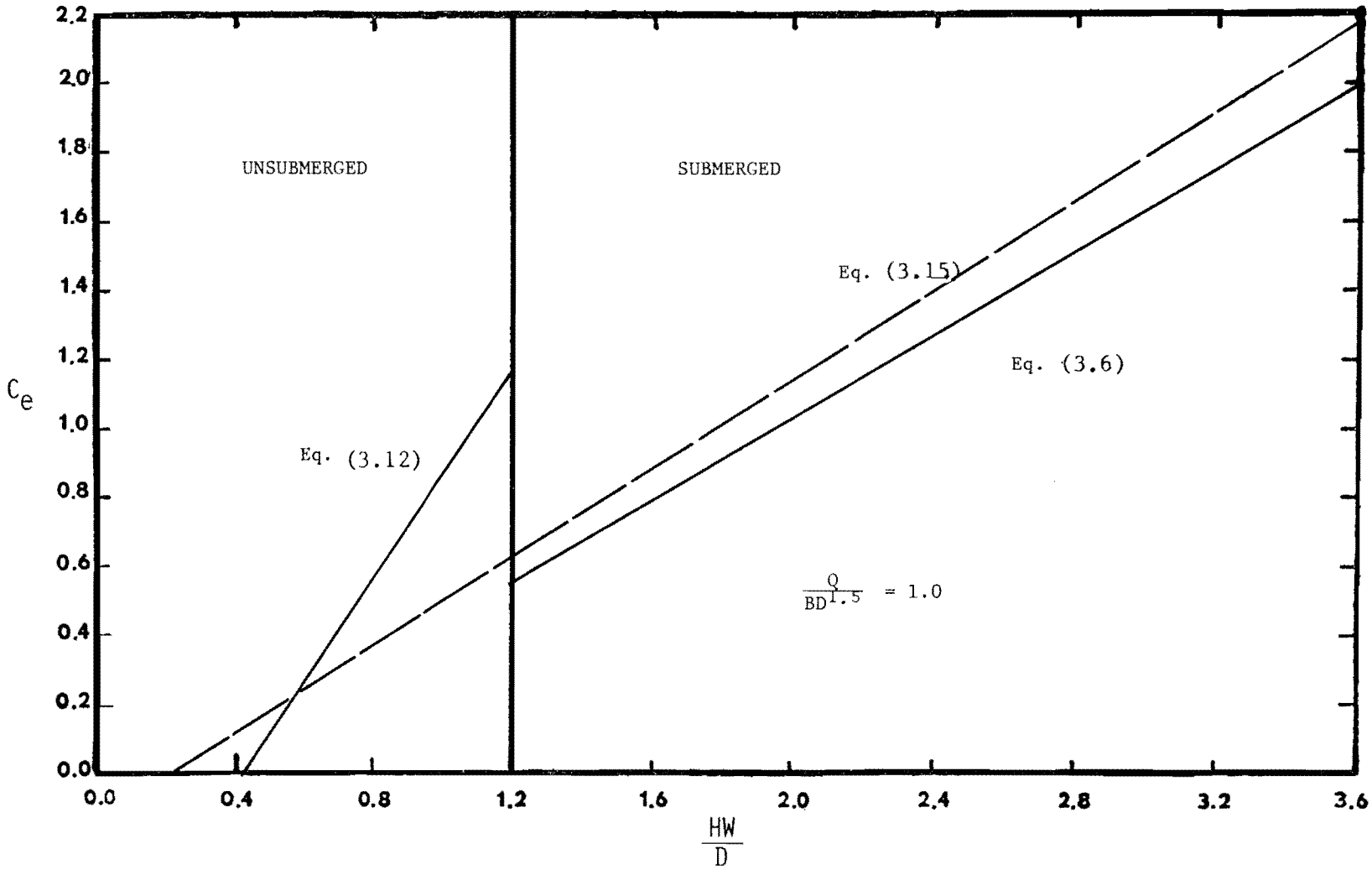


Figure 3.15 Entrance Headloss Coefficient, $\frac{Q}{BD^{1.5}} = 1.0$, for the Outlet Control Conditions, Bar Grates (Eqs. 3.6, 3.12, 3.15)

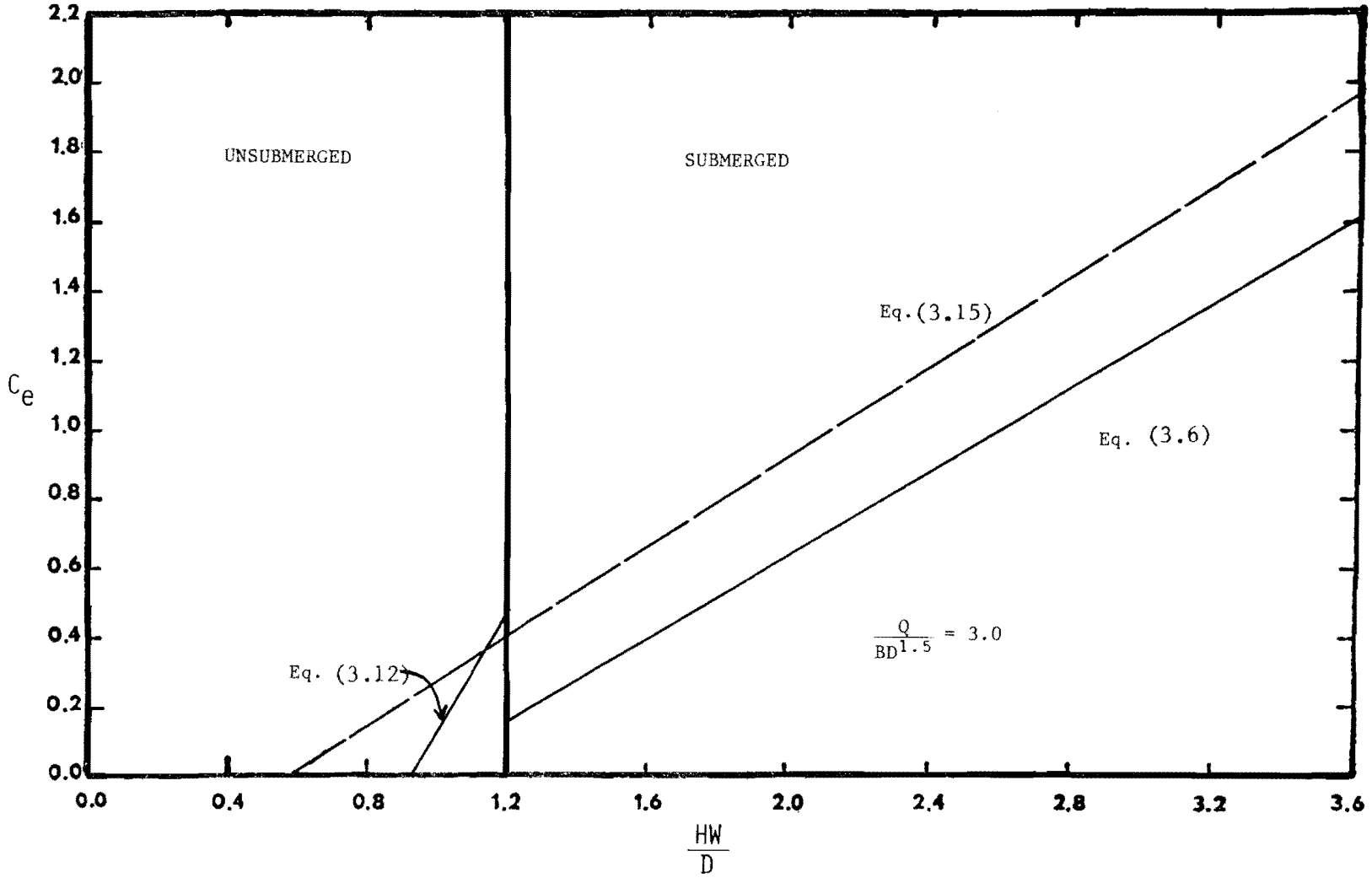


Figure 3.16 Entrance Headloss Coefficient, $\frac{Q}{BD^{1.5}} = 3.0$, for the Outlet Control Conditions, Bar Grates (Eqs. 3.6, 3.12, 3.15)

# CHAPTER 4 CLOGGING TESTS - BOX CULVERT

To demonstrate the effect of clogging, the open surface area of the safety grates was covered with boards. The simulated clogging ranged from 15 to 90 percent of the open surface area of the grates (Figs. 4.1-4.3). The bar and pipe safety grates were covered with boards (simulating clogging) in intervals of 15 percent of the original open surface area. The clogging was placed in three different patterns; from top to bottom, from bottom to top, and randomly positioned.

## 4.1 Test Procedure for Clogging

The clogging tests were used to determine the relative effects of various percentages of clogging. Empirical tests were difficult due to the unpredictability of field conditions. The measurements were made under free outfall conditions. The steps in the clogging tests were the following:

1. A constant discharge was established where the water surface was at or above the top of the culvert.

2. A 15 percent clogging was placed at the top of the grate and all measurements were taken after the water flow stabilized. The sequence of measurements were the same as the free outfall tests.

3. The rest of the clogging was placed from the top downward until 90 percent of the grate was clogged. All measurements were taken at each different percentage of clogging.

4. The entire procedure was repeated with the clogging placed from bottom to the top of the safety grates.

## 4.2 Relationship of Headwater - Percent Clogging

Figures D.1 through D.11 are graphs illustrating the headwater/depth ($\frac{HW}{D}$) versus percentage clogging for the pipe safety grates on the box culvert.

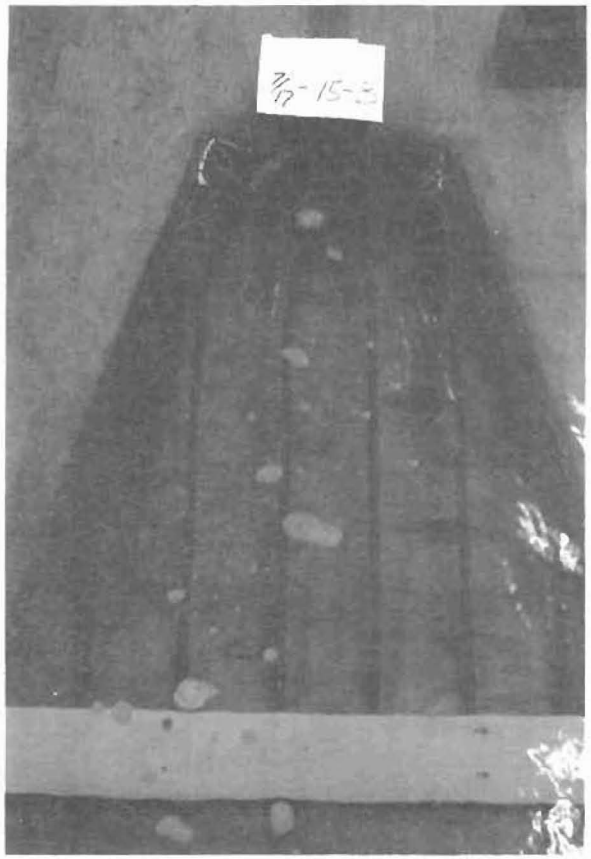

15% Clogging

30% Clogging

Figure 4.1 Clogging From Bottom To Top

45% Clogging

60% Clogging

Figure 4.2 Clogging From Bottom To Top

75% Clogging

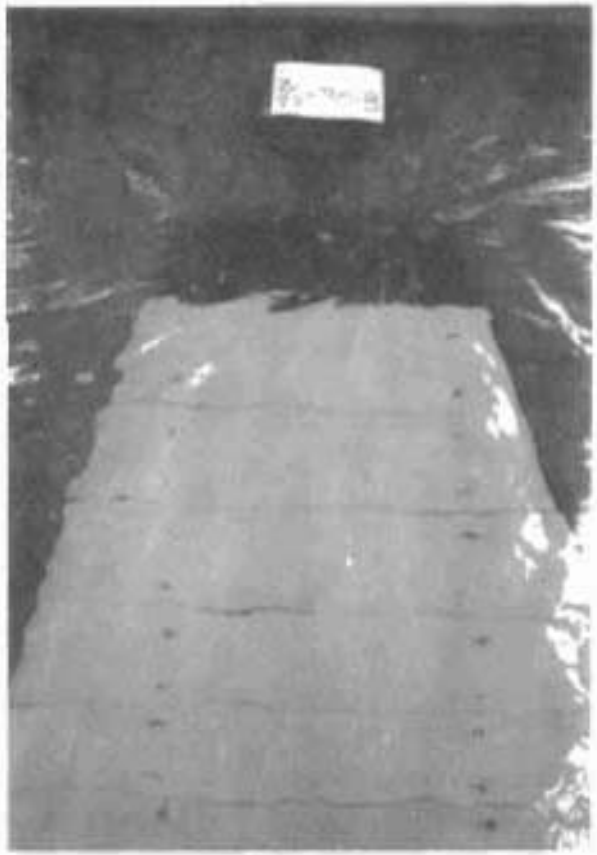

90% Clogging

Figure 4.3 Clogging From Bottom To Top

For slopes of 0.0008 and 0.0063, the results of placing the clogging from top to bottom and from bottom to top on the pipe grates are shown in Figs. D.1 through D.9 for several discharges. Figures D.9 through D.11 show the effect of various culvert slopes for the same or similar discharges. Basically, the steeper slopes do have smaller ($\frac{HW}{D}$) for the same discharges. Obviously, the general trend was an increase in headwater depth with an increase in percentage of clogging. Below 45 percent clogging, the headwater is affected very little by the clogging, while above 45 percent, the headwater is not only affected by the clogging, but also by the placement of clogging. The headwater depth increases much more rapidly when the clogging is placed from the top downward than placing clogging from the bottom upward.

The clogging tests for the bar safety grates were only conducted using a .0063 slope. Test data from top downward and from bottom upward clogging are presented in (Figures D.12 through D.16) with constant discharges. As for the clogging tests on pipe grates, the headwater increased very little for clogging less than 45 percent but increased rapidly for clogging greater than 45 percent. At the higher percentage of clogging, the headwater was higher for clogging starting at the top than for clogging starting at the bottom. Figures D.17 through D. 19 present clogging data for both the pipe and bar safety grates under similar conditions (slope and discharge).

## 4.3 Relationship of Entrance Headloss Coefficient - Percent Clogging

The effects of the percentage of clogging and the placement of clogging for the pipe safety grates are illustrated in Figures D.20 through D.35.

Figures D.20 through D.23 are the relationships of $C_e$ versus percent clogging for a culvert slope of 0.0008 and for the discharges of 9.02, 9.62, 10.7, and 11.2 cfs, respectively. Figures D.21 and D.23 illustrate the effect of the

position of clogging from top to bottom as opposed to clogging from bottom to top. The effect of clogging from top to bottom has a much more pronounced effect on increasing the $C_e$ for larger percentages of clogging. Figure D.24 shows the effect of increasing $C_e$ for a culvert slope of 0.0063 and dishcarges of 8.04, 9.10, 10.04 and 11.07 cfs.

Figures D.25 through D.28 are for the purpose of illustrating the effect of various culvert slopes for various percentages of clogging using pipe grates. Figure D.25 shows $C_e$ versus percent clogging for culvert slopes of 0.0008 and 0.0128 and each with a discharge of 9.02 cfs. This figure clearly illustrates the drastic effect of increasing the $C_e$ for larger percentages of clogging for the mild slope. This is also illustrated in Figure D.26 for the slopes of 0.0063 and 0.0128. Figures 0.27 shows the relationship for the three slopes, 0.0008, 0.0063, and 0.0128.

The effect of the placement of the clogging (bottom 1/3, middle 1/3, or top 1/3 of grate) on $C_e$ for various discharges and percentages of clogging are illustrated in Figures D.29 through D.31. Discharges of 7.94, 9.03, 10.00, and 10.82 cfs were considered for the various percentages and placements of clogging. Similar conclusions as before to the placement of clogging were found. Clogging closer to the tope of the grate causes larger values of $C_e$.

A comparison of the effect of clogging for the bar grates and the pipe grates was also performed. Figure D.32 shows the relationship of $C_e$ versus percent clogging for a culvert slope of 0.0063 and discharges of 9.09, 10.11 and 11.05 cfs for the bar safety grate. The larger dishcarges result in large $C_e$ values for the same percent clogging as shown before for the pipe grates. Figures D.33 through D.35 show a comparison of the effect of the pipe grates as

opposed to the bar grates for various percentages of clogging, for a culvert slope of 0.0063 and discharges of approximately 9, 10, and 11 cfs.

For the discharge of 9 and 10 cfs (Figures D.33 and D.34) it is difficult to say which Type grate had the greatest effect, except for the 90 percent clogging. However, for the discharge of 11 cfs (Figure D.35), the effect was definitely greater for the bar safety grates.

# CHAPTER 5 PIPE CULVERT RESULTS

The experimental tests of the safety grates for the pipe culvert model are presented and analyzed in this chapter. Figures are presented to compare the hydraulic effect with and without the pipe safety grates under various combinations of slopes, discharges, headwater depths, and tailwater depths. For comparison, the experimental tests without safety grates are also included on selected figures. Discussions of the tests are presented describing changes in the hydraulics due to the safety grates. Regression equations are presented for predicting entrance headloss coefficients for different conditions of outlet control. Also, regression equations are presented for determining headwater-discharge relationships for inlet control.

Geometric similarity (of the corrugations) is not completely satisfied in this experiment. The safety grate similarity is easily satisfied by the construction of a 1:4 scale model grate. However, geometric similarity of corrugations between the 15-inch diameter model pipe culvert and a prototype culvert is not possible due to the constant corrugation sizes in helical corrugated metal pipe for all pipe diameters. In other words, the relative size of the corrugations to the pipe diameter decreases with increasing diameter. Furthermore, the angle of corrugations for helical pipe as fabricated, is not constant throughout the various pipe diameters.

Kinematic similarity is partially upheld for reasons similar to those for geometric similarity. The velocity ratio is satisfied for increasing diameter. However, because of constant corrugation size, complete kinematic similarity cannot be satisfied. Satisfaction of dynamic similarity is not complete for

reasons also due to the constant pipe corrugations. The inability to precisely model the corresponding lengths and velocities of model and prototype may limit the application of regression equations for $C_e$. Data for the regression analysis is listed in Appendix G.

## 5.1 Entrance Headloss Coefficient With and Without Safety Grates

A direct comparison of the entrance headloss coefficient with grates installed and the entrance headloss coefficient without grates for the mild slopes, 0.0007 and 0.008, are presented in Figures E.1 and E.2. For the milder slope, 0.0007, the entrance headloss coefficients for grates installed are greater than those without the grates. This clearly indicates that the grates do have an effect; however, the effect does not seem to be major. For the steeper slope, .008, the entrance headloss coefficients are significantly greater for the lower discharges and seem to have little effect for the higher discharges. In fact, the effect of the grates on the entrance headloss coefficient at the high discharges was insignificant.

## 5.2 Headwater-Discharge Relationships

The headwater-discharge relationships for inlet control are shown in Figures E.3, E.4, and E.5 for the slopes 0.0007, 0.008, and 0.05, respectively. The curves are plotted as $\frac{HW}{D}$ vs $\frac{Q}{D^{2.5}}$ with and without the safety grates installed. The safety grates do show an increase in $\frac{HW}{D}$ which is relatively constant throughout the range of discharges.

Regression equations for inlet control were developed using the general form

$$\frac{HW}{D} = a_o + a_1\left(\frac{Q}{D^{2.5}}\right) + a_2\left(\frac{Q}{D^{2.5}}\right) + \ldots + a_n\left(\frac{Q}{D^{2.5}}\right)^n \qquad (5.1)$$

where $\frac{HW}{D}$ is the dependent variable and $\frac{Q}{D^{2.5}}$ is the independent variable. The results of the regression analysis are summarized in Table 5.1 for no grates and the grates installed. As an example of the equations developed, the simplest form for the no grates and grates installed are, respectively,

$$\frac{HW}{D} = 0.166 + 0.385 \left(\frac{Q}{D^{2.5}}\right) \tag{5.2}$$

and

$$\frac{HW}{D} = 0.158 + 0.389 \left(\frac{Q}{D^{2.5}}\right) \tag{5.3}$$

## 5.3 Entrance Headloss Coefficient - Headwater Relationship

Entrance headloss coefficient - headwater relationships are plotted in Figs. E.6 through E.13 for various flow regimes of the two slopes, 0.008 and 0.0007. Figure E.6 illustrates the $C_e$ vs $\frac{HW}{D}$ for flow regimes 1, 2, 4A and 4B with and without the grates for the slope of 0.008. Figures E.7, E.8, E.9, and E.11 are separate graphs of $C_e$ vs $\frac{HW}{D}$ for flow regimes, 1, 2, 4A, 4B respectively. Figures E.11, E.12, and E.13 are for the slope, of 0.0007, considering flow regimes 4A and 4B combined, 4A and 4B respectively. Probably the most significant conclusion from these graphs is that $C_e$ is significantly affected by $\frac{HW}{D}$. The entrance headloss coefficient for safety grates installed are greater than for no grates for unsubmerged inlets. The effect of safety grates on the entrance headloss coefficient is relatively constant for submerged inlets. The entrance headloss coefficient with and without grates installed, increases substantially for an unsubmerged inlet.

## 5.4 Entrance Headloss Coefficient - Discharge Relationship

Entrance headloss coefficient-discharge relationships ($C_e$ vs $\frac{Q}{D^{2.5}}$) are plotted in Figures E.14 through E.19 for various flow regimes for the two slopes, 0.008 and 0.0007. Figure E.14 illustrates the $C_e$ vs $\frac{Q}{D^{2.5}}$ relationship

Table 5.1 Headwater-Discharge Relationships for Inlet Control

(a) No Grates, 31 Data Points

| Equation | $a_0$ | $a_1$ | $a_2$ | $a_3$ | $a_4$ | $a_5$ | R |
|---|---|---|---|---|---|---|---|
| 1 | 0.166 | 0.385 | | | | | 0.9868 |
| 2 | 0.516 | 0.144 | 0.036 | | | | 0.9923 |
| 3 | -0.129 | 0.845 | -0.190 | 0.022 | | | 0.9943 |
| 4 | 2.267 | -2.606 | 1.524 | -0.331 | 0.026 | | 0.9977 |
| 5 | 0.236 | 1.088 | -1.00 | 0.482 | -0.099 | 0.007 | 0.9980 |

(b) Grates Installed, 30 Data Points

| Equation | $a_0$ | $a_1$ | $a_2$ | $a_3$ | $a_4$ | $a_5$ | R |
|---|---|---|---|---|---|---|---|
| 1 | 0.158 | 0.389 | | | | | 0.9839 |
| 2 | 0.645 | 0.053 | 0.049 | | | | 0.9941 |
| 3 | -0.082 | 0.846 | -0.206 | 0.025 | | | 0.996 |
| 4 | 1.656 | -1.656 | +1.035 | -0.230 | 0.019 | | 9.9983 |
| 5 | -0.774 | 2.775 | -1.999 | 0.749 | -0.132 | 0.009 | 0.9990 |

for flow regimes 1, 2, 4A, and 4B with and without grates for the slope of 0.008. Figures E.15, E.16, E.17 and E.18 are separate graphs of $C_e$ vs $\frac{Q}{D^{2.5}}$ for flow regimes 1, 2, 4A and 4B. Figure E.19 shows the relationship for flow regimes 4A and 4B for a slope of 0.0007. The most significant conclusion is that the entrance headloss coefficient increases substantially for increased discharges for submerged entrances.

## 5.5 Headwater-Tailwater Relationships

For the tailwater tests, the tailwater ranged from free outfall conditions to full flow. Figures E.20 through E. 23 show the relationship of $\frac{HW}{D}$ vs $\frac{TW}{D}$ with and without grates installed. Figure E.20 shows the relationships for a discharge of 5.6 cfs and a slope of 0.0007. Figures E.21, E.22, and E.23 are for the slope, of 0.008, and discharges 3.6, 4.5, and 5.5 cfs. The headwater depth is unaffected by rising tailwater depths less than critical depth. The flatter the culvert slope, the greater the effect of tailwater depth on the headwater depth.

## 5.6 Regression Equations for Submerged Inlet Conditions

Regression equations were developed for the entrance headloss coefficient for submerged inlet conditions, $\frac{HW}{D} < 1.2$. The various regression equations considered are listed in Table 5.2. The resulting coefficients, $B_o$, ..., $B_n$ for each of the regression equations are listed in Table 5.3 for no grates and in Table 5.4 for the grates installed.

From the viewpoint of design considerations regression equations for $C_e$ should be at the simplest form with the least number of independent variables. Equation 13 in Table 5.2 is one of the simpler forms considered. The regression equation for no grates is

$$C_e = -0.119 + 0.364 \left(\frac{Q}{D^{2.5}}\right) - 0.133 \left(\frac{HW-TW}{D}\right) \qquad (5.4)$$

Table 5.2 Regression Equations for Pipe Culvert Equation

1. $C_e = B_o + B_1 (\frac{Q}{D^{2.5}}) + B_2 (\frac{Q}{D^{2.5}})^2 + B_3 (\frac{Q}{D^{2.5}})^3 + B_4 (\frac{Q}{D^{2.5}})$

2. $C_e = B_o + B_1 (\frac{Q}{D^{2.5}}) + B_2(S_o)$

3. $C_e = B_o + B_1 (\frac{Q}{D^{2.5}})$

4. $C_e = B_o + B_1 (\frac{Q}{D^{2.5}})^2$

5. $C_e = B_o + B_1 (\frac{HW}{D}) + B_2 (\frac{Q}{D^{2.5}})$

6. $C_e = B_o + B_1 (\frac{Q}{D^{2.5}})^2 (\frac{HW}{D})$

7. $C_e = B_o + B_1 (\frac{Q}{D^{2.5}})^{-2} (\frac{HW}{D}) + B_2 (\frac{Q}{D^{2.5}})^{-2}$

8. $C_e = B_o + B_1 (\frac{Q}{D^{2.5}})^{-2} (\frac{HW}{D}) + B_2 (\frac{Q}{D^{2.5}})^{-2} + B_3 (\frac{Q}{D^{2.5}})^{-2} (S_o)$

9. $C_e = B_o + B_1 (\frac{Q}{D^{2.5}})^{-2}$

10. $C_e = B_o + B_1 (\frac{HW}{D}) + B_2 (\frac{Q}{D^{2.5}}) + B_3 (S_o)$

11. $C_e = B_o + B_1 (\frac{HW}{D})^2 + B_2 (\frac{Q}{D^{2.5}}) + B_3 (\frac{Q}{D^{2.5}}) + B_4 (S_o)$

12. $C_e = B_o + B_1 (\frac{HW}{D}) B_2 (\frac{HW}{D})^2 + B_3 (\frac{Q}{D^{2.5}}) + B_4 (\frac{Q}{D^{2.5}})^2 + B_5 (S_o)$

13. $C_e = B_o + B_1 (\frac{Q}{D^{2.5}}) + B_2 (\frac{HW-TW}{D})$

Table 5.3 Regression Results for Submerged Conditions, No Grates, 90 Data Points

| Equation | $B_o$ | $B_1$ | $B_2$ | $B_3$ | $B_4$ | $B_5$ | R |
|---|---|---|---|---|---|---|---|
| 1 | 9.1511 | -11.4430 | 5.5038 | 1.1215 | 0.0835 | | 0.823 |
| 2 | -0.0443 | 0.2623 | 17.1550 | | | | 0.877 |
| 3 | 0.1448 | 0.230 | | | | | 0.811 |
| 4 | 0.5071 | 0.0352 | | | | | 0.798 |
| 5 | 0.0853 | 0.0937 | 0.1929 | | | | 0.828 |
| 6 | 1.0738 | -1.0640 | | | | | 0.504 |
| 7 | 1.1041 | 1.2168 | -4.2980 | | | | 0.813 |
| 8 | 1.1996 | 1.2439 | -6.3351 | 205.8080 | | | 0.908 |
| 9 | 1.1585 | -2.5967 | | | | | 0.758 |
| 10 | -0.1160 | 0.1040 | 0.2221 | 17.6738 | | | 0.897 |
| 11 | -0.7412 | 0.0321 | 0.6744 | -0.0715 | 20.1376 | | 0.912 |
| 12 | -1.3816 | 1.0003 | -0.2317 | 0.4842 | -0.0398 | 21.1668 | 0.937 |
| 13 | -0.1190 | 0.3640 | -0.1330 | | | | 0.860 |

Table 5.4 Regression Results for Submerged Conditions, Grates Installed, 87 Data Points

| Equation | $B_o$ | $B_1$ | $B_2$ | $B_3$ | $B_4$ | $B_5$ | R |
|---|---|---|---|---|---|---|---|
| 1 | 13.4540 | -16.4665 | 7.6996 | -1.5431 | 0.1134 | | 0.896 |
| 2 | 0.1165 | 0.2314 | 11.2522 | | | | 0.913 |
| 3 | 0.2414 | 0.2102 | | | | | 0.877 |
| 4 | 0.5743 | 0.0319 | | | | | 0.864 |
| 5 | 0.2156 | 0.0501 | 0.1881 | | | | 0.883 |
| 6 | 1.1295 | -1.1600 | | | | | 0.582 |
| 7 | 1.1568 | 0.6726 | -3.4833 | | | | 0.855 |
| 8 | 1.2298 | 0.6702 | -4.9686 | 150.2440 | | | 0.921 |
| 9 | 1.1951 | -2.6103 | | | | | 0.834 |
| 10 | 0.0869 | 0.0541 | 0.2079 | 11.4102 | | | 0.920 |
| 11 | -0.4294 | 0.0164 | 0.5609 | -0.0549 | 13.4505 | | 0.931 |
| 12 | -0.7092 | -.5799 | -0.1356 | 0.3933 | -0.0279 | 13.7285 | 0.944 |
| 13 | 0.0190 | 0.3230 | -0.1110 | | | | 0.920 |

and for grates installed is

$$C_e = 0.019 + 0.323 \left(\frac{Q}{D^{2.5}}\right) - 0.111 \left(\frac{HW-TW}{D}\right) \qquad (5.5)$$

The coefficients of determination are 0.86 for Eq. (5.4) and 0.92 for Eq. (5.5). Equation (5.4) is plotted in Fig. 5.1 and Eq. (5.5) is plotted in Fig. 5.2. A comparison of the two equations with and without grates is given in Figure 5.3. The values of $C_e$ with grates are clearly greater than those without grates.

Another simple equation is Eq. 2 in Table 5.2. The regression equation for no grates is

$$C_e = -0.044 + 0.262 \left(\frac{Q}{D^{2.5}}\right) + 17.155 \left(S_o\right) \qquad (5.6)$$

and for grates installed is

$$C_e = 0.117 + 0.231 \left(\frac{Q}{D^{2.5}}\right) + 11.252 \left(S_o\right) \qquad (5.7)$$

The coefficients of determination for these equations are 0.877 for Eq. (5.6) and 0.913 for Eq. (5.7). These two equations (5.6) and (5.7) are plotted in Fig. 5.4 for three example slopes, $S_o$ = 0.0005, 0.005, and 0.01. These curves indicate that the differences in $C_e$ for no grates and grates installed decrease for the larger slopes and for larger values of $\left(\frac{Q}{D^{2.5}}\right)$.

An even simpler form for $C_e$ is Eq. 3 in Table 5.2. The regression equation for no grates is

$$C_e = 0.145 + 0.230 \left(\frac{Q}{D^{2.5}}\right) \qquad (5.8)$$

and for grates installed is

$$C_e = 0.241 + 0.210 \left(\frac{Q}{D^{2.5}}\right) \qquad (5.9)$$

The coefficients of determination for these equations are 0.81 for Eq. (5.8) and 0.88 for Eq. (5.9). These equations are plotted in Fig. 5.5.

$$C_e = -0.119 + 0.364 \left(\frac{Q}{D^{2.5}}\right) - 0.133 \left(\frac{HW-TW}{D}\right)$$

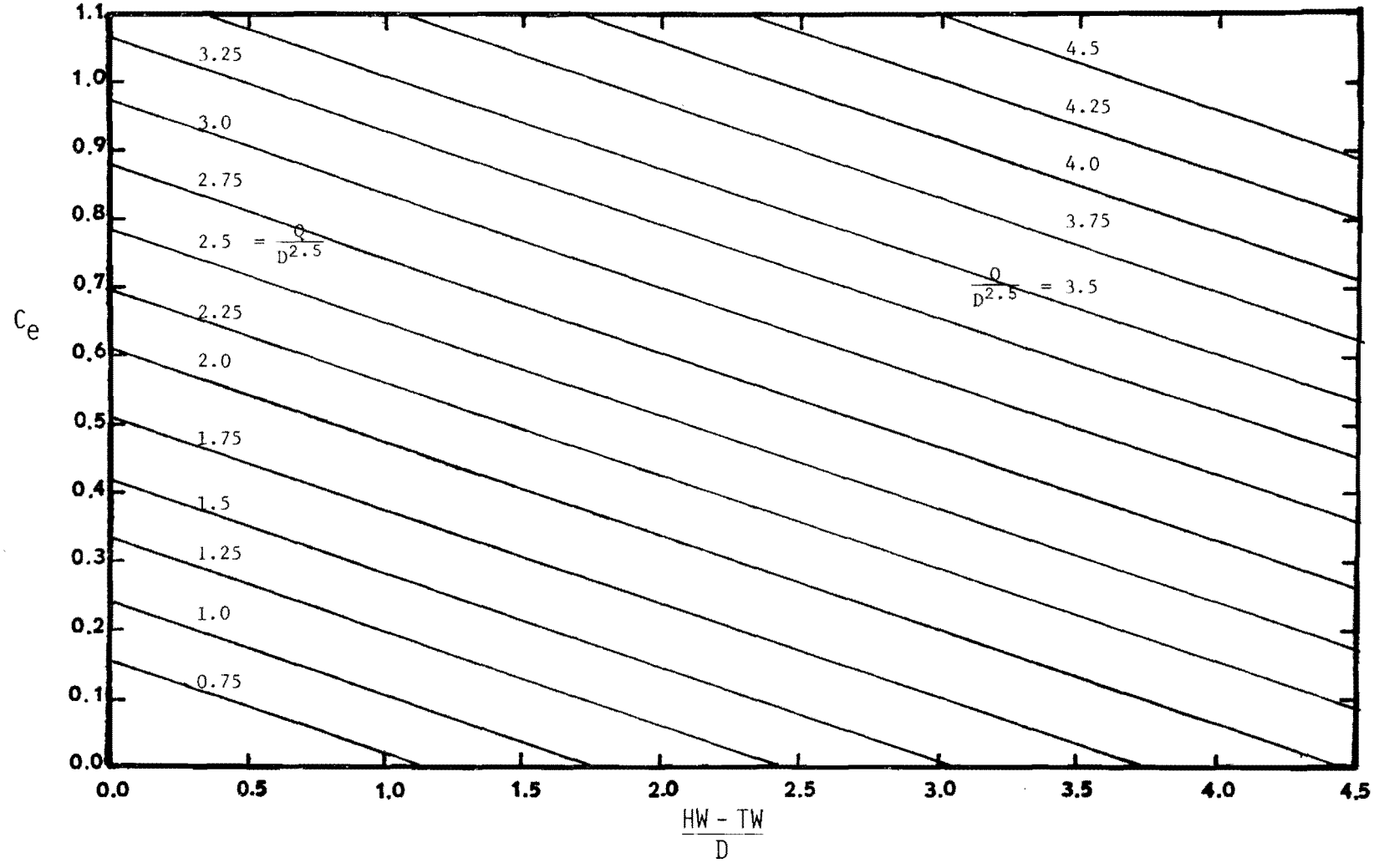


Figure 5.1 Entrance Headloss Coefficient for Submerged Conditions, No Grates (Eq. 5.4)

$$C_e = 0.019 + 0.323 \left(\frac{Q}{D^{2.5}}\right) - 0.111 \left(\frac{HW-TW}{D}\right)$$

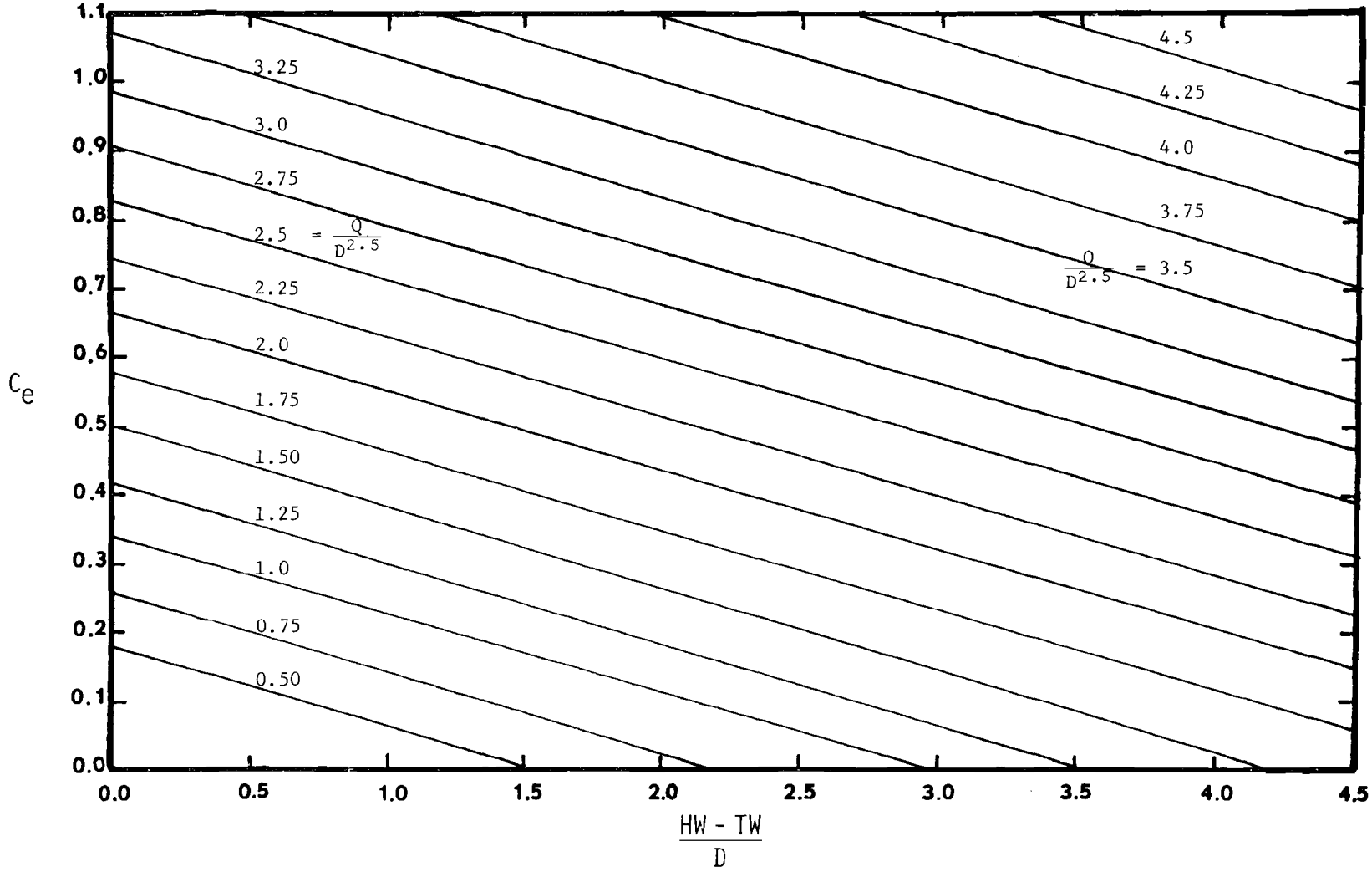


Figure 5.2 Entrance Headloss Coefficient for Submerged Conditions, Grates (Eq. 5.5)

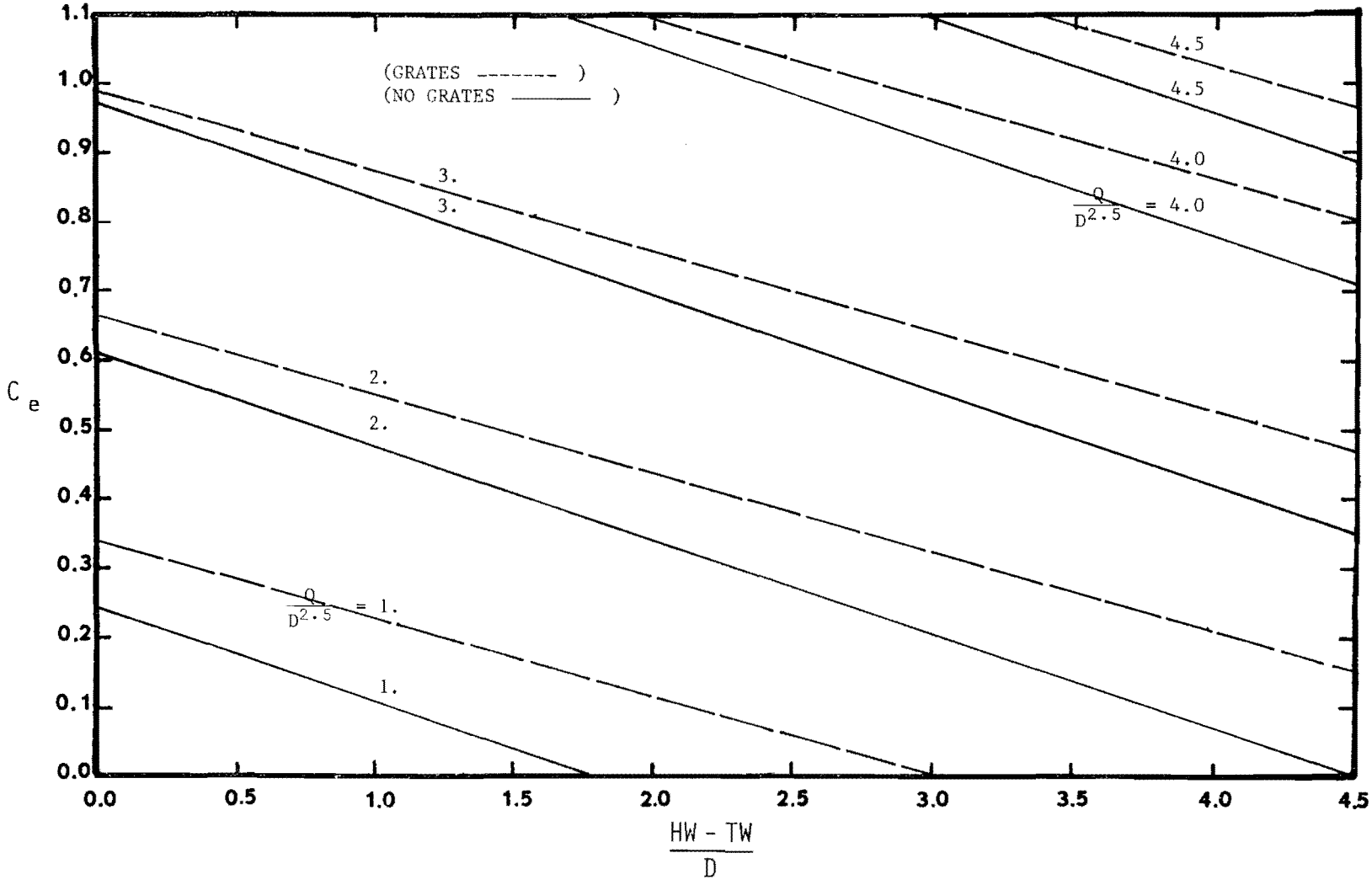


Figure 5.3 Entrance Headloss Coefficient for Submerged Conditions, Grates and No Grates (Eqs. 5.5, 5.4)

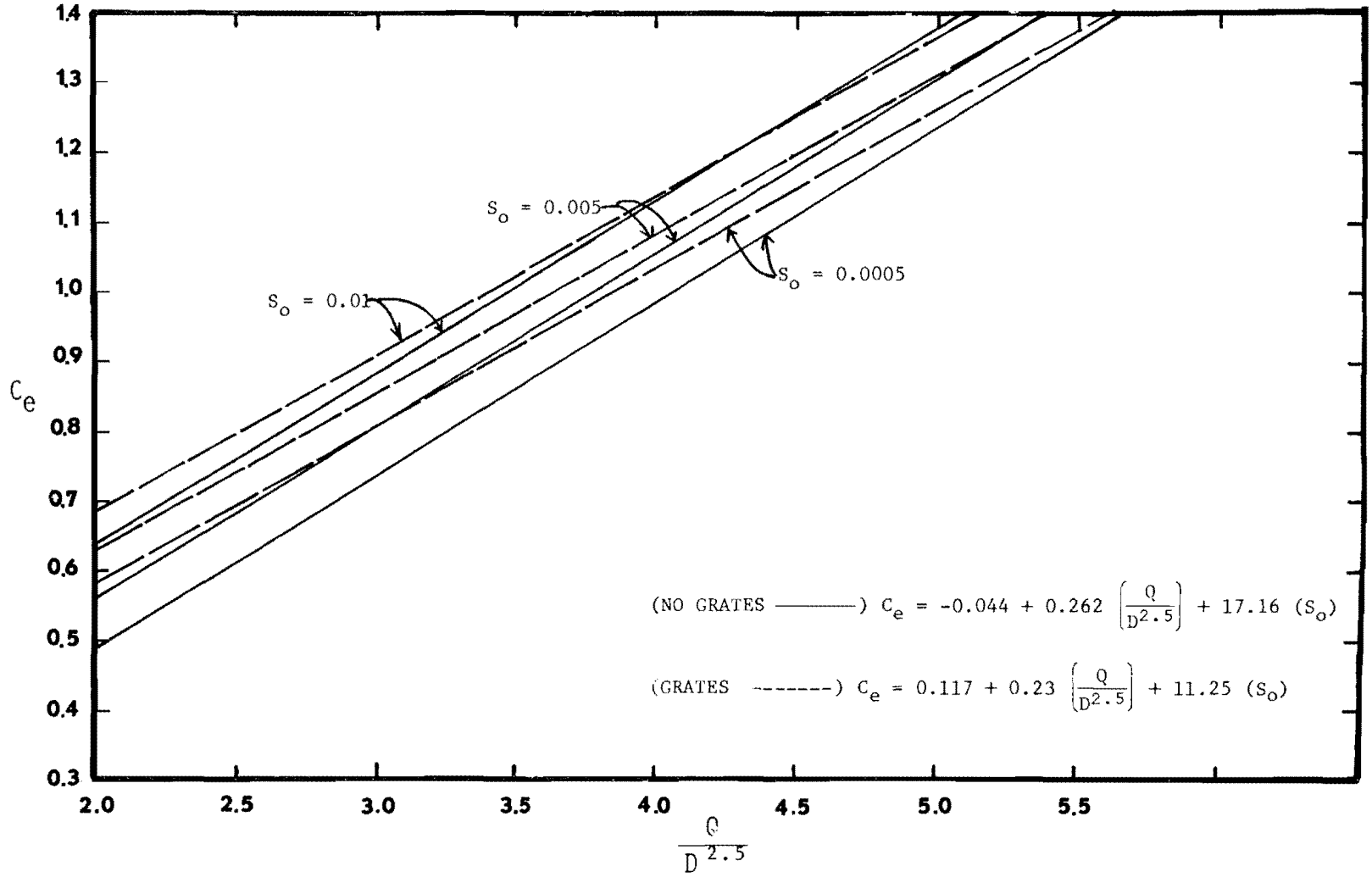


Figure 5.4 Entrance Headloss Coefficient for Submerged Conditions, Grates and No Grates (Eqs. 5.7, 5.6)

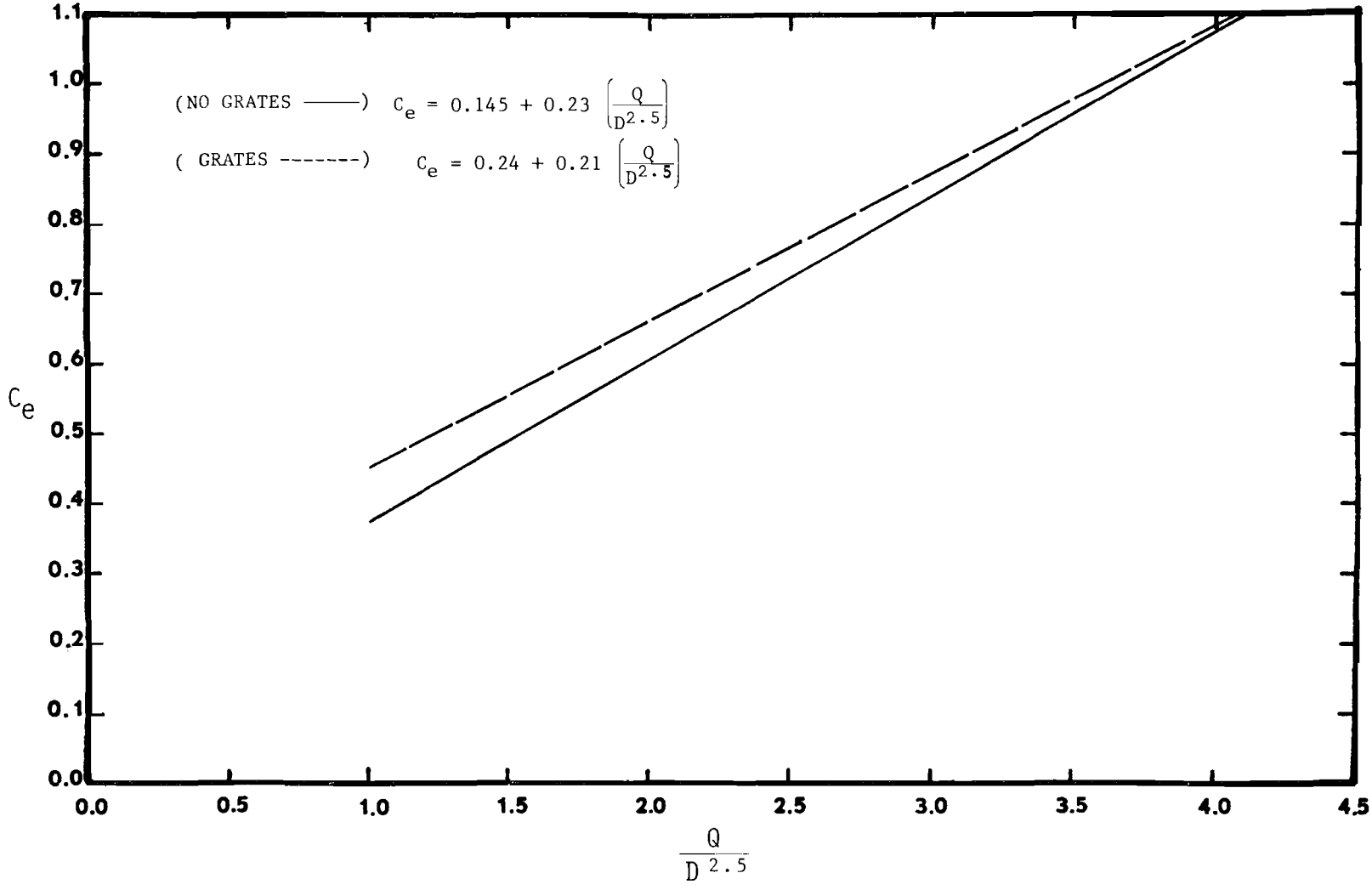


Figure 5.5 Entrance Headloss Coefficient for Submerged Conditions, Grates and No Grates (Eqs. 5.9, 5.8)

## 5.7 Regression Equations for Submerged and Unsubmerged Inlets Combined

Regression equations were developed for the entrance headloss coefficients for submerged and unsubmerged inlet conditions. The various regression equations considered are listed in Table 5.2. The resulting coefficients, $B_o$, ..., $B_n$ for each of the regression equations are listed in Table 5.5 for no grates and in Table 5.6 for the grates installed. The simple forms of the equations for $C_e$ used for the submerged conditions are also considered.

The first set of equations are 13 in Table 5.2. The regression equation for no grates is

$$C_e = -0.115 + 0.350 \left(\frac{Q}{D^{2.5}}\right) - 0.109 \left(\frac{HW-TW}{D}\right) \qquad (5.10)$$

and for grates installed is

$$C_e = 0.187 + 0.252 \left(\frac{Q}{D^{2.5}}\right) - 0.062 \left(\frac{HW-TW}{D}\right) \qquad (5.11)$$

The coefficients of determination for these equations are 0.90 for Eq. (5.10) and are 0.92 for Eq. (5.11). Equation (5.10) is plotted in Figure 5.6 and Eq. (5.11) is plotted in Fig. 5.7. A comparison of the two equations for no grates and grates installed is given in Fig. 5.8.

Utilizing Eq. 2 in Table 5.2, the regression equation for no grates is

$$C_e = -0.176 + 0.302 \left(\frac{Q}{D^{2.5}}\right) + 15.705 \, (S_o) \qquad (5.12)$$

and for grates installed is

$$C_e = 0.133 + 0.227 \left(\frac{Q}{D^{2.5}}\right) + 10.754 \, (S_o). \qquad (5.13)$$

The coefficients of determination for these equations are 0.901 for Eq. (5.12) and 0.93 for Eq. (5.13). These two equations are plotted in Fig. 5.9 for four example slopes 0.0005, 0.005, 0.010 and 0.015. These curves clearly indicate that the differences in $C_e$ for no grates and grates installed decrease for the larger slopes and for larger values of $\left(\frac{Q}{D^{2.5}}\right)$.

Table 5.5 Regression Results for Submerged and Unsubmerged Conditions Combined, No Grates, 106 Data Points

| Equation | $B_1$ | $B_2$ | $B_3$ | $B_4$ | $B_5$ | $B_6$ | R |
|---|---|---|---|---|---|---|---|
| 1 | 0.1940 | 0.0414 | 0.0417 | 0.0191 | -0.0046 | | 0.886 |
| 2 | -0.1764 | 0.3024 | 15.7059 | | | | 0.901 |
| 3 | -0.0003 | 0.2721 | | | | | 0.874 |
| 4 | 0.3925 | 0.0446 | | | | | 0.848 |
| 5 | -0.0329 | 0.1374 | 0.2016 | | | | 0.894 |
| 6 | 1.1026 | -1.4156 | | | | | 0.563 |
| 7 | 1.0012 | 0.1119 | -1.6237 | | | | 0.730 |
| 8 | 1.0452 | 0.0637 | -2.5535 | 109.9870 | | | 0.747 |
| 9 | 1.0151 | -1.5487 | | | | | 0.730 |
| 10 | -0.2230 | 0.1489 | 0.2279 | 16.7126 | | | 0.924 |
| 11 | -0.5012 | 0.0368 | 0.5103 | -0.0459 | 17.8104 | | 0.926 |
| 12 | -0.6018 | 0.7528 | -0.1697 | 0.1509 | 0.0109 | 17.5524 | 0.939 |
| 13 | -0.1150 | 0.3500 | -0.1090 | | | | 0.900 |

Table 5.6 Regression Results for Submerged and Unsubmerged Conditions Combined, Grates Installed, 101 Data Points

| Equation | $B_o$ | $B_1$ | $B_2$ | $B_3$ | $B_4$ | $B_5$ | R |
|---|---|---|---|---|---|---|---|
| 1 | 1.4217 | -1.3742 | 0.7437 | -0.1453 | 0.0100 | | 0.914 |
| 2 | 0.1329 | 0.2266 | 10.7540 | | | | 0.926 |
| 3 | 0.2530 | 0.2062 | | | | | 0.904 |
| 4 | 0.5471 | 0.0341 | | | | | 0.895 |
| 5 | 0.2431 | 0.0491 | 0.1800 | | | | 0.908 |
| 6 | 1.1242 | -1.2200 | | | | | 0.631 |
| 7 | 1.0594 | -0.3908 | -0.8262 | | | | 0.703 |
| 8 | 1.0926 | -0.4388 | -1.4950 | 80.3584 | | | 0.720 |
| 9 | 1.0092 | -1.0820 | | | | | 0.693 |
| 10 | 0.1197 | 0.0540 | 0.1982 | 10.9763 | | | 0.932 |
| 11 | 0.1074 | 0.0129 | 0.2386 | -0.0060 | 11.0500 | | 0.930 |
| 12 | 0.0765 | 0.3324 | -0.0765 | 0.0685 | 0.2070 | 10.8565 | 0.935 |
| 13 | 0.1870 | 0.2520 | -0.0620 | | | | 0.920 |

$$C_e = -0.115 + 0.35 \left(\frac{Q}{D^{2.5}}\right) - 0.109 \left(\frac{HW-TW}{D}\right)$$

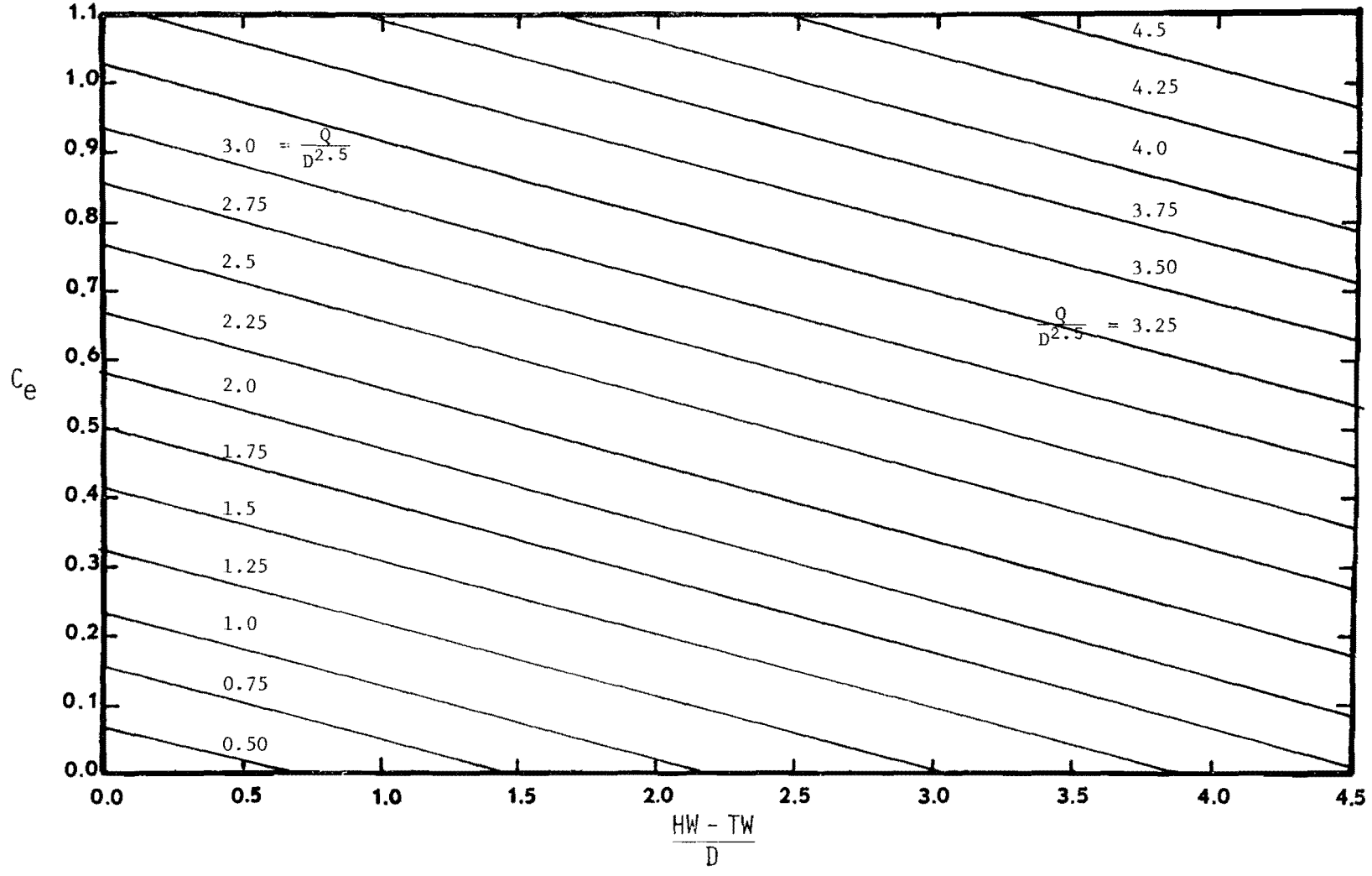


Figure 5.6 Entrance Headloss Coefficient for Submerged and Unsubmerged Conditions Combined, No Grates (Eq. 5.10)

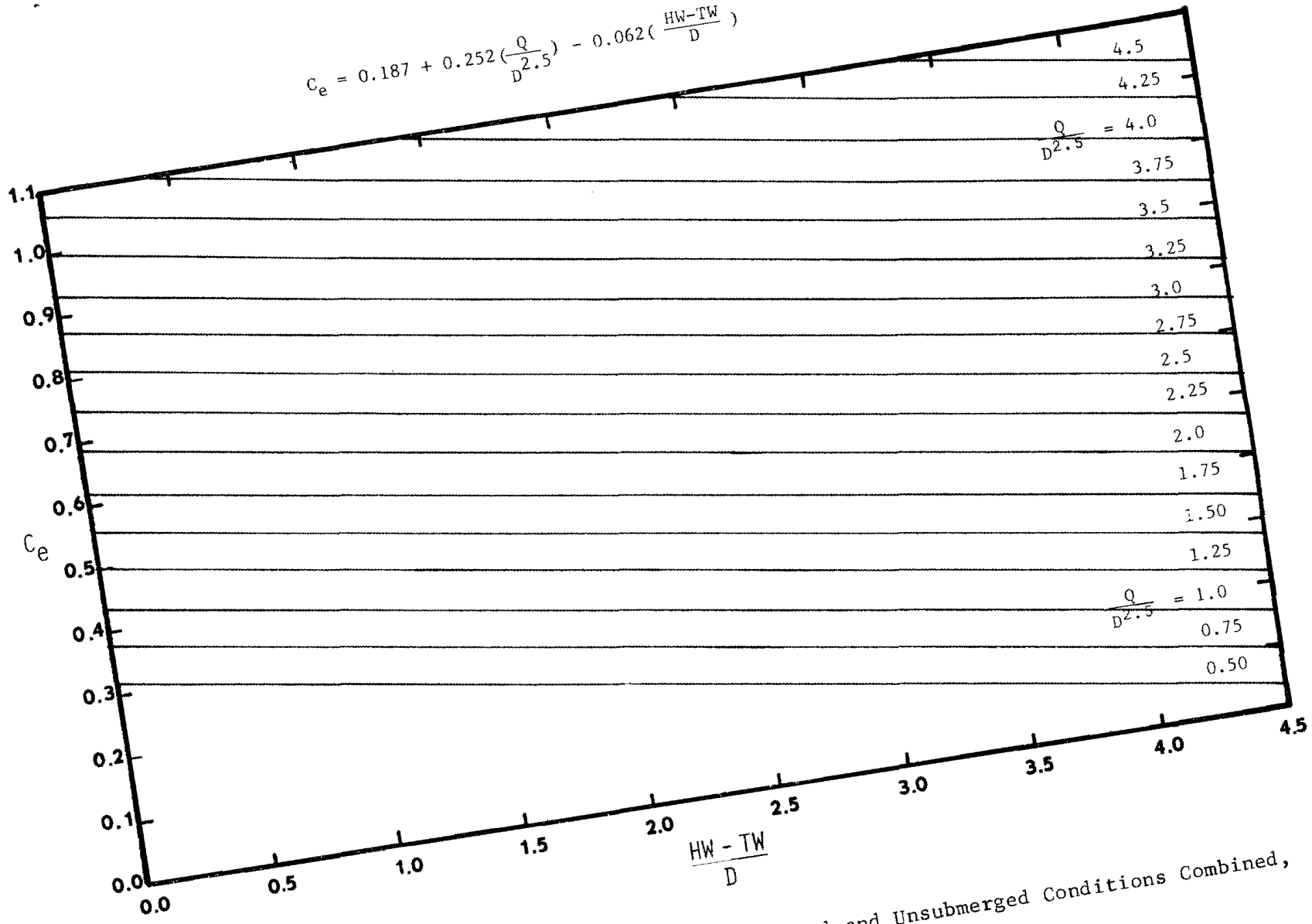


Figure 5.7 Entrance Headloss Coefficient for Submerged and Unsubmerged Conditions Combined, Grates (Eq. 5.11)

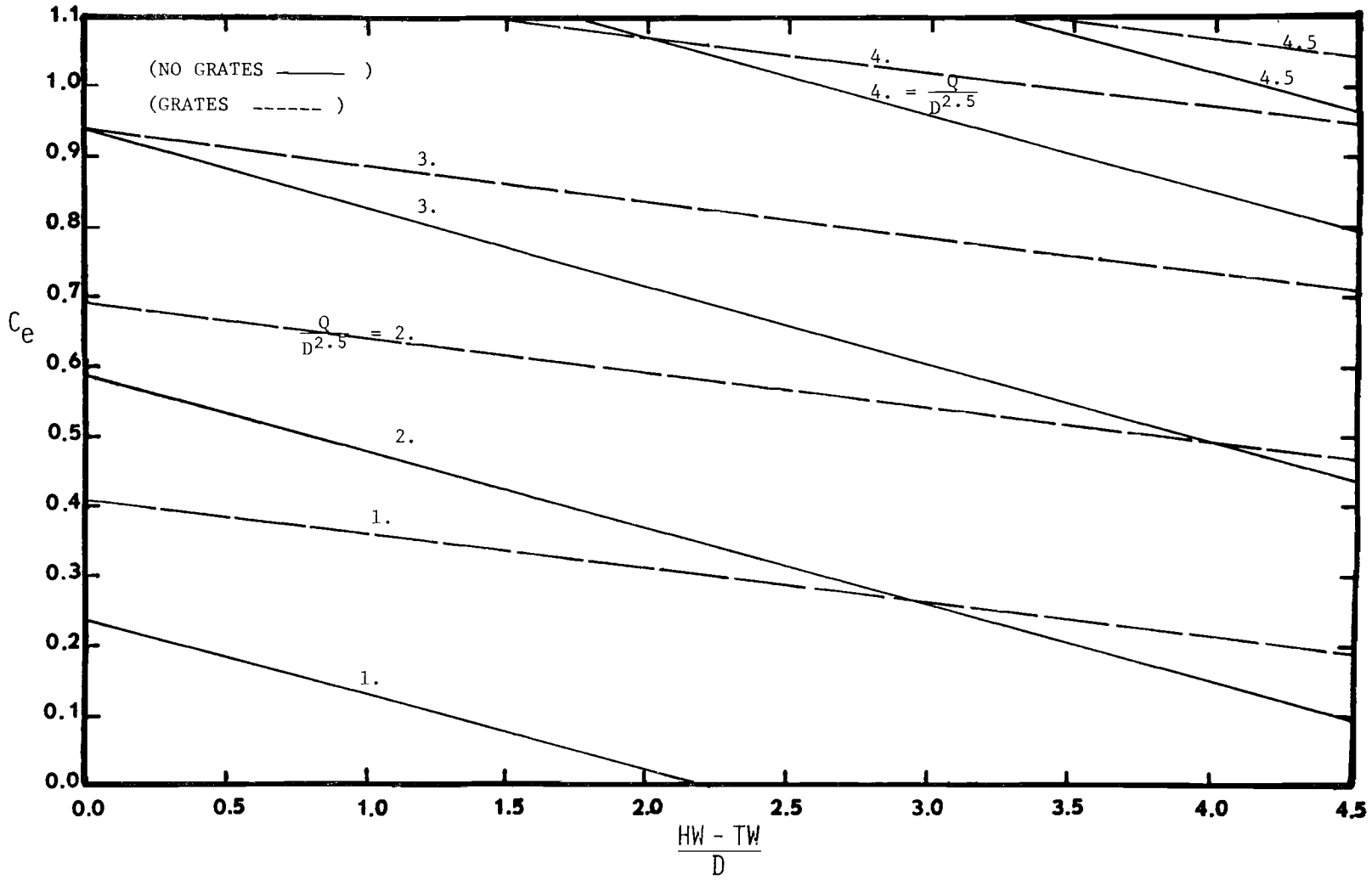


Figure 5.8 Entrance Headloss Coefficient for Submerged and Unsubmerged Conditions Combined, Grates and No Grates (Eqs. 5.11, 5.10)

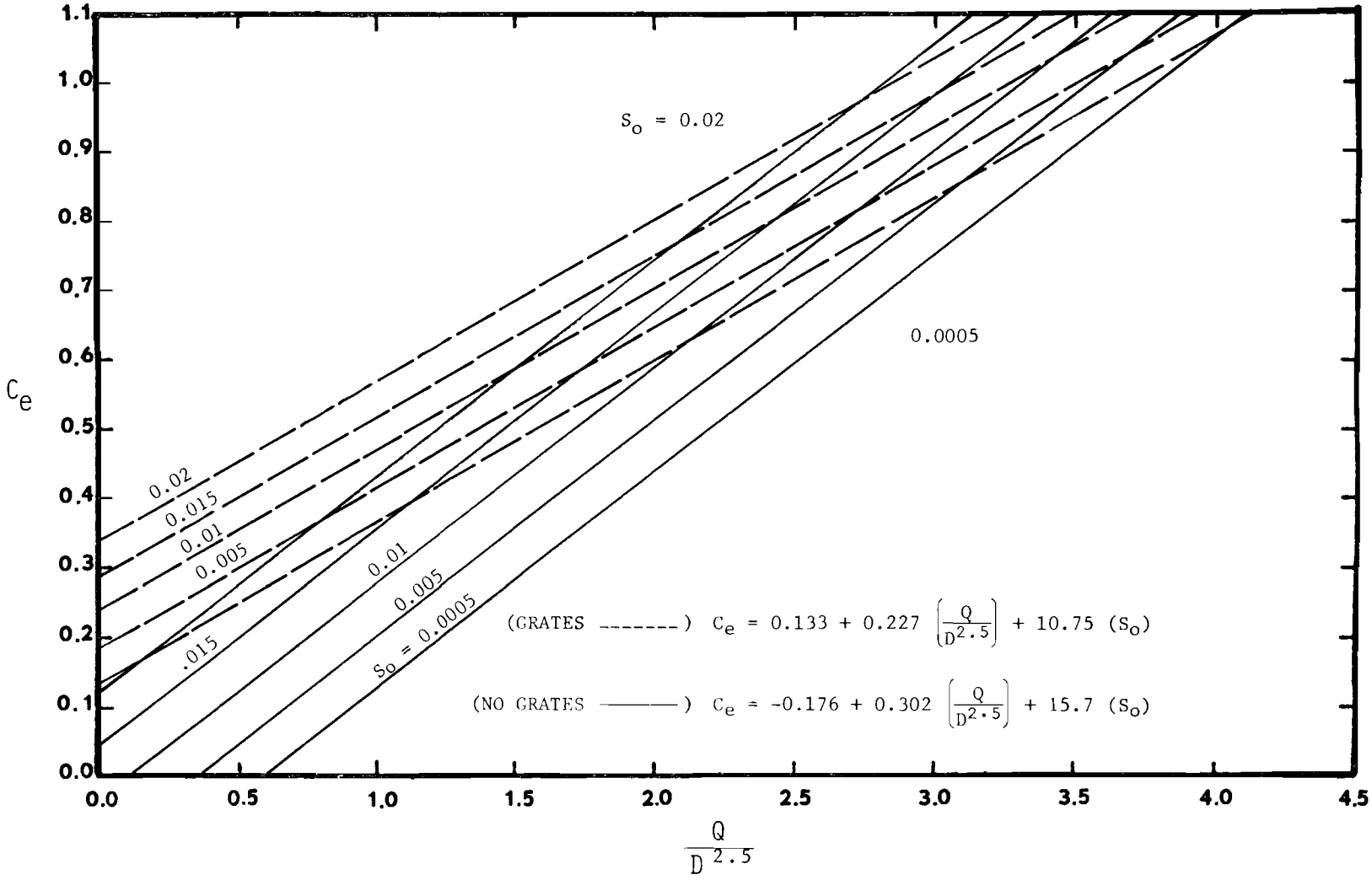


Figure 5.9 Entrance Headloss Coefficient for Submerged and Unsubmerged Conditions Combined, Grates and No Grates (Eqs. 5.13, 5.12)

The simplest form of the equation for $C_e$ is 3 in Table 5.2 The regression equation for no grates is

$$C_e = -0.0003 + 0.272 \left(\frac{Q}{D^{2.5}}\right) \tag{5.14}$$

and for grates installed is

$$C_e = 0.253 + 0.206 \left(\frac{Q}{D^{2.5}}\right) \tag{5.15}$$

The coefficients of determination for these equations are 0.874 for Eq. (5.14) and 0.904 for Eq. (5.15). These equations are plotted in Fig. 5.10.

Figure 5.11 is a comparison for no grates of Eqs. 5.12 (for $S_o$ = 0.0007 and 0.008), Eq. 5.14 and Eq. 5.16 (from Eq. 4 in Table 5.2),

$$C_e = 0.392 + 0.045 \left(\frac{Q}{D^{2.5}}\right)^2 \tag{5.16}$$

The coefficient of determination for Eq. 5.16 is 0.85.

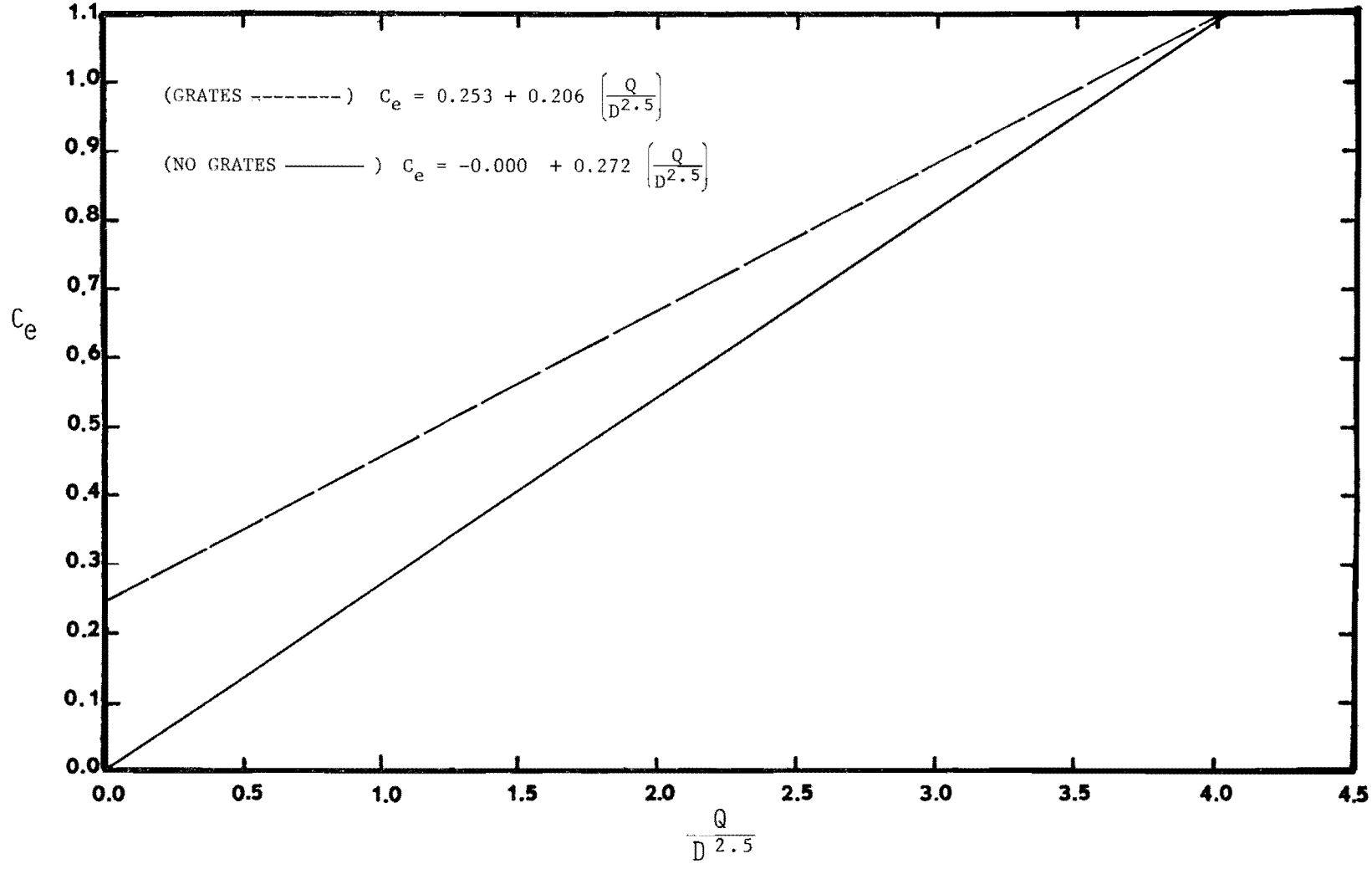


Figure 5.10 Entrance Headloss Coefficient for Submerged and Unsubmerged Conditions Combined, Grates and No Grates (Eqs. 5.15, 5.14)

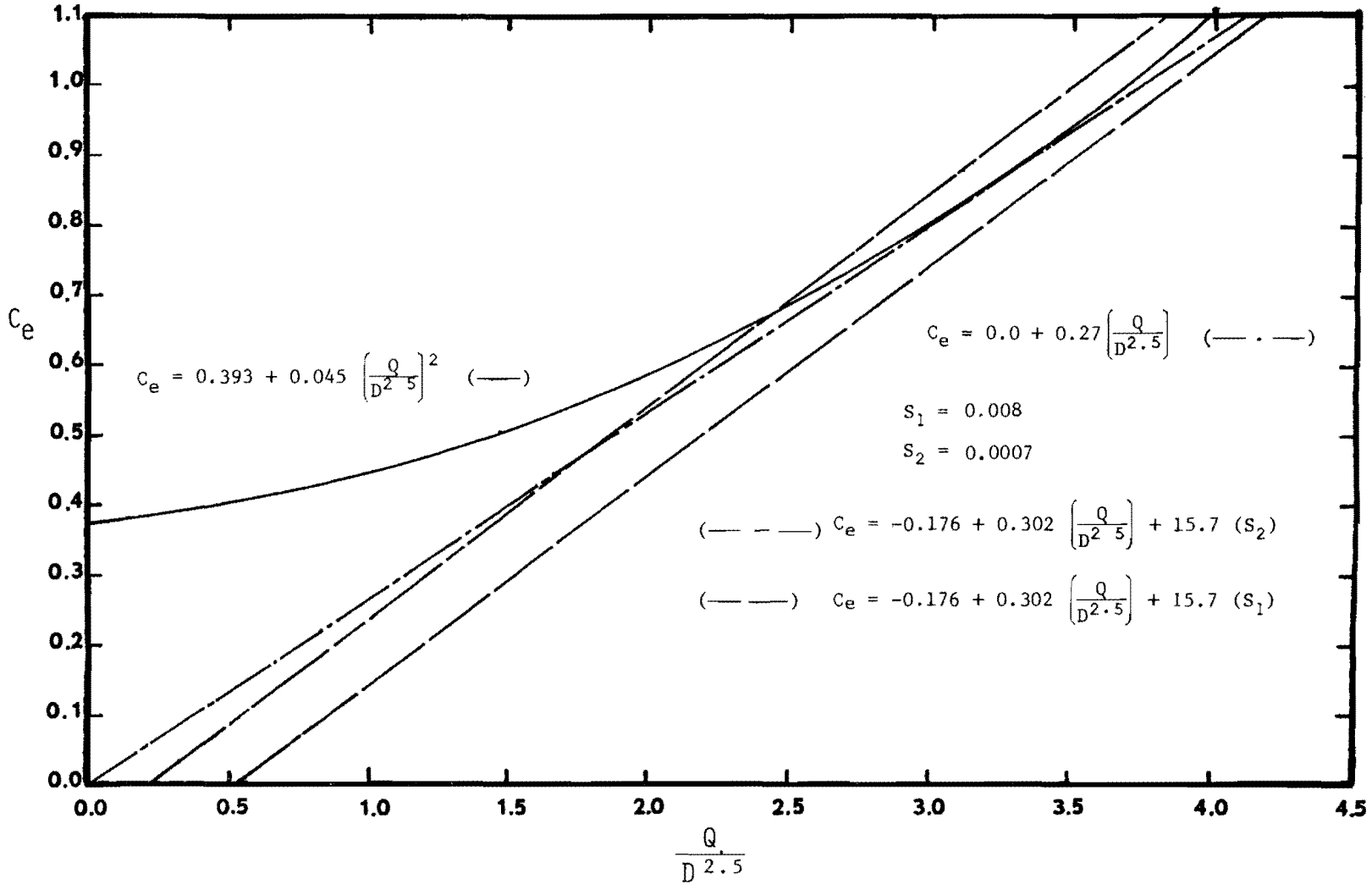


Figure 5.11 Entrance Headloss Coefficient for Submerged and Unsubmerged Conditions Combined, No Grates (Eqs. 5.12, 5.14, 5.16)

# CHAPTER 6 CONCLUSIONS

## 6.1 Conclusions for Box Culvert Model

### 6.1.1 Pipe Safety Grates

Based on the experimental study for the box culvert using pipe safety grates, the following conclusions are made:

1. For steep and mild slope regimes with full barrel flow, the pipe safety grates increased the entrance headloss only slightly. The comparison of $C_e$ values with and without the safety grates (Figs. B.1 - B.5) indicate only a small increase in the entrance headloss coefficient for outlet control with slopes .0008 and .0063 and for inlet control with slopes .0108 and .0128. For slope .0013 (outlet control) the entrance headloss coefficient was not affected by the safety grates.
2. For full flow conditions and for submerged entrance conditions (Type 4A and 4B flow regimes), the pipe safety grates have little effect on the entrance headloss coefficient. Referring to the comparison plots of the $C_e$ values with and without safety grates installed (Figures B.1 - B.5), the data points for Type 4A and 4B flow regimes appear scattered and the regression lines generally have the lowest correlation coefficients (Table 3.1).
3. The headwater depth was not measurably affected by the installation of the pipe safety grates. Referring to the headwater versus discharge plots (Figures B.9 -B.13), the data points

with the safety grates plotted almost identical with the data points without safety grates. Referring to the headwater versus tailwater plots (Figures B.33 - B.47), the data points with and without the pipe safety grates are approximately the same.

4. Conventional hydraulic design of culverts uses a constant entrance headloss coefficient for all Types of flow conditions. However, based upon this experimental study, the entrance headloss coefficient can vary with headwater, discharge, tailwater, and consequently with flow regime. From the entrance headloss coefficient versus headwater plots (Figures B.17 - B.21), the entrance headlosses increased with an increase in headwater depth. The increase in headwater was due to increases in tailwater and/or discharge. The maximum entrance headloss coefficients were obtained for $(\frac{HW}{D})$ greater than approximately 1.5. The lower $C_e$ values were generally for outlet control with an unsubmerged entrance. The higher entrance headloss coefficients were for full culvert flow conditions.

5. The entrance headloss coefficient can be determined by regression equations based on combinations of headwater, tailwater, slope, and dishcarge. The regression equations with the best fit were for outlet control with unsubmerged entrance conditions (Type 1 and 2 flow regimes) and for submerged entrance with outlet control conditions (Type 4B flow regimes).

6. When the pipe safety grates experience clogging greater than 45 percent, the headwater and the entrance headloss coeffici-

ents increased dramatically (Figures B.1 - B.11 and B.20 - B.31, respectively), and the efficiency of the culvert was substantially decreased. The increase in headwater and entrance headloss coefficient was higher for the larger discharges. While there is an obvious propensity for clogging with safety grates, this study did not incude an evaluation of that propensity.

6.1.2 Bar Safety Grates

Based on the experimental testing program for the bar safety grates, the following conclusions are made:

1. The entrance headloss coefficients for the bar safety grates were higher than without the safety grates. The comparison of entrance headloss coefficients with and without bar safety grates (Figs. B.7 - B.9) indicate an increase in $C_e$ for all flow regimes tested on slopes 0.0008 and 0.0108 and an increase in $C_e$ for Type 2 and 4B flow regimes for the slope 0.0063. The data points for Type 1 and 4A flow regimes were rather scattered for slope 0.0063.

2. Along with the increase in the entrance headloss coefficients, there was a corresponding increase in the headwater due to the bar safety grates. Referring to the headwater versus discharge plots (Figs. B.14 - B.16), the bar safety grates caused higher headwaters than with no safety grates under similar condtions. The increase in headwater was also evident in the headwater versus tailwater plots (Figs. B.34 - B.47). The headwater depths with the bar safety grates were higher than the headwater depths without the safety grates for the same discharge and

tailwater. The increase in headwater due to the bar safety grates was less obvious for higher tailwater depths. The higher tailwater depths were less stable in this experiment, and thus less accurate.

3. The entrance headloss coefficient with the bar safety grates were also varied with headwater, discharge, tailwater, and flow regime. The entrance headloss coefficient increased with an increase in headwater as evident by the entrance headloss coefficient versus headwater plots (Figs. B.22 - B.24). The maximum $C_e$ values were again obtained for $\frac{HW}{D}$ greater than 1.5. Outlet control with unsubmerged entrance (Type 1 flow regime) and full flow conditions (Type 4A flow regime) had the lowest and highest entrance headloss coefficients, respectively.

4. The developed regression equations for the bar safety grates can be used to determine the entrance headloss coefficients for Type 1, 2, 4B, and to a lesser extent, 4A flow regimes (Table 3.5). For the bar safety grates, the empirical curves (Table 3.6) were also determined for inlet control flow conditions (Type 3A flow regime).

5. The bar safety grates experienced the same response as the pipe safety grates did to clogging. The entrance headloss coefficient and headwater increased rapidly above 45 percent clogging and the increase was greater for the higher discharges (Figs. B.15 - B.12 and B.22 - B.35, respectively).

6.1.3 Summary of Regression Equations for Design

1. Regression equations have been developed for determining the headwater-discharge relationships for inlet control. Five equations (1st order to 5th order polynomials) were developed for each situation, with or without pipe safety grates and with bar safety grates. The effect of pipe grates were insignificant so the same equations can be used with or without these grates. The regression coefficients are summarized in Table 3.3. The fifth order equation for no grates is

$$\frac{HW}{D} = 1.888 - 3.745 \left(\frac{Q}{BD^{1.5}}\right) + 3.631 \left(\frac{Q}{BD^{1.5}}\right)^2 - 1.539 \left(\frac{Q}{BD^{1.5}}\right)^3 + 0.307 \left(\frac{Q}{BD^{1.5}}\right)^4 - 0.231 \left(\frac{Q}{BD^{1.5}}\right)^5$$

and for the bar grates installed is

$$\frac{HW}{D} = 1.3236 - 2.661 \left(\frac{Q}{BD^{1.5}}\right) + 2.907 \left(\frac{Q}{BD^{1.5}}\right)^2 - 1.333 \left(\frac{Q}{BD^{1.5}}\right)^3 + 0.2843 \left(\frac{Q}{BD^{1.5}}\right)^4 - 0.0226 \left(\frac{Q}{BD^{1.5}}\right)^5$$

2. Recommended regression equations for design considering submerged inlet, outlet control conditions are:

No Grates

$$C_e = 0.421 + 0.102 \left(\frac{Q}{BD^{1.5}}\right) - 0.348 \left(\frac{HW-TW}{D}\right) \qquad (6.1)$$

Pipe Safety Grates

$$C_e = 0.474 + 0.080 \left(\frac{Q}{BD^{1.5}}\right) - 0.254 \left(\frac{HW - TW}{D}\right) \qquad (6.2)$$

Bar Safety Grates

$$C_e = 0.616 + 0.063 \left(\frac{Q}{BD^{1.5}}\right) - 0.433 \left(\frac{HW - TW}{D}\right) \quad (6.3)$$

3. Recommended regression equations for design considering unsubmerged inlet, outlet control conditions are:

No Grates

$$C_e = -0.040 + 1.000 \left(\frac{HW}{D}\right) - 0.276 \left(\frac{Q}{BD^{1.5}}\right) \quad (6.4)$$

Pipe Safety Grates

$$C_e = -0.122 + 1.046 \left(\frac{HW}{D}\right) - 0.262 \left(\frac{Q}{BD^{1.5}}\right) \quad (6.5)$$

Bar Safety Grates

$$C_e = -0.213 + 1.448 \left(\frac{HW}{D}\right) - 0.366 \left(\frac{Q}{BD^{1.5}}\right) \quad (6.6)$$

4. Recommended regression equations for design developed considering both submerged and unsubmerged inlet, outlet control conditions are:

No Grates

$$C_e = -0.187 + 0.614 \left(\frac{HW}{D}\right) - 0.060 \left(\frac{Q}{BD^{1.5}}\right) \quad (6.7)$$

Pipe Safety Grates

$$C_e = -0.172 + 0.479 \left(\frac{HW}{D}\right) + 0.001 \left(\frac{Q}{BD^{1.5}}\right) \quad (6.8)$$

Bar Safety Grates

$$C_e = 0.025 + 0.643 \left(\frac{HW}{D}\right) - 0.111 \left(\frac{Q}{BD^{1.5}}\right) \quad (6.9)$$

5. The inclusion of the $(\frac{HW}{D})$ term in Eqs. 6.1-6.9 will add yet another level of trial and error manipulations to the standard procedure of culvert design. A possible procedure would use a first estimate of $C_e$ to obtain, as per standard procedures, values for $(\frac{HW}{D})$ and $(\frac{Q}{BD^{1.5}})$. Next a new value for $C_e$ could be obtained using the appropriate equation (6.1-6.9), etc, until a solution is converged upon.

## 6.2 Conclusions for Pipe Culvert Model

The following conclusions were made based upon the experimental study using the 15-inch diameter helical corrugated metal pipe culvert:

1. At low discharges, the entrance coefficients are substantially higher for the grate treatment than for the no grate conditions. The effect of the grates on the entrance coefficient is more significant at higher discharges. (Figs. E.1 - E.2, E.14 - E.19).
2. Headwater depth increases linearly with increasing discharge up to headwater depths equal to approximately 1.2 times the culvert diameter. The effect of the safety grates on headwater depth is virtually constant throughout the discharge range. (Figs. E.3 - E.5).
3. The entrance coefficient for the safety grate condition is higher than that for the no grate condition for unsubmerged inlets. The effect of safety grates on the entrance coefficient is relatively constant for a submerged inlet (Fig. E.12). The coefficient for both conditions increses substantially for an unsubmerged inlet (Fig. E.11).

4. The entrance coefficient increases substantially for increasing discharge for a submerged entrance (Fig. E.14).

5. Headwater depth is unaffected by rising tailwater depth for less than critical depths (Figs. E.20 - E.23).

6. The flatter the slope, the greater the effect of tailwater depth on headwater depth (Figs. E.22 - E.23).

7. For available headwall elevations greater than 1.2 times the culvert diameter, the effects of safety grate treatment on design criteria is insignificant. For available headwall elevations less than 1.2 times the culvert diameter, the effect of safety grate treatment on design criteria is substantial.

8. Regression equations have been developed for determining the headwater-discharge relationships for inlet control for no grates and for grates installed. Five equations (1st order to 5th order polynomials) were developed for each situation, with and without grates. The regression coefficients are summarized in Table 5.1. The fifth order equation for no grates is

$$\left(\frac{HW}{D}\right) = 0.236 + 1.088\left(\frac{Q}{BD^{1.5}}\right) + \left(\frac{Q}{BD^{1.5}}\right)D^2 + 0.482\left(\frac{Q}{BD^{1.5}}\right)^3 + 0.099\left(\frac{Q}{BD^{1.5}}\right)^4 + 0.007\left(\frac{Q}{BD^{1.5}}\right)^5$$

and for grates installed is

$$\left(\frac{HW}{D}\right) = -\ 0.774 + 2.775\left(\frac{Q}{BD^{1.5}}\right) - 1.999\left(\frac{Q}{BD^{1.5}}\right)^2 + 0.749\left(\frac{Q}{BD^{1.5}}\right)^3 - 0.732\left(\frac{Q}{BD^{1.5}}\right)^4 + 0.009\left(\frac{Q}{BD^{1.5}}\right)^5$$

9. Regression equations for outlet control conditions were developed for determining $C_e$ for use in design procedures. The

suggested equations for submerged conditions are summarized as follows:

No Grates - Submerged Inlet

$$C_e = -0.044 + 0.262 \left(\frac{Q}{D^{2.5}}\right) + 17.155 (S_o) \quad (6.10)$$

or

$$C_e = 0.145 + 0.230 \left(\frac{Q}{D^{2.5}}\right) \quad (6.11)$$

Grates Installed - Submerged Inlet

$$C_e = 0.117 + 0.231 \left(\frac{Q}{D^{2.5}}\right) + 11.252 (S_o) \quad (6.12)$$

or

$$C_e = 0.241 + 0.210 \left(\frac{Q}{D^{2.5}}\right) \quad (6.13)$$

The suggested equations for submerged and unsubmerged conditions combined are summarized as follows:

No Grates - Submerged and Unsubmerged Inlets

$$C_e = -0.176 + 0.302 \left(\frac{Q}{D^{2.5}}\right) + 15.705 (S_o) \quad (6.14)$$

or

$$C_e = -0.0000 + 0.272 \left(\frac{Q}{D^{2.5}}\right) \quad (6.15)$$

Grates Installed - Submerged and Unsubmerged Inlets

$$C_e = 0.133 + 0.227 \left(\frac{Q}{D^{2.5}}\right) + 10.754 (S_o) \quad (6.16)$$

or

$$C_e = 0.253 + 0.206 \left(\frac{Q}{D^{2.5}}\right) \quad (6.17)$$

10. As discussed in Chapter 5, the extrapolation of the test results for the pipe culvert model should be done with caution keeping in mind that the corrugation sizes were not properly modeled.

## 6.3 Final Discussion

In the process of investigating the hydraulic performance of culverts with safety grates, experimental data was also collected and analysed for the same culverts with no safety grates in place. Typical design procedure incorporates conservative estimates for $C_e$ which vary with entrance geometry and culvert type, but are considered independent of slope, HW, TW and Q. The equations presented here suggest that $C_e$ can vary with slope, HW, TW and/or Q. Comparison for a given flow situation, of the $C_e$ values calculated from the noted equations, whether with or without safety grates, with the value provided by typical practice can provide insight leading to more effective design of highway culverts.

## REFERENCES


1. American Iron and Steel Institute, Handbook of Steel Drainage and Highway Construction, 2nd Edition, 1971.

2. Blaisdell, F. W., "Flow in Culvert and Related Design Philosophies", Journal of the Hydraulics Division, ASCE, Vol. 92, March, 1966, pp. 19-31.

3. Bossey, H. G., "Hydraulics of Conventional Highway Culverts", U.S. Department of Commerce, Bureau of Public Roads, Unpublished paper, August, 1961.

4. Chow, V. T., Open Channel Hydraulics, Mc-Graw-Hill Book Co., 1959, pp. 475-480.

5. French, J. L., Discussion of "Tests on Circular-Pipe-Culvert Inlets", Highway Research Board, Bulletin 126, January, 1955, pp. 20-22.

6. French, J. L., "Effect of Approach Channel Characteristics on Model Pipe Culvert Operation", National Bureau of Standards Report No. 5306, June 3, 1957.

7. French, J. L., "Tapered Box Culvert Inlets - Sixth Progress Report on Hydraulics of Culverts", National Bureau of Standards Report 9355, June, 1966.

8. Mavis, F. T., "The Hydraulics of Culverts", Bulletin 56, Engineering Experiment Station, Pennsylvania State College, 1942, pp. 1-29.

9. Schiller, R. E., "Tests on Circular-Pipe-Culvert Inlets", Highway Research Board, Bulletin 126, January 1955, pp. 11-19.

10. Shoemaker, R. H. and Clayton, L. A., "Model Studies of Tapered Inlets for Box Culvert", Highway Research Board, Research Report 15-B, January, 1953.

11. State Department of Highways and Public Transportation in Texas, THYSYS, Bridge Division.

12. State Department of Highways and Public Transportation in Texas, Hydraulic Manual, Bridge Division, September, 1970, pp. IV 1-68.

13. Statistical Engineering Laboratory at The National Bureau of Standards, OMNITAB, 1966.

14. University of Texas Computation Center, RLFOR, Austin, Texas.

15. U.S. Department of Transportation, "Hydraulic Charts for the Selection of Highway Culverts", Hydraulic Engineering Circular No. 5, December, 1965, pp. 1-54.

16. U.S. Department of Transportation, "Capacity Chart for the Hydraulic Design of Highway Culverts", Hydraulic Engineering Circular No. 10, March, 1965, pp. 1-90.

17. U.S. Department of Transportation, "Hydraulic Design of Improved Inlets for Culverts", Hydraulic Engineering Circular No. 13, August, 1972, pp. 1-172.

# APPENDIX A

User's Manual And Fortran Listing

For Computer Program

"CULVERT"

## Appendix A.1

## User's Manual for Computer Program "CULVERT"

The computer program, CULVERT, was designed to convert test data into headwater, tailwater, discharge, energy gradeline, and hydraulic gradeline measurements. CULVERT was able to analyze test data from both box and cirular culverts. The output from the program consisted of two entrance headloss coefficients, the critical depth, the critical slope, and HW/D, TW/D, and $Q/BD^{1.5}$ values. The entrance headloss coefficient was determined by both the energy and the hydraulic gradelines. The CULVERT output format was modified for use in several plotting routines and for the OMNITAB II and RLFOR statistical programs.

The arrangements and descriptions of the input cards are given as follows.

Input Data

The first data card will identify the culvert type being tested. a one or a two will mean a circular culvert, while a three or a four will identify a box culvert. The format is

| FORTRAN Name | Format | Card Column | Description |
|---|---|---|---|
| SHAPE | I5 | 1- 5 | Type of culvert being tested |

The second data card will read in the slope, the physical dimensions, and the Manning's n for the culvert. The format is as follows:

| FORTRAN Name | Format | Card Column | Description |
|---|---|---|---|
| SLOPE | F10.5 | 1-10 | The measured slope of the culvert |
| LENGTH | F10.5 | 11-20 | The measured length of the culvert in feet |
| MANN | F10.5 | 21-30 | The assumed Manning's n for the culvert |
| WIDE | F10.5 | 31-40 | The width of the culvert in feet. Diameter (DIAM) if the culvert is circular. |
| HIGH | F10.5 | 41-50 | The height of the culvert in feet. Leave blank for circular culvert. |

The third data set contains conversion factors which will change the raw measured data into actual measurements of headwater, tailwater, discharge, and hydraulic depth in the culvert. The determination of each conversion factor is given in Section 2.6, Testing of Data Reduction. The format is

| FORTRAN Name | Format | Card Column | Description |
|---|---|---|---|
| HWLELE | F10.5 | 1-10 | Conversion factor for the left upstream gauge measurement |
| HWRELE | F10.5 | 11-20 | Conversion factor for the right upstream gauge measurement |
| TWLELE | F10.5 | 21-30 | Conversion factor for the discharge channel piezometer |
| WEIREL | F10.5 | 31-40 | Conversion factor for the weir point gauge reading |
| GAGEL | F10.5 | 41-50 | Conversion factor for gauges 1 through 12 |

(continued)

| FORTRAN Name | Format | Card Column | Description |
|---|---|---|---|
| GAGOUT | F10.5 | 51-60 | Conversion factor for gauge 12 |

The fourth and fifty data cards will read in the distances that the twelve piezometers are from the culvert entrance. The format is

| FORTRAN Name | Format | Card Column | Description |
|---|---|---|---|
| DY(I) | F10.5 | 1-80 | Location of each piezometer along the culvert in feet. I = 1 through 12. |

The sixth data card reads in the discharge, date, and other information for each different safety grate test. This card, along with the following cards, will be repeated for each test conducted. The format is as follows:

| FORTRAN Name | Format | Card Column | Description |
|---|---|---|---|
| HWEIR | F10.5 | 1-10 | Measurement of the weir point gauge in feet. A 9999.0 will terminate the program. |
| B | A10 | 21-80 | The date, the tailwater conditions, the grate type, and other pertinent information of the test. |

The next two data cards will give the actual measurement for each safety grate test. These data cards are repeated each time the safety grates are removed or installed. A one in column 5 of the first card will mean the test was run without any safety grates in place. A test with just an upstream safety grate will have a two. With both safety grates, a three will be in column 5. The format of the first card is as follows:

| FORTRAN Name | Format | Card Column | Description |
|---|---|---|---|
| ICOND | I5 | 1- 5 | Location of the safety grates<br>1 = No safety grates,<br>2 = Upstream safety grate,<br>3 = Both safety grates |
| DX(I) | F10.0 | 11-80 | Piezometric readings inside the culvert. |

The format of the second card is as follows:

| FORTRAN Name | Format | Card Column | Description |
|---|---|---|---|
| DX(I) | F10.0 | 1-50 | Remaining piezometric readings |
| HWL | F10.0 | 51-60 | Upstream left point gauge measurement |
| HWR | F10.0 | 61-70 | Upstream right point gauge measurement |
| TWL | F10.0 | 71-80 | Discharge channel piezometer reading. |

# APPENDIX A.2

Listing of Computer Program

"CULVERT"

```
      PROGRAM CULVERT(INPUT,OUTPUT,TAPE1,TAPE2,TAPE3,TAPE4,TA
PE5,TAPE6,
     1TAPE7,TAPE8,TAPE9)
      REAL MANN,LENGTH
      INTEGER SHAPE
      DIMENSION A(3),B(6),DY(12),DX(12),EGL(12)
      DATA A(1)/1HW-O GRATES/,A(2)/1HW-US GRATE/,A(3)/1HBO
THGRATES/
      DATA C/1H*NO--DATA*/,NT/1/
C
C*****************************************************************
C**   INPUT CULVERT PROPERTIES
C**   SLOPE,LENGTH,MANNING'S N,AND CULVERT DIMENSIONS
C**     SHAPE  = 1 FOR CIRCULAR CULVERT
C**              4 FOR BOX CULVERT
C**     DIAM   = CIRCULAR CULVERT DIAMETER
C**     WIDE   = BOX CULVERT WIDTH
C**     HIGH   = BOX CULVERT HEIGHT
C*****************************************************************
C
      REWIND NT
      READ 100,SHAPE
      GO TO (1,1,2,2),SHAPE
    1 READ 101,SLOPE,LENGTH,MANN,DIAM
      PRINT 301,DIAM,LENGTH,SLOPE
  301 FORMAT(1H1,4X*CIRCULAR CULVERT MODEL*/5X*DIAMETER (IN F
T.) =*F10.3
     1          ,5X*LENGTH =*F10.3,5X*SLOPE =*F10.4///)
      GO TO 3
    2 READ 101,SLOPE,LENGTH,MANN,WIDE,HIGH
      PRINT 302,HIGH,WIDE,LENGTH,SLOPE
  302 FORMAT(1H1,4X*BOX CULVERT MODEL*/5X*DIMENSION (IN FT.)
:*F10.3,2X,
     1           *BY*F10.3,5X*LENGTH =*F10.3,5X*SLOPE =*F10.4
///)
C
C*****************************************************************
C**   INPUT CONVERSION FACTORS
C**   HWLELE=LEFT UPSTREAM GAGE
C**   HWRELE=RIGHT UPSTREAM GAGE
C**   TWLELE=TAILWATER GAGE
C**   WEIREL=WEIR CONVERSION
C**   GAGEL= GAGES 1 THRU 11
C**   GAGOUT = GAGE 12
C*****************************************************************
C
    3 READ 101,HWLELE,HWRELE,TWLELE,WEIREL,GAGEL,GAGOUT
C
C*****************************************************************
C**   INPUT PIEZOMETERS LOCATIONS IN CULVERT
C*****************************************************************
C
      READ 101,(DY(I),I=1,12)
  100 FORMAT(I5)
  101 FORMAT(8F10.5)
C
C*****************************************************************
C**   READ IN DISCHARGE DATA
C**     HWEIR  = WEIR READING
C**     QPP    = DISCHAGE (CFS)
C*****************************************************************
```

```
C
    4 READ 103,HWEIR,B
  103 FORMAT(F10.5,10X,6A10)
      IF(HWEIR .EQ. 9999) GO TO 999
      HWEIR=HWEIR+WEIREL
      QPP=3.33*4.*HWEIR**1.5
C
C*****************************************************************
C**    COMPUTE CRITICAL DEPTH,CRITICAL SLOPE, AND NORMAL DEPTH
C**      CRITD  = CRITICAL DEPTH
C**      CRSLPE = CRITICAL SLOPE
C**      UDEP   = NORMAL DEPTH
C*****************************************************************
C
      CALL CRITIC(SHAPE,DIAM,HIGH,WIDE,MANN,QPP,CRSLPE,CRITD)
      CALL NOXUD (SHAPE,DIAM,HIGH,WIDE,MANN,QPP,SLOPE,UDEP)
      PRINT 201,QPP,B,MANN,CRITD,UDEP,CRSLPE,SLOPE
  201 FORMAT(//5X,*DISCHARGE = *,F10.5,* CFS*,5X,6A10,/
     1          5X*MANNING =*F7.4,5X*CRITICAL DEPTH =*F7.4,
     1          5X*NORMAL DEPTH =*F7.4,5X*CRITICAL SLOPE=*F7.4

     1          5X*SLOPE=*F7.4//
     1        1X,*CONDITIONS*,5X,*HEAD-WATER*,5X,* E.G.L. DE*
     2         5X,*  H-OVER-D*,5X,*NON-DIMENO*,5X,*HYD.G.L.CE*
     3         5X,* E.G.L. CE*,5X,* TW-OVER-D*/)
C
C*****************************************************************
C**    READ IN HEADWATER,TAILWATER,AND DEPTH DATA IN CULVERT
C**      DX(I)  = PIEZOMETER READINGS
C**      HWL    = LEFT UPSTREAM POINT GAGE
C**      HWR    = RIGHT UPSTREAM POINT GAGE
C**      TWL    = DISCHARGE CHANNEL GAGE
C*****************************************************************
C
    5 READ 102,ICOND,(DX(I),I=1,12),HWL,HWR,TWL
  102 FORMAT(I5,5X,7F10.0/8F10.0)
      IF(HWL .EQ. 0.0) GO TO 9
      IF(TWL .EQ. 0.0) GO TO 10
C
C*****************************************************************
C**    CONVERT TEST DATA INTO ACTUAL MEASUREMENTS
C**      HW     = AVERAGE HEADWATER DEPTH
C**      TW     = TAILWATER DEPTH
C
C*****************************************************************
C
      TW=(TWL/12.)+TWLELE
      GO TO 11
   10 TW=0.0
   11 CONTINUE
      HW=(HWL+HWLELE+HWR+HWRELE)/2.
C
C*****************************************************************
C**    START OF LINEAR REGRESSION BY DETERMING THE
C**    ENERGY AND HYDRAULIC GRADE LINES
C*****************************************************************
C
      XGS=0.0
      XS=0.
      YS=0.
      DN=5.
      DO 25 J=6,10
```

```
      DEPTH=DX(J) + GAGEL
      DEP=DEPTH + SLOPE*DY(J)
      GO TO (35,32,31,31),SHAPE
   32 CALL CIRCLE(DEP,AREA,FSLOPE,DIAM,QPP,MANN)
      GO TO 32
   31 CALL BOX(DEP,AREA,FSLOPE,WIDE,HIGH,MANN,QPP)
   32 VEL=QPP/AREA
      EGL(J)=DEPTH + VEL**2/64.4
      XS=XS + DEPTH
      XGS = XGS + EGL(J)
   25 YS = YS + DY(J)
      XM = XS/DN
      YM=YS/DN
      XGLM=XGS/DN
      EGP=0.0
      XP=0.0
      YP=0.0
      DO 26 K=6,10
      XP=XP+(DX(K)+GAGEL-XM)*(DY(K)-YM)
      EGP=EGP+(EGL(K)-XGLM)*(DY(K)-YM)
   26 YP=YP+(DY(K)-YM)**2
C
C*****************************************************************
C**   CALCULATION OF DEPTH AT ENTRANCE BY EXTRAPOLATION OF
C**   THE ENERGY AND HYDRAULIC GRADELINES
C**     DE      = HYDRAULIC DEPTH
C**     PGAMMA  = ENERGY DEPTH
C*****************************************************************
C
      DE=XM-(XP/YP)*YM
      PGAMMA=XGLM-(EGP/YP)*YM
      TWOD=TW/DIAM
C
C*****************************************************************
C**   CALCULATION OF H-OVER-D,TW-OVER-D,AND AREA OF FLOW
C**     F       = QPP/(B*D**1.5)
C**     HWOD    = HEADWATER/HIGH
C**     TWOD    = TAILWATER/HIGH
C*****************************************************************
C
      GO TO(6,6,7,7),SHAPE
    6 CALL CIRCLE(DE,AREA,FSLOPE,DIAM,QPP,MANN)
      HWOD=HW/DIAM
      F=QPP/DIAM**2.5
      IF(TW.EQ.0.0) GO TO 8
      TWOD=TW/DIAM
      GO TO 8
    7 CALL BOX(DE,AREA,FSLOPE,WIDE,HIGH,MANN,QPP)
      HWOD=HW/HIGH
      F=QPP/(WIDE*HIGH**1.5)
      IF(TW.EQ.0.0) GO TO 8
      TWOD=TW/HIGH
C
C*****************************************************************
C**   DETERMINATION OF AVERAGE VELOCITY
C*****************************************************************
C
    8 VEL=QPP/AREA
C
C*****************************************************************
C**   DETERMINATION OF CE BY USE OF BOTH ENERGY AND
C**   HYDRAULIC GRADE LINES
```

```
C*****************************************************************
C
      CE=(HW-PGAMMA)/(VEL**2/64.4)
      HGCE=(HW-DE)/(VEL**2/64.4)-1
      PRINT 202,A(ICOND),HW,PGAMMA,HWOD,F,HGCE,CE,TWOD
C
C*****************************************************************
C**   SEPARATION OF DATA INTO DIFFERENT FLOW REGIMES
C**   USING TEXAS HWY. DEPT. CRETERIA
C*****************************************************************
C
      SC=CRSLPE
      SL=SLOPE*LENGTH
      DC=CRITD
      IC=ICOND
      IF (SLOPE.GE.SC) GO TO 41
      IF (TW.GT.DC) GO TO 42
      IF (HW.GE.(1.2*HIGH)) GO TO 49
      IF (TW.EQ.0.0) GO TO 46
C
C*****************************************************************
C**   FLOW TYPE 1
C**      SLOPE L.T. CRSLPE
C**      HW    L.T. 1.2*HIGH
C**      TW    L.T. CRITD
C*****************************************************************
C
      WRITE(2,202) A(ICOND),HW,PGAMMA,HWOD,F,HGCE,CE,TWOD
      GO TO 9
   46 IF (ICOND.EQ.2) GO TO 9
      IF (ICOND.EQ.3) IC=2
      WRITE(IC,202) A(ICOND),HW,PGAMMA,HWOD,F,HGCE,CE,TWOD
      GO TO 9
C
C*****************************************************************
C**   FLOW TYPE 4B
C**      HW    G.T. 1.2*HIGH
C**      TW    L.T. HIGH
C*****************************************************************
C
   49 IF (TW.NE.0.0)GO TO 47
      IF (ICOND.EQ.2) GO TO 9
      IF (ICOND.EQ.1) IC=7
      IF (ICOND.EQ.3) IC=8
      GO TO 43
   47 IC=8
   43 WRITE(IC,202) A(ICOND),HW,PGAMMA,HWOD,F,HGCE,CE,TWOD
      GO TO 9
   42 IF (TW.GE.HIGH) GO TO 44
      IF (HW.GE.(1.2*HIGH)) GO TO 47
C
C*****************************************************************
C**   FLOW TYPE 2
C**      SLOPE L.T. CRSLPE
C**      HW    L.T. 1.2*HIGH
C**      TW    G.T. CRITD BUT
C**            L.T. HIGH
C*****************************************************************
C
      WRITE(3,202) A(ICOND),HW,PGAMMA,HWOD,F,HGCE,CE,TWOD
      GO TO 9
   41 IF (TW.GE.SL.AND.TW.LT.(SL+HIGH)) GO TO 45
```

```
      IF (TW.GE.(SL+HIGH)) GO TO 44
C
C*****************************************************************
C**    FLOW TYPE 3A
C**      SLOPE G.T. CRSLPE
C**      TW     L.T. SLOPE*LENGTH
C*****************************************************************
C
      IF (TW.NE.0.0) GO TO 48
      IF (ICOND.EQ.2) GO TO 9
      IF (ICOND.EQ.1) IC=4
      IF (ICOND.EQ.3) IC=5
      GO TO 50
   48 IC=5
    5 WRITE(IC,202) A(ICOND),HW,PGAMMA,HWOD,F,HGCE,CE,TWOD
      GO TO 9
C
C*****************************************************************
C**    FLOW TYPE 4A
C**      SLOPE L.T. CRSLPE AND
C**      TW     G.T. HIGH
C**             OR
C**      SLOPE G.T. CRSLPE AND
C**      TW     G.T. SLOPE*LENGTH + HIGH
C*****************************************************************
C
   44 WRITE(6,202) A(ICOND),HW,PGAMMA,HWOD,F,HGCE,CE,TWOD
      GO TO 9
C
C*****************************************************************
C**    FLOW TYPE 3B
C**      SLOPE G.T. CRSLPE
C**      TW     G.T. SLOPE*LENGTH BUT
C**             L.T. SLOPE*LENGTH + HEIGHT
C*****************************************************************
C
   45 WRITE(9,202) A(ICOND),HW,PGAMMA,HWOD,F,HGCE,CE,TWOD
      GO TO 9
  202 FORMAT(1X,A10,5X,7(F10.5,5X))
    9 IF (ICOND .EQ. 3) GO TO 4
      GO TO 5
  999 STOP
      END
C
C*****************************************************************
      SUBROUTINE BOX(DS,A,S,WIDE,HIGH,MANN,QPP)
C**    ROUTINE TO COMPUTE FLOW AREA, WETTED PARAMETER,
C**    AND NORMAL SLOPE
C**      A       = FLOW AREA
C**      WP      = WETTED PARAMETER
C**      S       = NORMAL SLOPE
C**
C*****************************************************************
C
      REAL MANN
      D=DS
      IF (DS .GE. HIGH) D=HIGH
      A=D*WIDE
      WP=WIDE+D*2.
      R=A/WP
      S=QPP**2.*MANN**2./(2.22*A**2.*R**(4./3.))
      RETURN
```

```
      END
      SUBROUTINE CIRCLE(D5,A,S,DIAM,QPP,MANN)
      REAL MANN
  100 VAL=(2*D5-DIAM)/DIAM
      IF(ABS(VAL).LT.1.) GO TO 20
      THETA=3.
      GO TO 21
   20 THETA=2.*ACOS(VAL)
   21 A=DIAM**2./8.*(6.2832-THETA+SIN(THETA))
      AK=1.486*((((6.2832-THETA+SIN(THETA))/8.)**5)/(((6.2832
-THETA)
     1   /2.)**2*(D5/DIAM)**8))**(1./3.)
      S=(QPP*MANN/(AK*D5**(8./3.)))**2
      DC=D5
      SC=S
      RETURN
      END
C*************************************************************
**********
      SUBROUTINE CRITIC(SHAPE,DIAM,HIGH,WIDE,MANN,QPP,CRSLPE,
CRITD)
C     ROUTINE TO COMPUTE CRITICAL DEPTH AND CRITICAL SLOPE
C*************************************************************
**********
      INTEGER SHAPE
      REAL MANN
      GO TO (11,11,12,12), SHAPE
   11 ONE=QPP**2/32.2
      D5=DIAM/2.-.01
      DENOM=2.
    1 IF (DIAM/DENOM .LT. .005) GO TO 3
      CALL CIRCLE(D5,A,CRSLPE,DIAM,QPP,MANN)
      TWO=A**3/(2.*SQRT(D5*DIAM-D5*D5))
      DENOM=DENOM*2.
      IF (ONE - TWO) 2,3,4
    2 D5=D5-DIAM/DENOM
      GO TO 1
    4 D5=D5+DIAM/DENOM
      GO TO 1
    3 CRITD=D5
      GO TO 14
   12 CRITD=(QPP**2./(32.2*WIDE**2.))**(1/3.)
      CALL BOX(CRITD,A,CRSLPE,WIDE,HIGH,MANN,QPP)
   14 RETURN
      END
C
C
C*************************************************************
**********
      SUBROUTINE BOXUD(SHAPE,DIAM,HIGH,WIDE,MANN,QPP,SLOPE,UD
EP)
C     ROUTINE TO COMPUTE THE UNIFORM OR NORMAL DEPTH
C*************************************************************
**********
      REAL MANN
      INTEGER SHAPE
      GO TO (1,2,12,4), SHAPE
    1 THIGH=DIAM*.93818
      HIMAX=DIAM
      GO TO 5
    2 THIGH=HIGH*.9257
      HIMAX=HIGH
```

```
      GO TO 5
    4 THIGH=HIGH
      HIMAX=HIGH
    5 D5=THIGH/2.
      DENOM=4.
    6 GO TO (7,7,10,10), SHAPE
    7 CALL CIRCLE (D5,A,S,DIAM,QPP,MANN)
      GO TO 11
   10 CALL BOX(D5,A,S,WIDE,HIGH,MANN,QPP)
   11 IF(S .GT. SLOPE) GO TO 13
      D5=D5-THIGH/DENOM
      GO TO 14
   13 D5=D5+THIGH/DENOM
   14 IF(THIGH/DENOM .LT. 0.0005) GO TO 12
      DENOM=DENOM*2.
      GO TO 6
   12 UDEP=D5
C     IF((THIGH-UDEP) .LT. 0.0005) UDEP=HIMAX
      RETURN
      END
```

# APPENDIX B

## Graphical Results For Box Culverts

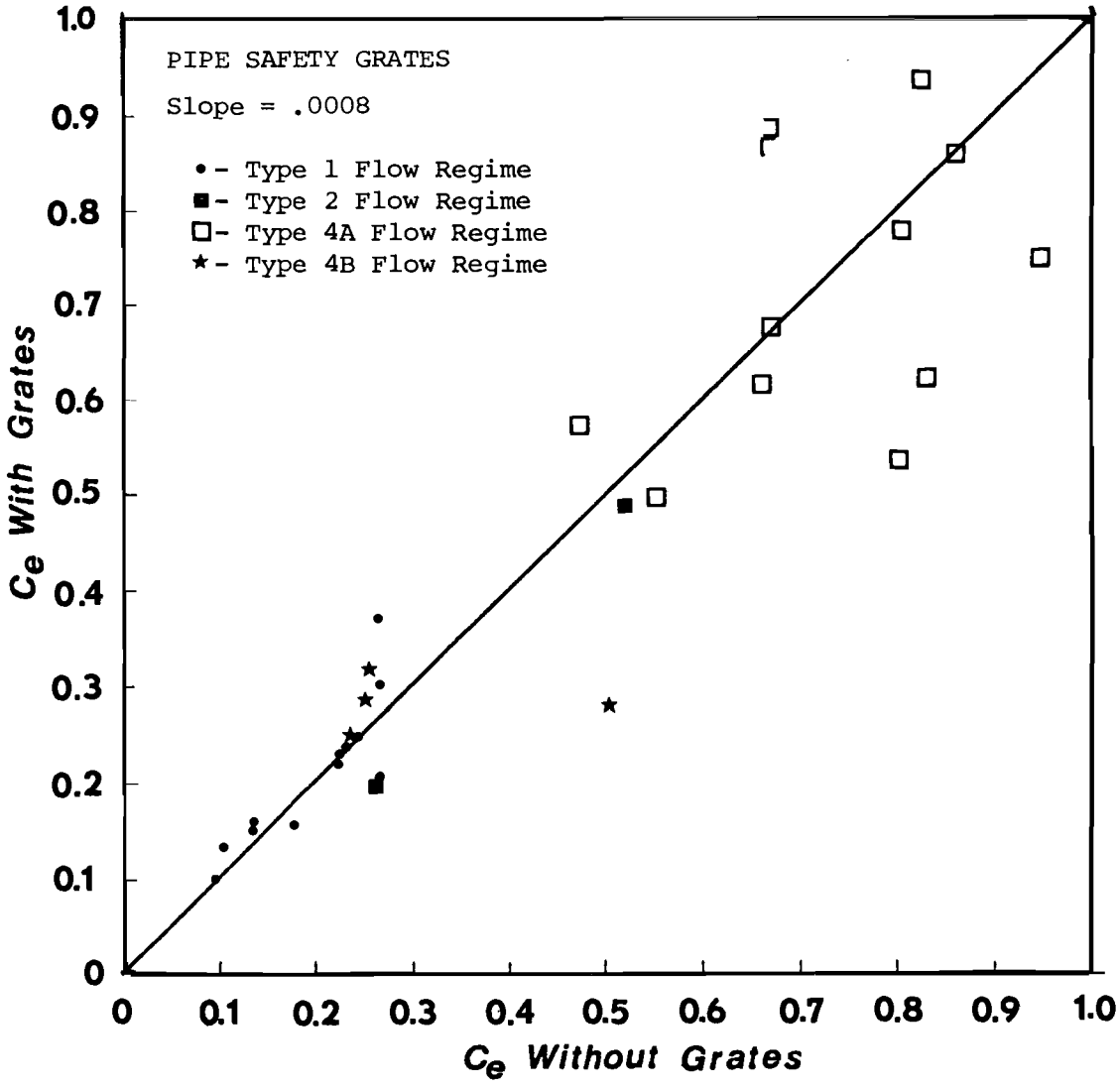


Figure B.1 Comparison of Entrance Headloss Coefficients With and Without Safety Grates, Slope = .0008

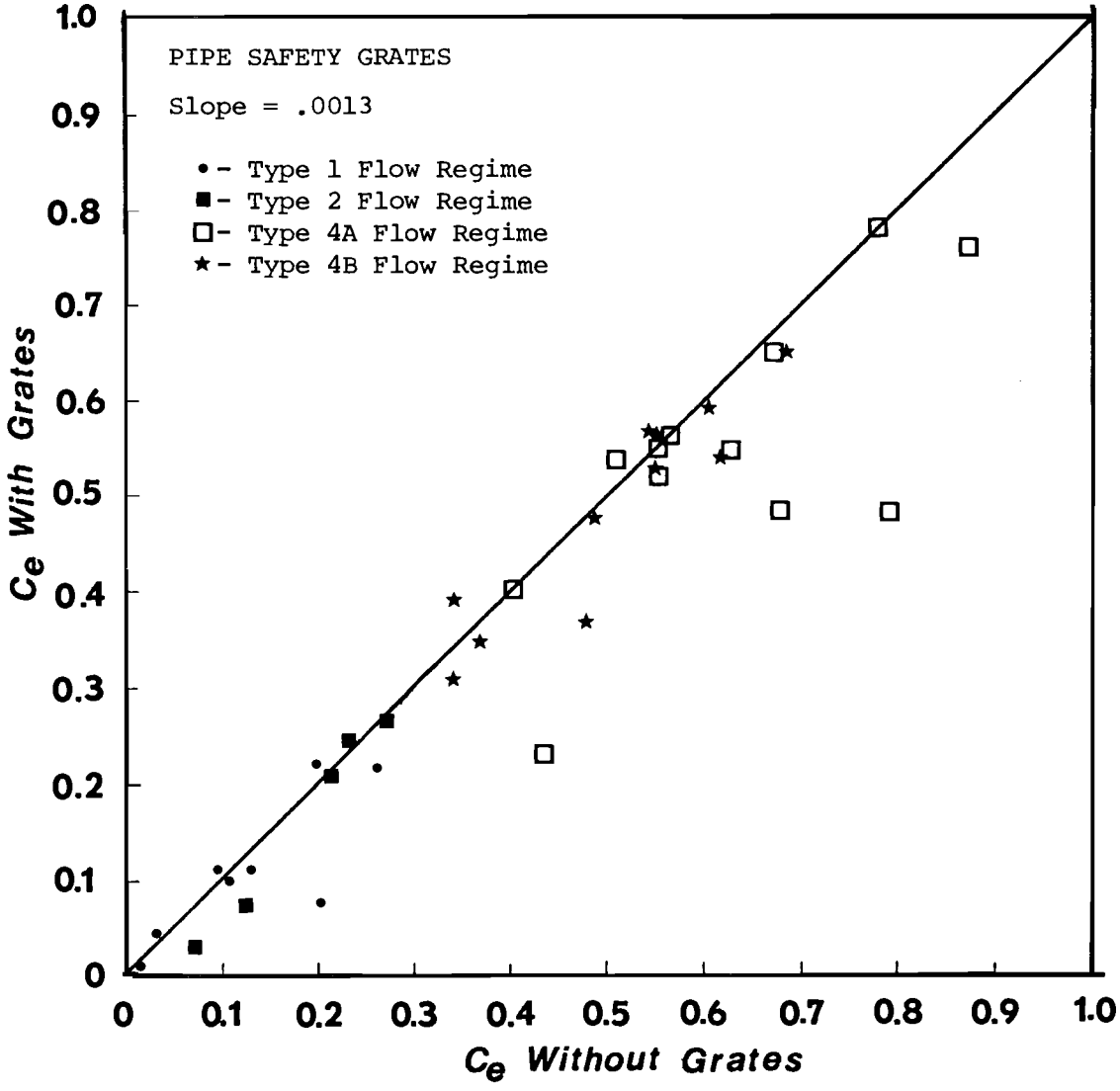


Figure B.2 Comparison of Entrance Headloss Coefficients With and Without Safety Grates, Slope = .0013

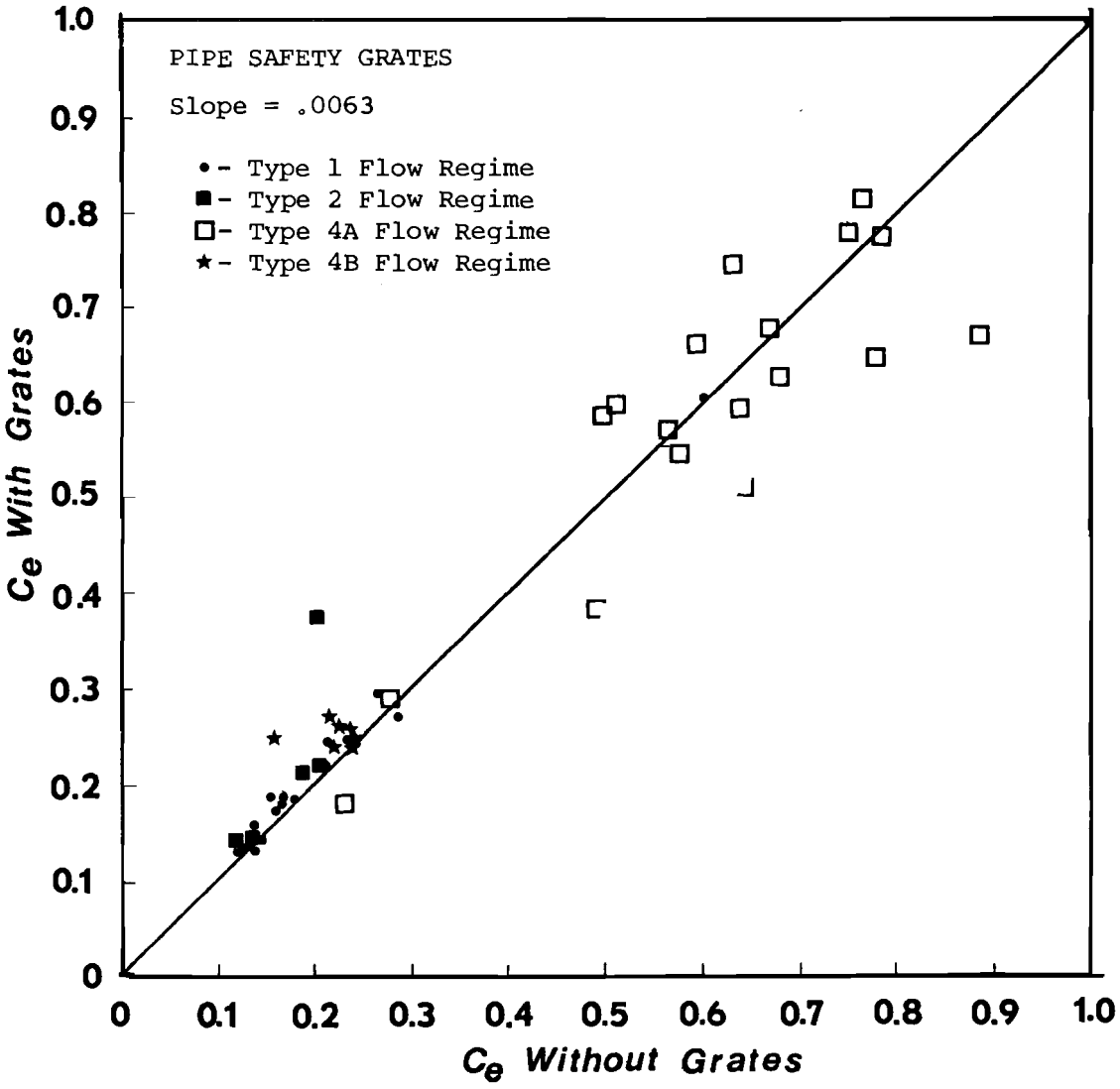


Figure B.3 Comparison of Entrance Headloss Coefficients With and Without Safety Grates, Slope = .0063

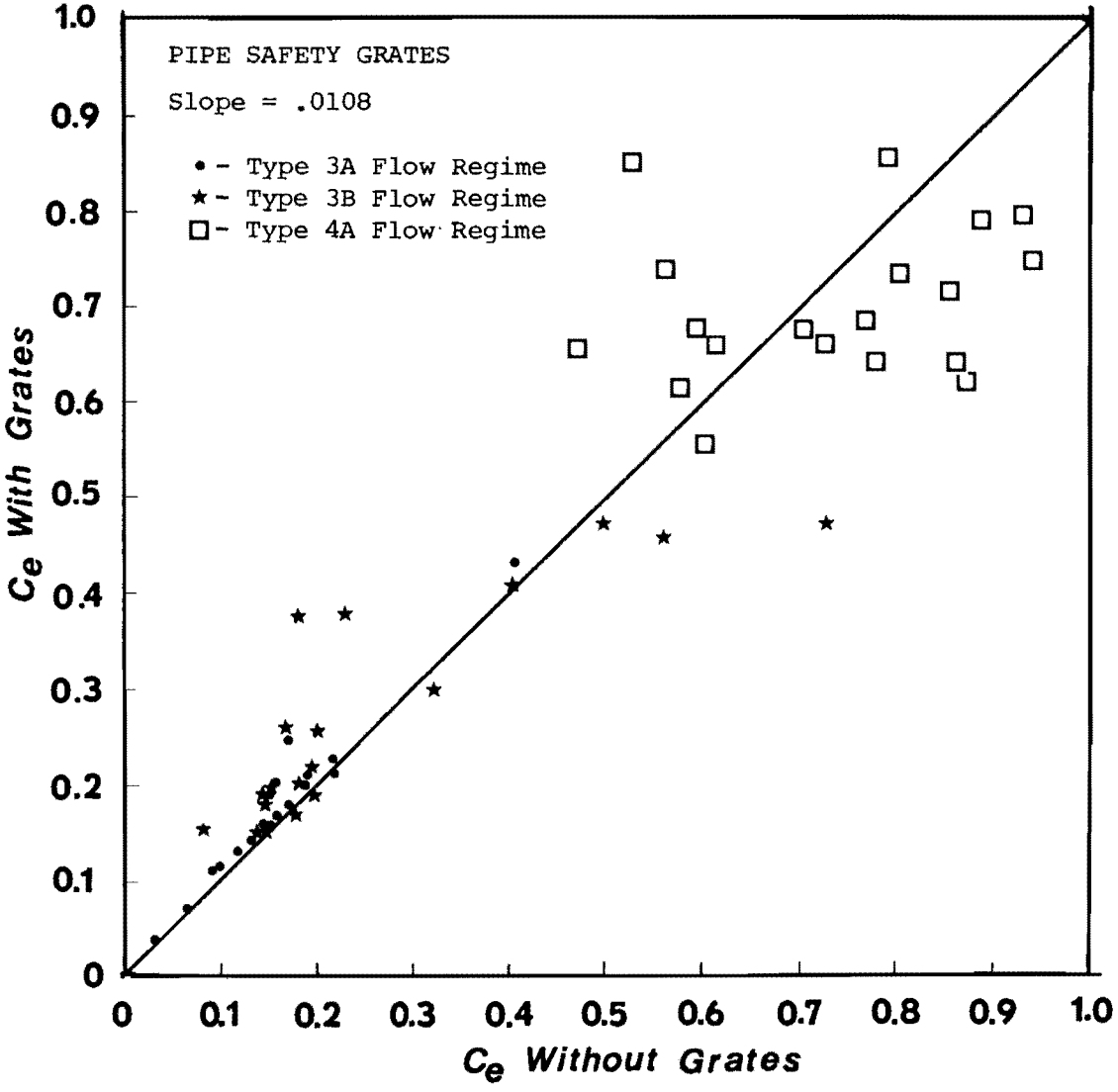


Figure B.4 Comparison of Entrance Headloss Coefficients With and Without Safety Grates, Slope = .0108

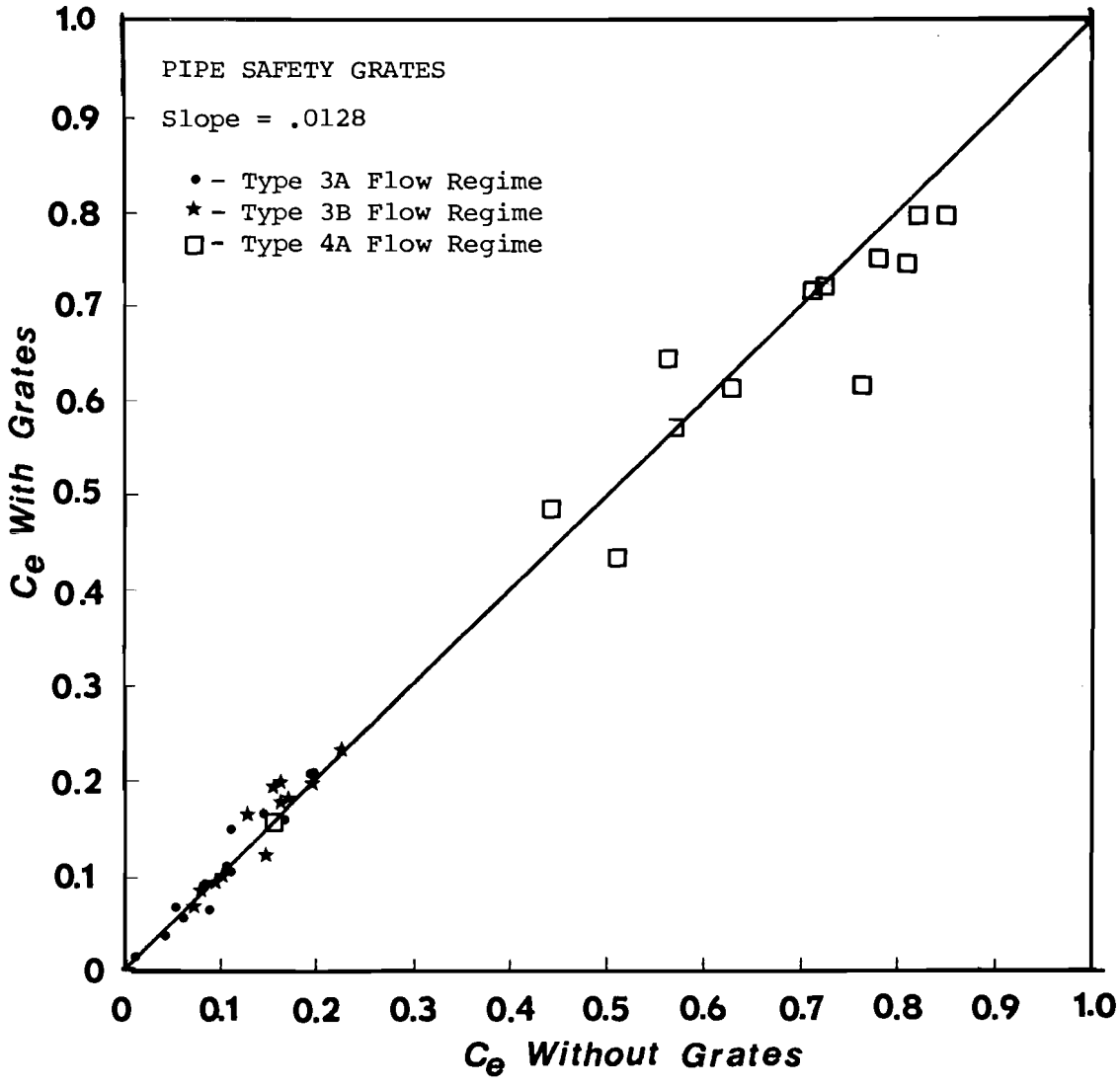


Figure B.5 Comparison of Entrance Headloss Coefficients With and Without Safety Grates, Slope = .0128

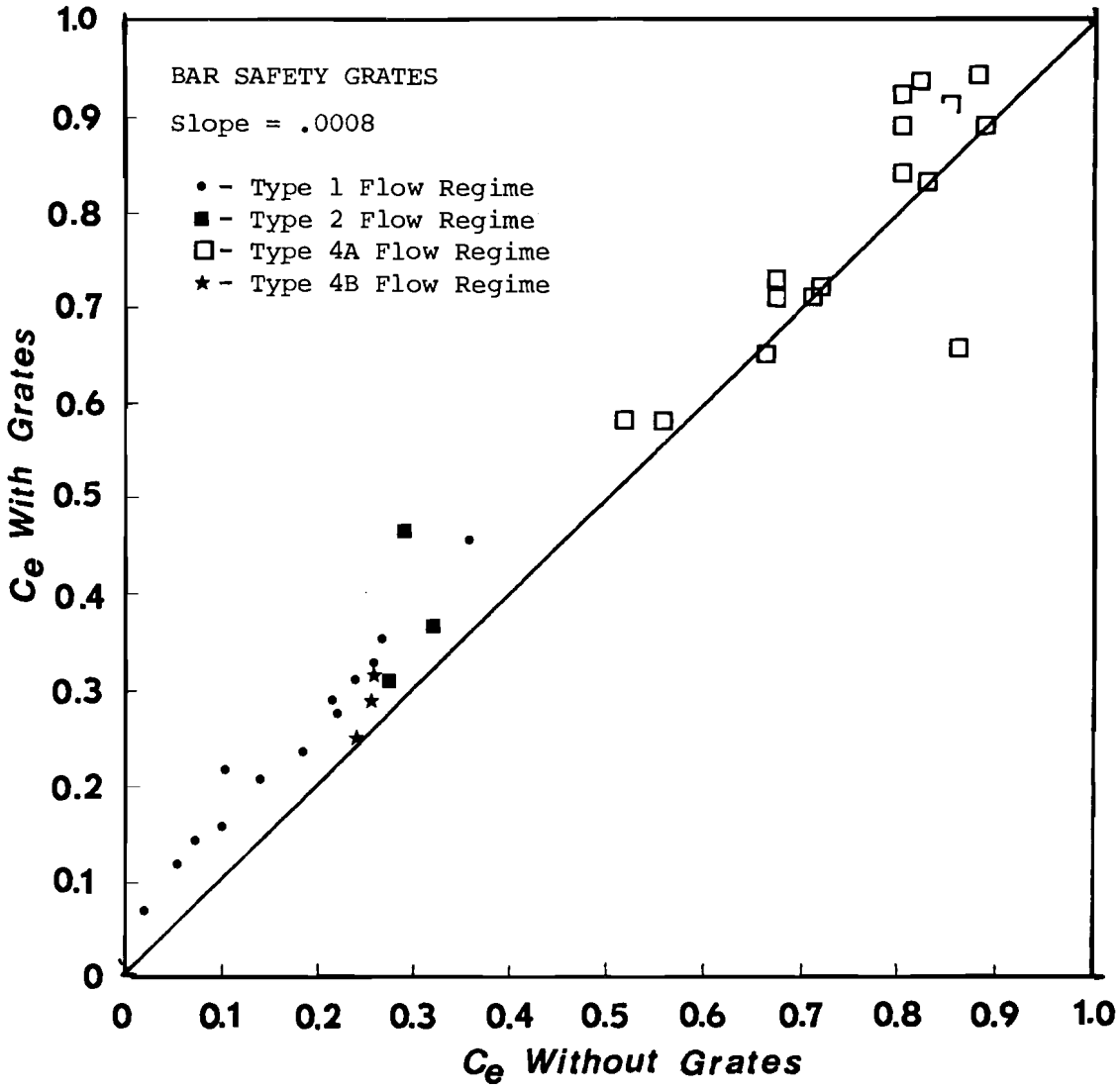


Figure B.6 Comparison of Entrance Headloss Coefficients With and Without Safety Grates, Slope = .0008

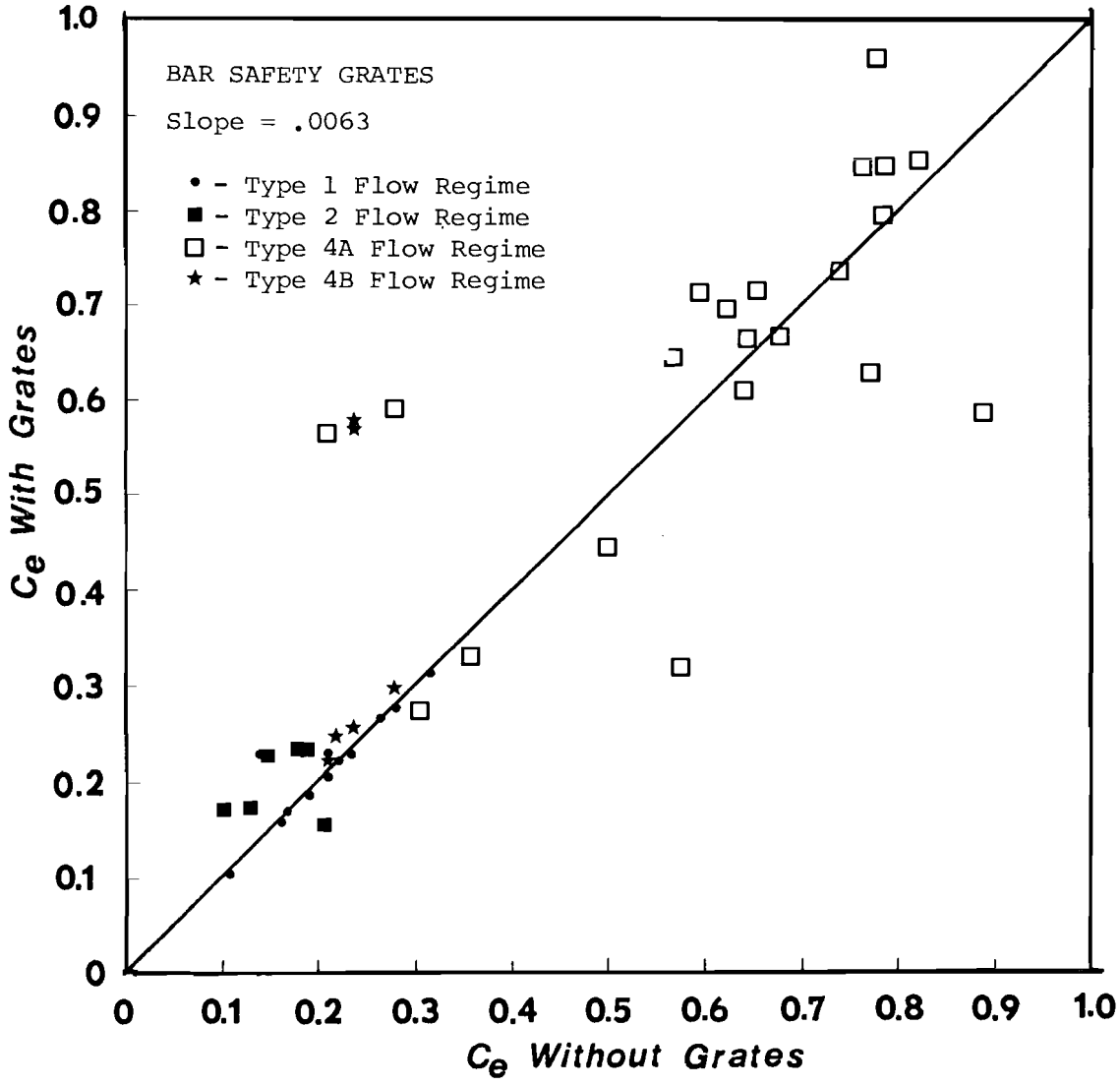


Figure B.7 Comparison of Entrance Headloss Coefficients With and Without Safety Grates, Slope = .0063

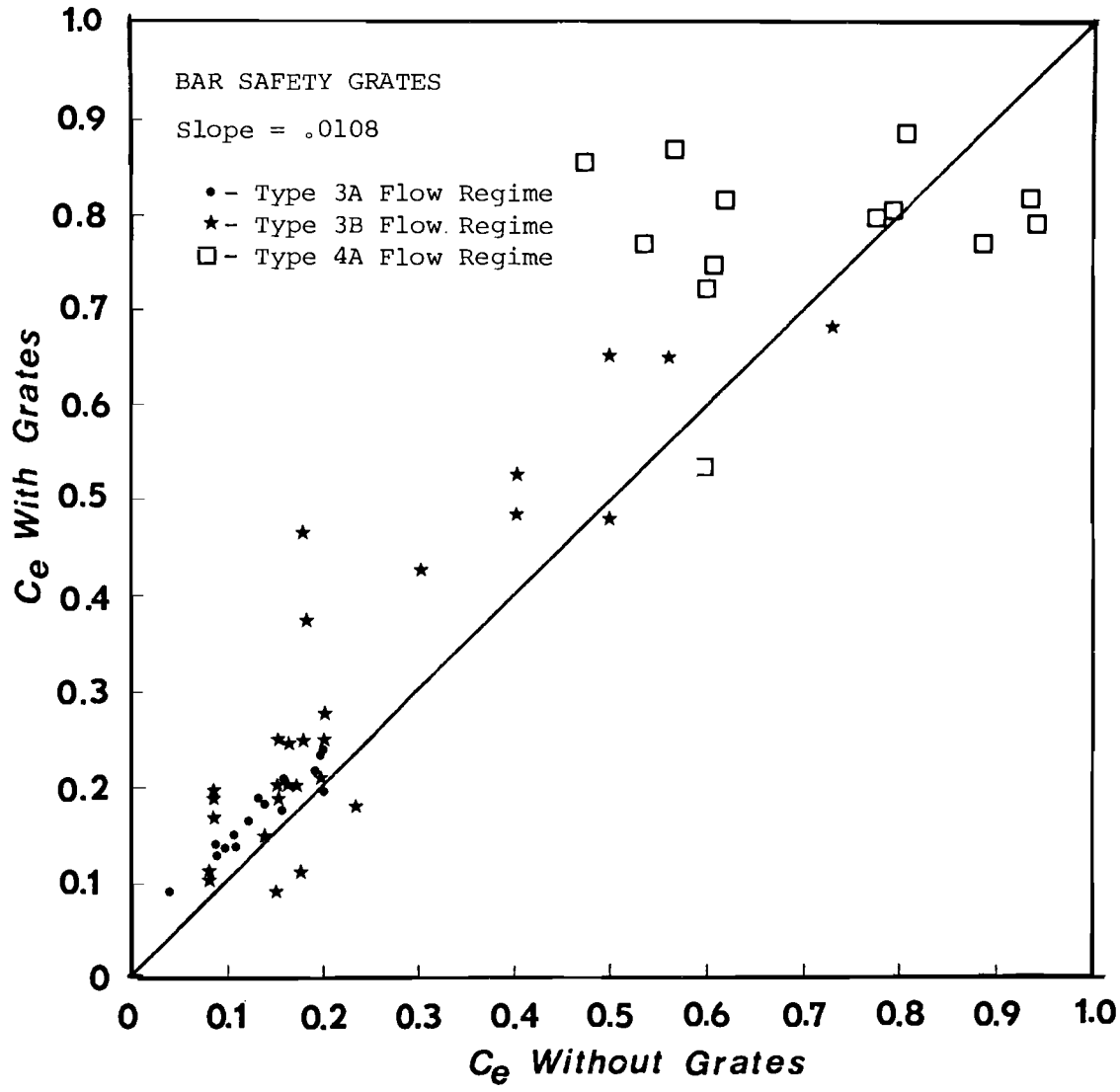


Figure B.8 Comparison of Entrance Headloss Coefficients With and Without Safety Grates, Slope = .0108

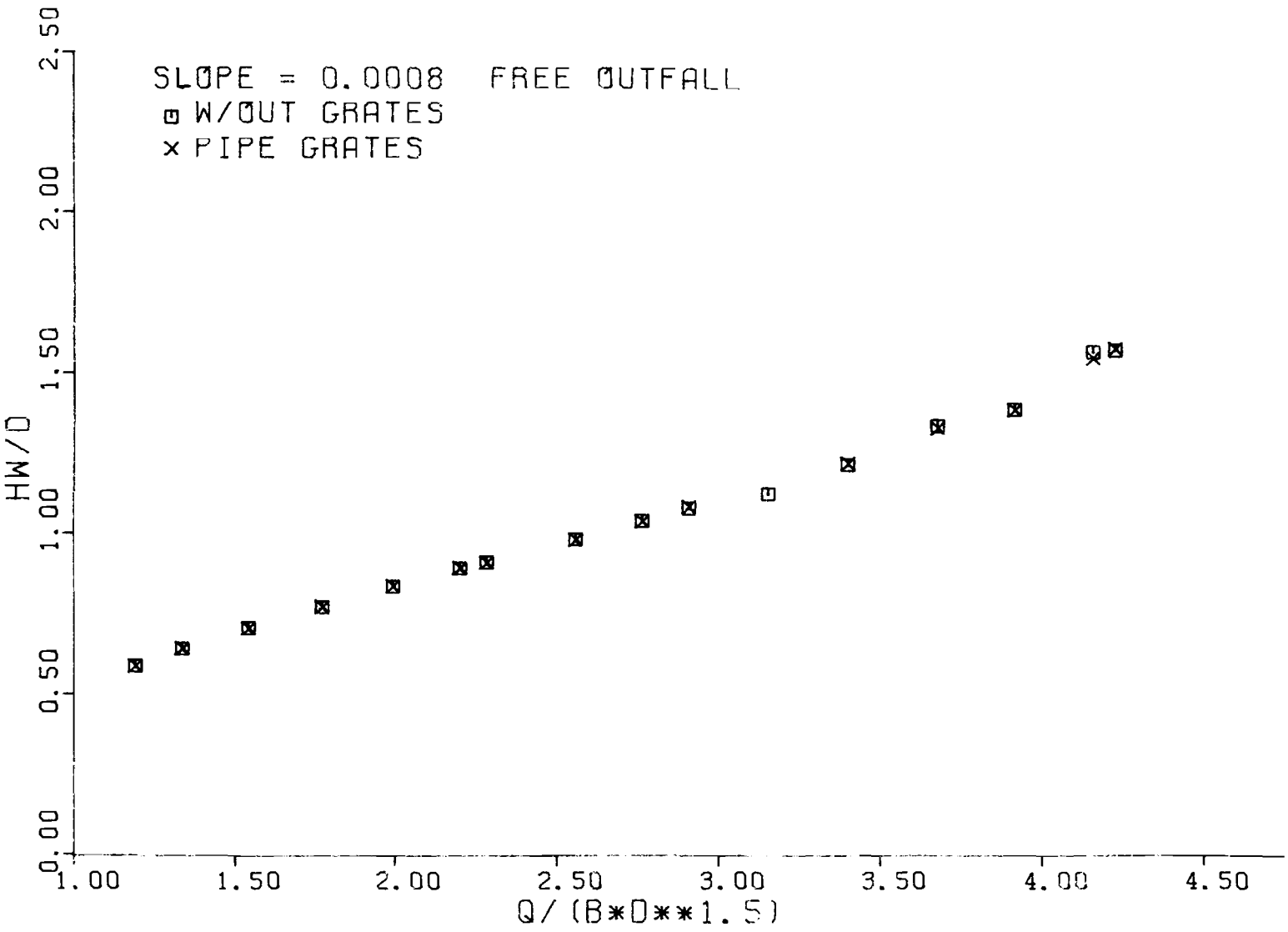


Figure B.9 Headwater vs. Discharge with and without Pipe Grates, Slope = .0008

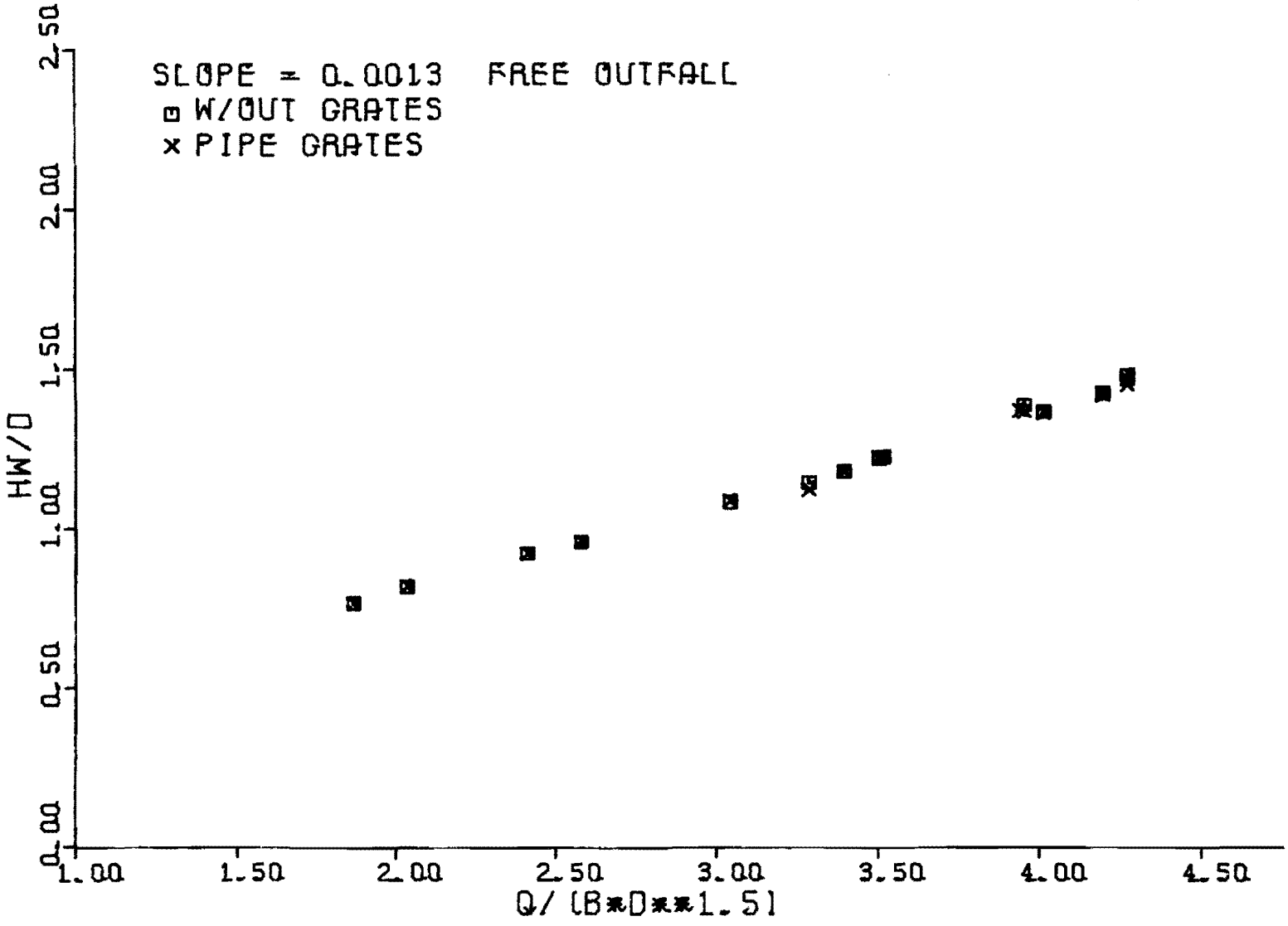


Figure B.10 Headwater vs. Discharge with and without Pipe Grates, Slope = .0013

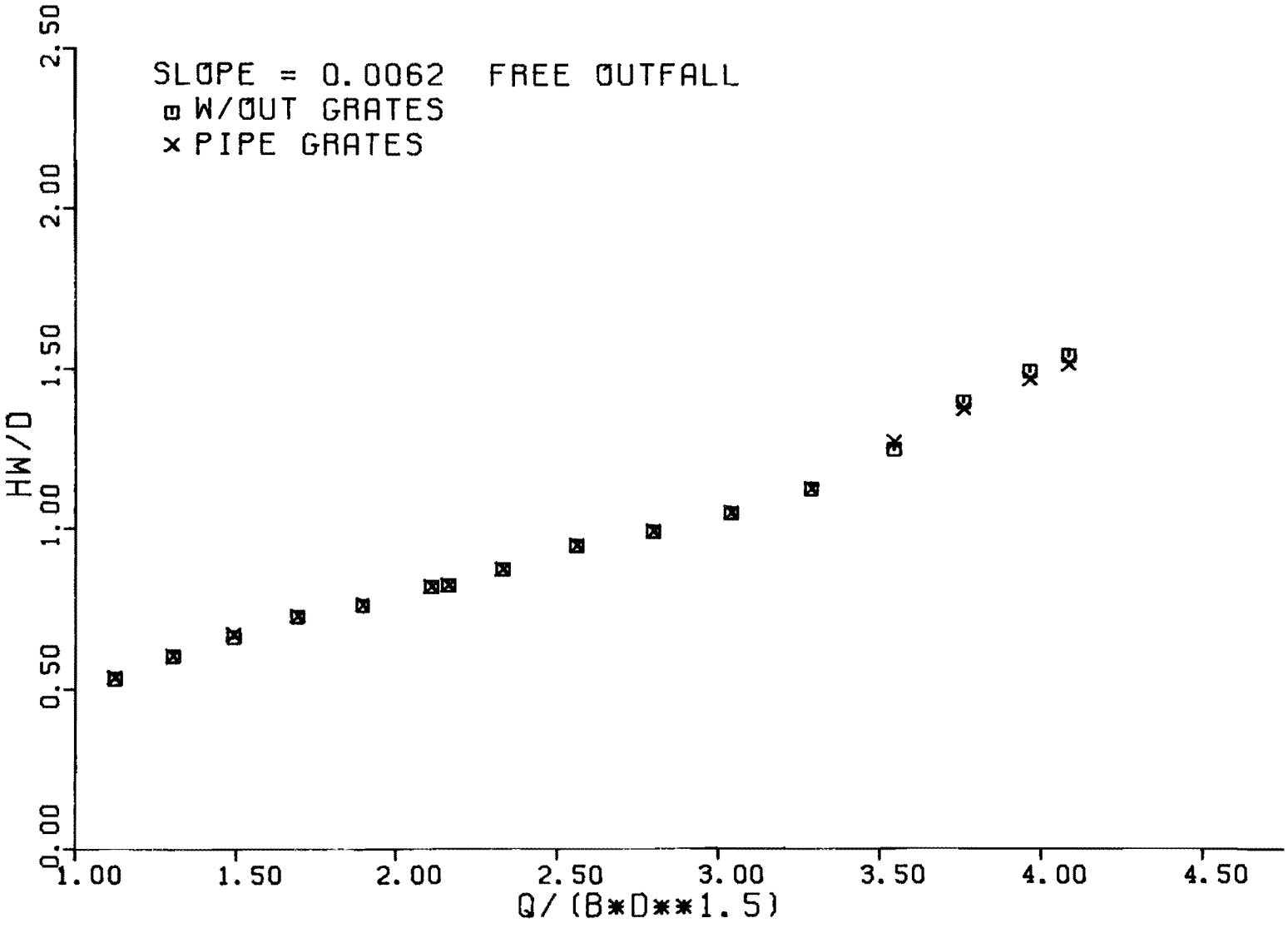


Figure B.11 Headwater vs. Discharge with and without Pipe Grates, Slope = .0062

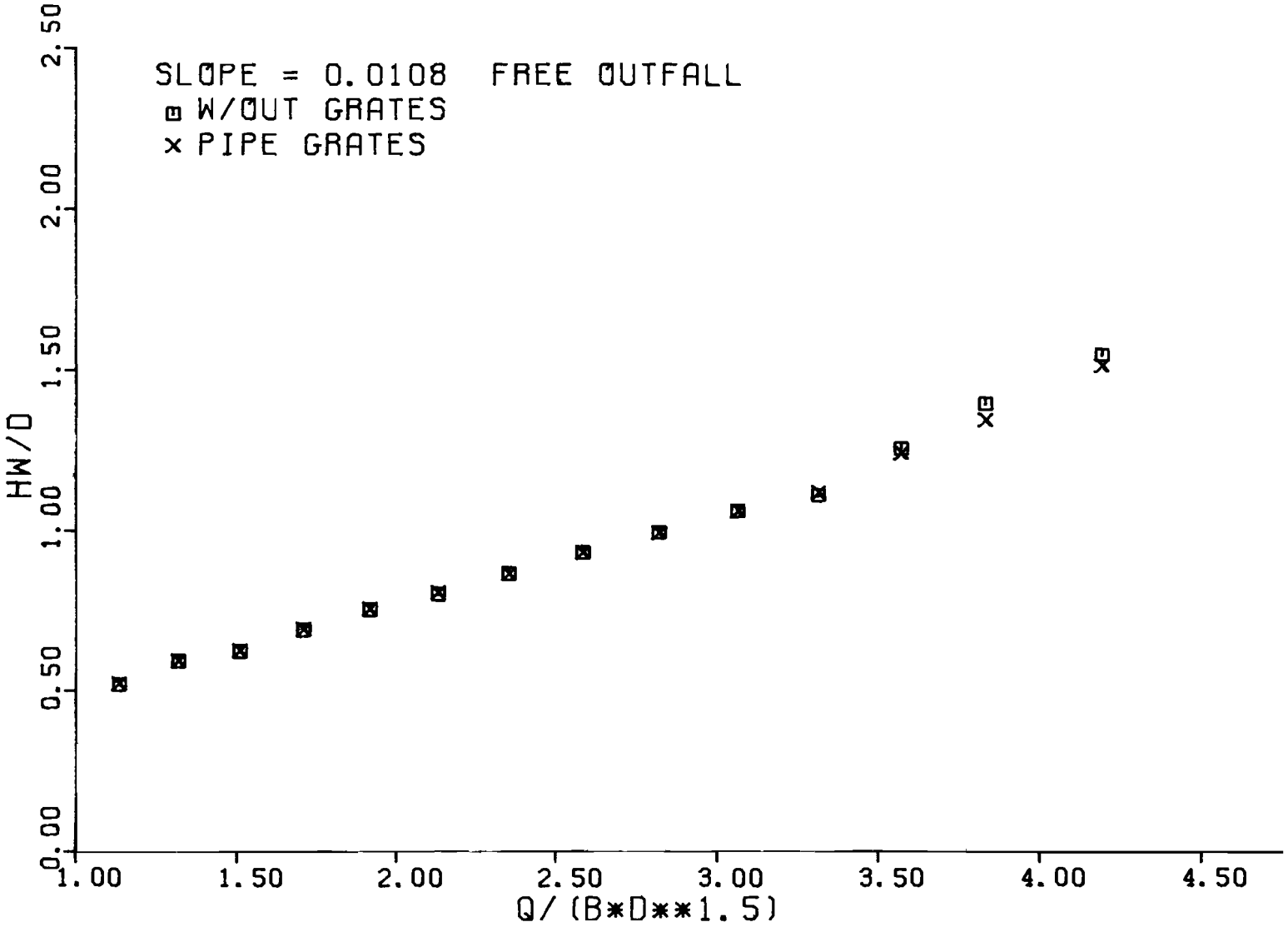


Figure B.12 Headwater vs. Discharge with and without Pipe Grates, Slope = .0108

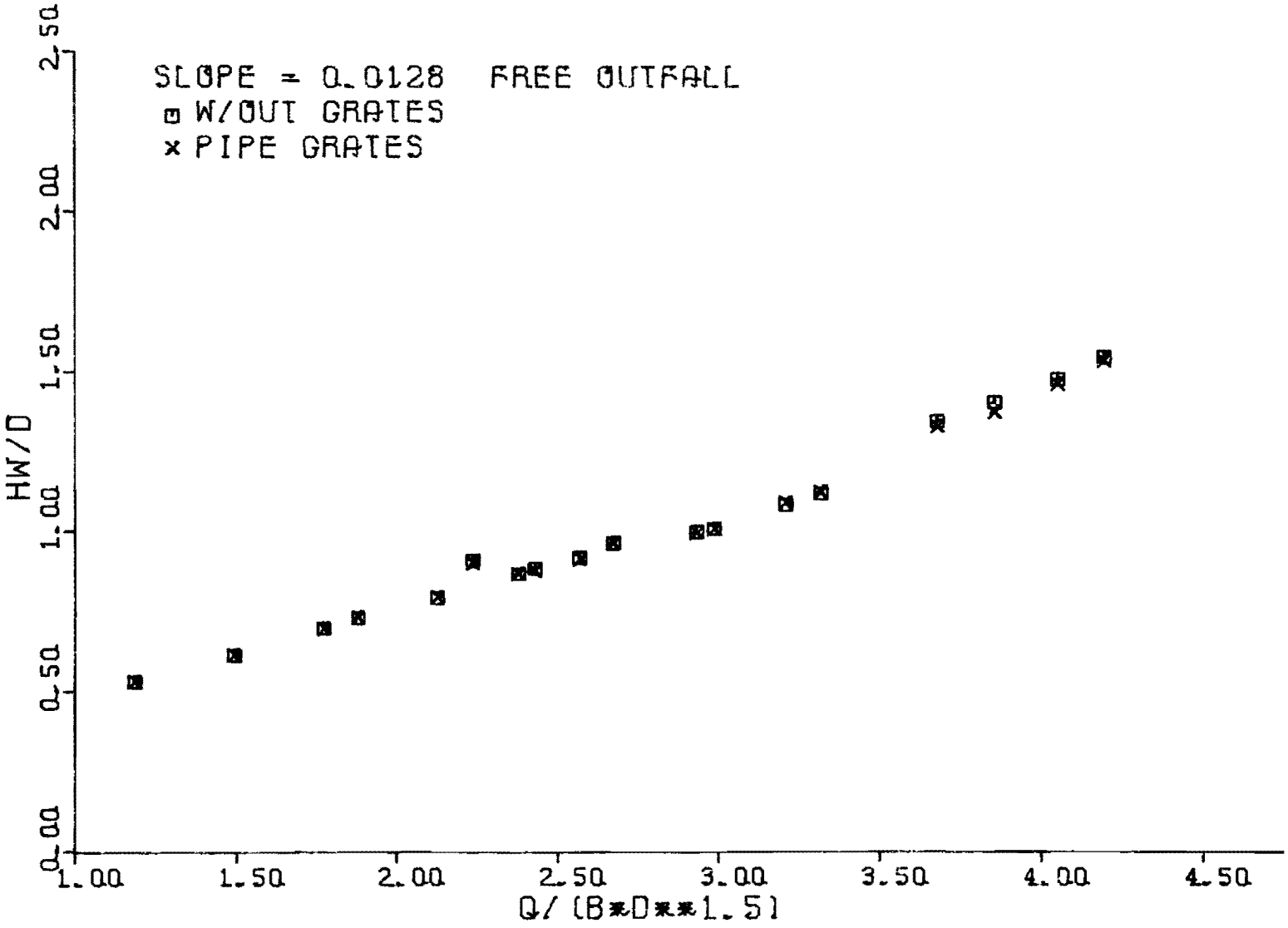


Figure B.13 Headwater vs. Discharge with and without Pipe Grates, Slope = .0128

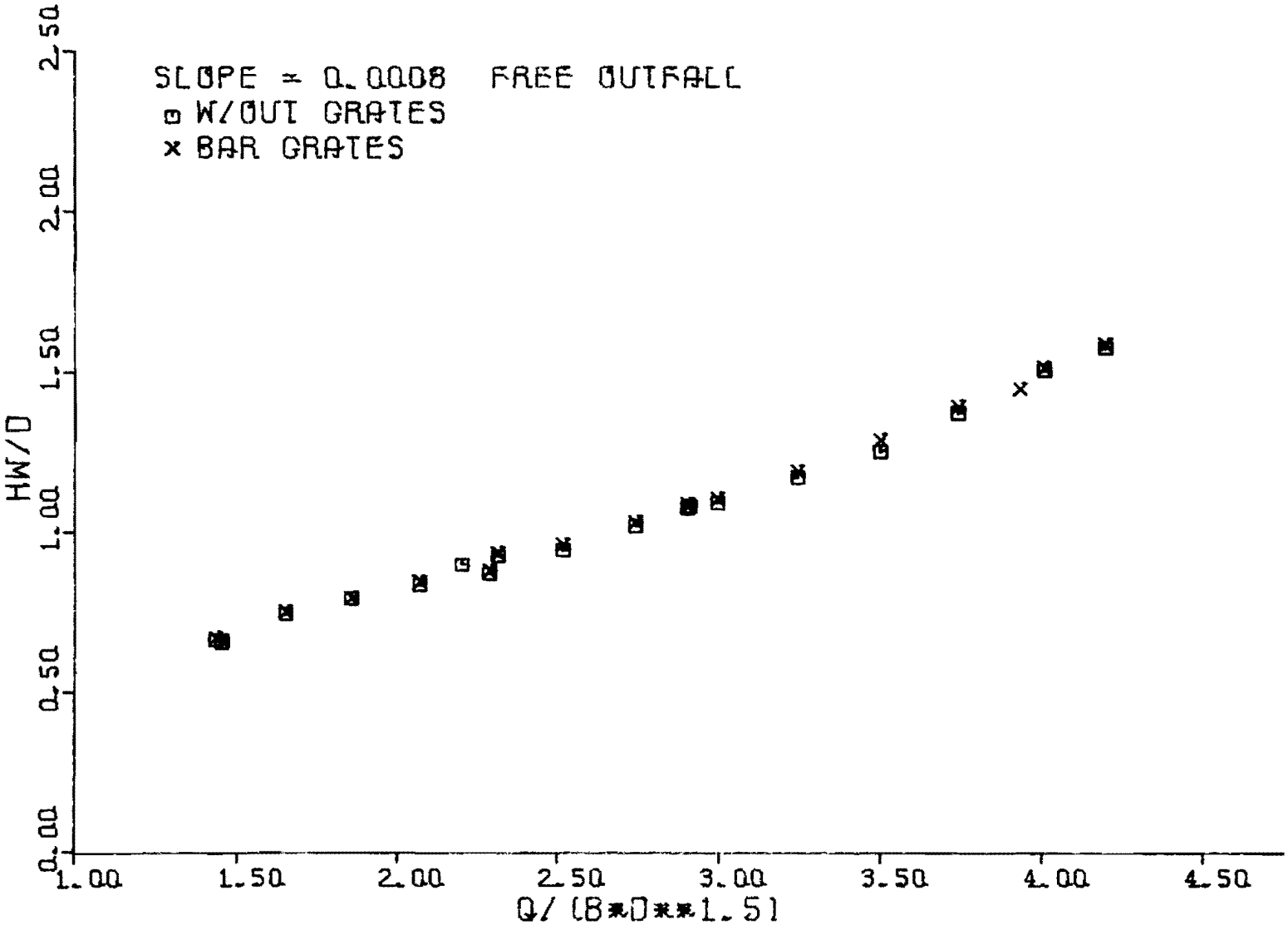


Figure B.14 Headwater vs. Discharge with and without Bar Grates, Slope = .0008

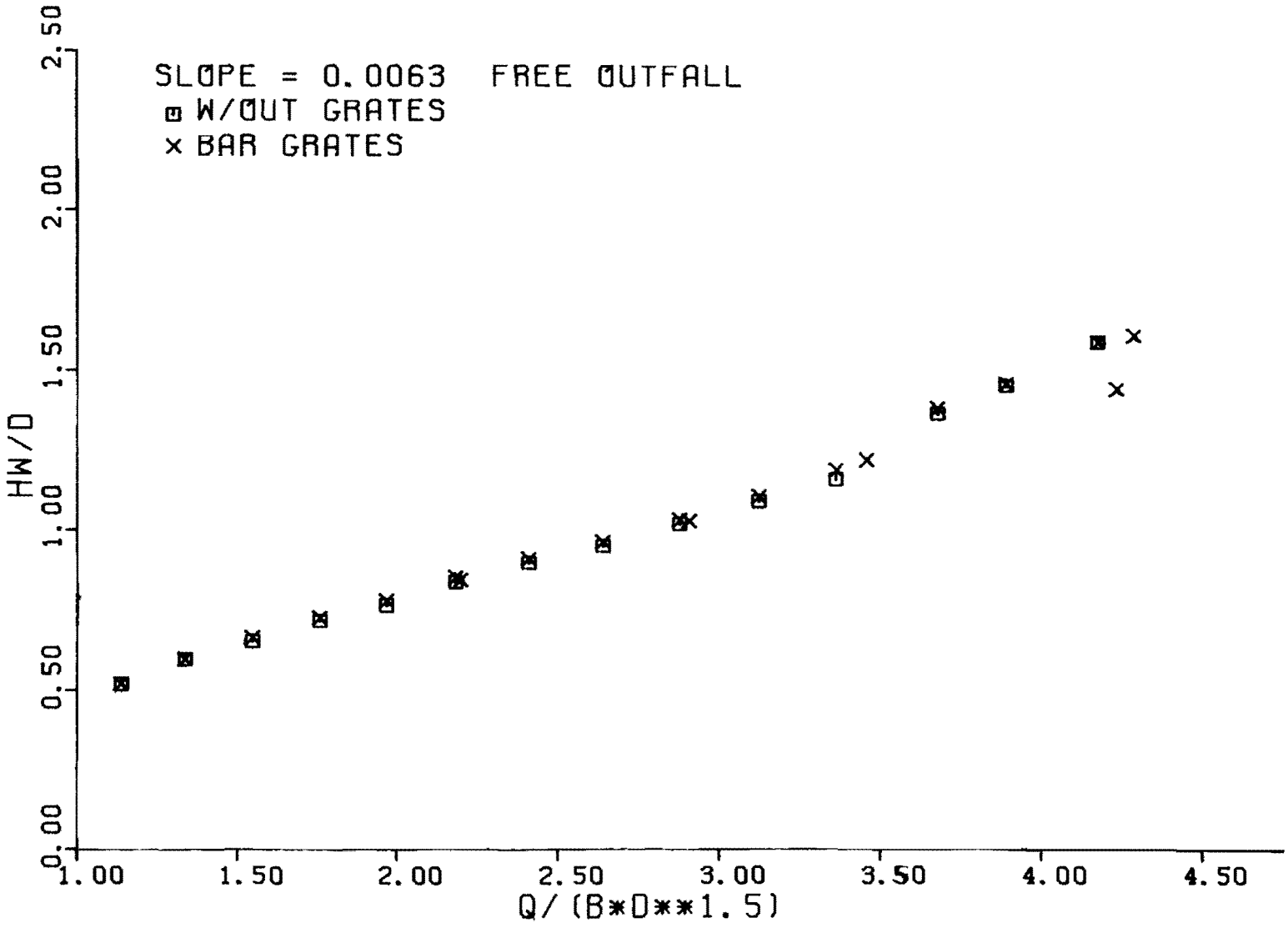


Figure B.15 Headwater vs. Discharge with and without Bar Grates, Slope = .0063

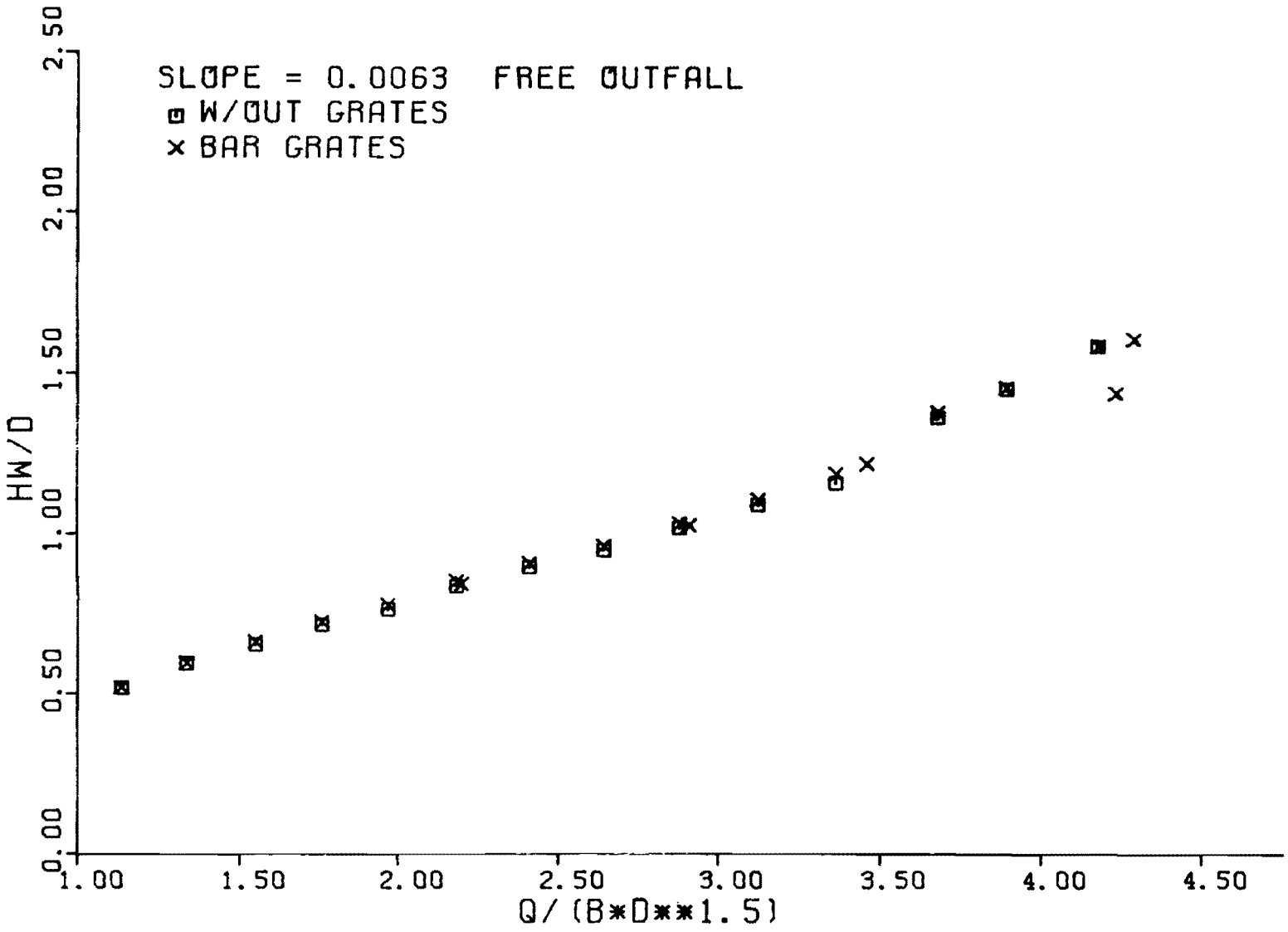


Figure B.16 Headwater vs. Discharge with and without Bar Grates, Slope = .0063

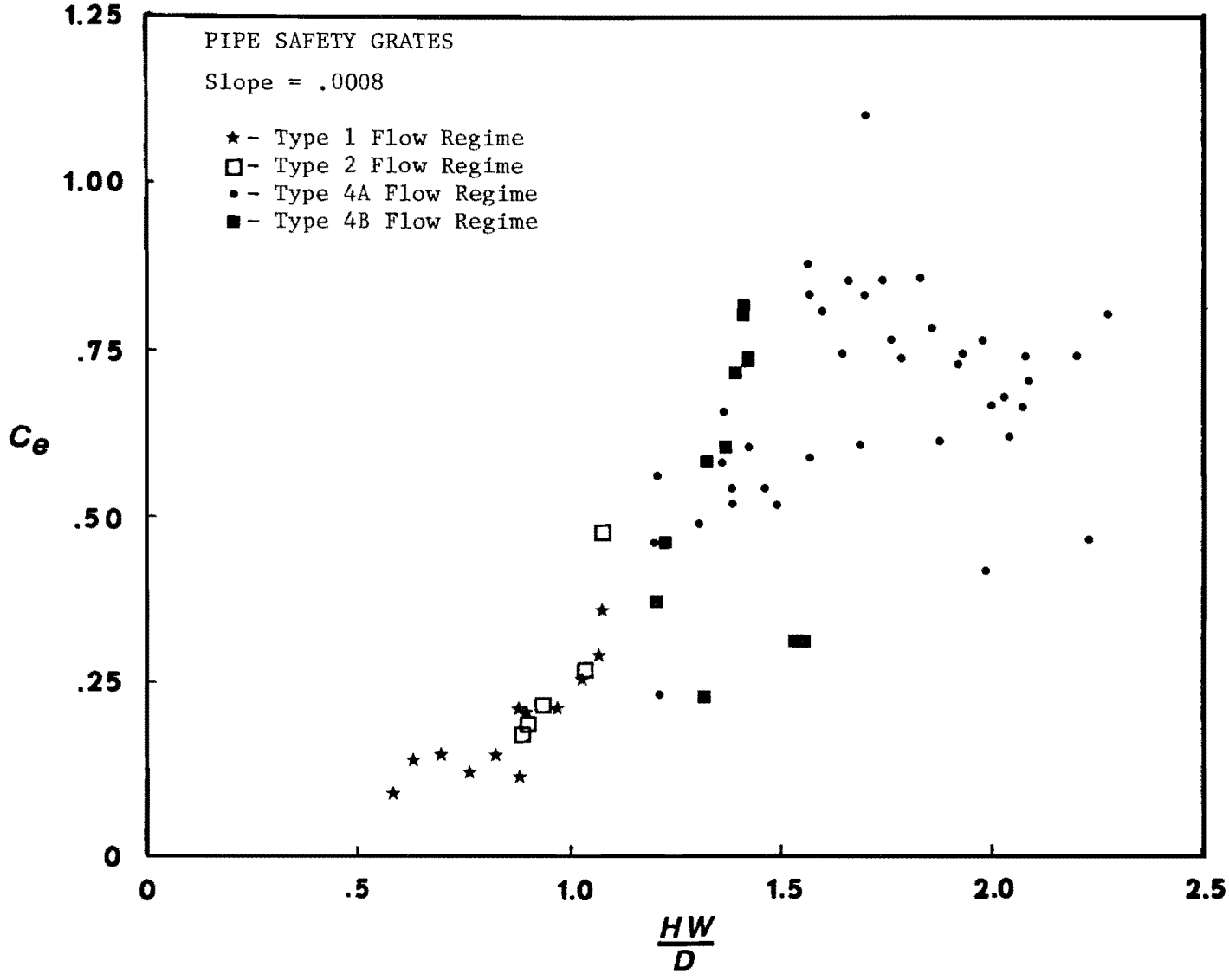


Figure B.17 Entrance Headloss Coefficient vs. Headwater
For Pipe Safety Grates, Slope = .0008

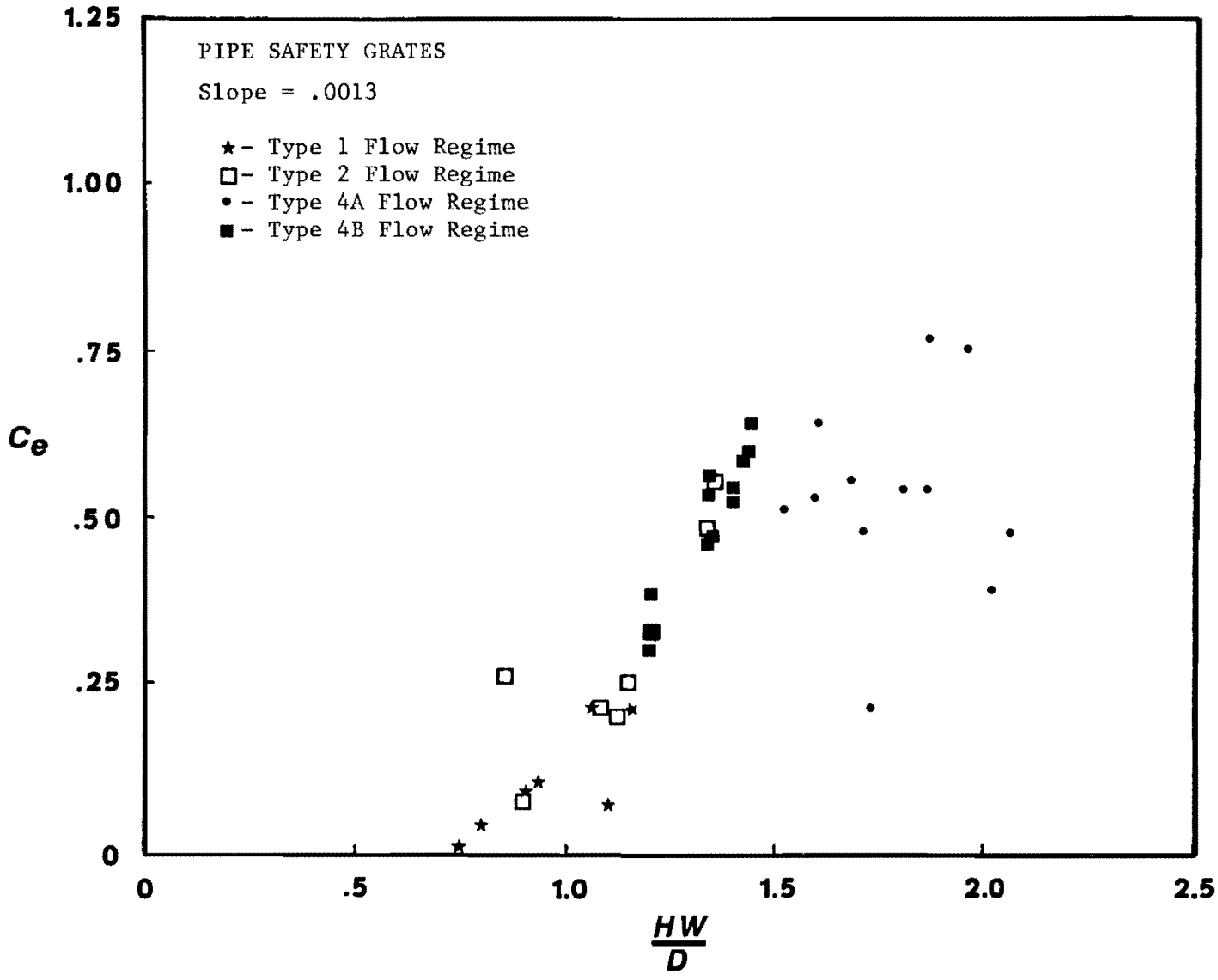


Figure B.18 Entrance Headloss Coefficient vs. Headwater For Pipe Safety Grates, Slope = .0013

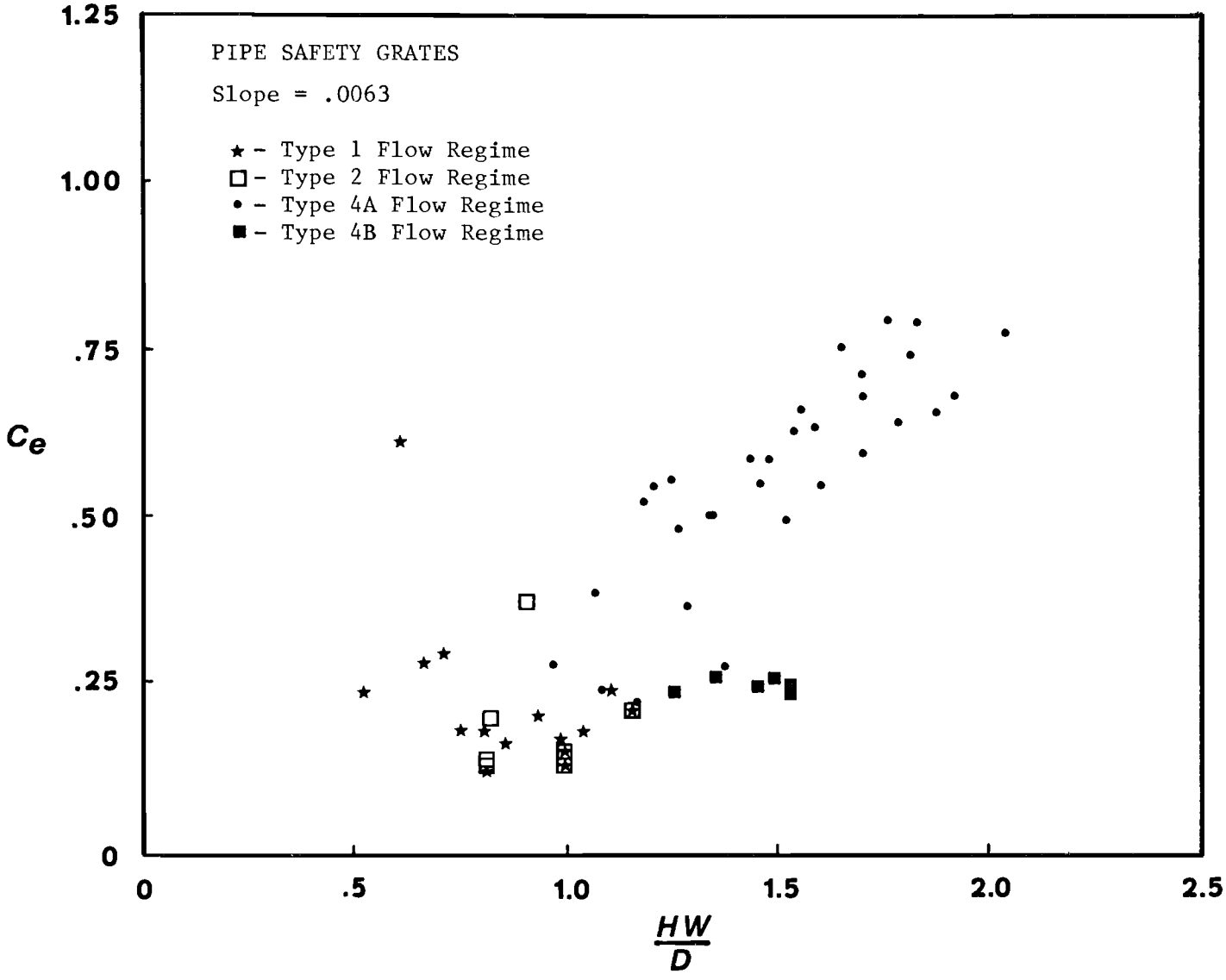


Figure B.19 Entrance Headloss Coefficient vs. Headwater For Pipe Safety Grates, Slope = .0063

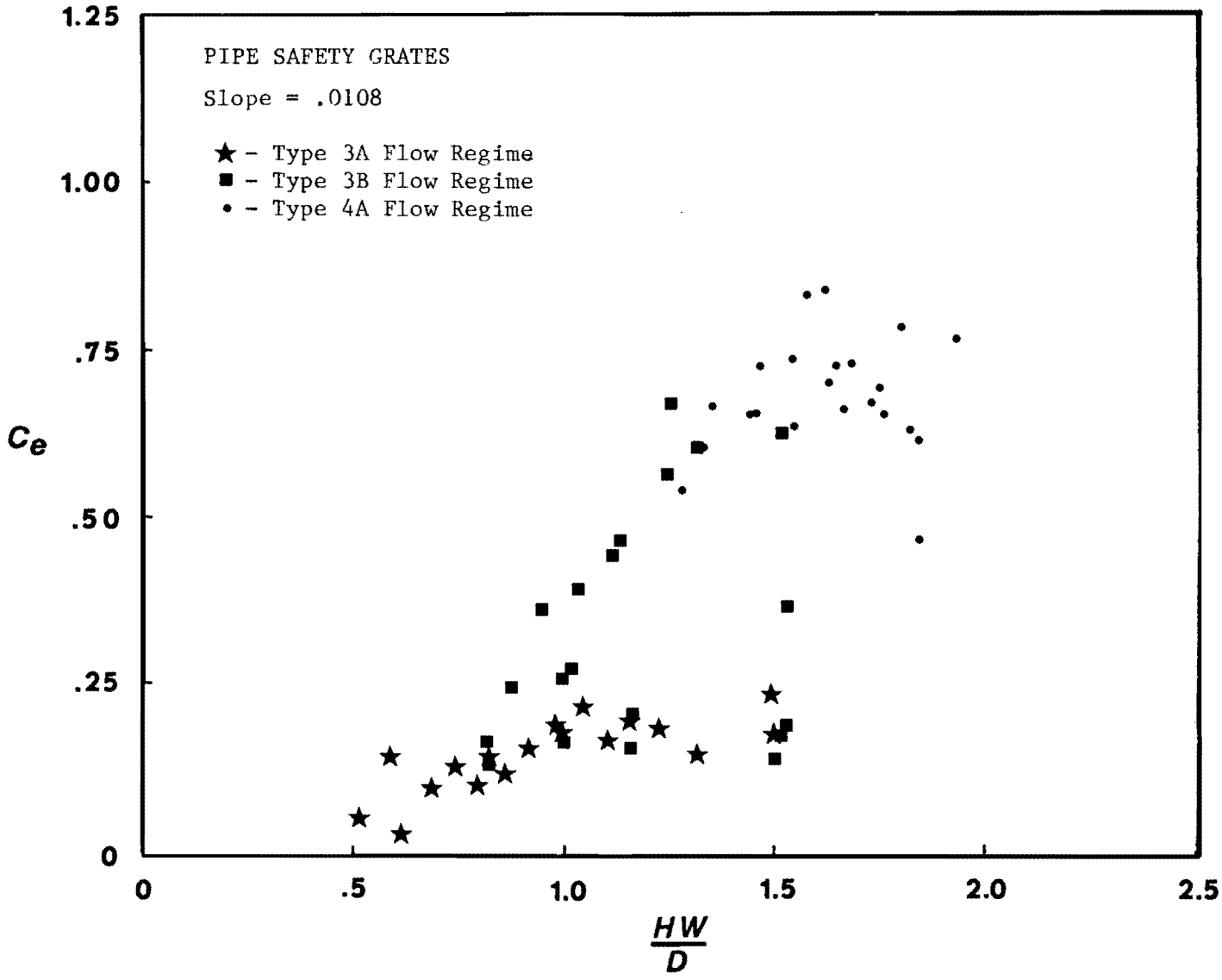


Figure B.20 Entrance Headloss Coefficient vs. Headwater
For Pipe Safety Grates, Slope = .0108

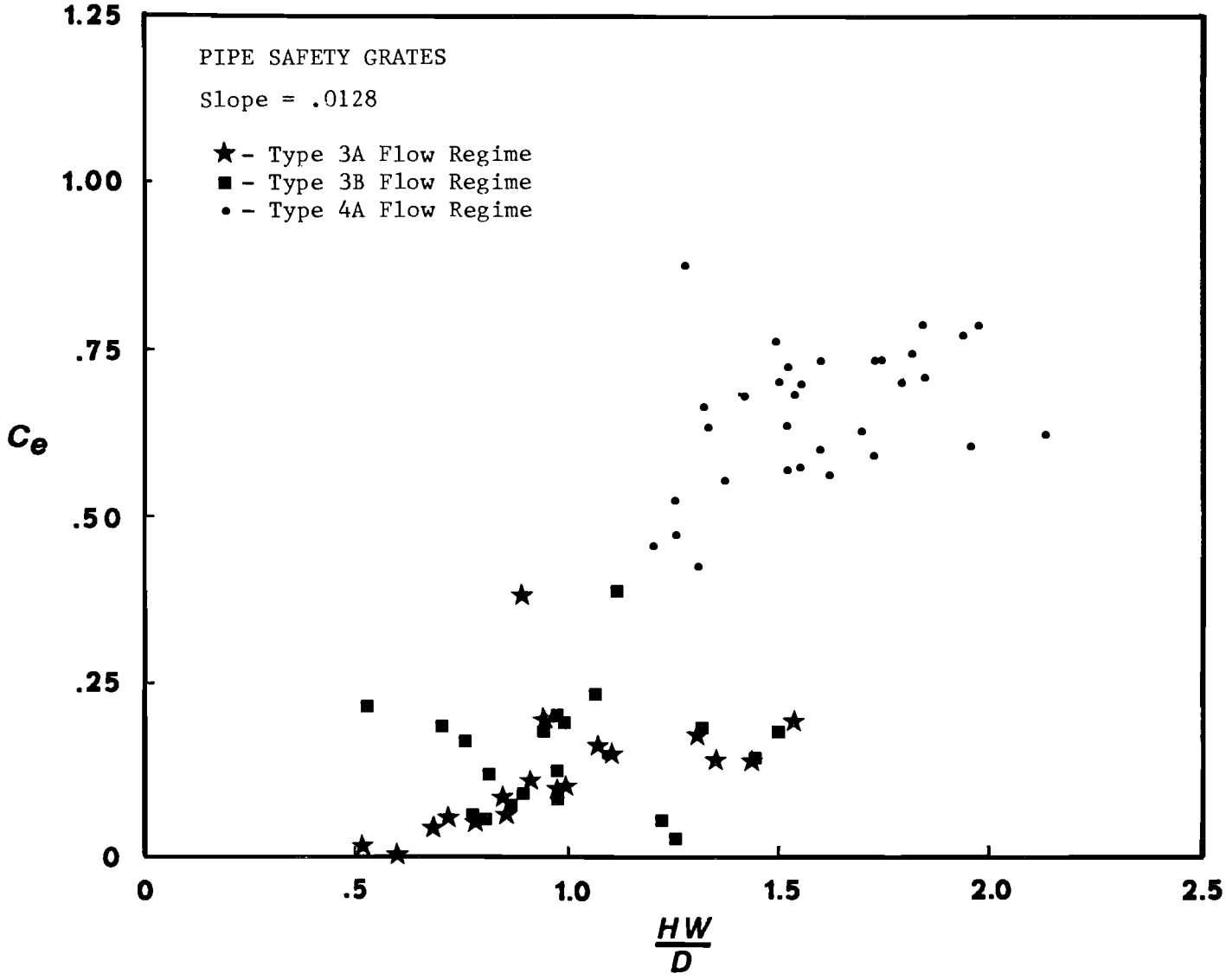


Figure B.21 Entrance Headloss Coefficient vs. Headwater For Pipe Safety Grates, Slope = .0128

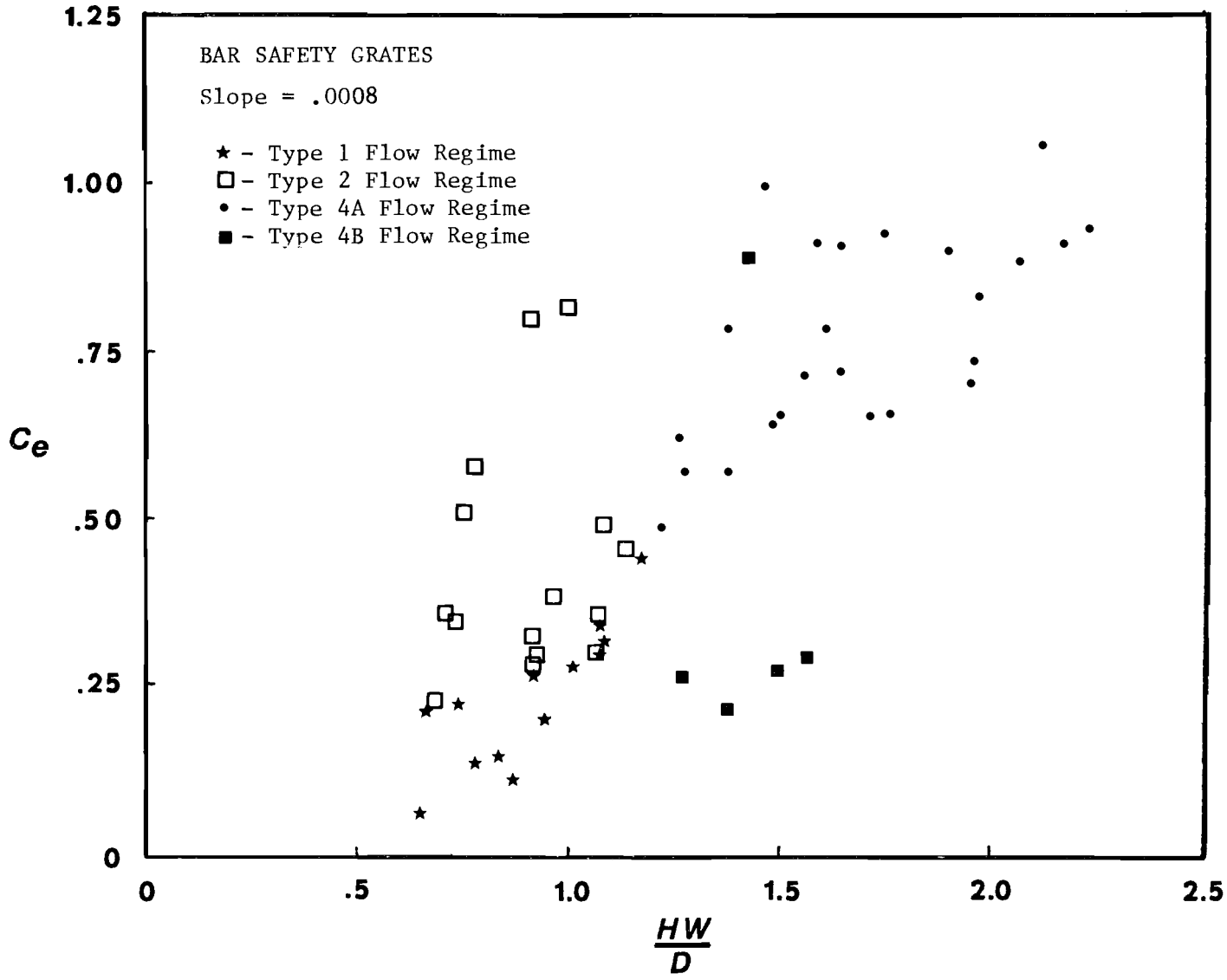


Figure B.22 Entrance Headloss Coefficient vs. Headwater For Bar Safety Grates, Slope = .0008

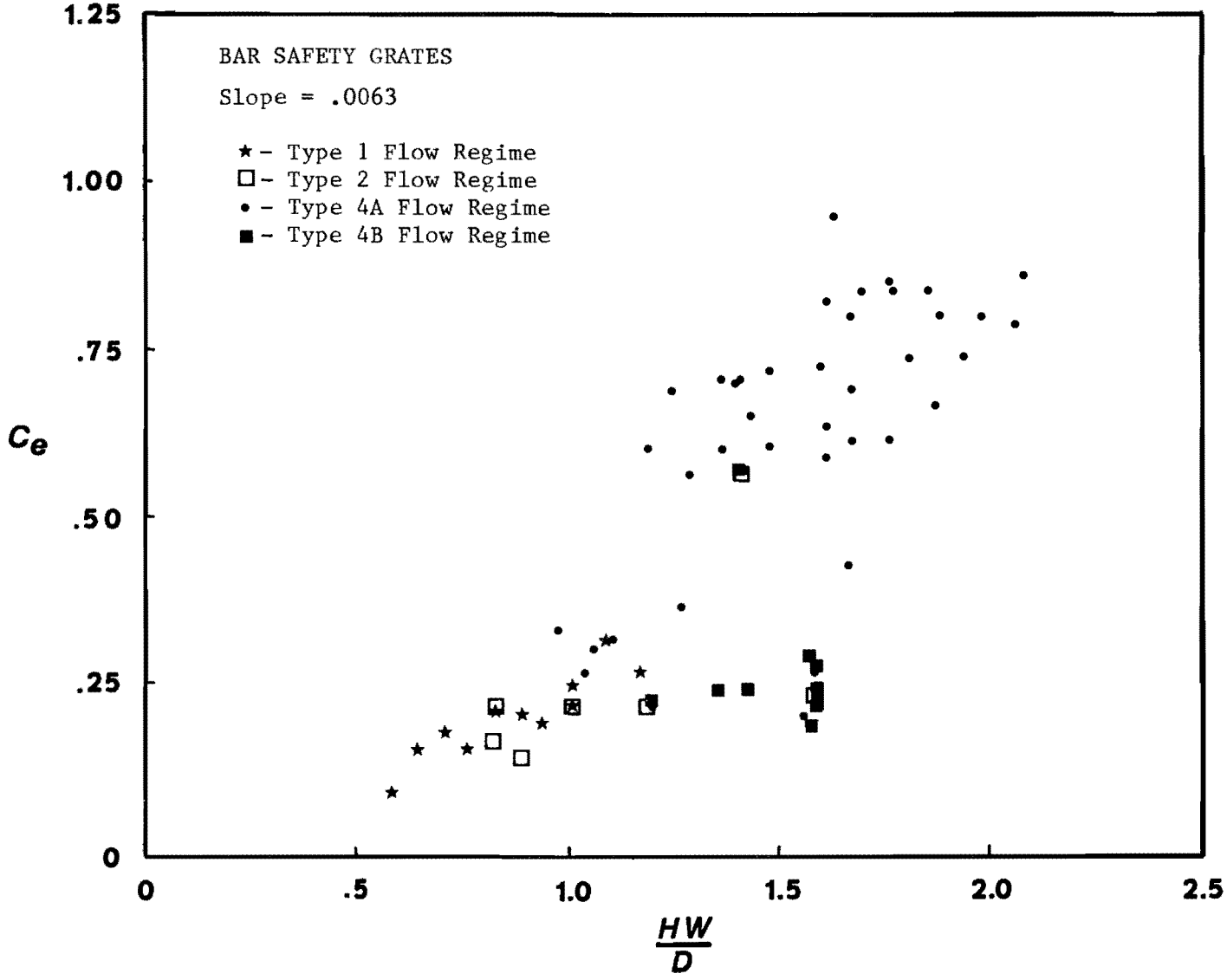


Figure B.23 Entrance Headloss Coefficient vs. Headwater For Bar Safety Grates, Slope = .0063

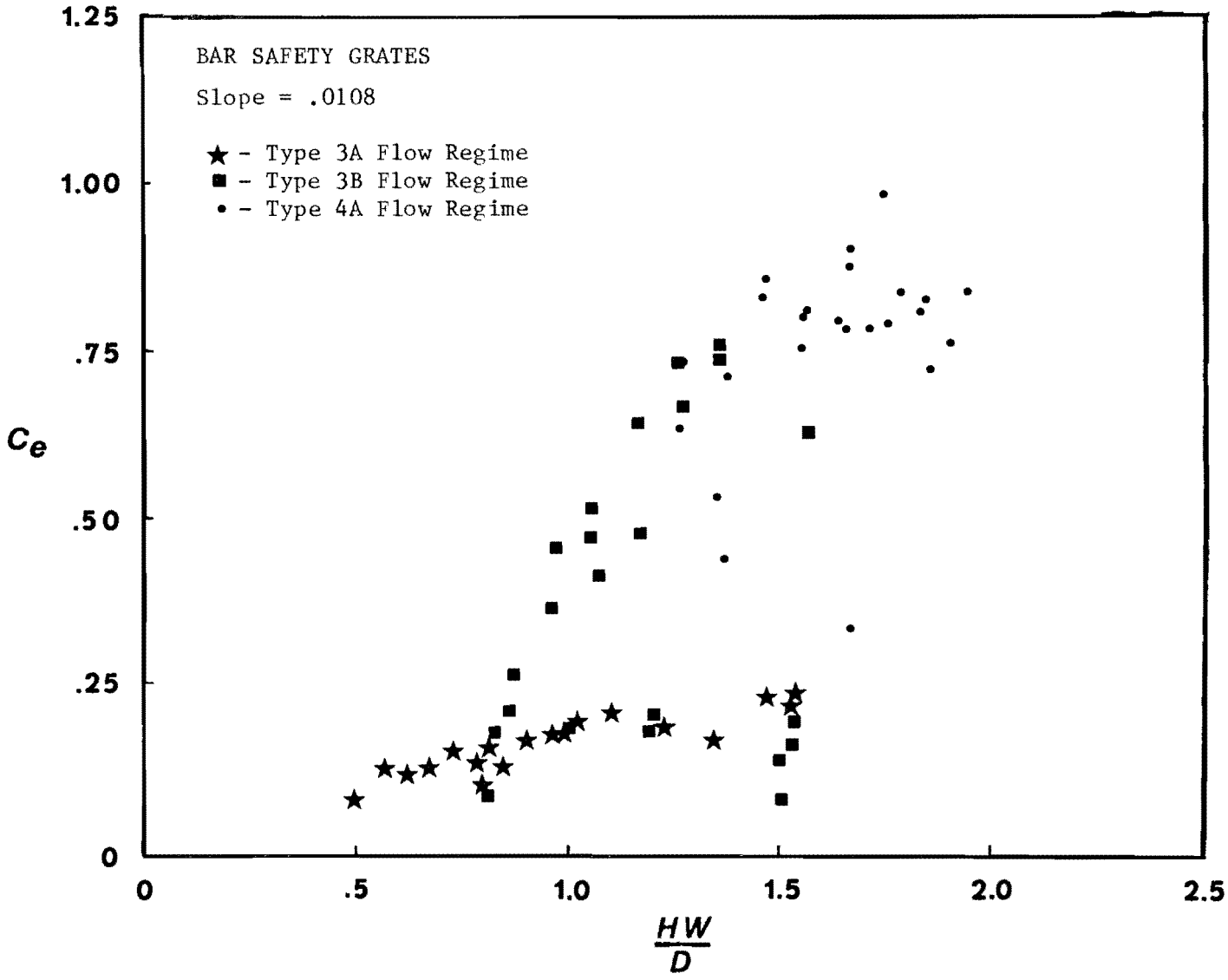


Figure B.24 Entrance Headloss Coefficient vs. Headwater For Bar Safety Grates, Slope = .0108

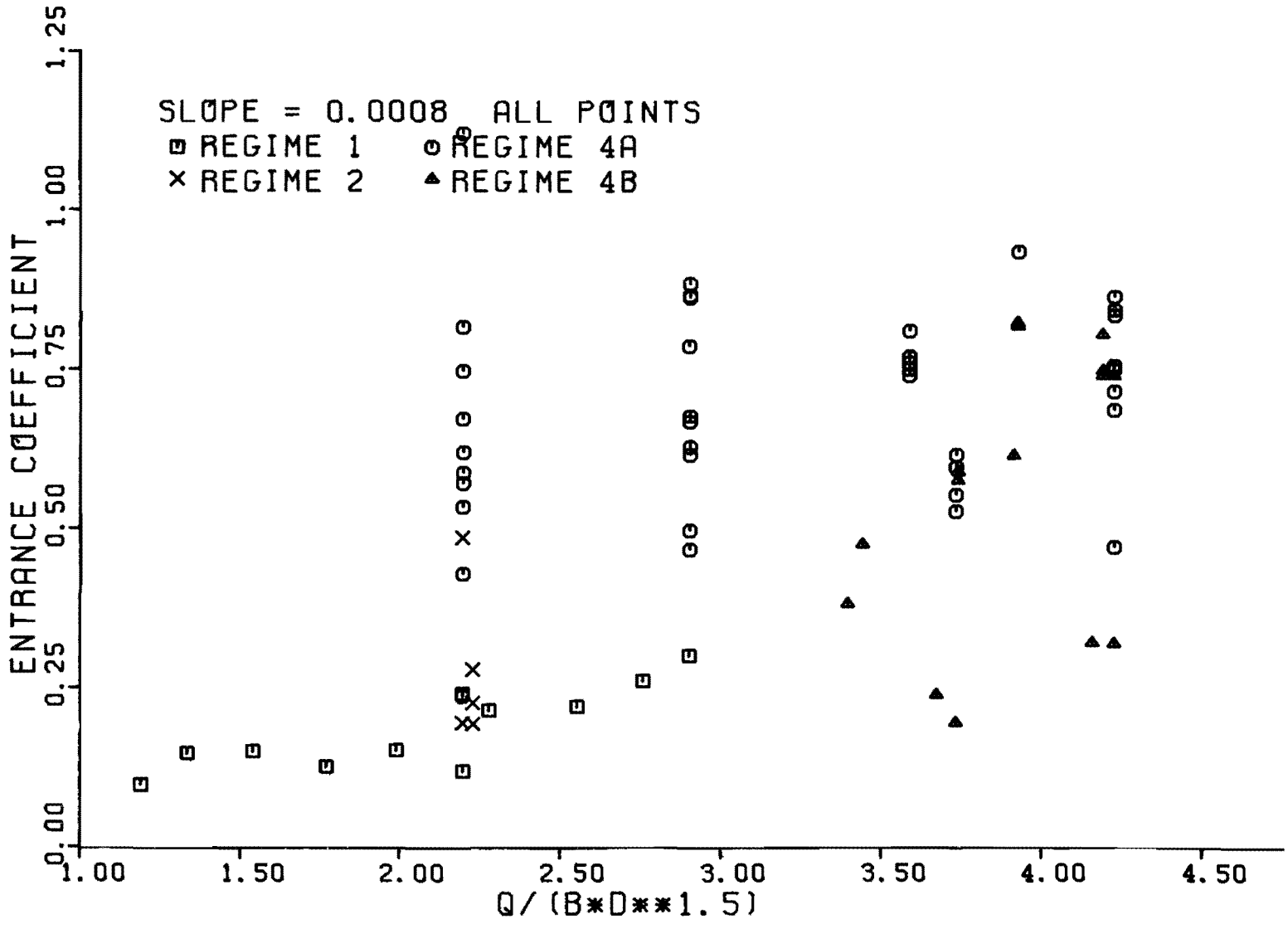


Figure B.25 Entrance Headloss Coefficient vs. Headwater For Pipe Safety Grates, Slope = .0008

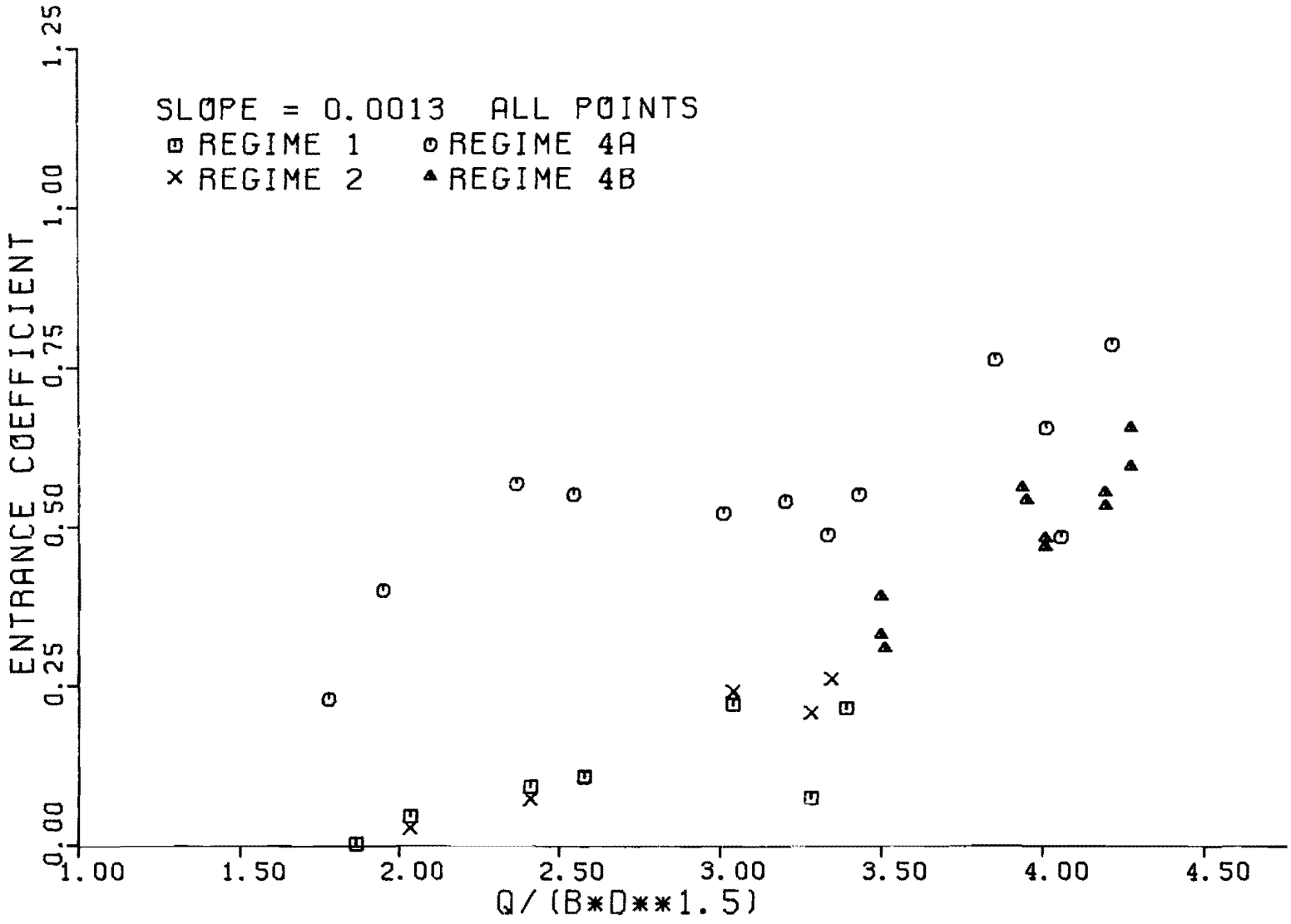


Figure B.26 Entrance Headloss Coefficient vs. Headwater For Pipe Safety Grates, Slope = .0013

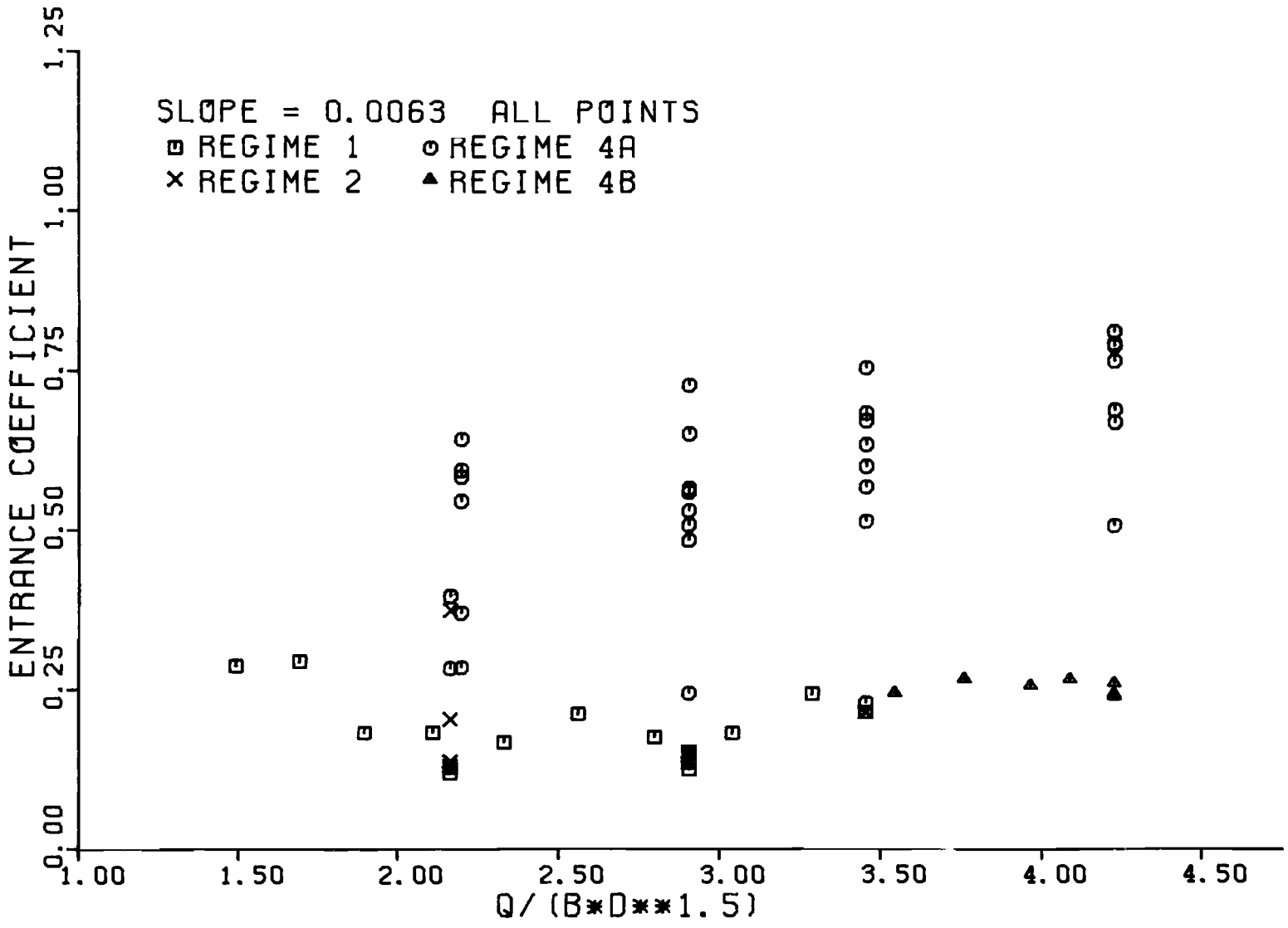


Figure B.27 Entrance Headloss Coefficient vs. Headwater For Pipe Safety Grates, Slope = .0063

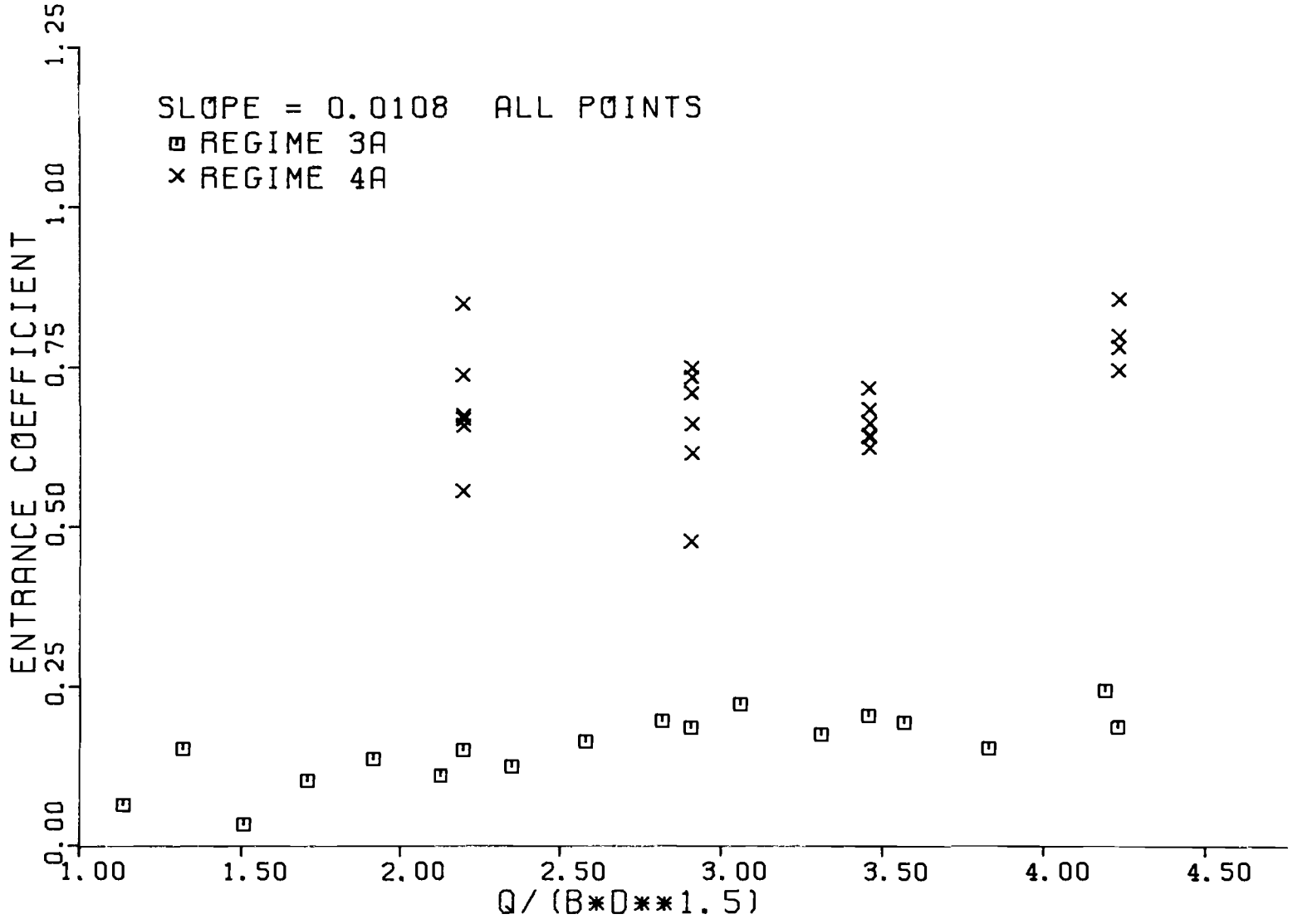


Figure B.28 Entrance Headloss Coefficient vs. Headwater For Pipe Safety Grates, Slope = .0108

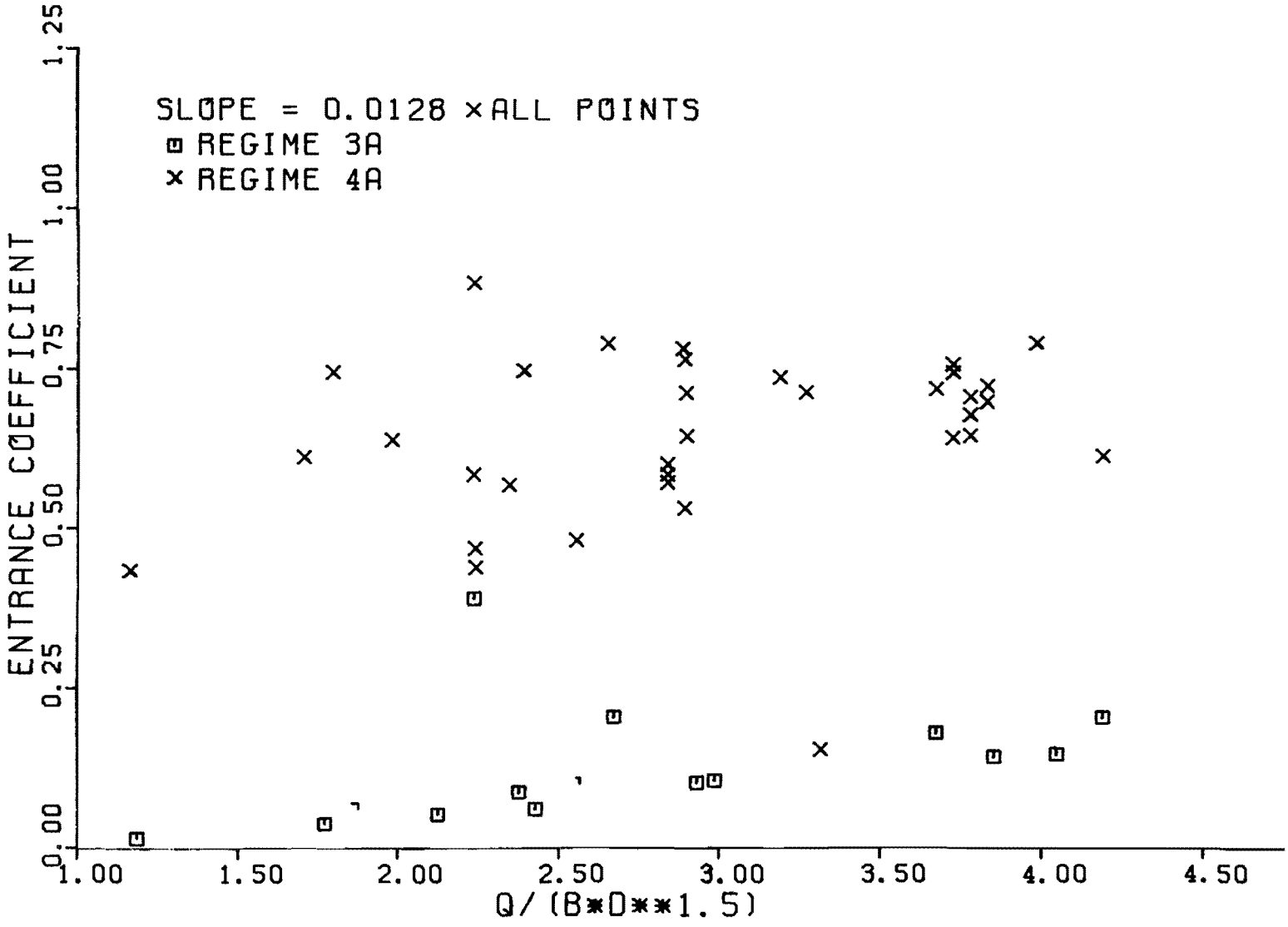


Figure B.29 Entrance Headloss Coefficient vs. Headwater For Pipe Safety Grates, Slope = .0128

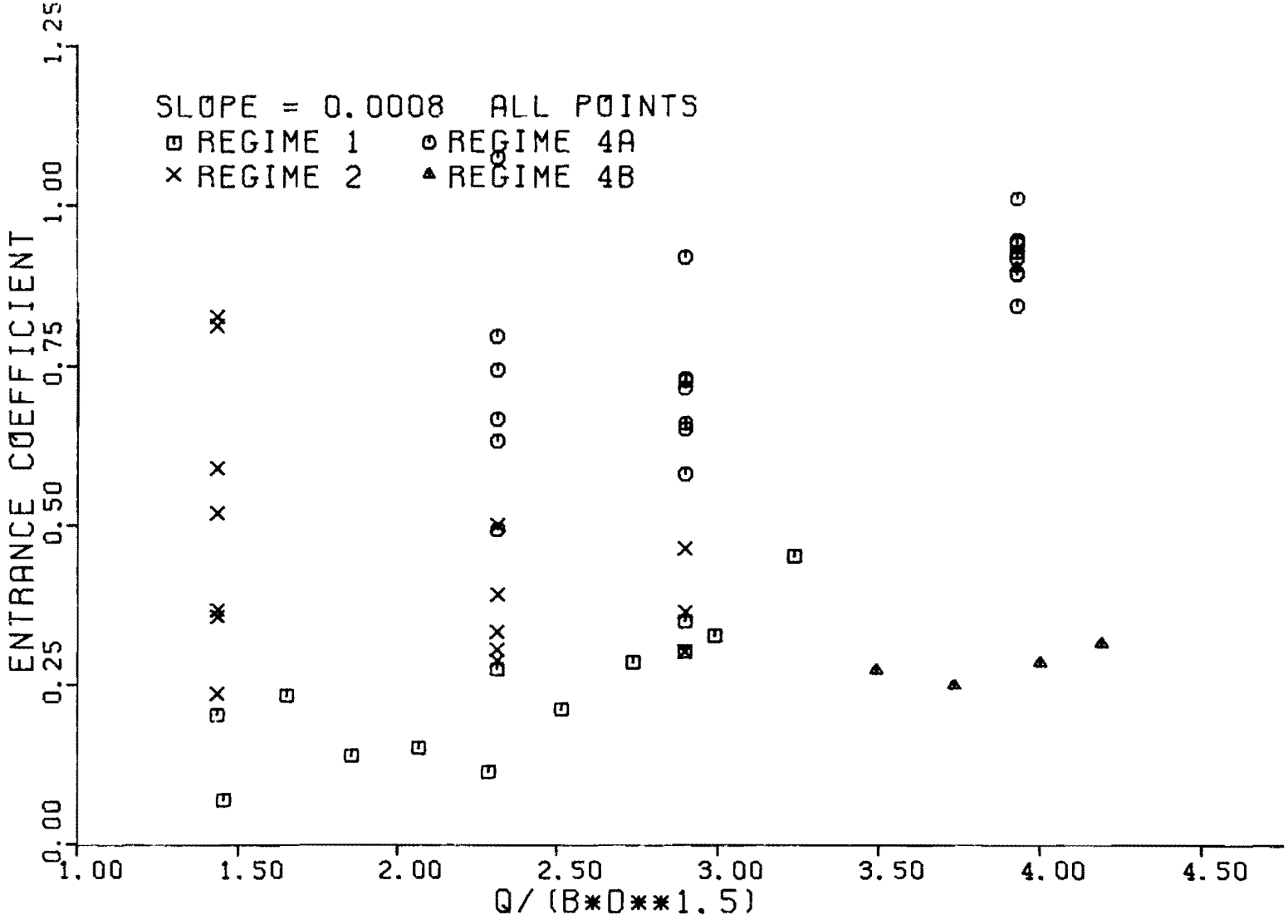


Figure B.30 Entrance Headloss Coefficient vs. Headwater For Bar Safety Grates, Slope = .0008

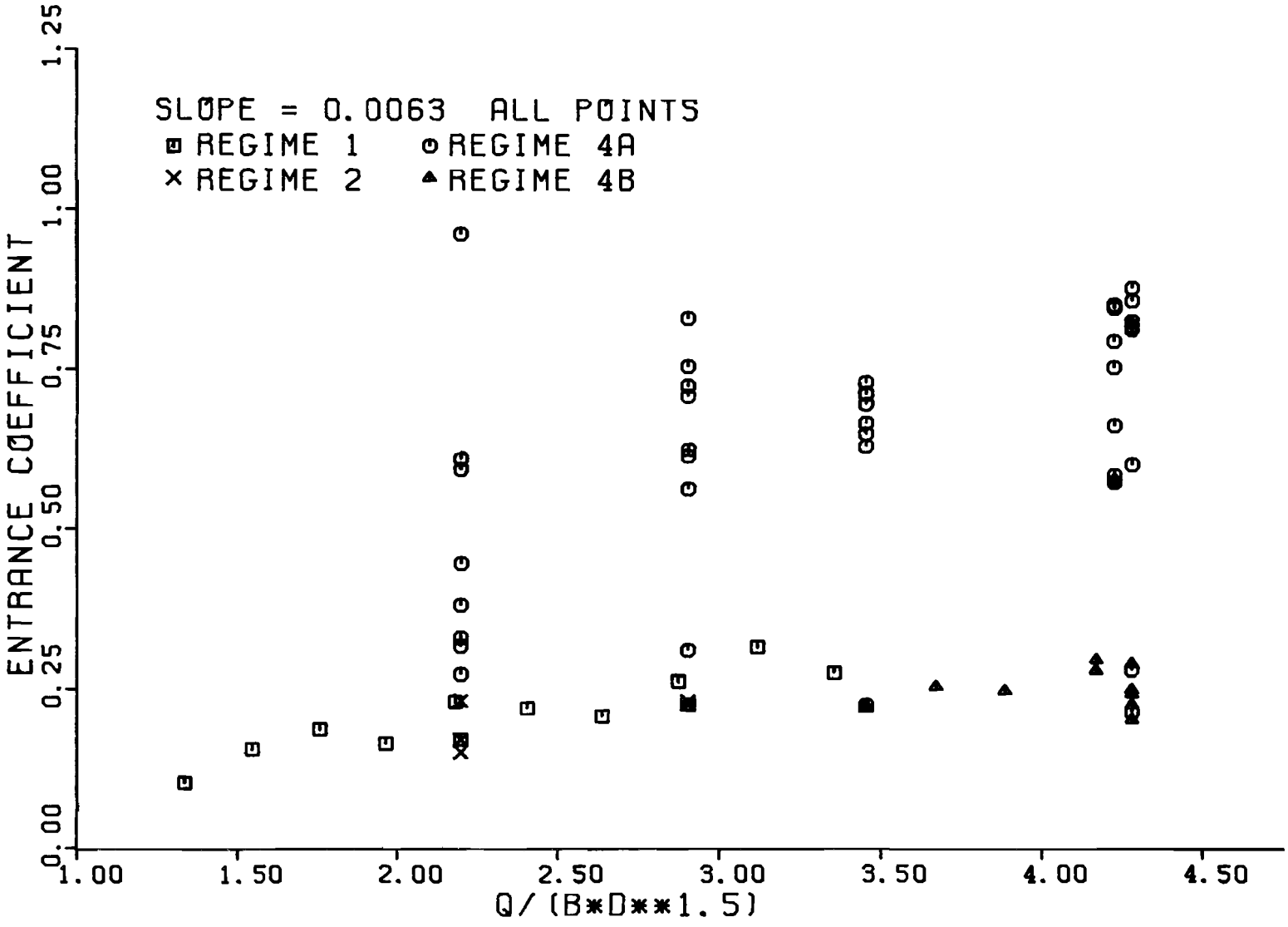


Figure B.31 Entrance Headloss Coefficient vs. Headwater for Bar Safety Grates, Slope = .0063

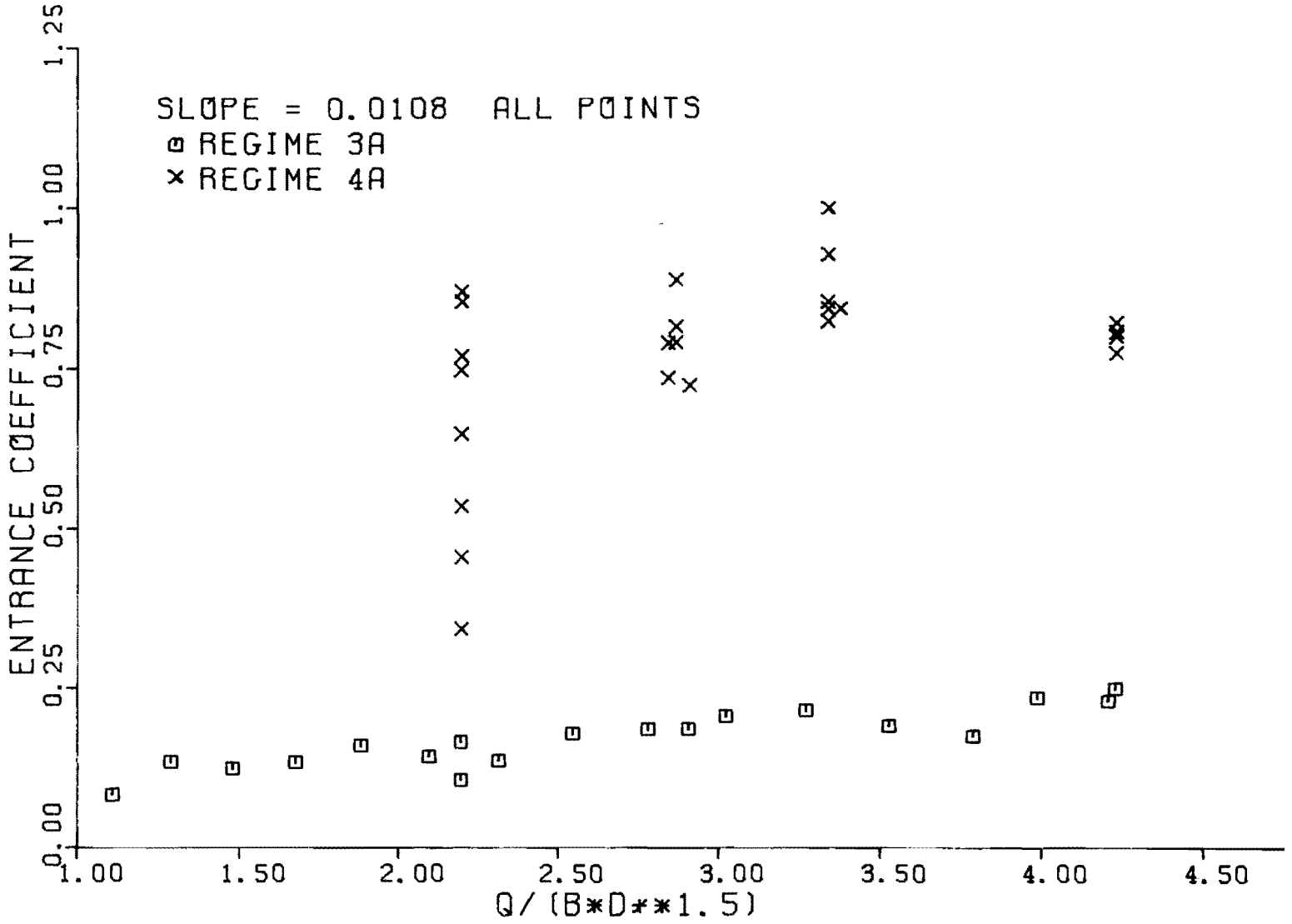


Figure B.32 Entrance Headloss Coefficient vs. Headwater For Bar Safety Grates, Slope = .0108

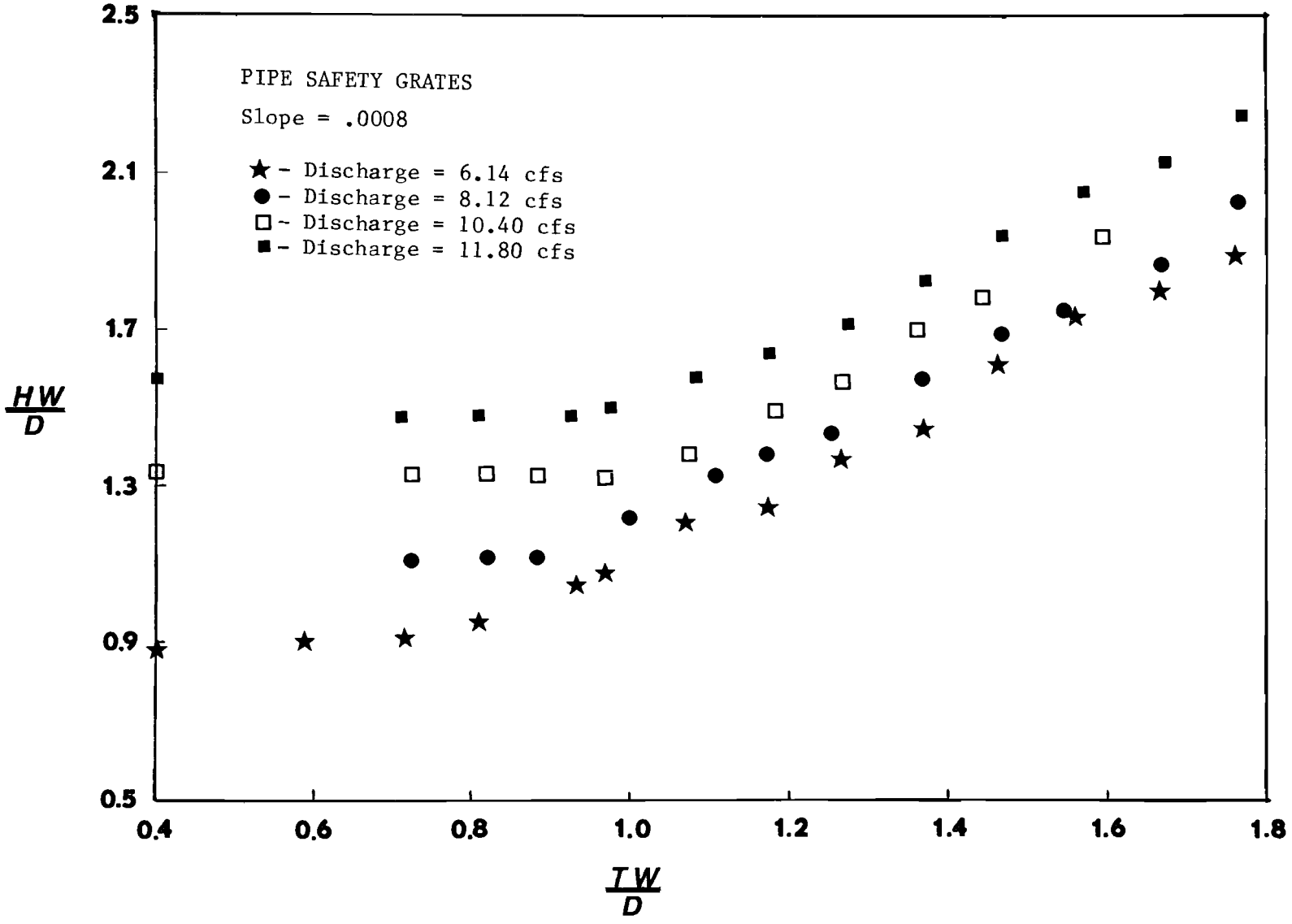


Figure B.33 Headwater vs. Tailwater For Pipe Safety Grates, Slope = .0008

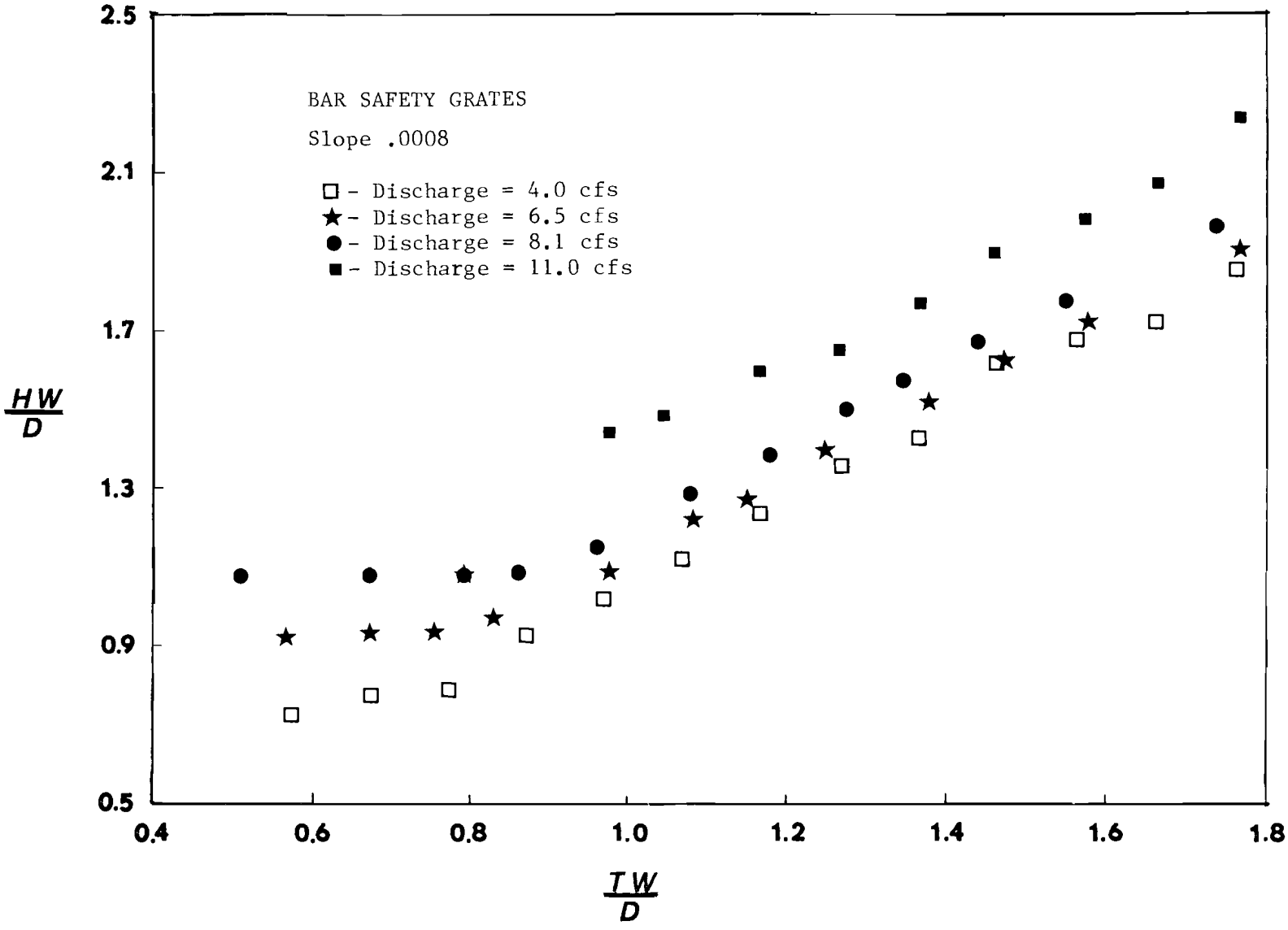


Figure B.34 Headwater vs. Tailwater For Bar Safety Grates, Slope = .0008

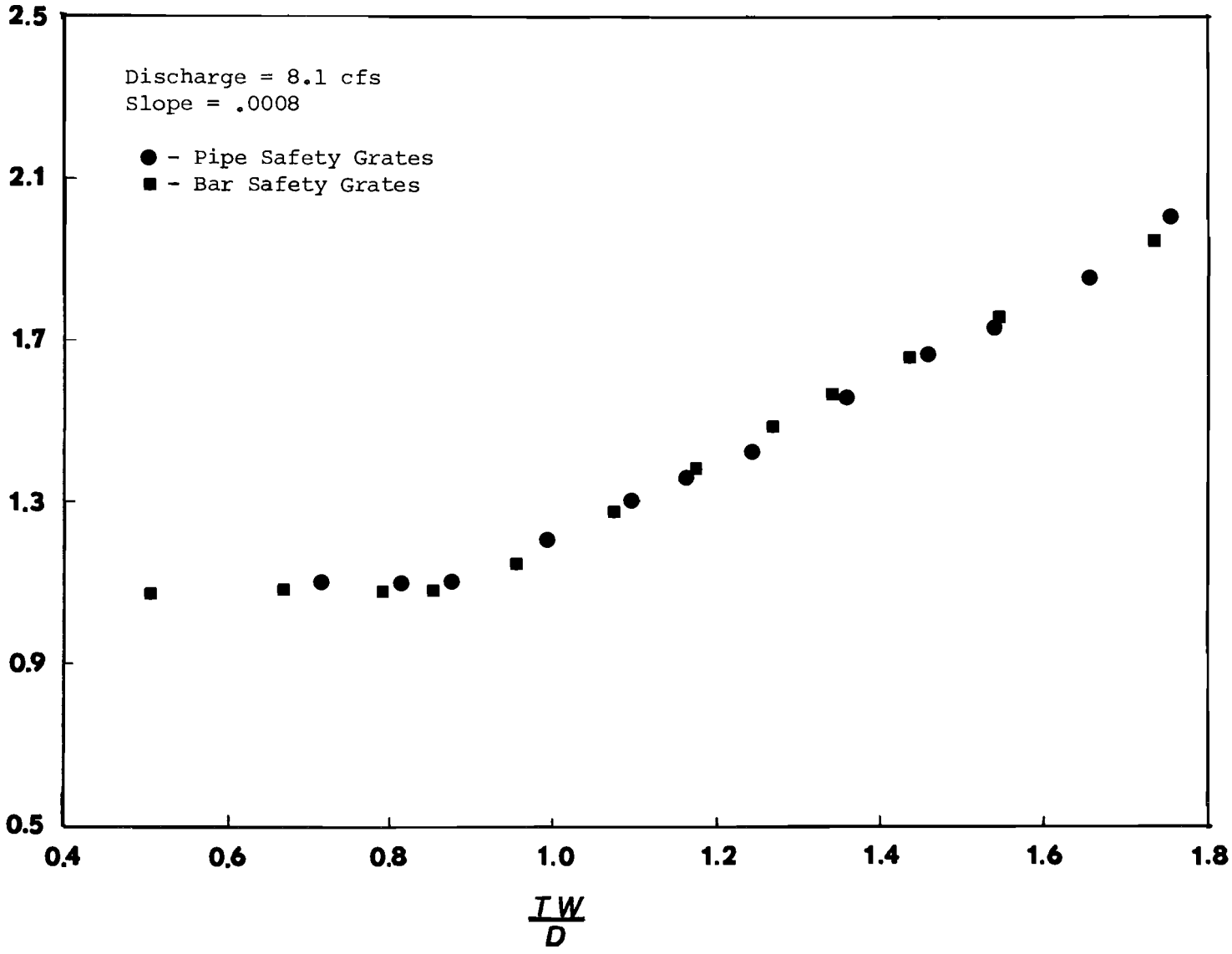


Figure B.35 Headwater vs. Tailwater for both Pipe Safety Grates and Bar Safety Grates, Discharge = 8.1 cfs, Slope = .0008

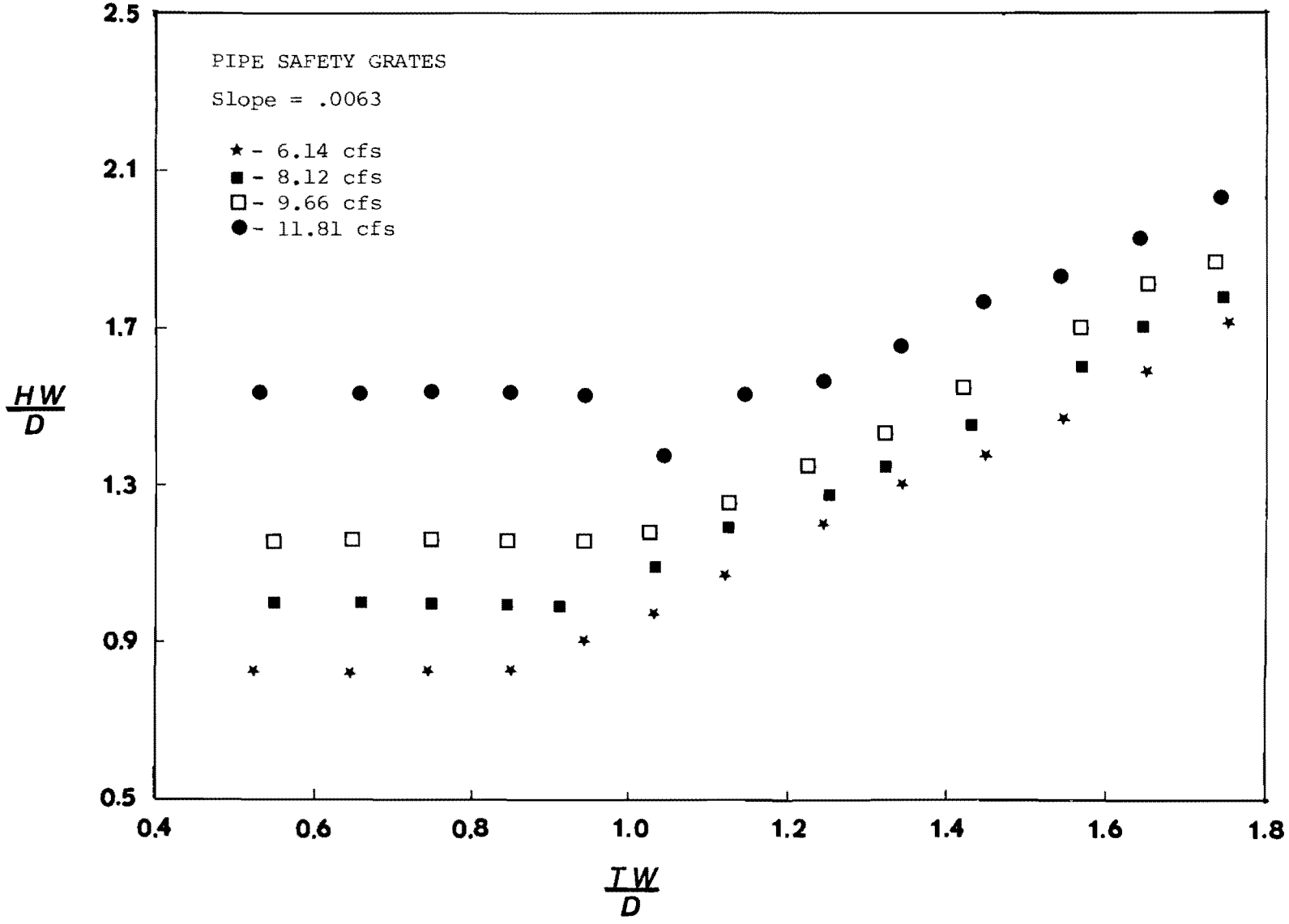


Figure B.36 Headwater vs. Tailwater for Pipe Safety Grates, Slope = .0063

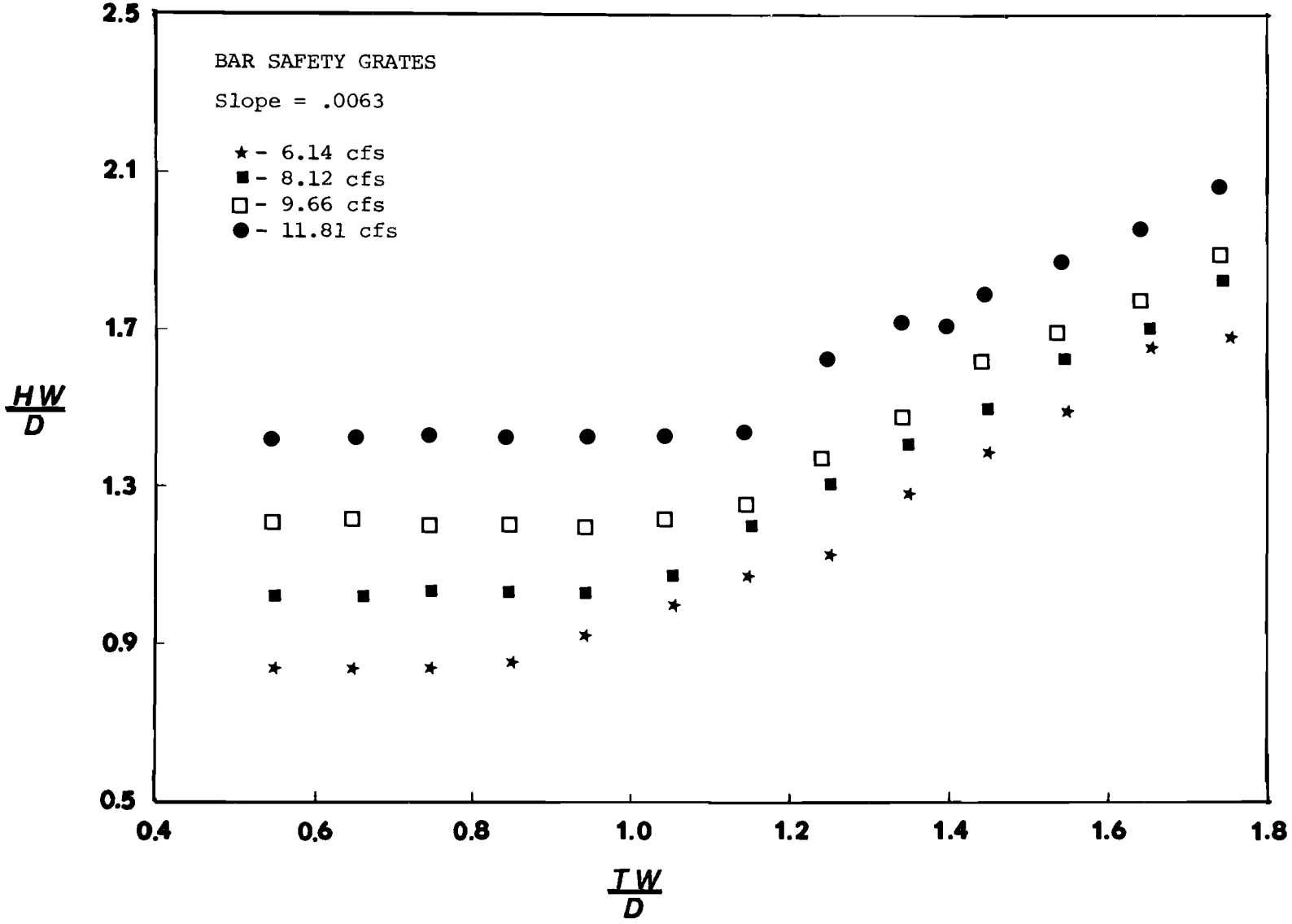


Figure B.37 Headwater vs. Tailwater for Bar Safety Grates, Slope = .0063

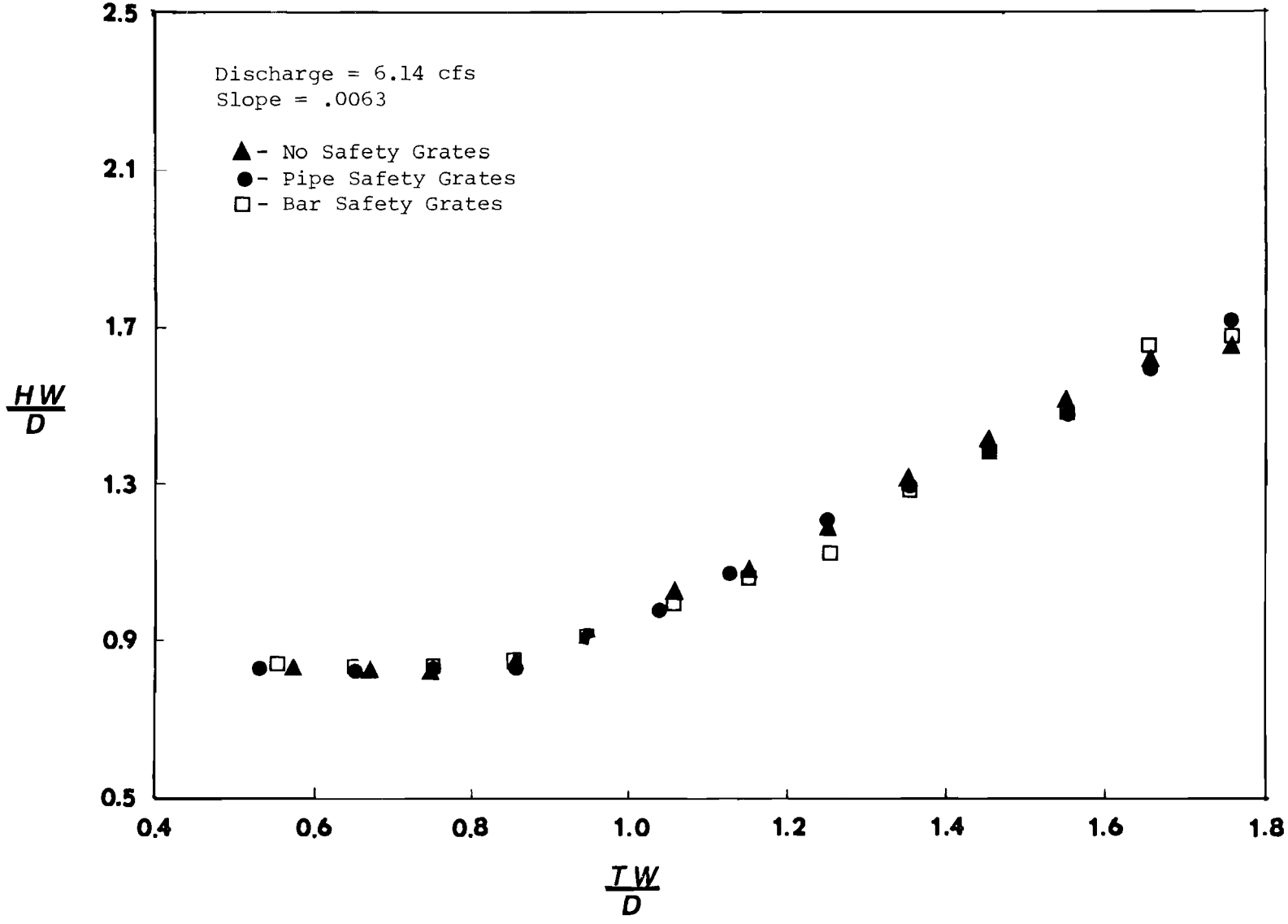


Figure B.38 Headwater vs. Tailwater For No Safety Grates, Pipe Safety Grates, and Bar Safety Grates, Discharge = 6.14 cfs, Slope = .0063

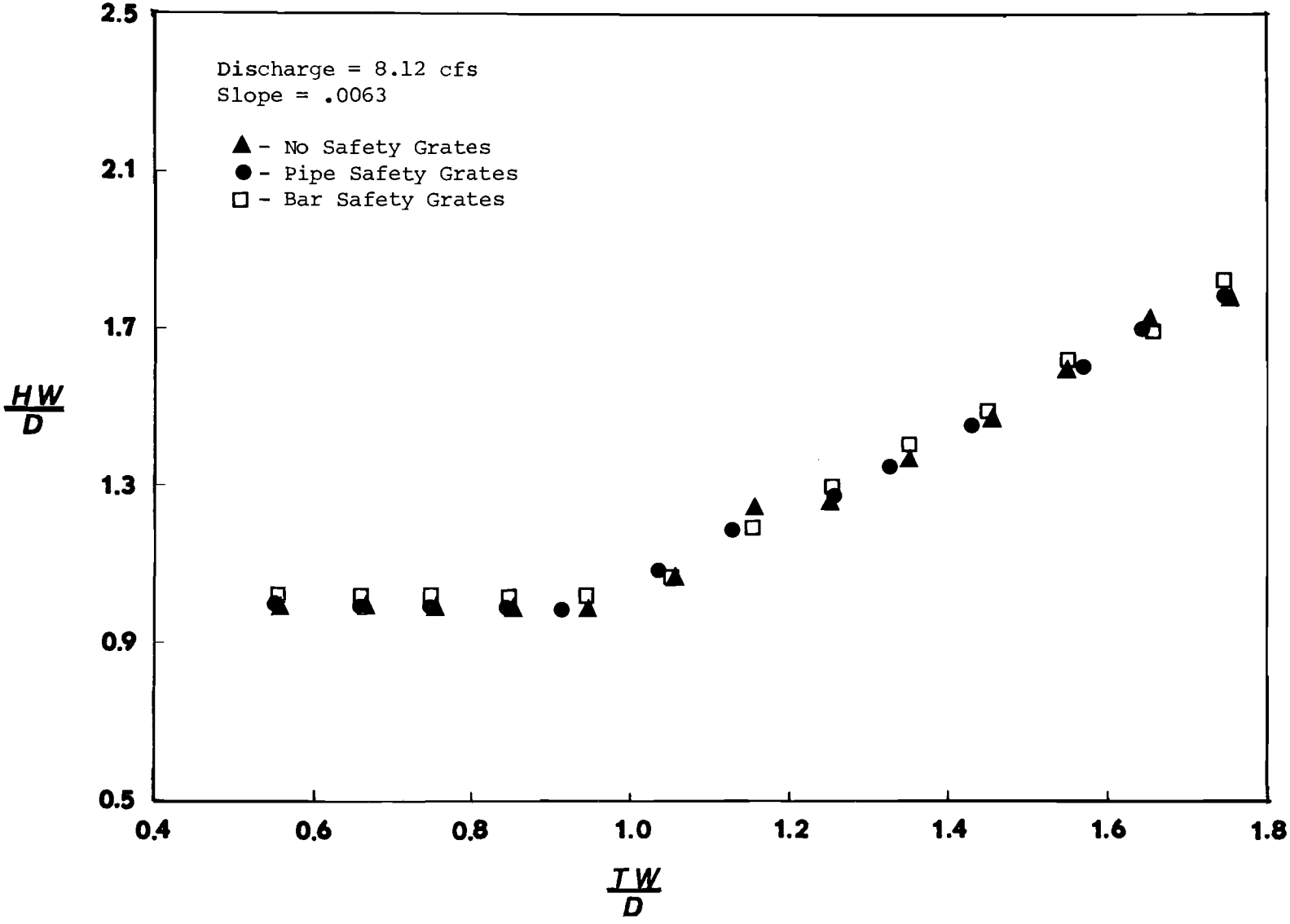


Figure B.39 Headwater vs. Tailwater For No Safety Grates, Pipe Safety Grates and Bar Safety Grates, Discharge = 8.12 cfs, Slope = .0063

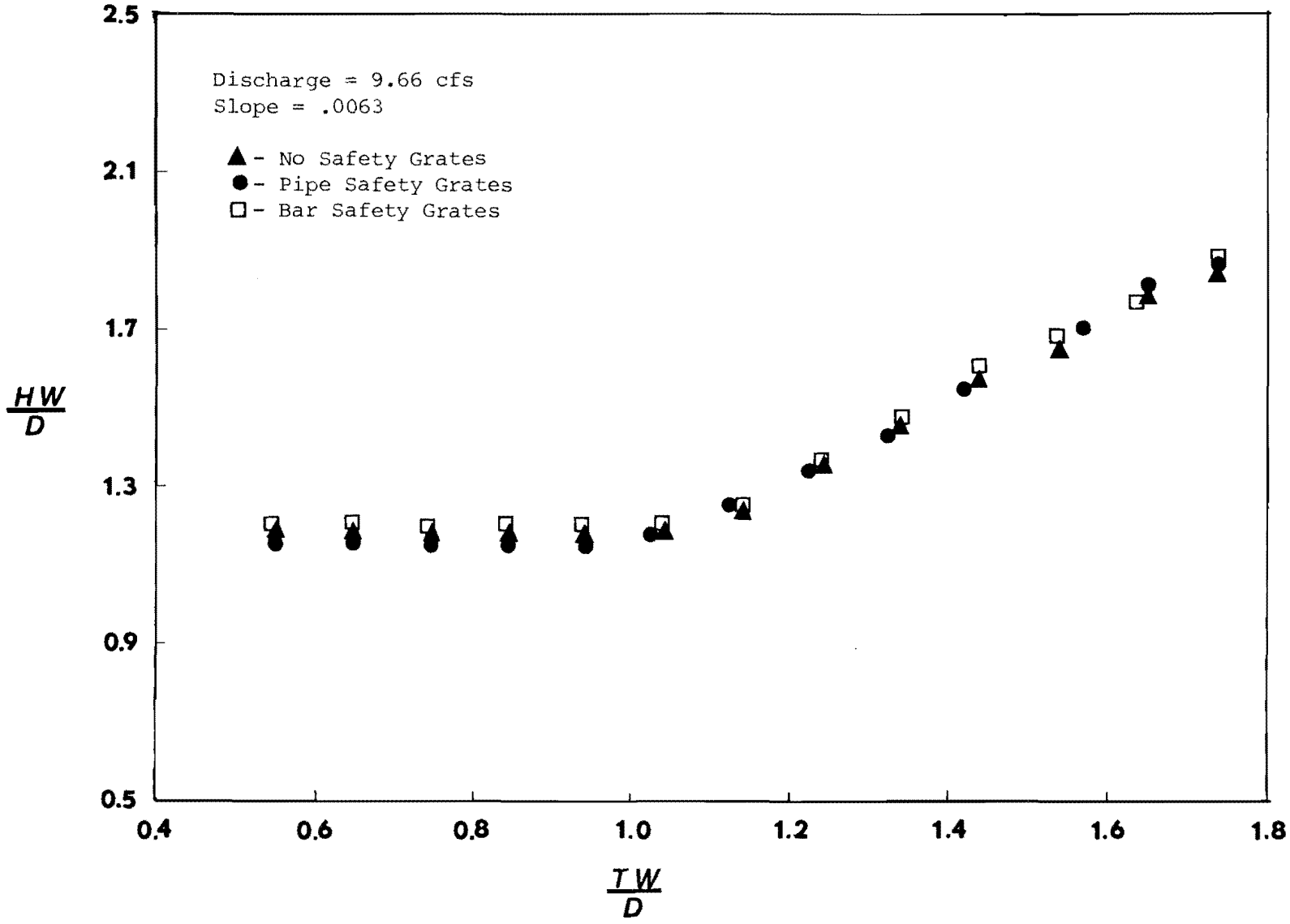


Figure B.40 Headwater Vs. Tailwater For No Safety Grates, Pipe Safety Grates and Bar Safety Grates, Discharge = 9.66 cfs, Slope = .0063

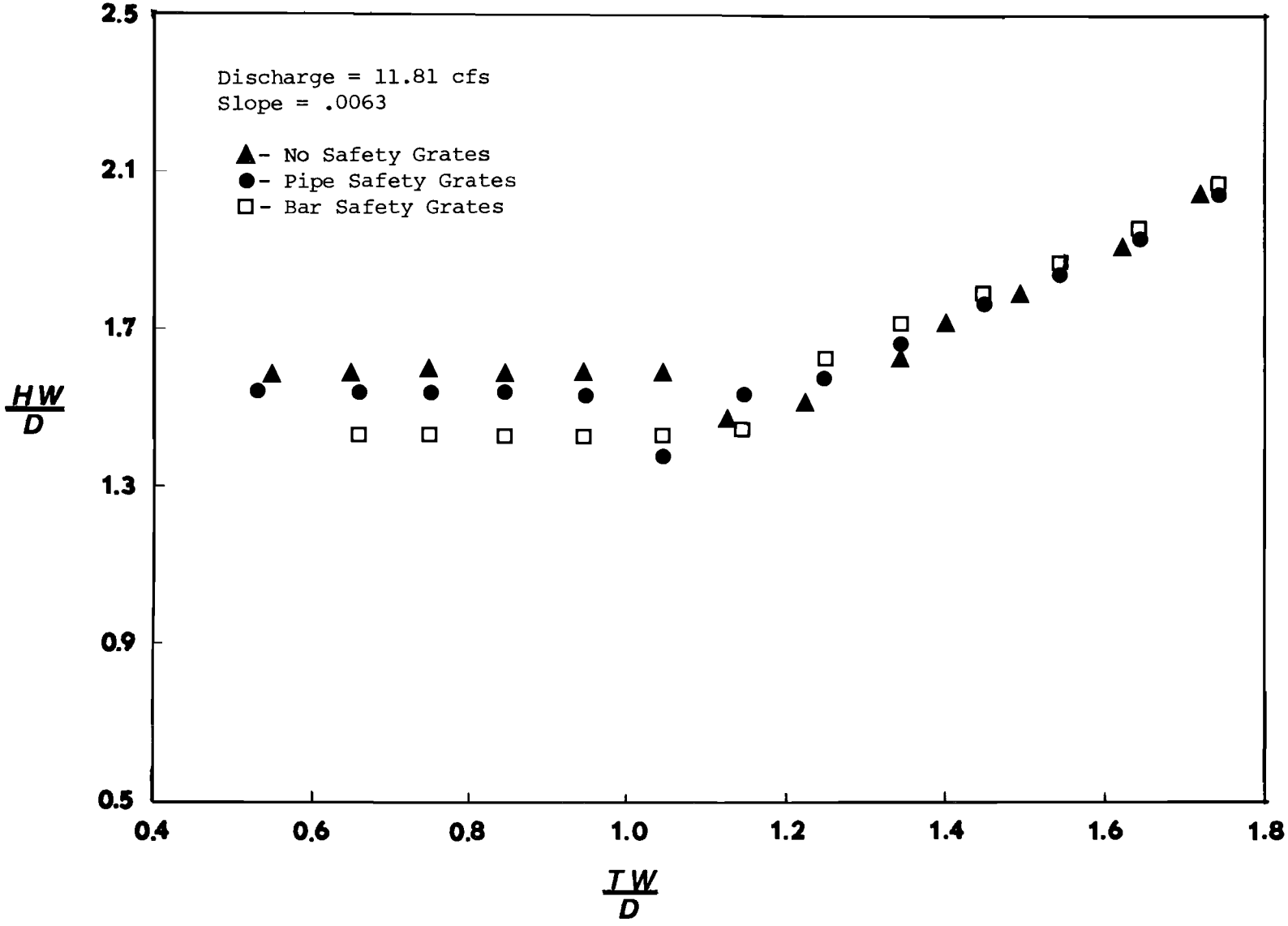


Figure B.41 Headwater vs. Tailwater for No Safety Grates, Pipe Safety Grates, and Bar Safety Grates, Discharge = 11.81 cfs, Slope = .0063

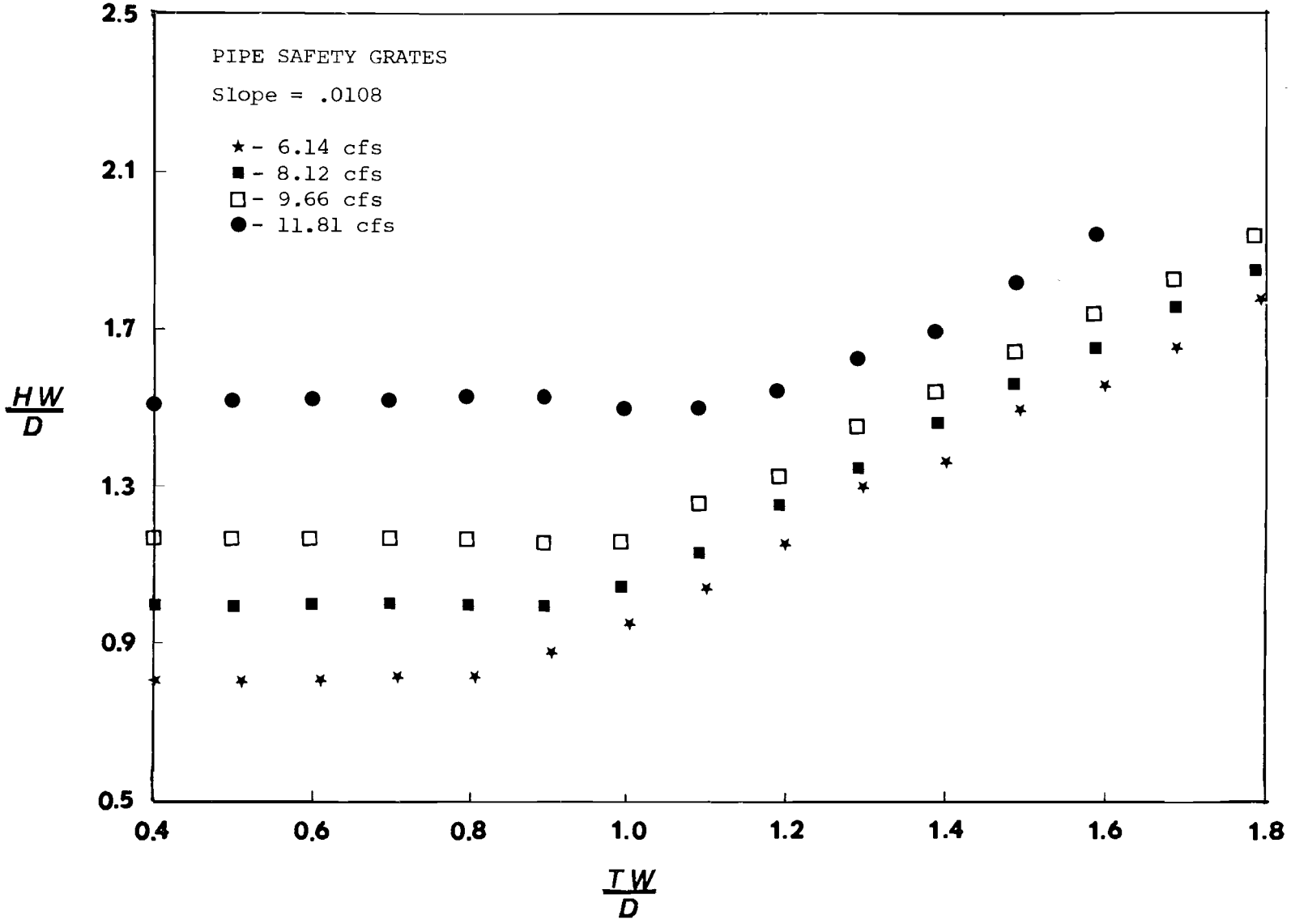


Figure B.42 Headwater vs. Tailwater for Pipe Safety Grates, Slope = .0108

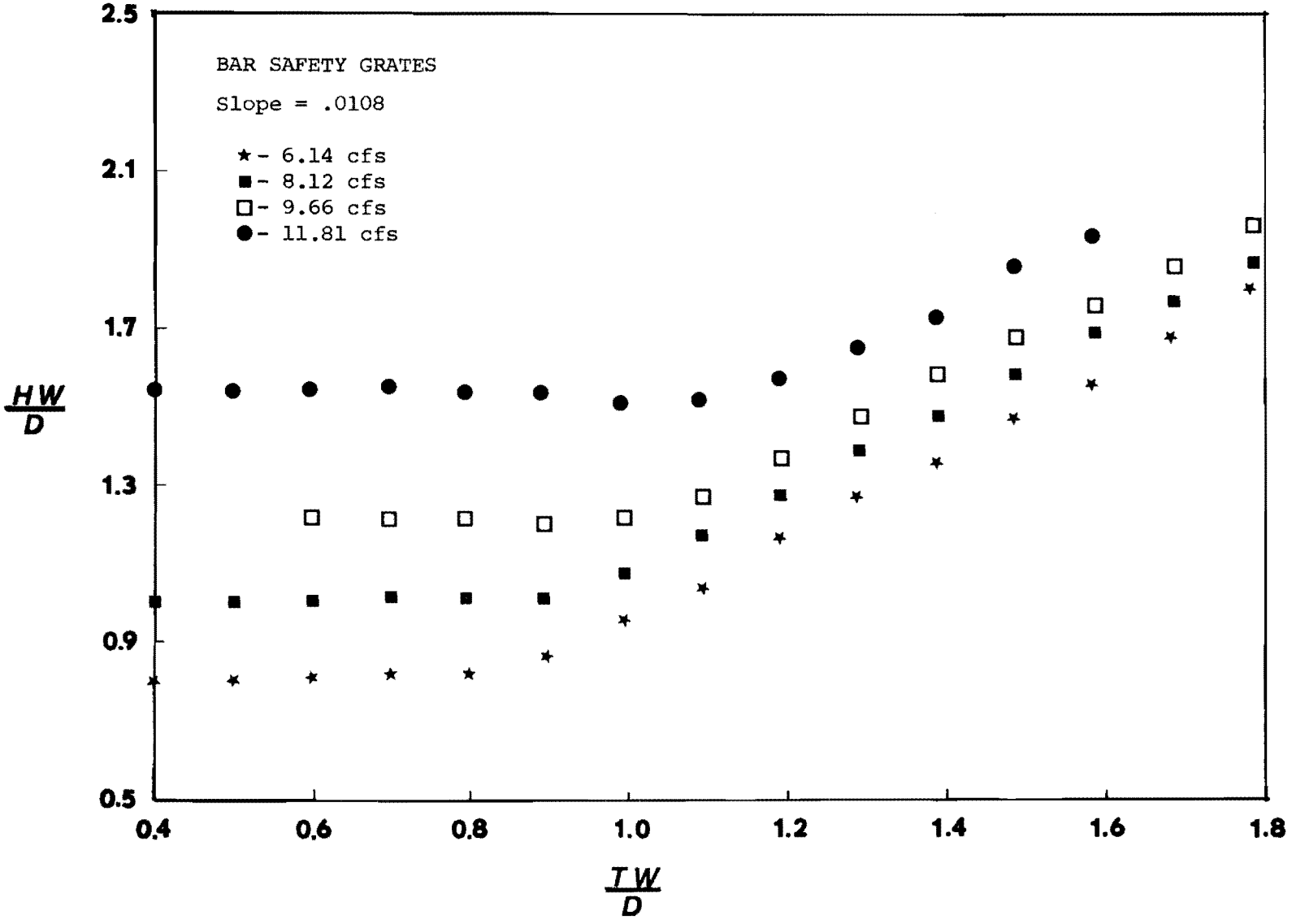


Figure B.43 Headwater vs. Tailwater for Bar Safety Grates, Slope = .0108

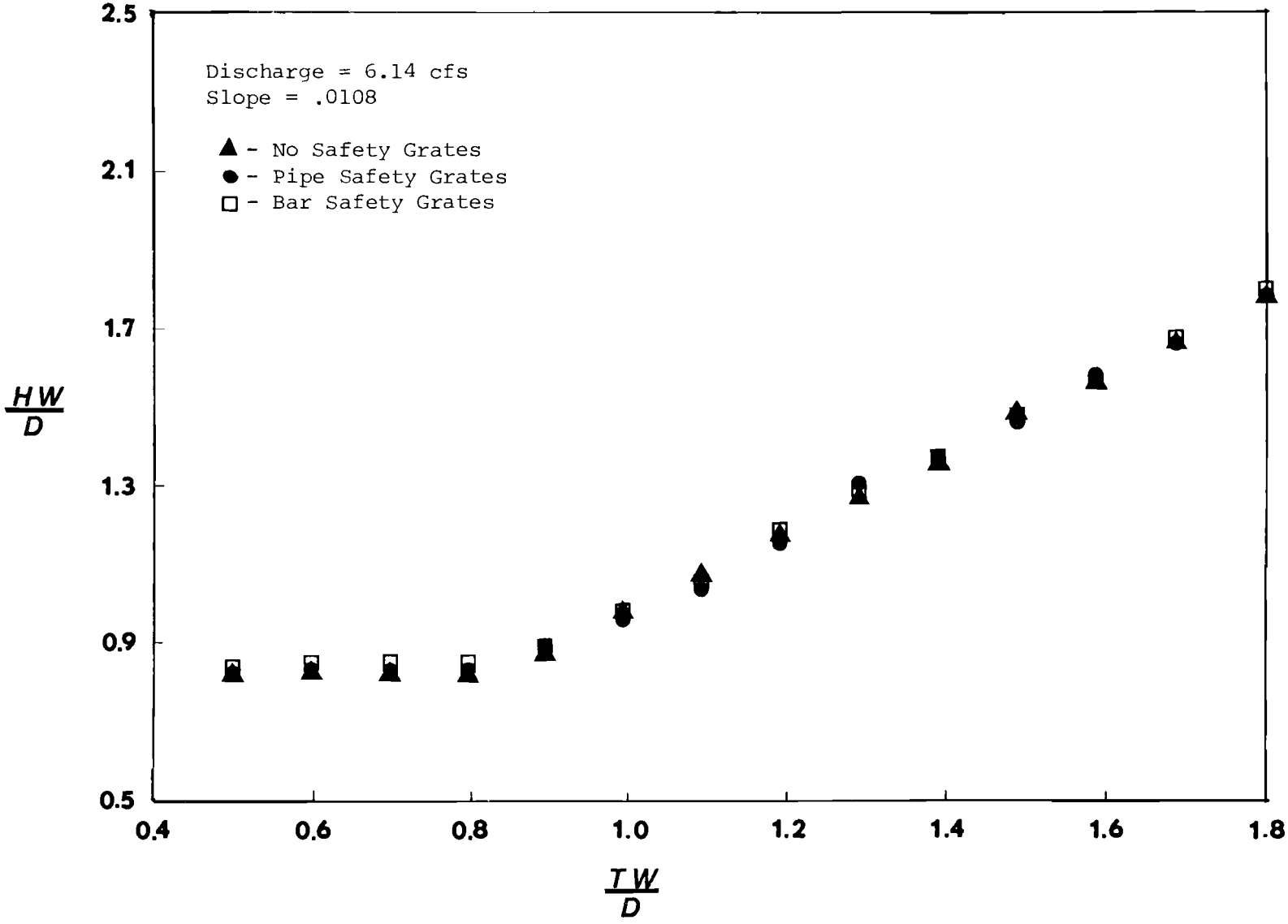


Figure B.44 Headwater vs. Tailwater for No Safety Grates, Pipe Safety Grates and Bar Safety Grates, Discharge = 6.14 cfs, Slope = .0108

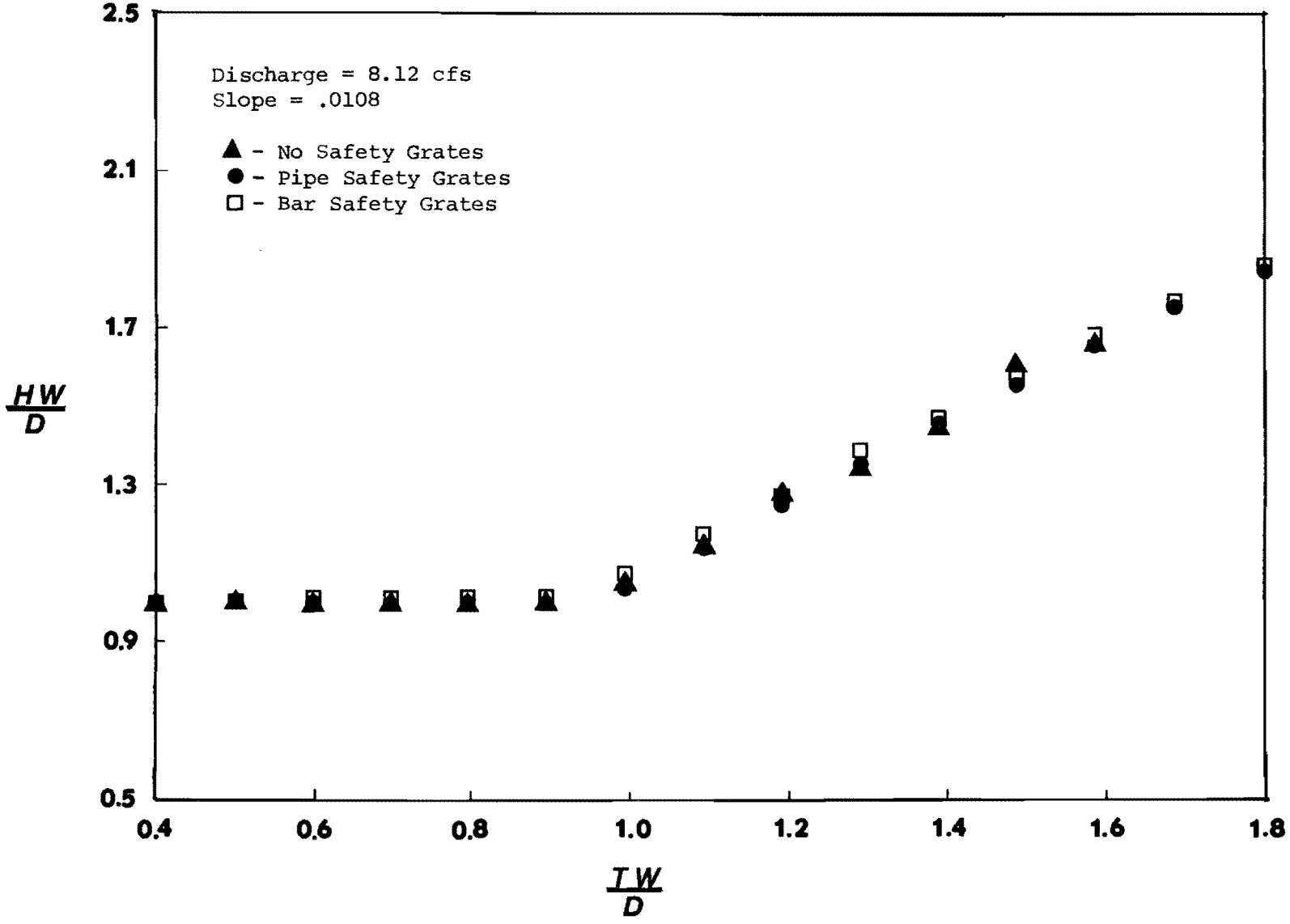


Figure B.45 Headwater vs. Tailwater for No Safety Grate, Pipe Safety Grate, Bar Safety Grate, Discharge = 8.12 cfs, Slope = .0108

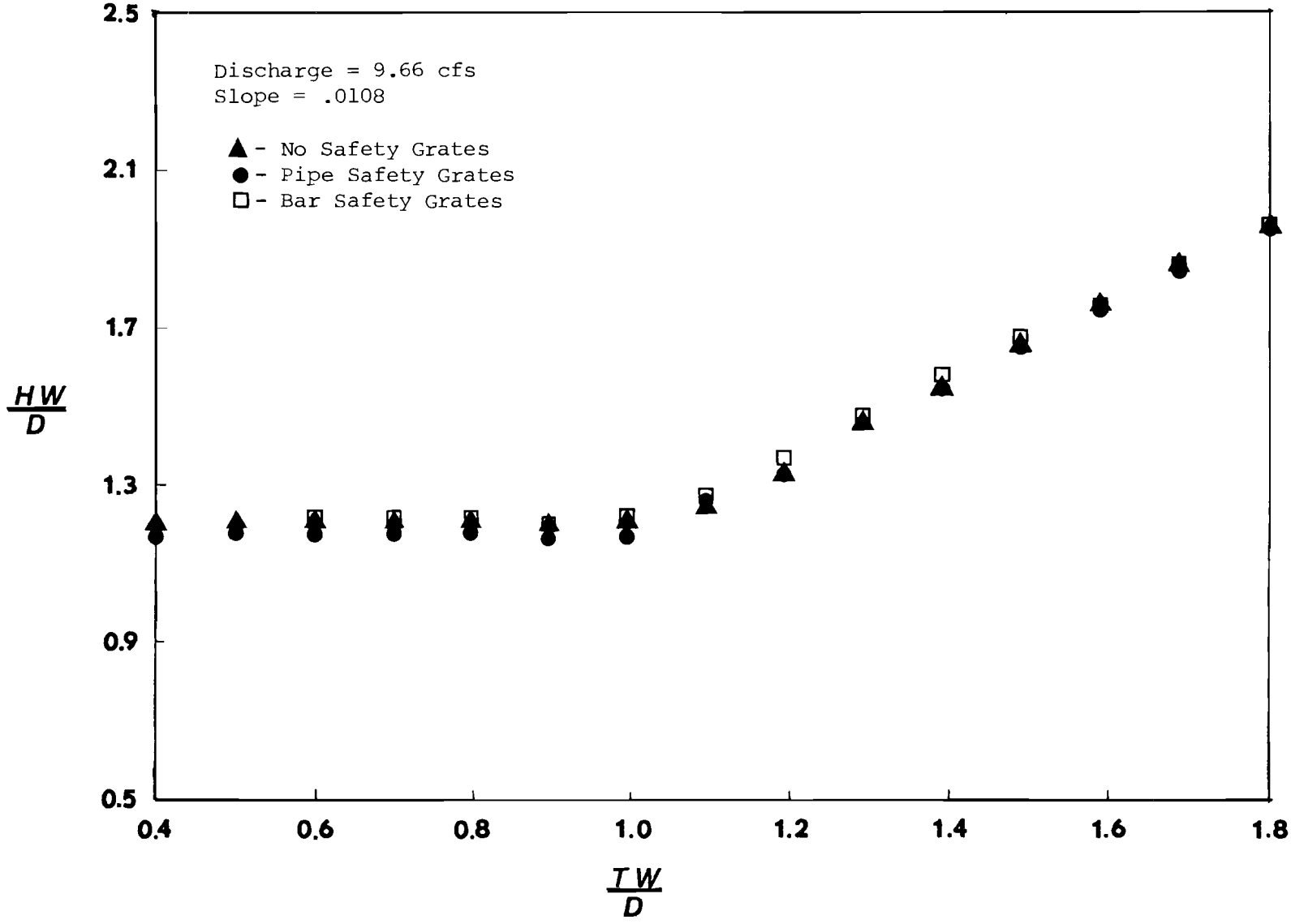


Figure B.46 Headwater vs. Tailwater for No Safety Grate, Bar Safety Grate, Pipe Safety Grate, Discharge = 0.66 cfs, Slope = .0108

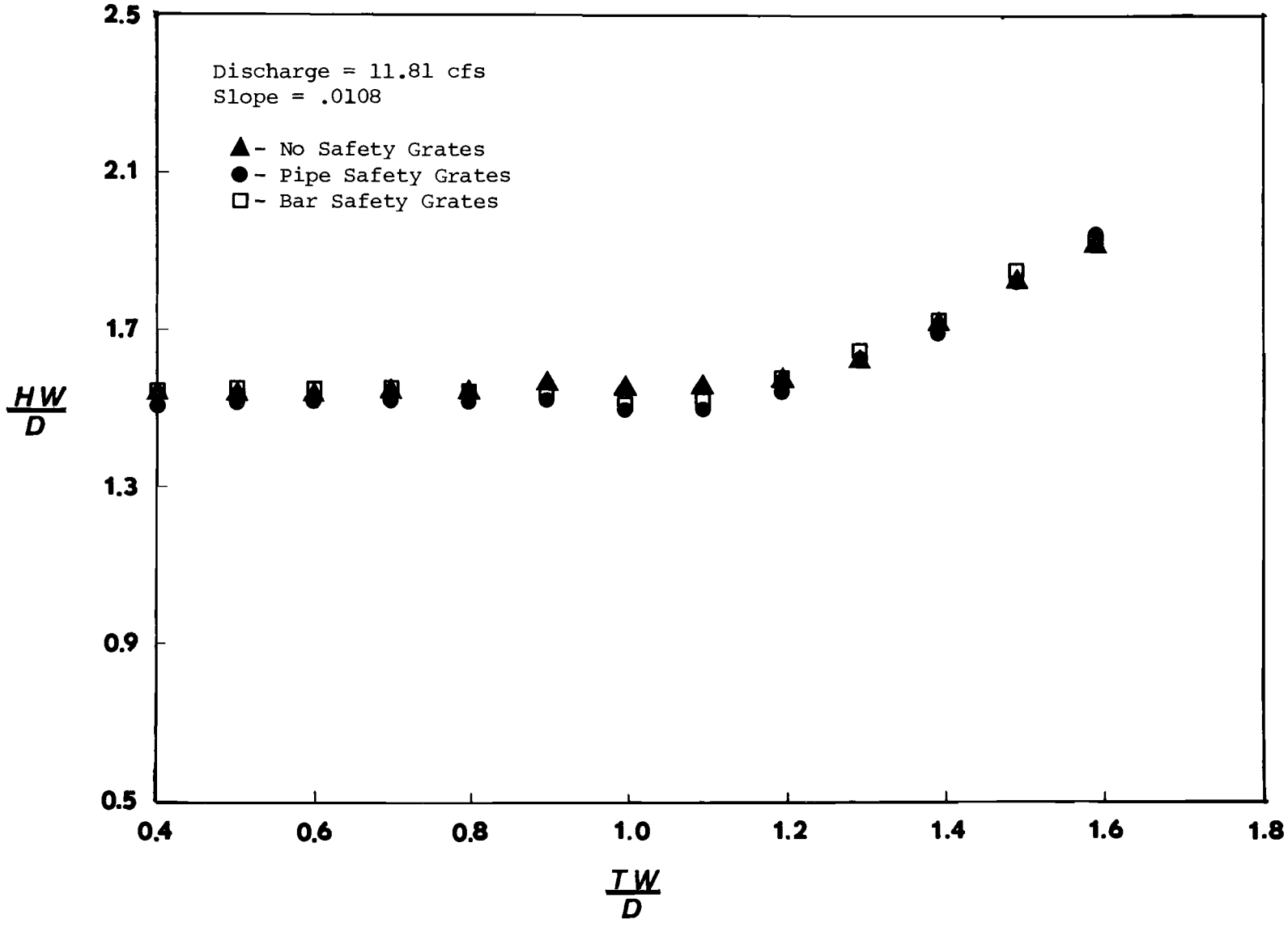


Figure B.47 Headwater vs. Tailwater for No Safety Grates, Pipe Safety Grates, Bar Safety Grates, Discharge = 11.81 cfs, Slope = .0108

# APPENDIX C

## Summary of Regression Results: Box Culvert

## DEVELOPMENT OF REGRESSION EQUATIONS CONSIDERING VARIOUS FLOW REGIMES

To determine the regression equations, the experimental data was divided into the different flow regimes. Several regression equations using different combinations of controlling factors (headwater, tailwater, etc) were considered. As an example, for Type 1 flow regime, the headwater, tailwater, and slope are factors used in culvert design while tailwater depth is not. Therefore, the regression equations were developed using different combinations of discharge, headwater, and slope for Type 1 flow regime conditions.

The statistical package program, OMITAB II, was utilized to determine the best fit equations for each combination of controlling factors. OMNITAB II (1966) was developed by the Statistical Engineering Laboratory of the National Bureau of Standards and uses the ordinary least squares method to determine the regression coefficients.

The regression equations to predict $C_e$ were also used to identify outliers in the data. To identify outliers, the deviation of the measured $C_e$ values from the predicted $C_e$ values were computed and were assumed to be normally distributed. The frequency of occurrence for the maximum deviation was computed $\frac{1}{n+1}$ where n is the number of observed data points. A normal distribution table was used to determine the maximum deviation associated with the computed frequency. Outliers were identified as having deviations larger than the maximum expected deviation.

### Regression Equations for $C_e$

Basically, the regression equations to determine entrance headloss coefficients were divided into two groups. The first set of regression equations were theoretical models based upon the energy equation. The second set of

regression equations predicted the entrance headloss coefficient from different combinations of headwater depth, discharge, tailwater depth and slope.

To develop the theoretical regression models, the energy equation for the entrance of the culvert was considered. The energy equation was rearranged so that the entrance headloss coefficient was the dependent variable and all other terms in the equation were independent variables. The resulting equation is

$$C_e = 2g\left(\frac{HW}{D}\right)\left(\frac{Q}{BD^{1.5}}\right)^{-2} - 2g\left(\frac{Q}{BD^{1.5}}\right)^{-2} - 1 \qquad (C.1)$$

For the statistical analysis, the terms 2g, -2g, and -1 were replaced with the regression constants $B_o$, $B_1$, and $B_2$. The final equation form is

$$C_e = B_0 + B_1\left(\frac{HW}{D}\right)\left(\frac{Q}{BD^{1.5}}\right)^{-2} + B_2\left(\frac{Q}{BD^{1.5}}\right)^{-2} \qquad (C.2)$$

To introduce different terms to the theoretical model, the variables were multiplied by $\left(\frac{Q}{BD^{1.5}}\right)^{-2}$ and added to the equation. As an example, if tailwater was included, then the final equation form would be

$$C_e = B_0 + B_1\left(\frac{HW}{D}\right)\left(\frac{Q}{BD^{1.5}}\right)^{-2} + B_2\left(\frac{Q}{BD^{1.5}}\right)^{-2} + B_3\left(\frac{TW}{D}\right)\left(\frac{Q}{BD^{1.5}}\right)^{-2} \qquad (C.3)$$

For the second set of equations, the regression models were in the general form

$$C_e = B_0 + B_1\left(\frac{HW}{D}\right) + B_2\left(\frac{Q}{BD^{1.5}}\right) + B_3\left(\frac{TW}{D}\right) \qquad (C.4)$$

where all terms have been previously defined. It should be emphasized that the selection of independent variables for the regression analysis must be done so that independence is maintained. For example, if $S_o$ was also included in Eq.

(C.4) then the variables would not be independent in $\frac{HW}{D}$ which is a function of $\frac{Q}{BD^{1.5}}$, $\frac{TW}{D}$, and $S_o$.

Table C-1

| Equation Reference | Equation Form |
|---|---|
| 1 | $C_e = B_0 + B_1 \left(\frac{HW}{D}\right)\left(\frac{Q}{BD^{1.5}}\right)^{-2} + B_2 \left(\frac{Q}{BD^{1.5}}\right)^{-2}$ |
| 2 | $C_e = B_0 + B_1 \left(\frac{HW}{D}\right)\left(\frac{Q}{BD^{1.5}}\right)^{-2} + B_2 \left(\frac{Q}{BD^{1.5}}\right)^{-2} + B_3 \left(\frac{TW}{D}\right)\left(\frac{Q}{BD^{1.5}}\right)^{-2}$ |
| 3 | $C^2_e = B_0 + B_1 \left(\frac{HW}{D}\right)\left(\frac{Q}{BD^{1.5}}\right)^{-2} + B_2 \left(\frac{Q}{BD^{1.5}}\right)^{-2} + B_3 \left(\frac{TW}{D}\right)\left(\frac{Q}{BD^{1.5}}\right)^{-2}$ |
| 4 | $C_e = B_0 + B_1 \left(\frac{HW}{D}\right)\left(\frac{Q}{BD^{1.5}}\right)^{-2} + B_2 \left(\frac{Q}{BD^{1.5}}\right)^{-2} + B_3 (S_o)\left(\frac{Q}{BD^{1.5}}\right)^{-2}$ |
| 5 | $C_e = B_0 + B_1 \left(\frac{Q}{BD^{1.5}}\right)^{-2} + B_2 \left(\frac{TW}{D}\right)\left(\frac{Q}{BD^{1.5}}\right)^{-2} + B_3 (S_o)\left(\frac{Q}{BD^{1.5}}\right)^{-2}$ |
| 6 | $C_e = B_0 + B_1 \left(\frac{HW}{D}\right)\left(\frac{Q}{BD^{1.5}}\right)^{-2}$ |
| 7 | $C_e = B_0 + B_1 \left(\frac{Q}{BD^{1.5}}\right)^{-2} + B_2 \left(\frac{TW}{D}\right)\left(\frac{Q}{BD^{1.5}}\right)^{-2}$ |

Table C.1 (continued)

| Equation Reference | Equation Form |
|---|---|
| 8 | $C_e = B_0 + B_1 (\frac{HW}{D}) + B_2 (\frac{Q}{BD^{1.5}})$ |
| 9 | $C_e = B_0 + B_1 (\frac{HW}{D}) + B_2 (\frac{Q}{BD^{1.5}}) + B_3 (\frac{TW}{D})$ |
| 10 | $C_e = B_0 + B_1 (\frac{Q}{BD^{1.5}}) + B_2 (\frac{TW}{D})$ |
| 11 | $C_e = B_0 + B_1 (\frac{HW}{D}) + B_2 (\frac{Q}{BD^{1.5}}) + B_3 (S_o)$ |
| 12 | $C_e = B_0 + B_1 (\frac{HW}{D}) + B_2 (\frac{HW}{D})^2 + B_3 (\frac{Q}{BD^{1.5}}) + B_4 (\frac{Q}{BD^{1.5}})^2 + B_5 (S_o)$ |
| 13 | $C_e = B_0 + B_1 (\frac{HW}{D})^2 + B_2 (\frac{Q}{BD^{1.5}}) + B_3 (\frac{Q}{BD^{1.5}})^2 B_4(S_o)$ |
| 14 | $C_e = B_0 + B_1 (\frac{Q}{BD^{1.5}}) + B_2 (\frac{TW}{D}) + B_3 (S_o)$ |
| 15 | $C_e = B_0 + B_1 (S_o)$ |
| 16 | $C_e = B_0 + B_1 (\frac{Q}{BD^{1.5}}) + B_2 (S_o)$ |

Table C.1

| Equation Reference | Equation Form |
|---|---|
| 17 | $C_e = B_0 + B_1 (\frac{HW}{D}) + B_2 (S_o)$ |
| 18 | $C_e = B_0 + B_1 (\frac{HW}{D})$ |
| 19 | $C_e = B_0 + B_1 (\frac{HW}{D}) + B_2 (\frac{TW}{D})$ |
| 20 | $C_e = B_0 + B_1 (\frac{Q}{BD^{1.5}})$ |
| 21 | $C_e = B_0 + B_1 (\frac{Q}{BD^{1.5}}) + B_2 (\frac{HW-TW}{D})$ |

TABLE C.2

BOX CULVERT
RESULTS OF REGRESSION ANALYSIS: NO GRATES

| Regime | Equation | $B_o$ | $B_1$ | $B_2$ | $B_3$ | $B_4$ | R | Number of Points |
|---|---|---|---|---|---|---|---|---|
| 1 | 1 | .222 | -.431 | .207 | | | .076 | 36 |
| | 4 | .072 | 1.822 | -1.132 | -55.845 | | .461 | |
| | 8 | -.071 | .825 | -.206 | | | .248 | |
| | 11 | -1.164 | 4.274 | -1.113 | 36.786 | | .710 | |
| | 13 | .210 | 2.956 | -.842 | -.112 | 42.682 | .884 | |
| 2 | 2 | -.047 | 6.189 | -4.171 | -40.477 | | .943 | 34 |
| | 8 | -.333 | 1.367 | -.309 | | | .958 | |
| 3A | 1 | .344 | -2.823 | 1.154 | | | .586 | 36 |
| 4A | 1 | .738 | 2.943 | -5.167 | | | .601 | 103 |
| | 2 | .726 | 3.480 | -4.778 | -.739 | | .605 | |
| | 9 | .003 | .525 | .014 | -.153 | | .653 | |
| 4B | 2 | 2.720 | -36.654 | 16.641 | -31.577 | | .604 | 42 |
| | 3 | 2.268 | -32.40 | 14.443 | -25.911 | | .572 | |
| | 9 | -.832 | -2.601 | 1.250 | -.047 | | .572 | |
| | 11 | -.354 | -1.664 | .827 | -41.657 | | .779 | |

TABLE C. 3

BOX CULVERT
RESULTS OF REGRESSION ANALYSIS: PIPE GRATES

| Regime | Equation | $B_o$ | $B_1$ | $B_2$ | $B_3$ | $B_4$ | R | Number of Points |
|---|---|---|---|---|---|---|---|---|
| 1 | 1 | .430 | -.384 | .181 | | | .054 | 39 |
| | 3 | .053 | 2.030 | -1.251 | 59.330 | | .453 | |
| | 8 | -.121 | .977 | -.245 | | | .294 | |
| | 11 | -1.288 | 4.542 | -1.160 | 36.741 | | .791 | |
| | 12 | .127 | .333 | 2.111 | -.723 | -.072 | .918 | |
| | 13 | .203 | 2.258 | -.651 | -.084 | 34.185 | .918 | |
| | 15 | .159 | 7.929 | | | | .246 | |
| | 16 | .135 | .011 | 7.836 | | | .258 | |
| | 17 | .258 | .092 | .072 | 8.273 | | .258 | |
| 2 | 2 | -.042 | 6.103 | -4.771 | .625 | | .828 | 32 |
| | 5 | .163 | -1.232 | 2.554 | -109.0 | | .804 | |
| | 8 | -.339 | 1.308 | -.286 | | | .922 | |
| | 9 | -.355 | 1.313 | -.287 | .014 | | .913 | |
| | 10 | -.023 | -.061 | .521 | | | .598 | |
| 4A | 2 | .646 | 5.105 | -2.084 | -4.085 | | .511 | 129 |
| | 3 | .805 | 3.162 | -1.470 | -2.456 | | .517 | |
| | 8 | .132 | .240 | .042 | | | .543 | |
| | 9 | .365 | .688 | -.0362 | -.498 | | .591 | |
| | 10 | .158 | .077 | .180 | | | .423 | |
| | 14 | .176 | .077 | .183 | -5.708 | | .444 | |
| | 18 | .511 | .195 | .283 | | | .511 | |
| 4B | 2 | 1.130 | -13.674 | 8.337 | 3.256 | | .444 | 44 |
| | 8 | .219 | -1.356 | .561 | | | .273 | |
| | 9 | .526 | -1.179 | .397 | .205 | | .462 | |
| | 11 | -.813 | 2.700 | -.554 | -123.532 | | .987 | |

TABLE C. 4

BOX CULVERT
RESULTS OF REGRESSION ANALYSIS: BAR GRATES

| Regime | Equation | $B_o$ | $B_1$ | $B_2$ | $B_3$ | $B_4$ | R | Number of Points |
|---|---|---|---|---|---|---|---|---|
| 1 | 1 | .321 | -.0060 | -.420 | | | .675 | 26 |
| | 8 | -.364 | 1.339 | -.268 | | | .861 | |
| | 11 | -.849 | 3.066 | -.755 | 17.429 | | .904 | |
| | 13 | -.091 | 1.581 | -.196 | -.108 | 16.073 | .919 | |
| 2 | 2 | .033 | 4.652 | -2.555 | -.356 | | .848 | 28 |
| | 8 | -.269 | 1.782 | -.470 | | | .941 | |
| | 9 | -.157 | 1.471 | -.417 | .078 | | .839 | |
| 3A | 6 | .543 | -.608 | | | | .818 | 28 |
| | 18 | .059 | .137 | | | | .744 | |
| 4A | 1 | .825 | 2.419 | -4.591 | | | .675 | 38 |
| | 2 | .747 | 5.091 | -3.648 | -3.081 | | .700 | |
| | 3 | .557 | 6.559 | -5.052 | -3.707 | | .666 | |
| | 8 | .100 | .308 | .041 | | | .627 | |
| | 9 | .343 | .738 | -.035 | -.484 | | .663 | |
| | 19 | .256 | .586 | -.330 | | | .658 | |
| 4B | 1 | -.571 | -1.576 | .803 | | | .661 | 26 |
| | 9 | -.660 | -2.039 | .998 | -.099 | | .952 | |
| | 10 | -.473 | .196 | .047 | | | .509 | |
| | 11 | -.612 | -2.031 | .999 | -19.941 | | .957 | |
| | 13 | -8.193 | -.689 | 4.210 | -.421 | -12.012 | .980 | |

# APPENDIX D

## Clogging Test Results For Box Culverts

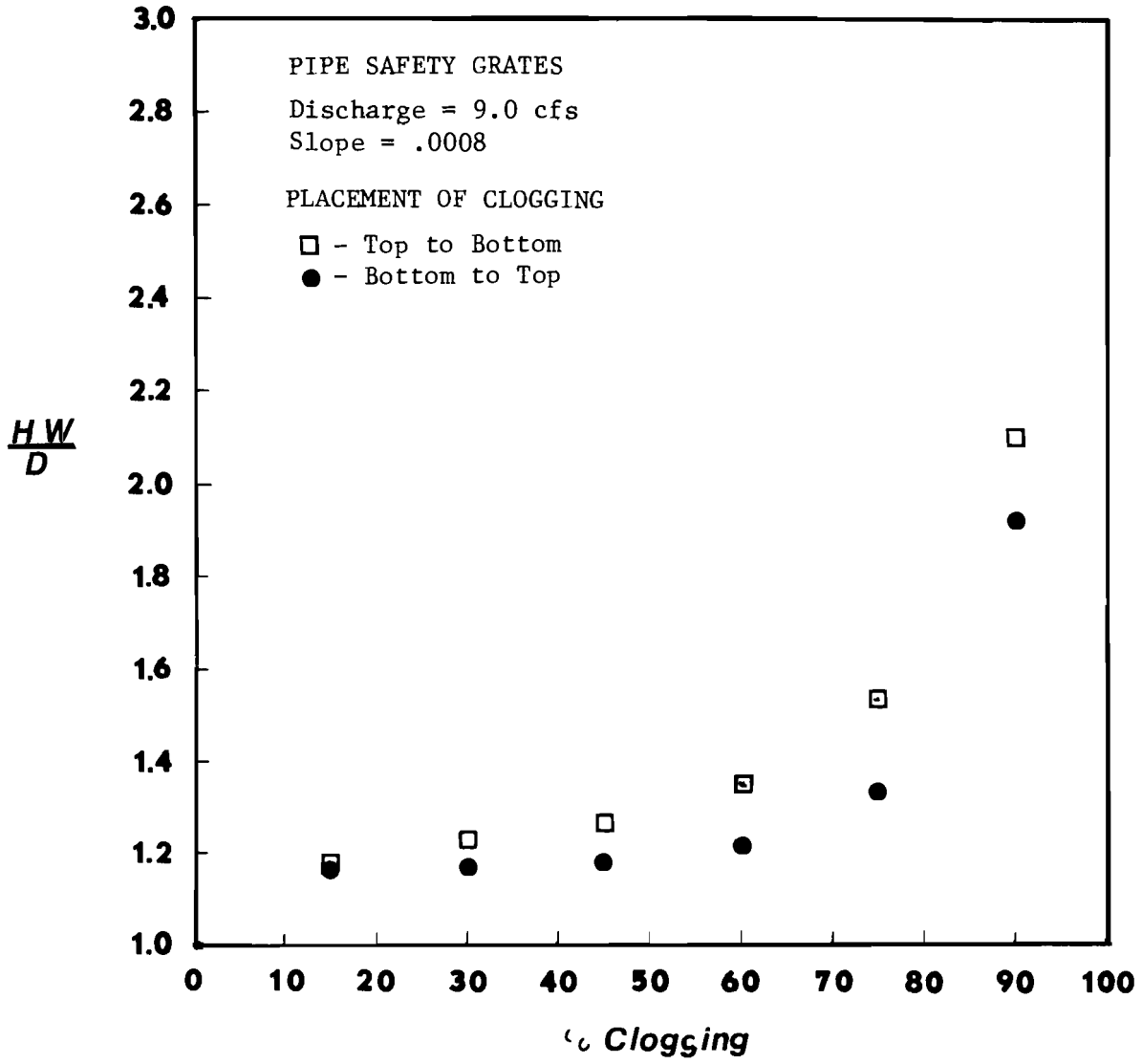


Figure D.1 Headwater vs. Percentage Clogging
($S_o$ = .0008, Q = 9 cfs)

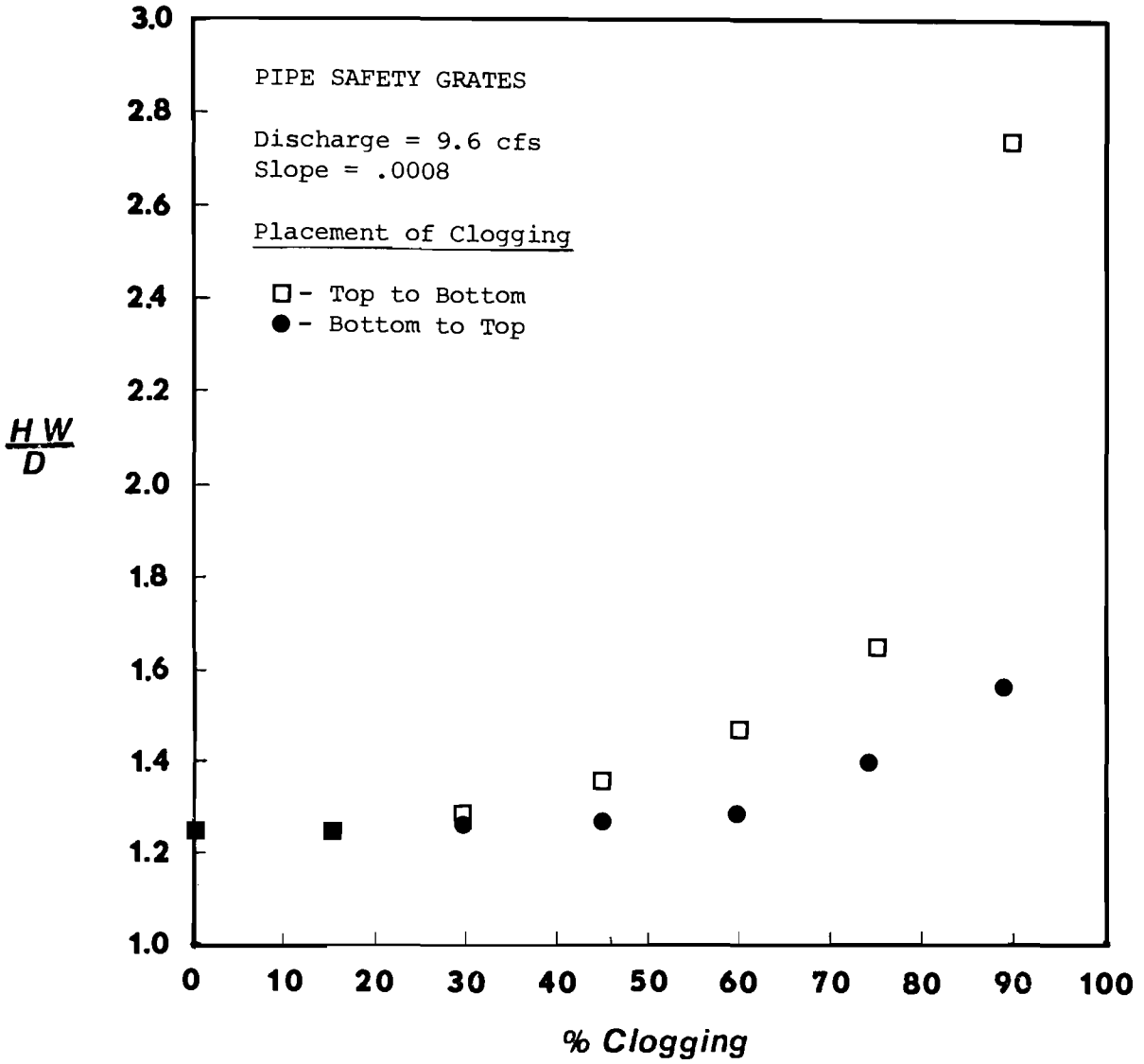


Figure D.2 Headwater vs. Percentage Clogging
($S_o$ = .0008, Q = 9.6 cfs)

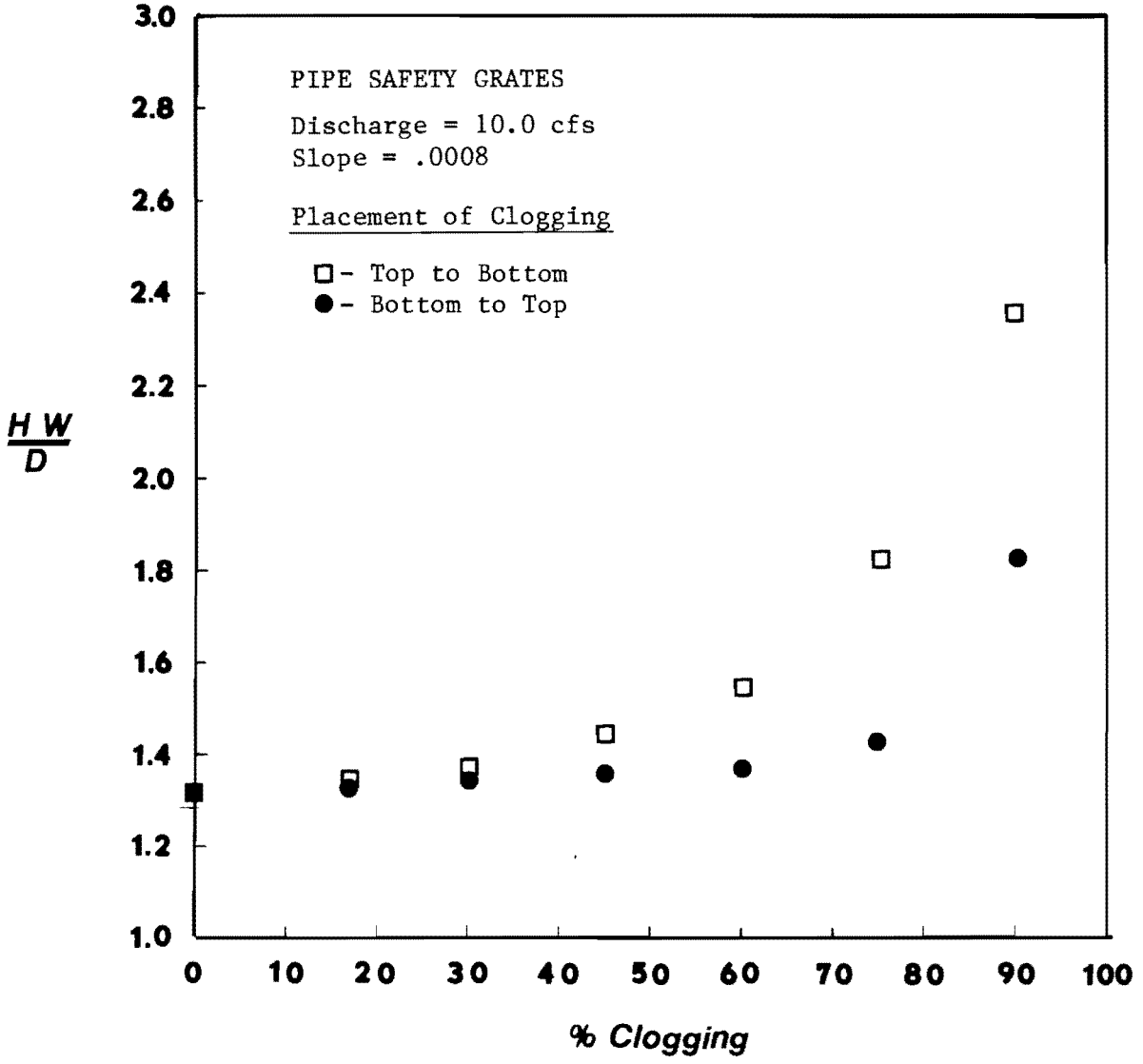


Figure D.3 Headwater vs. Percentage Clogging
($S_o$ = .0008, Q = 10 cfs)

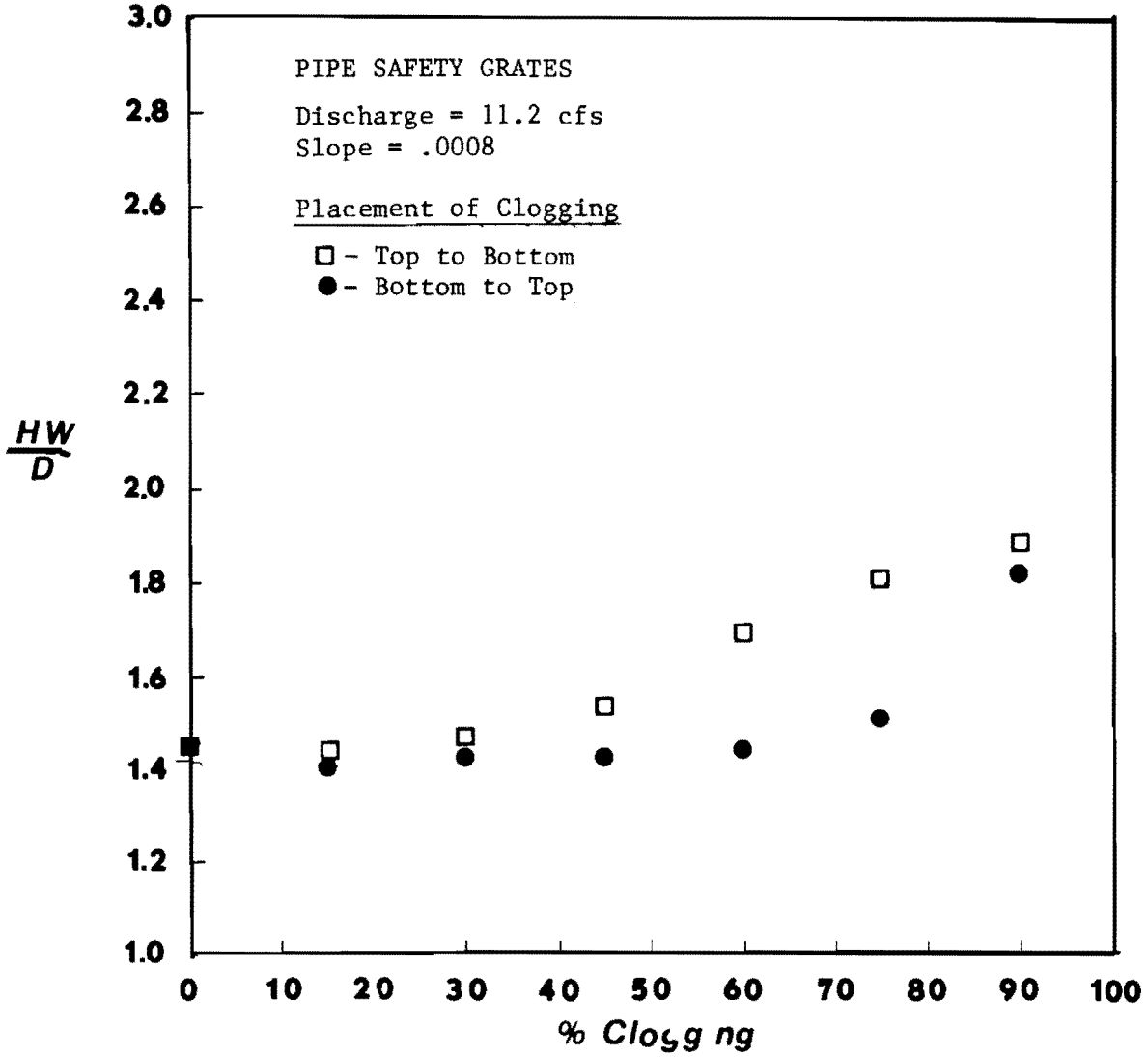


Figure D.4 Headwater vs. Percentage Clogging
($S_o$ = .0008, Q = 11.2 cfs)

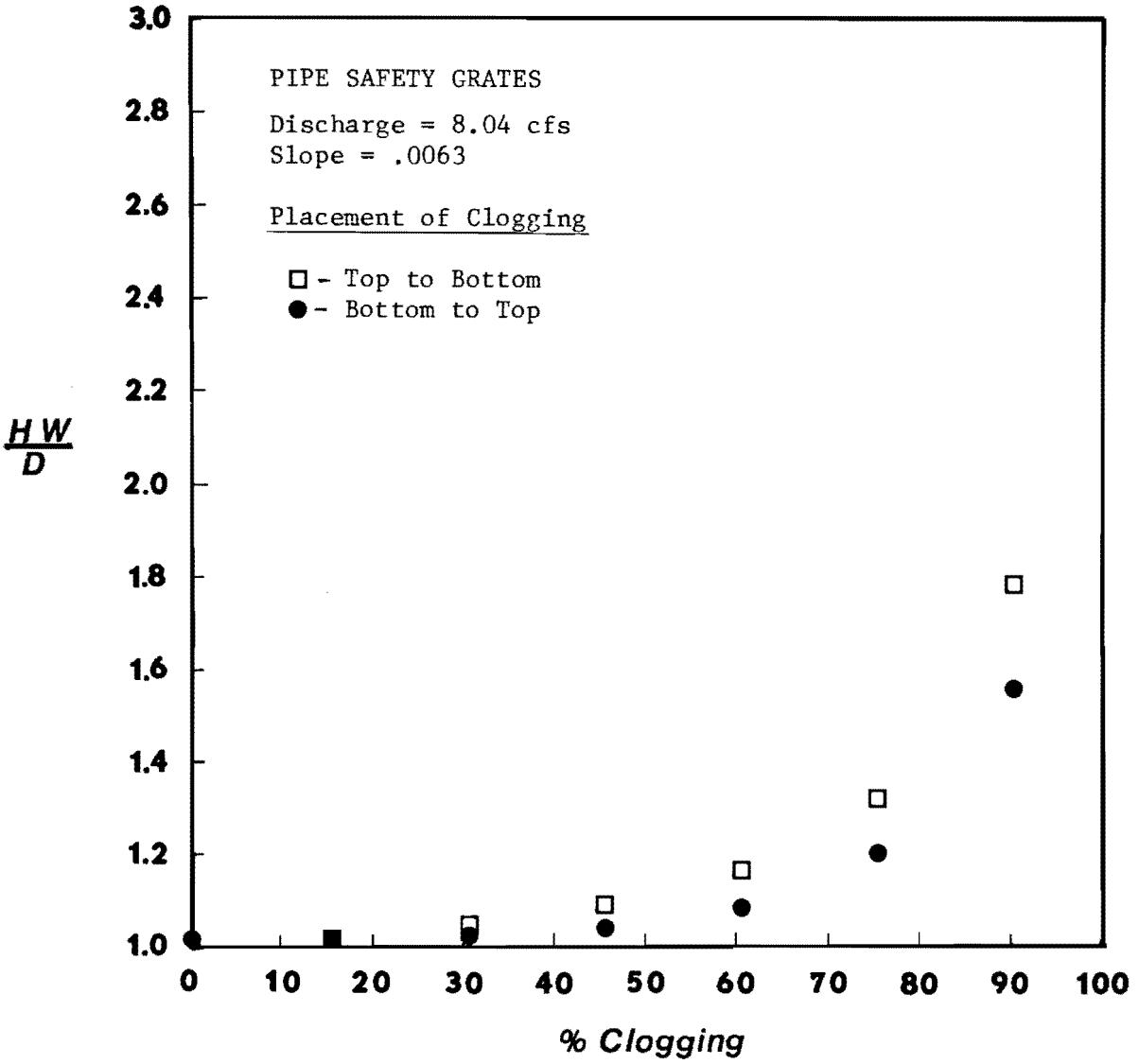


Figure D.5 Headwater vs. Percentage Clogging
($S_o$ = .0063, Q = 8.04 cfs)

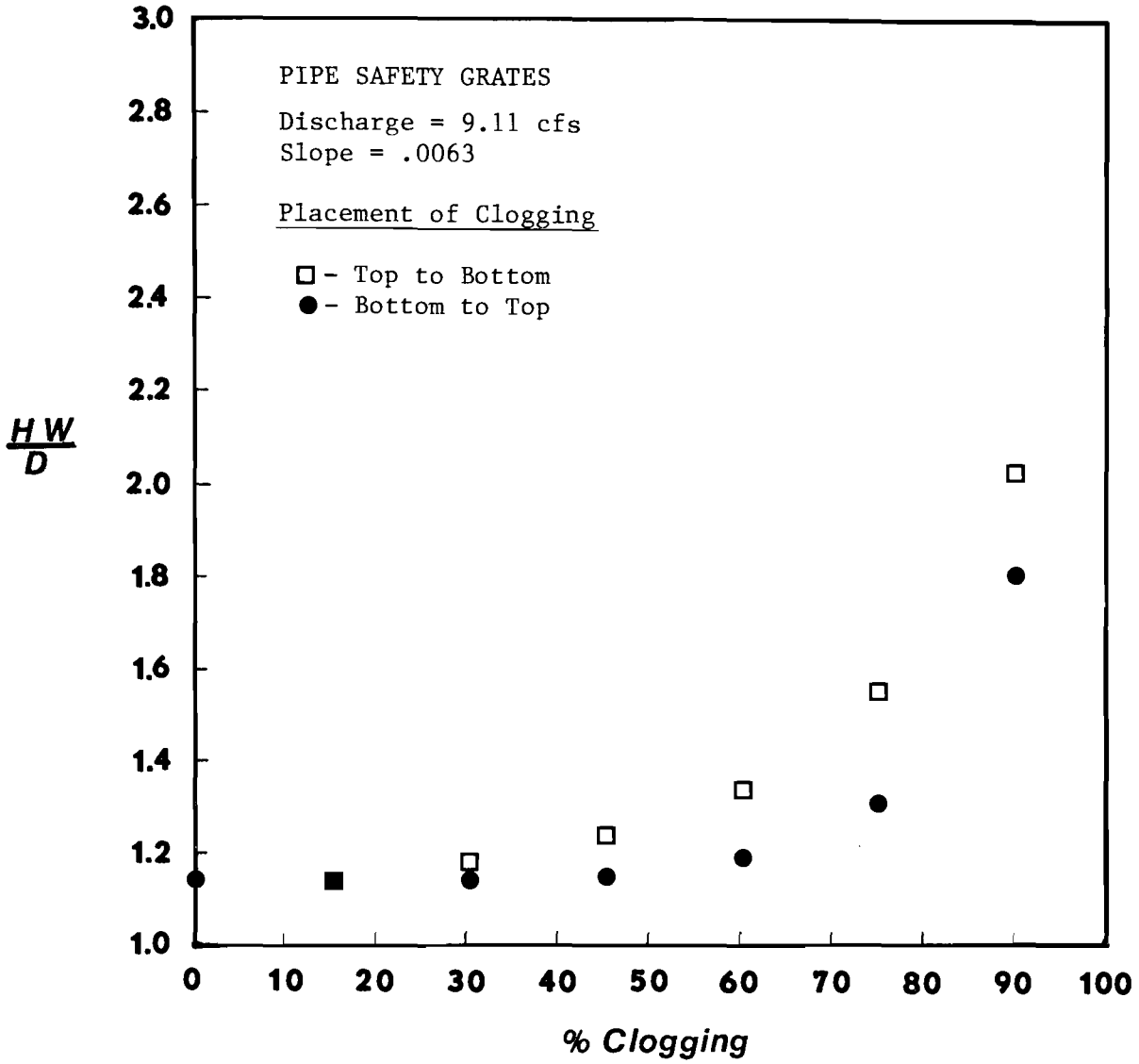


Figure D.6 Headwater vs. Percentage Clogging
($S_o$ = .0063, Q = 9.11 cfs)

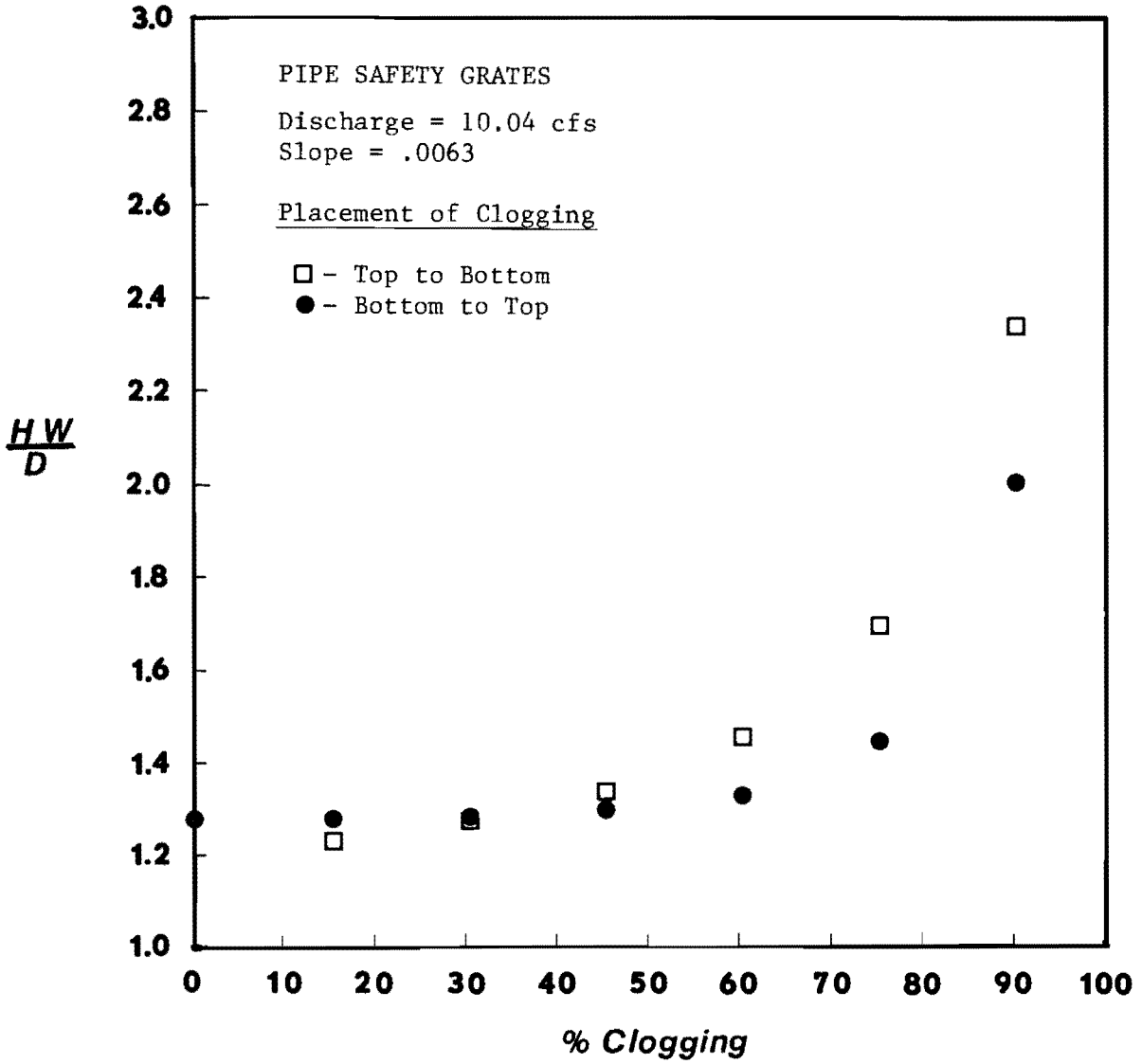


Figure D.7 Headwater vs. Percentage Clogging
($S_o$ = .0063, Q = 10.04cfs)

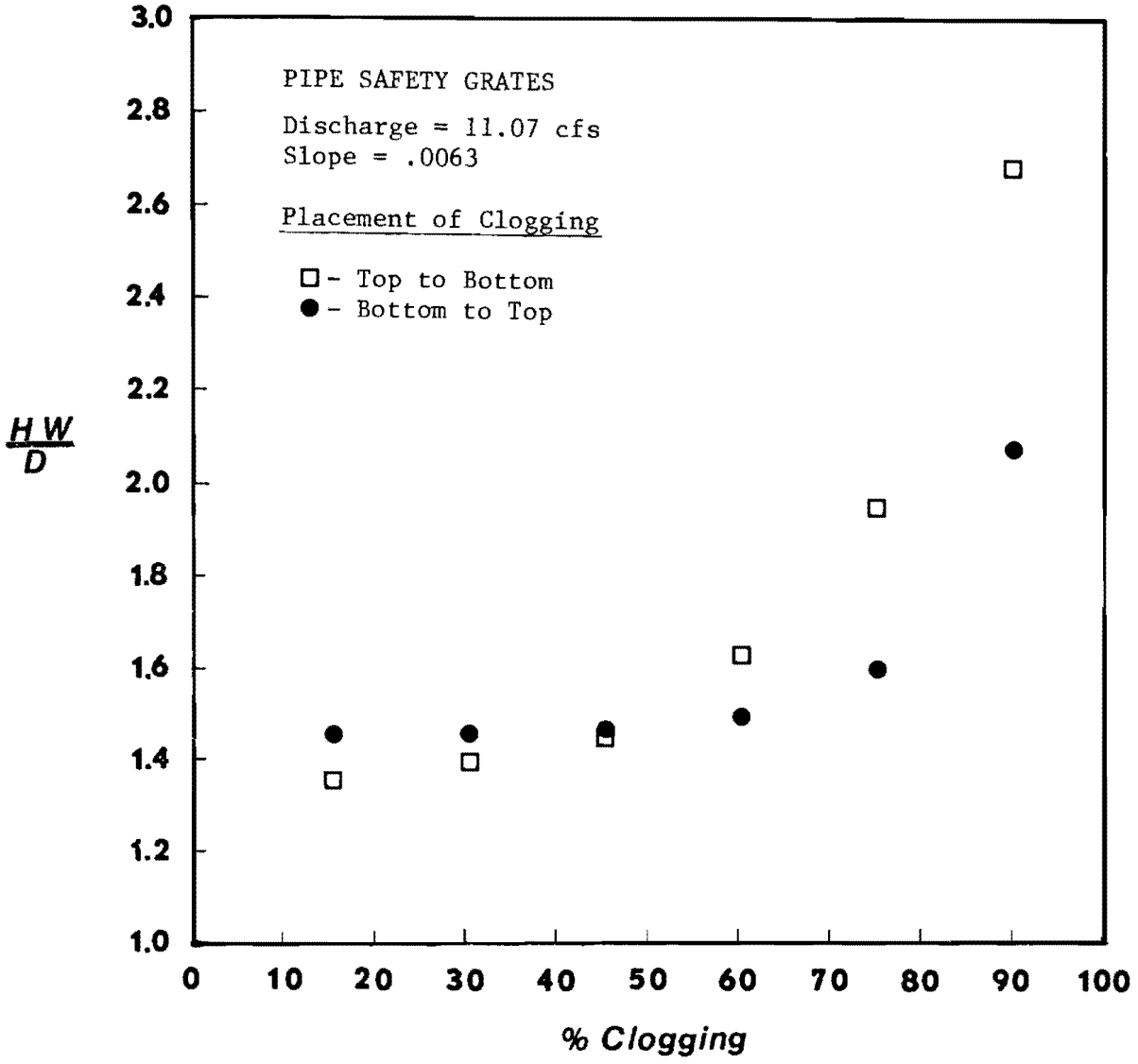


Figure D.8 Headwater vs. Percentage Clogging
($S_O$ = .0063, Q = 11.07cfs)

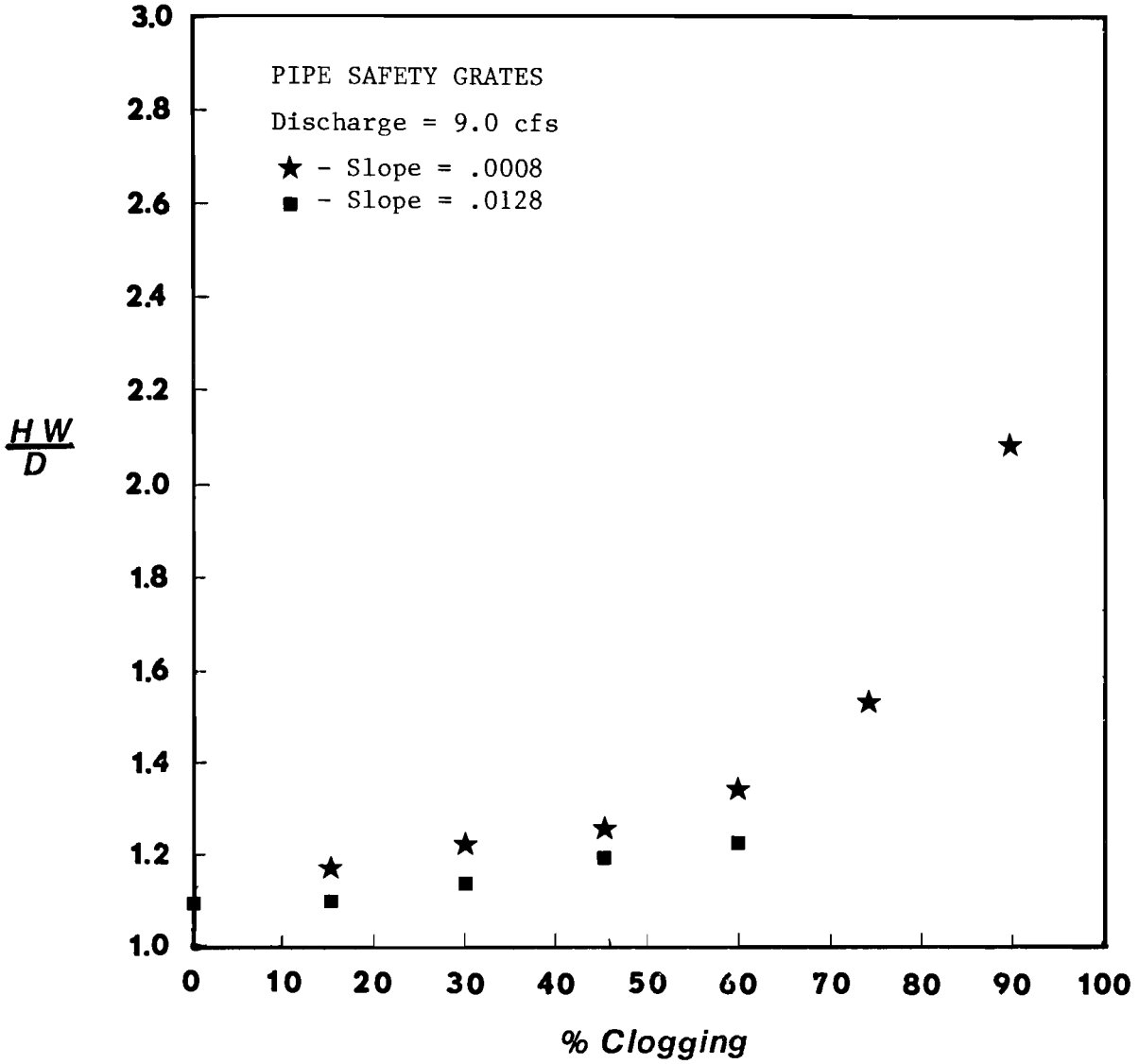


Figure D.9 Headwater vs. Percentage Clogging
($S_o$ = .0008, Q = 9.cfs)
($S_o$ = .0128, Q = 9.cfs)

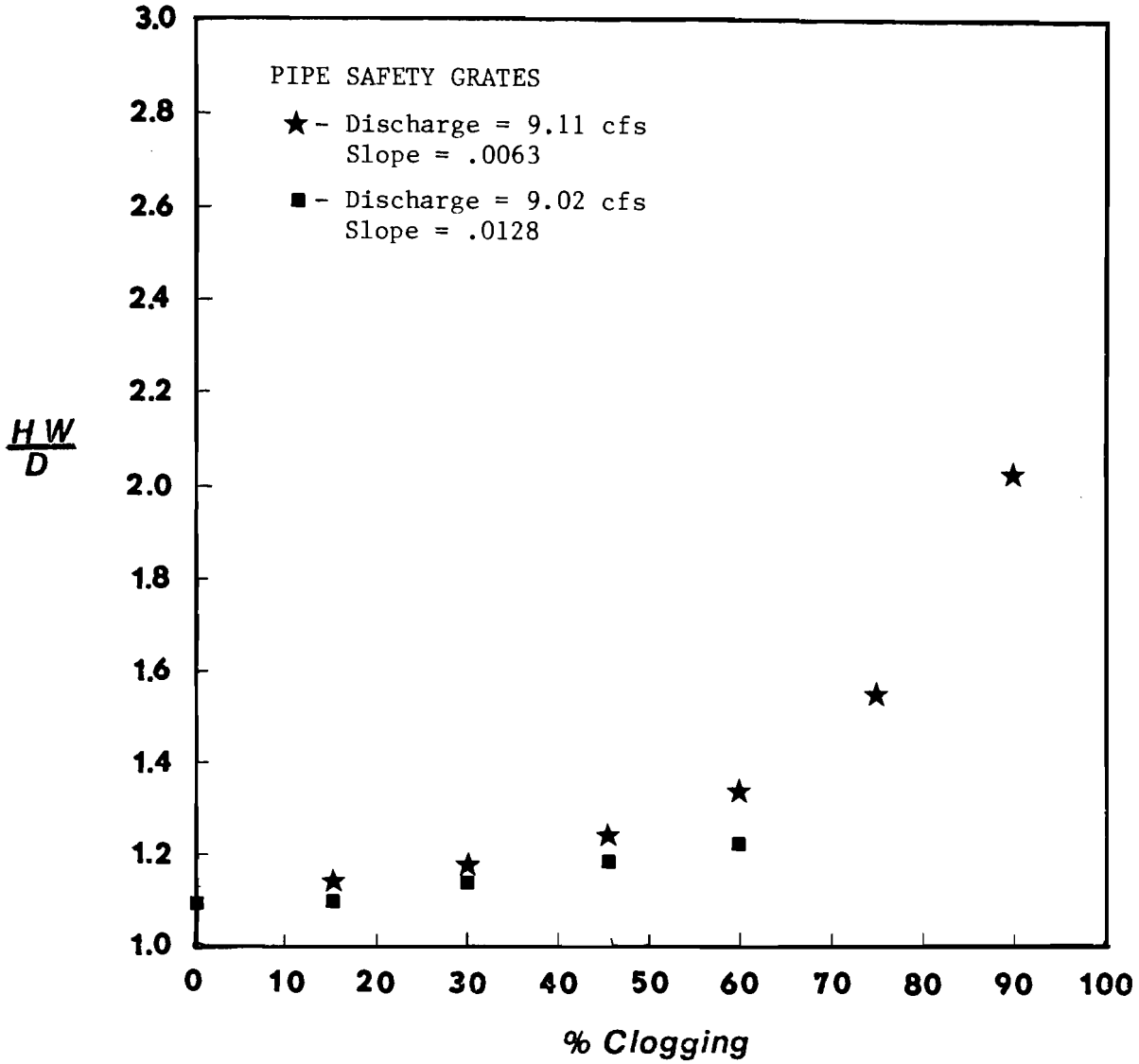


Figure D.10 Headwater vs. Percentage Clogging
($S_o$ = .0063, Q = 9.11cfs)
($S_o$ = .0128, Q = 9.02cfs)

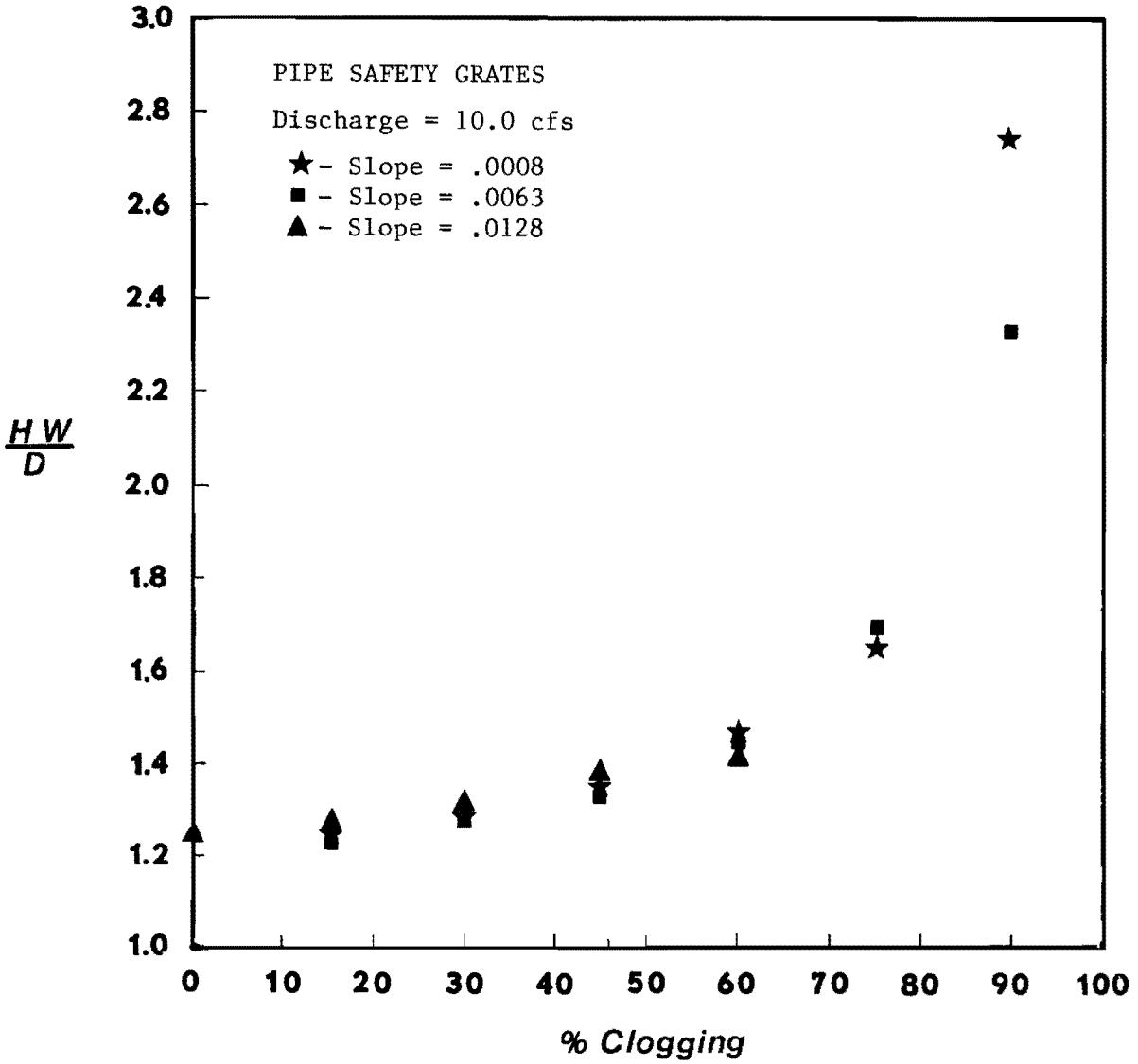


Figure D.11 Headwater vs. Percentage Clogging
($S_o$ = .0008, $S_o$ = .0063,
$S_o$ = .0128, Q = 10cfs)

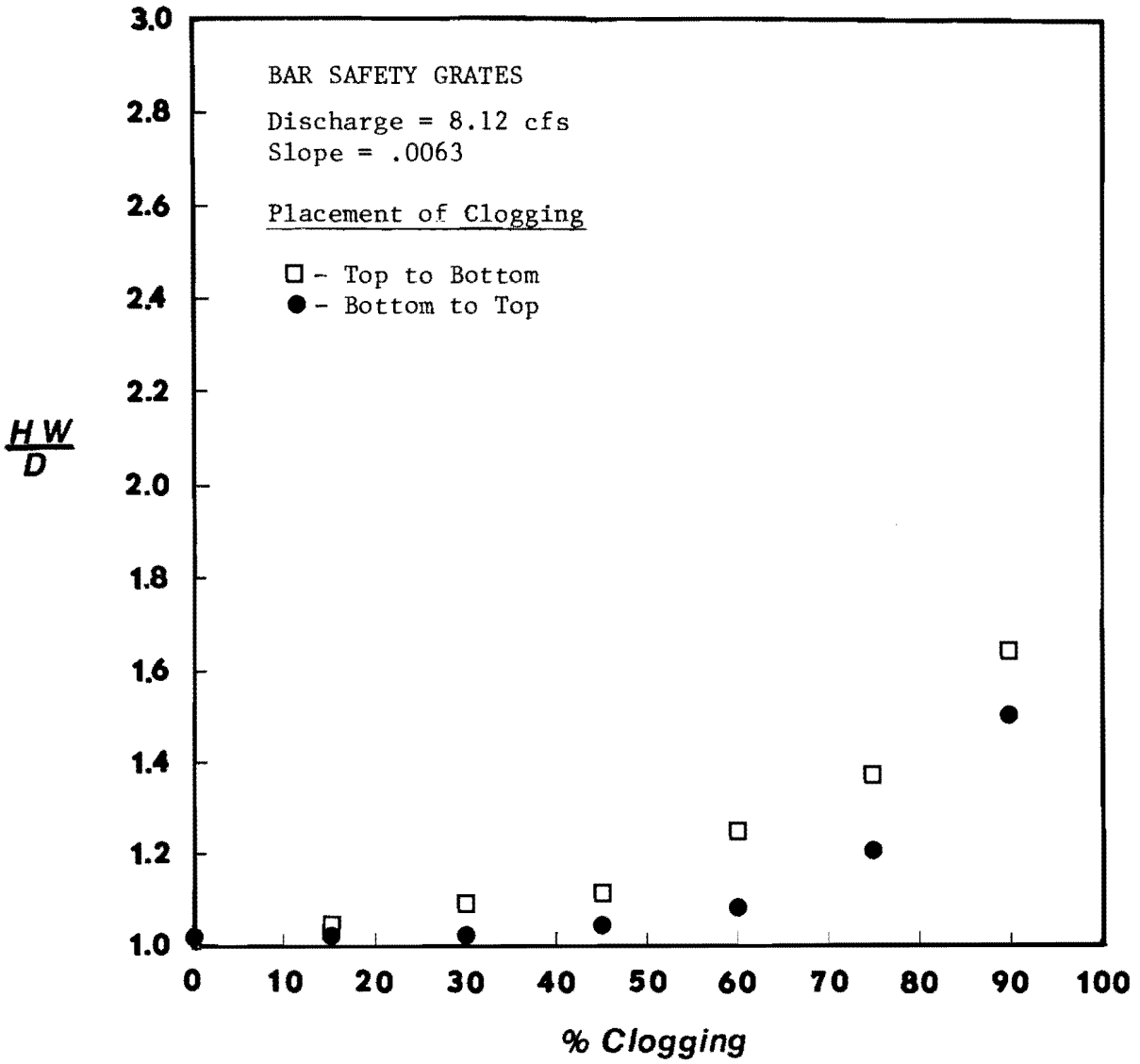


Figure D.12 Headwater vs. Percentage Clogging
($S_o$ = .0063, Q = 8.12cfs)

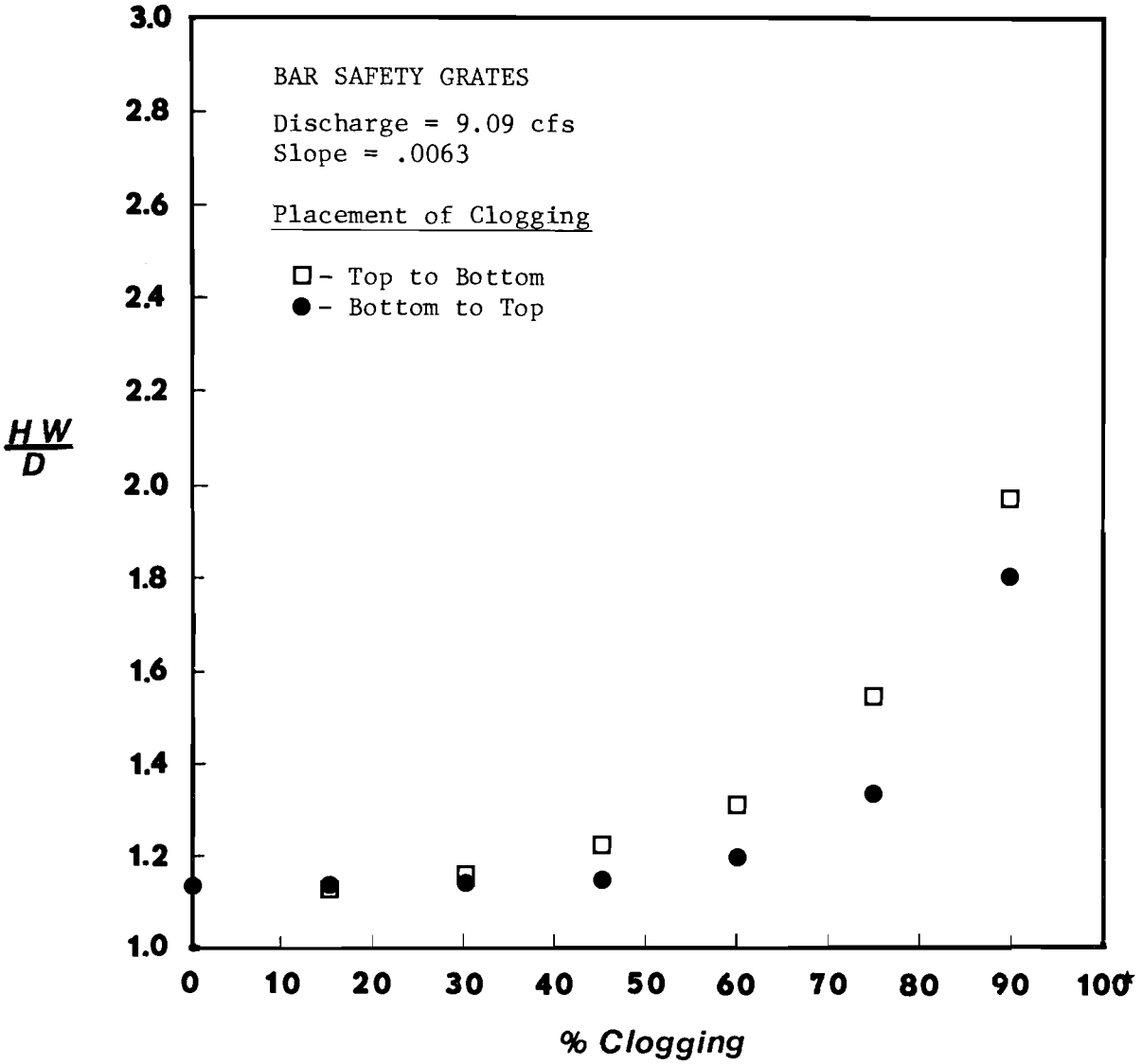


Figure D.13 Headwater vs. Percentage Clogging
($S_o$ = .0063, Q = 9.09cfs)

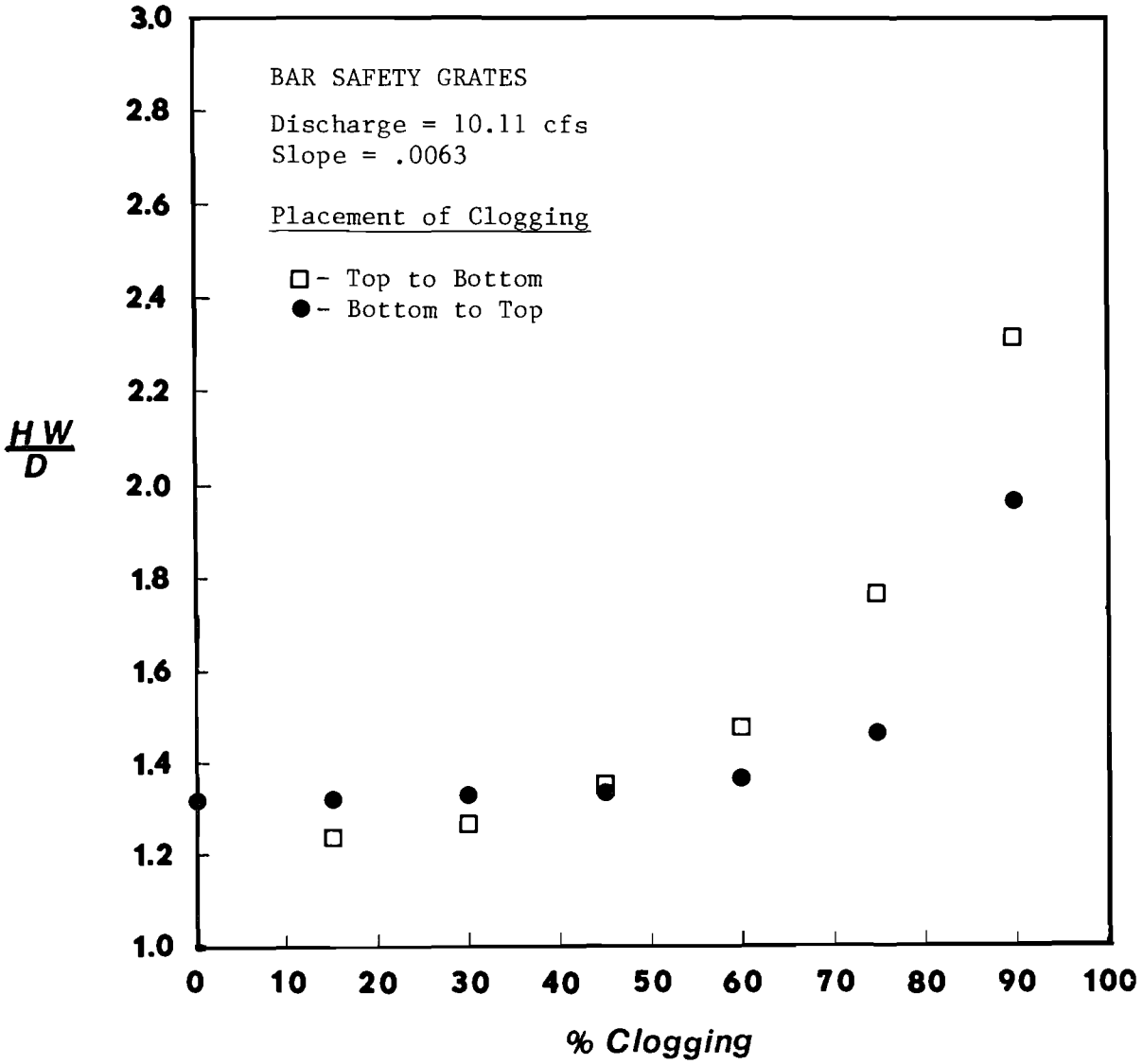


Figure D .14 Headwater vs. Percentage Clogging

($S_o$ = .0063, Q = 10.11cfs)

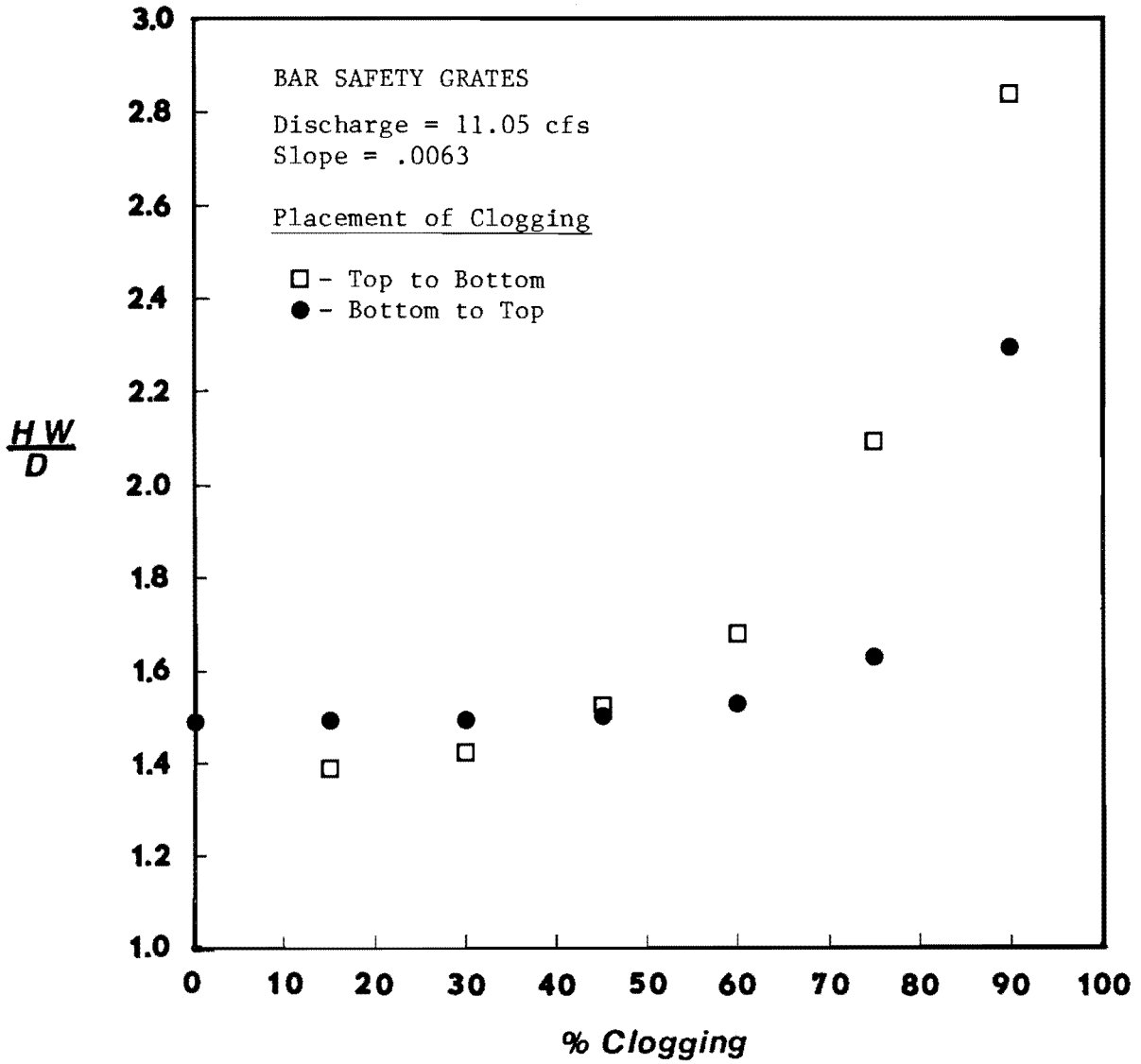


Figure D.15 Headwater vs. Percentage Clogging
($S_o$ = .0063, Q = 11.05cfs)

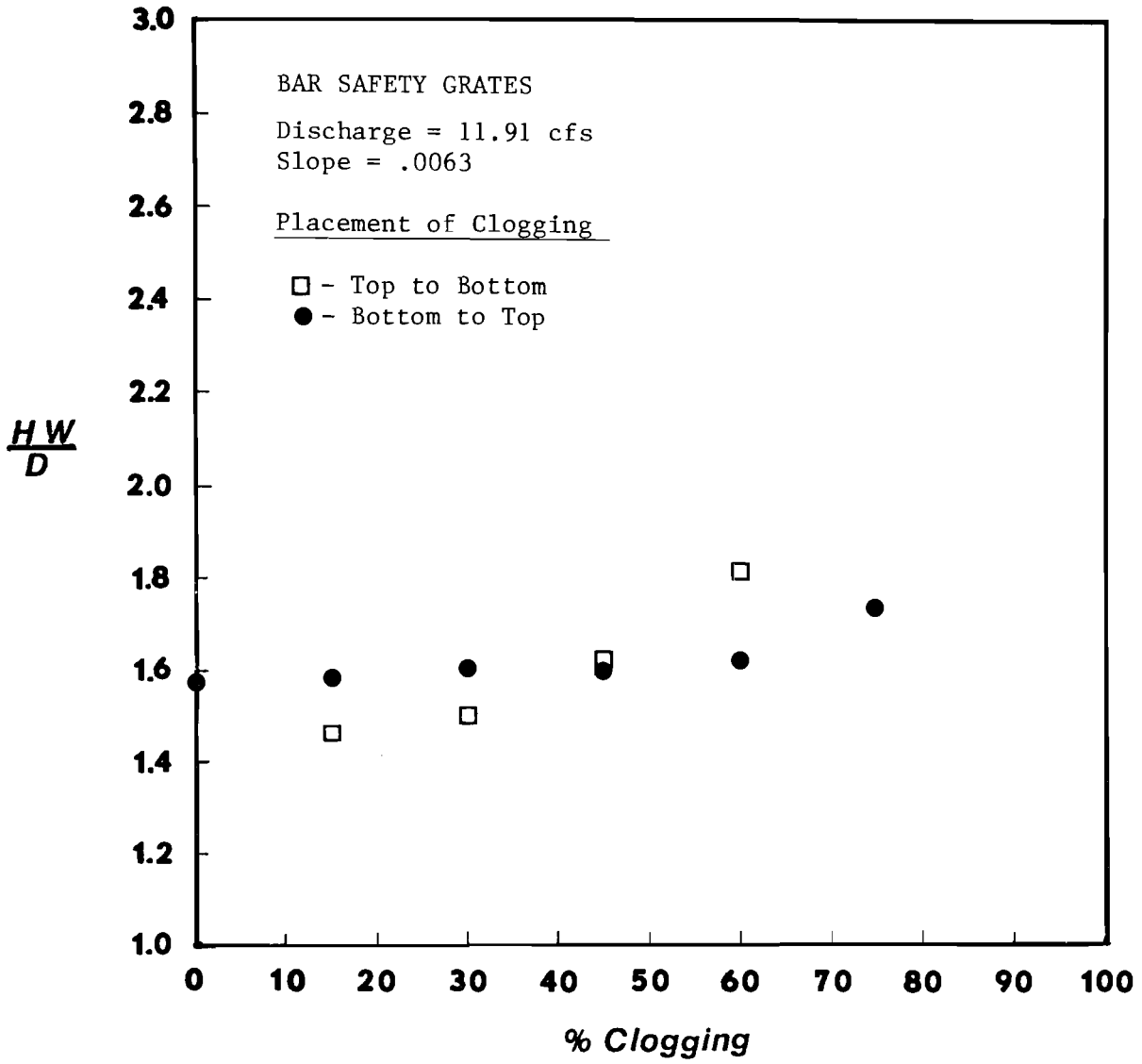


Figure D.16 Headwater vs. Percentage Clogging
($S_o$ = .0063, Q = 11.91 cfs)

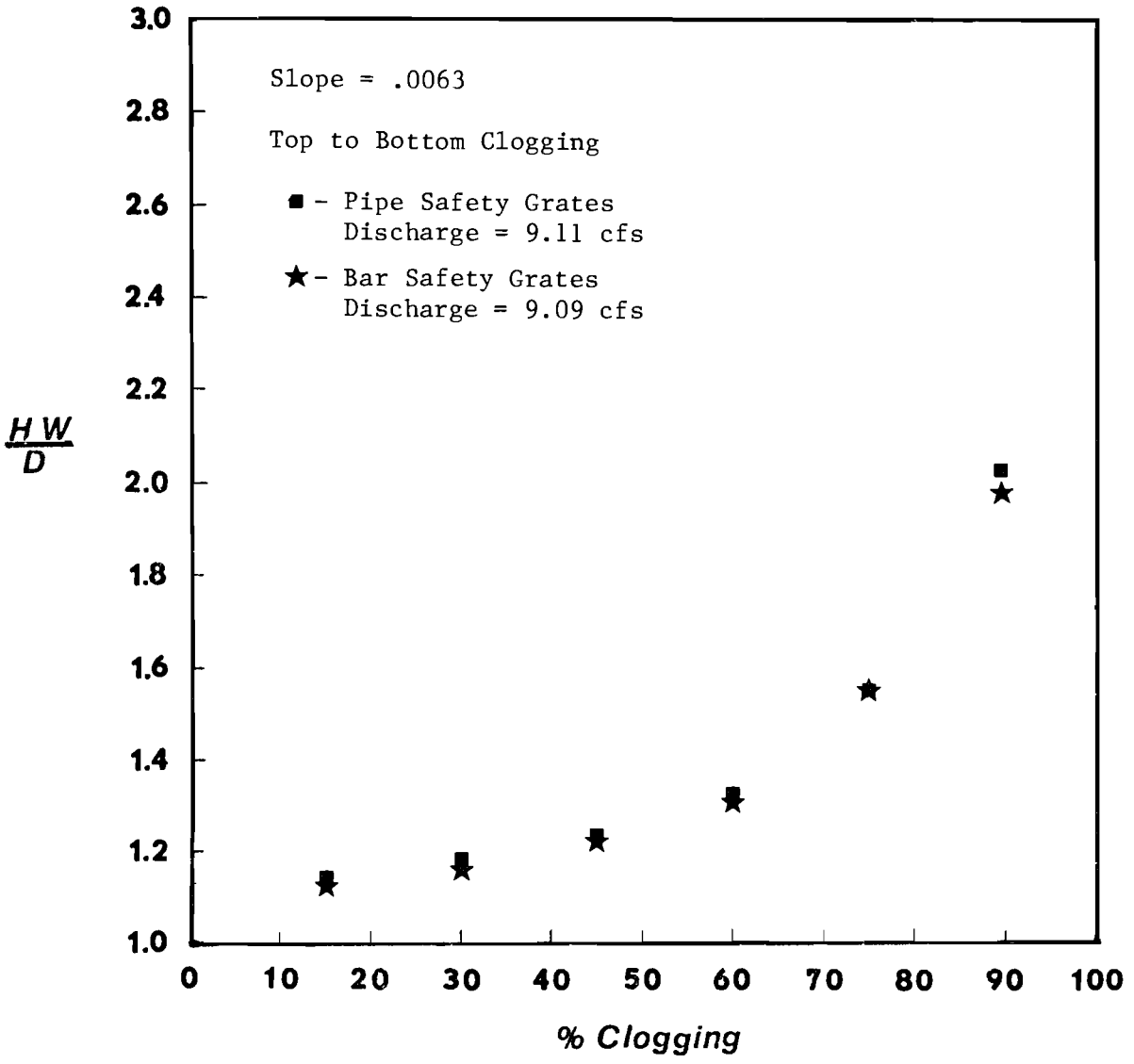


Figure D.17 Headwater vs. Percentage Clogging
Pipe Safety Grates ($S_o$ = .0063, Q = 9.11 cfs)
Bar Safety Grates ($S_o$ = .0063, Q = 9.09 cfs)

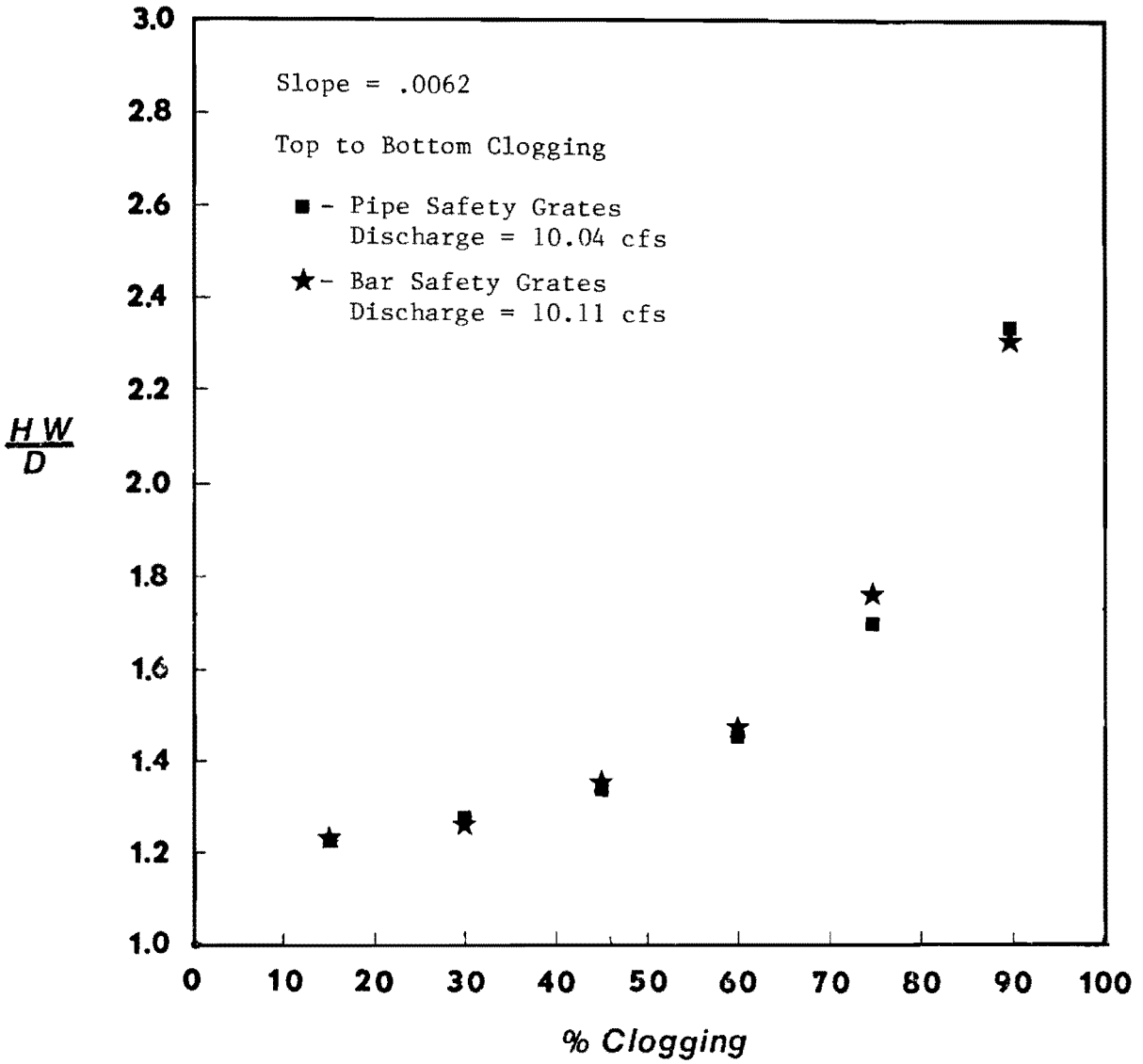


Figure D.18 Headwater vs. Percentage Clogging
Pipe Safety Grates ($S_o$ = .0062, Q = 10.04 cfs)
Bar Safety Grates ($S_o$ = .0062, Q = 10.11 cfs)

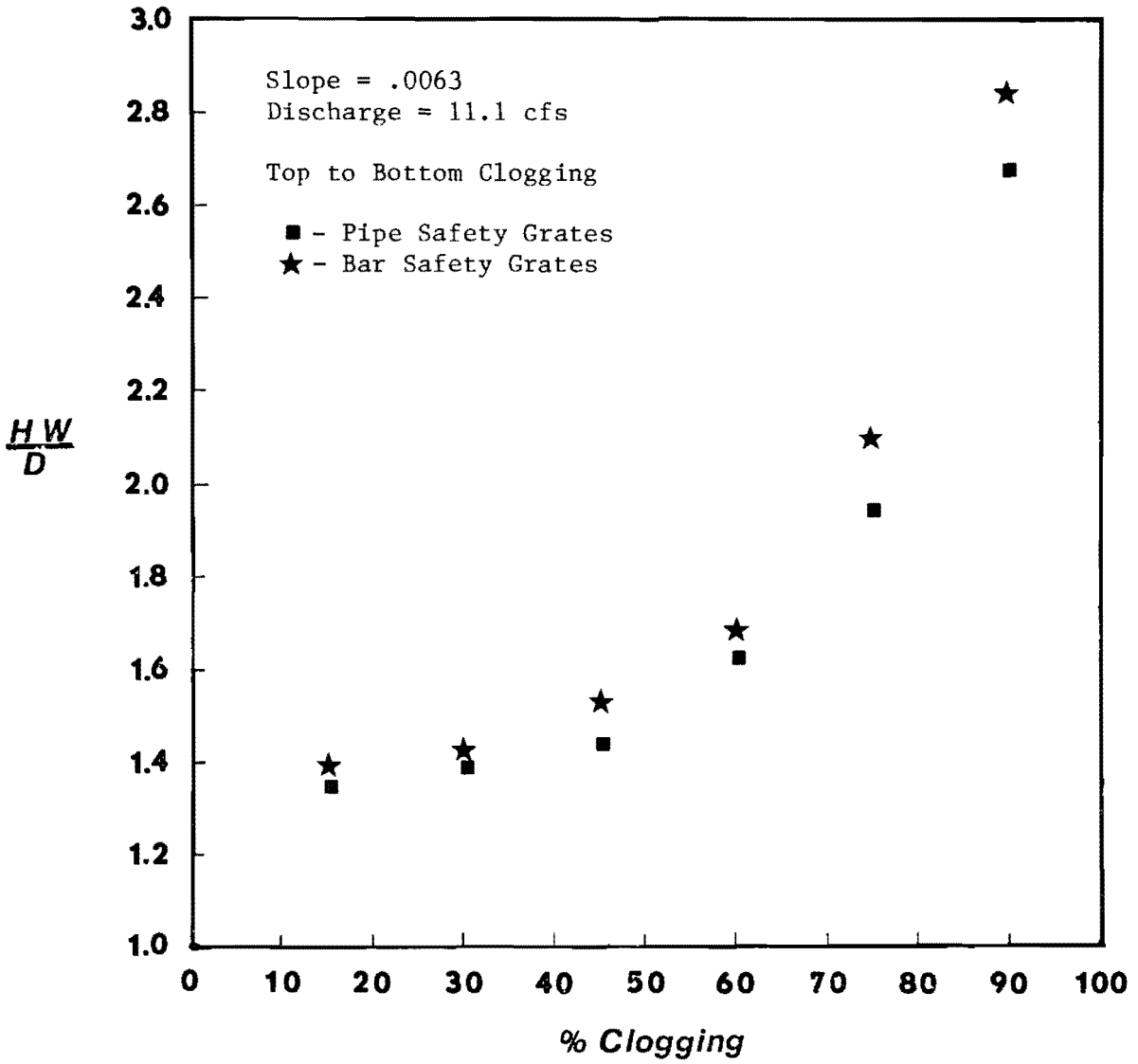


Figure D.19 Headwater vs. Percentage Clogging
Pipe Safety Grates ($S_o$ = .0063, Q = 11.1 cfs)
Bar Safety Grates ($S_o$ = .0063, Q = 11.1 cfs)

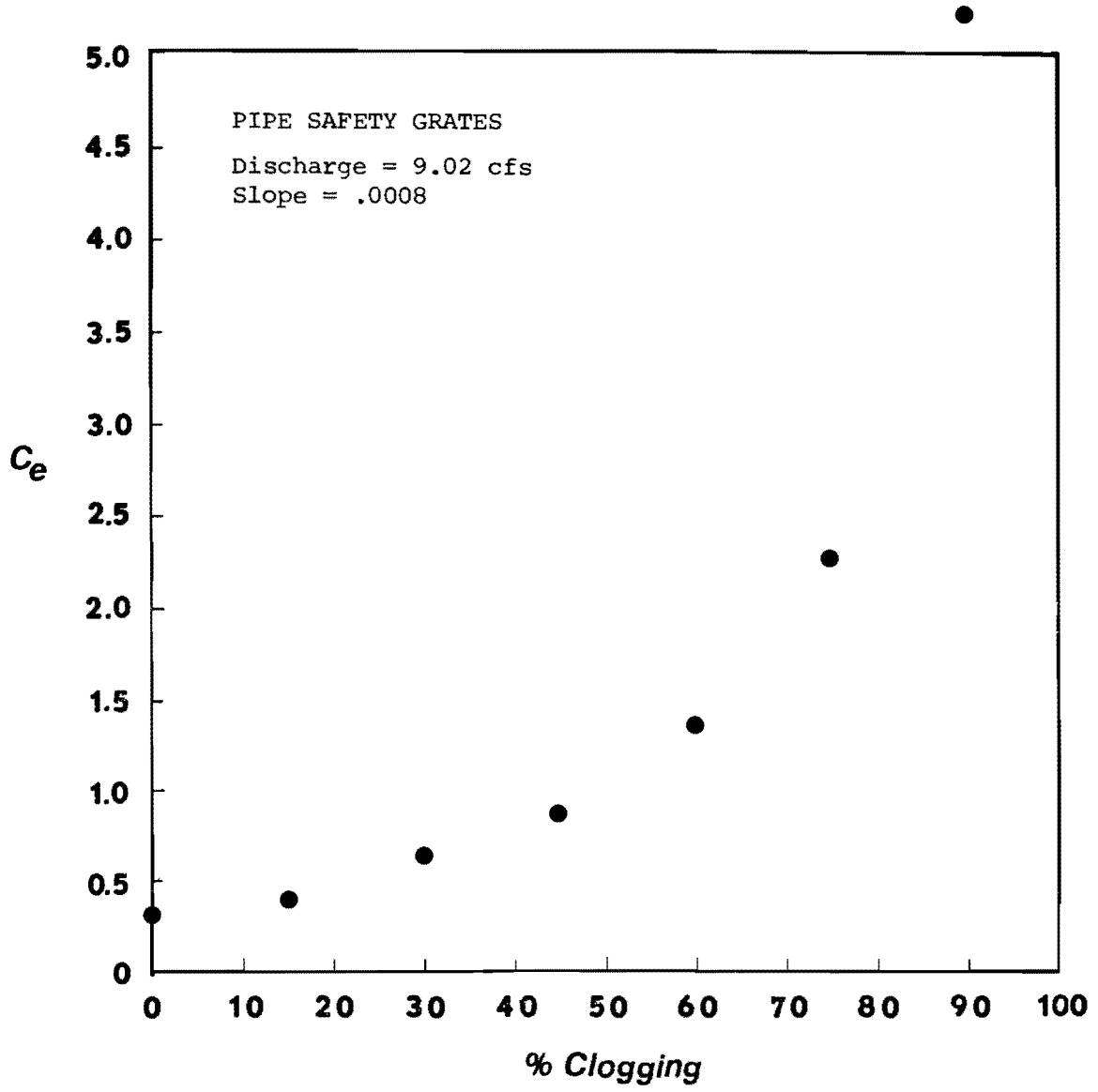


Figure D.20 Entrance Headloss Coefficient vs. Percentage Clogging ($S_o$ = .0008, Q = 9.02 cfs)

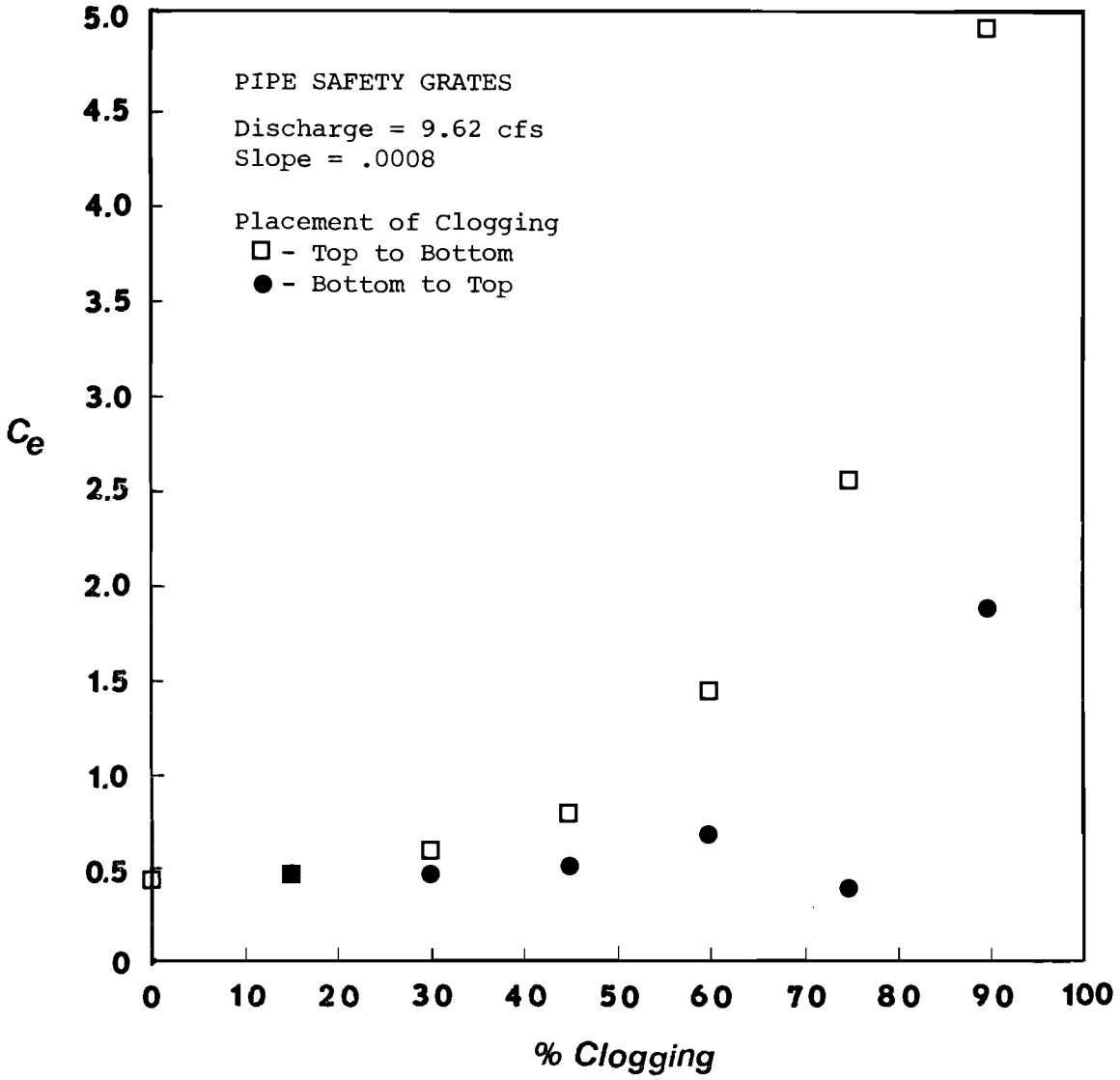


Figure D.21 Entrance Headloss Coefficient vs. Percentage Clogging ($S_o$ = .0008, Q = 9.62 cfs)

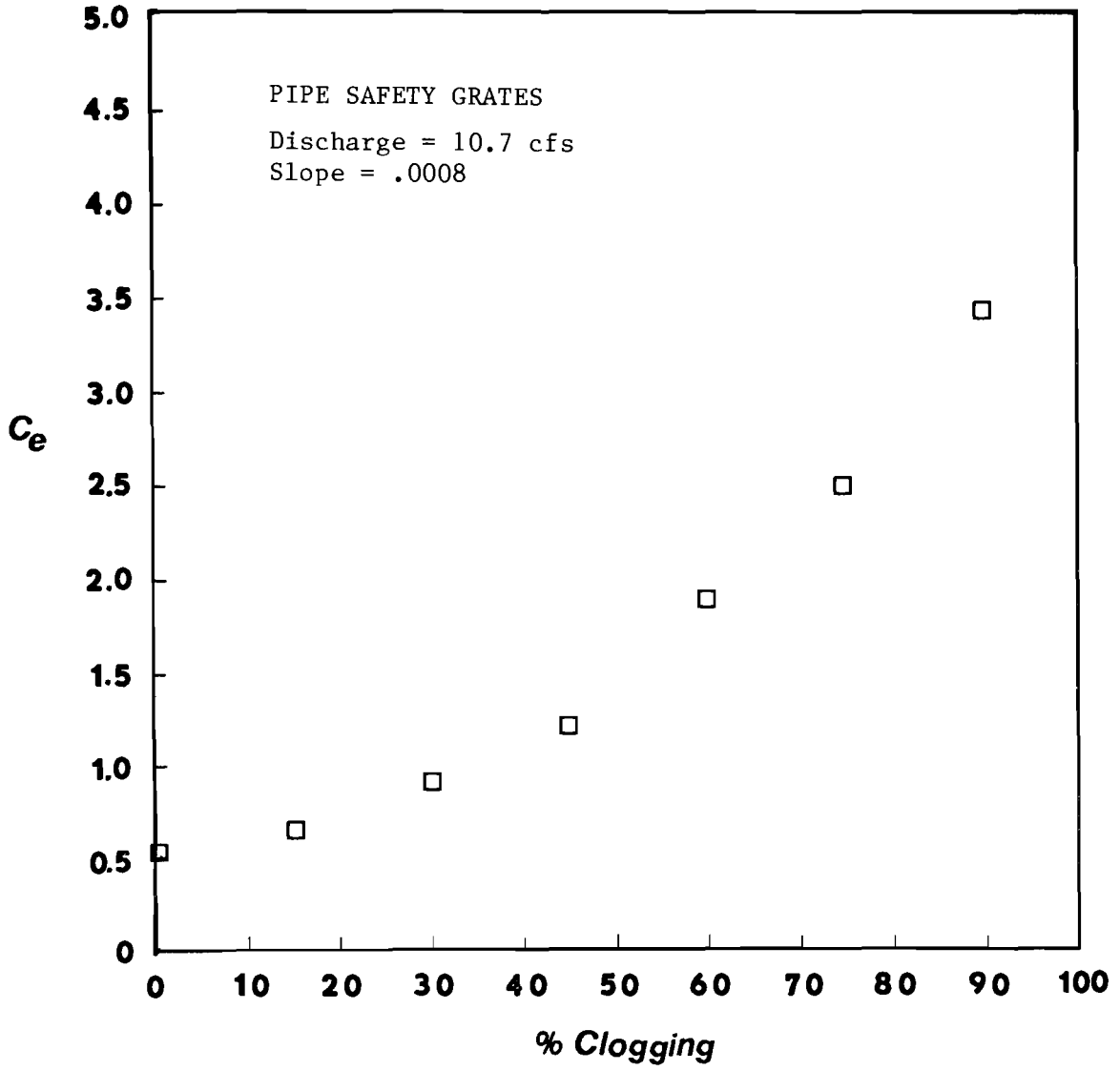


Figure D.22 Entrance Headloss Coefficient vs. Percentage Clogging

($S_0$ = .0008, Q = 10.7cfs)

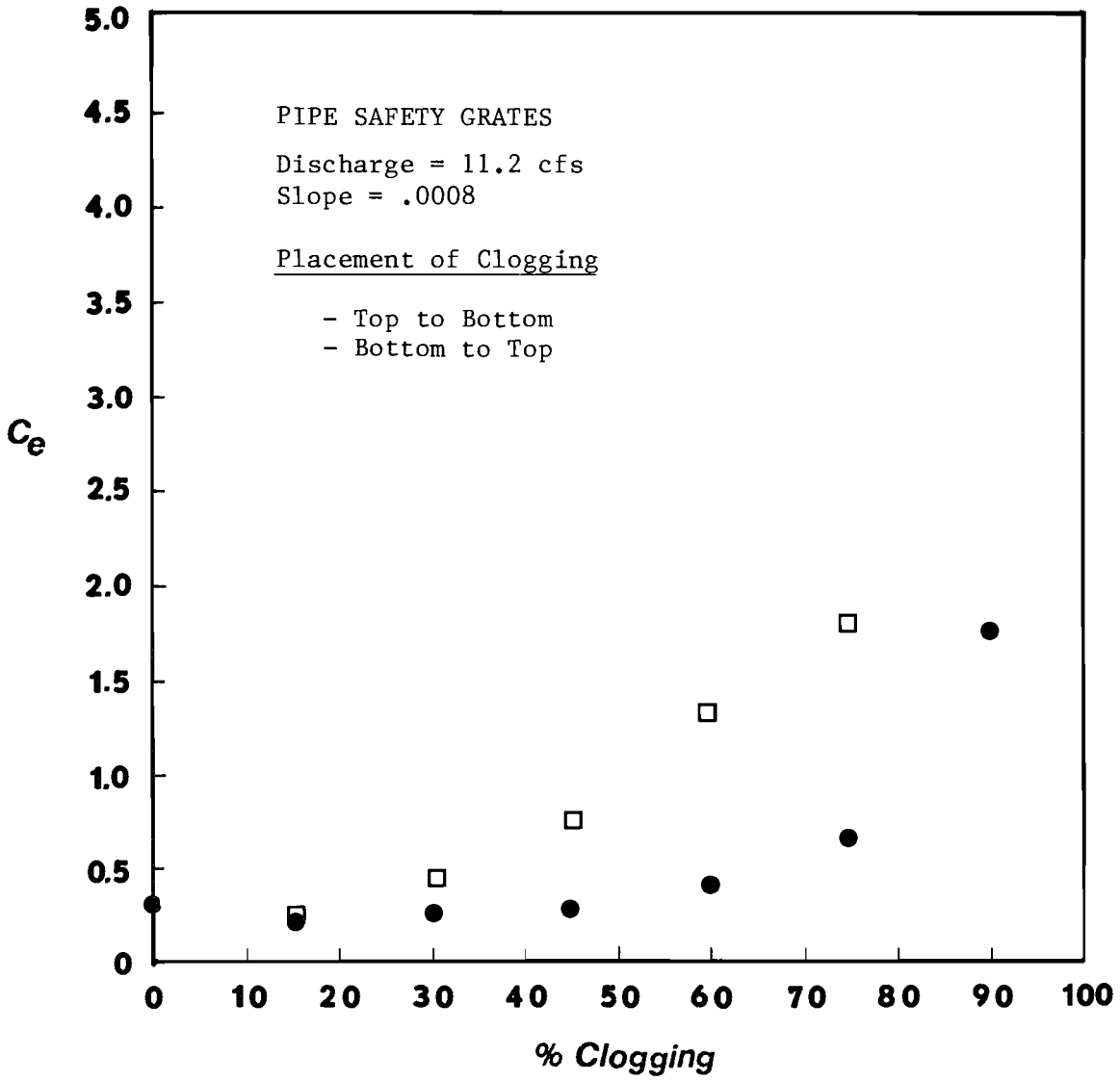


Figure D.23 Entrance Headloss Coefficient vs. Percentage Clogging

($S_o$ = .0008, Q = 11.2cfs)

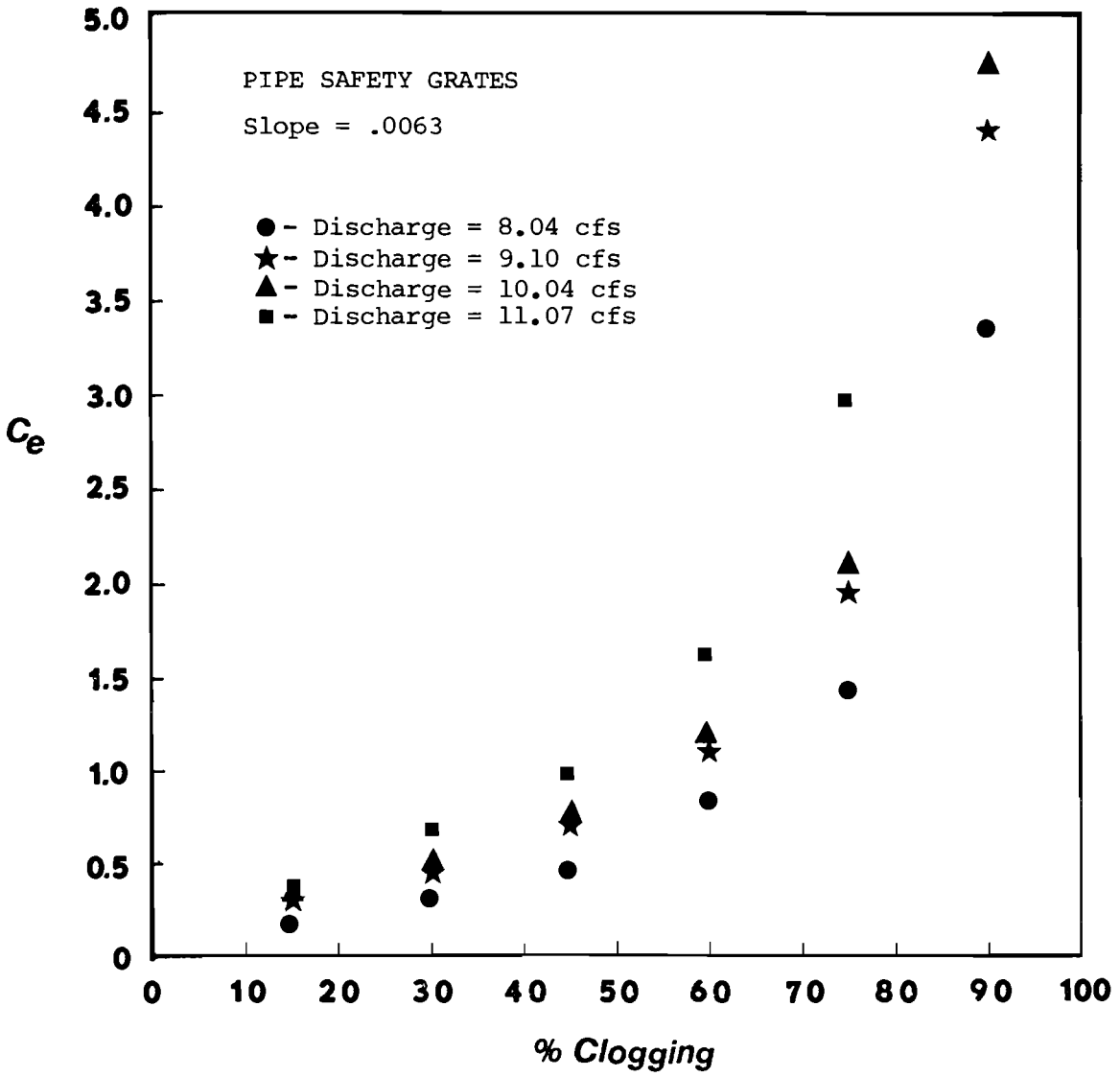


Figure D.24 Entrance Headloss Coefficient vs. Percentage Clogging ($S_o$ = .0063, Q = 8.04 cfs , Q = 9.1 cfs , Q = 10.04 cfs, Q = 11.07 cfs)

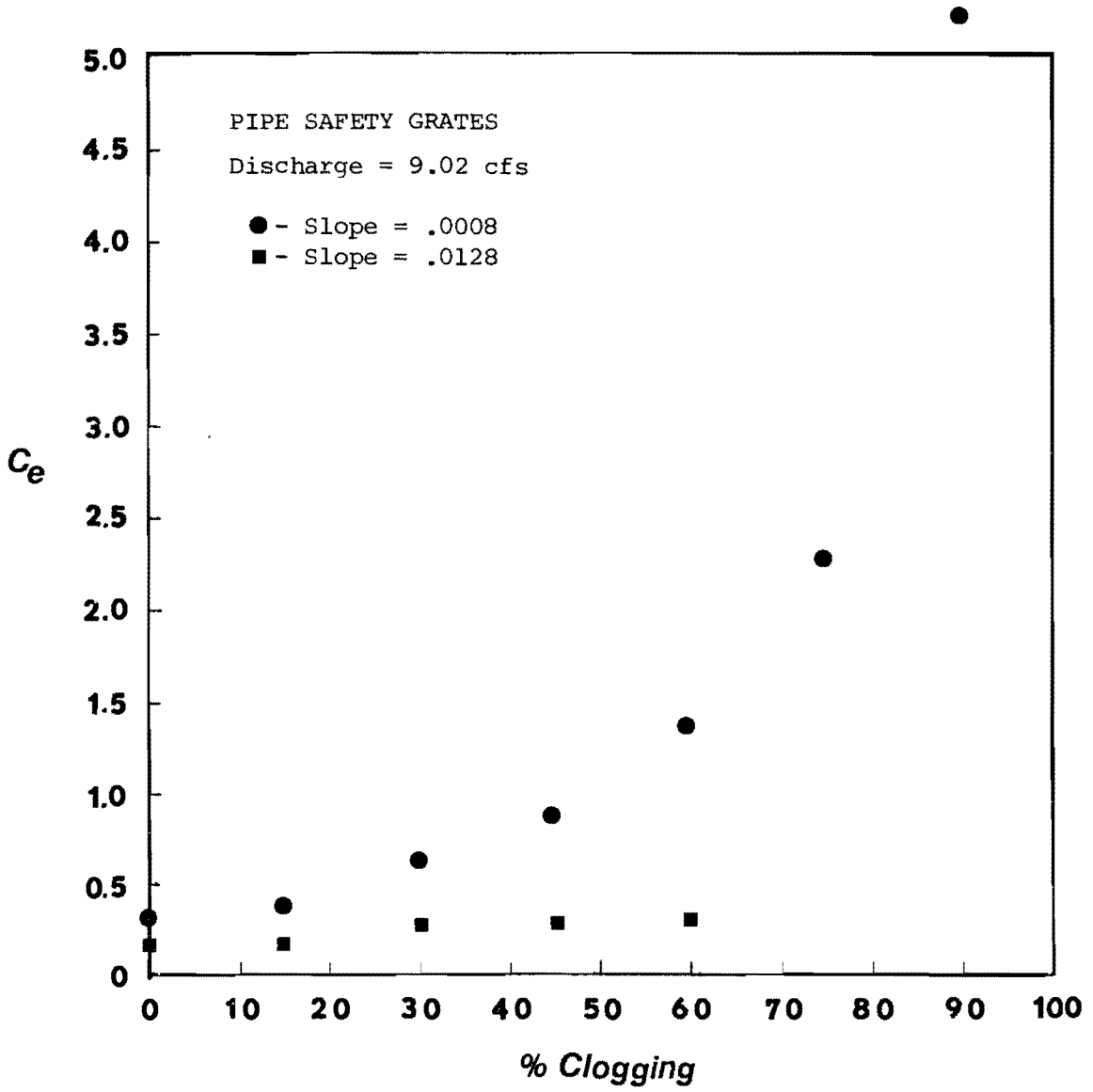


Figure D.25 Entrance Headloss Coefficient vs. Percentage Clogging ($S_o$ = .0008, $S_o$ = .0128, Q = 9.02 cfs)

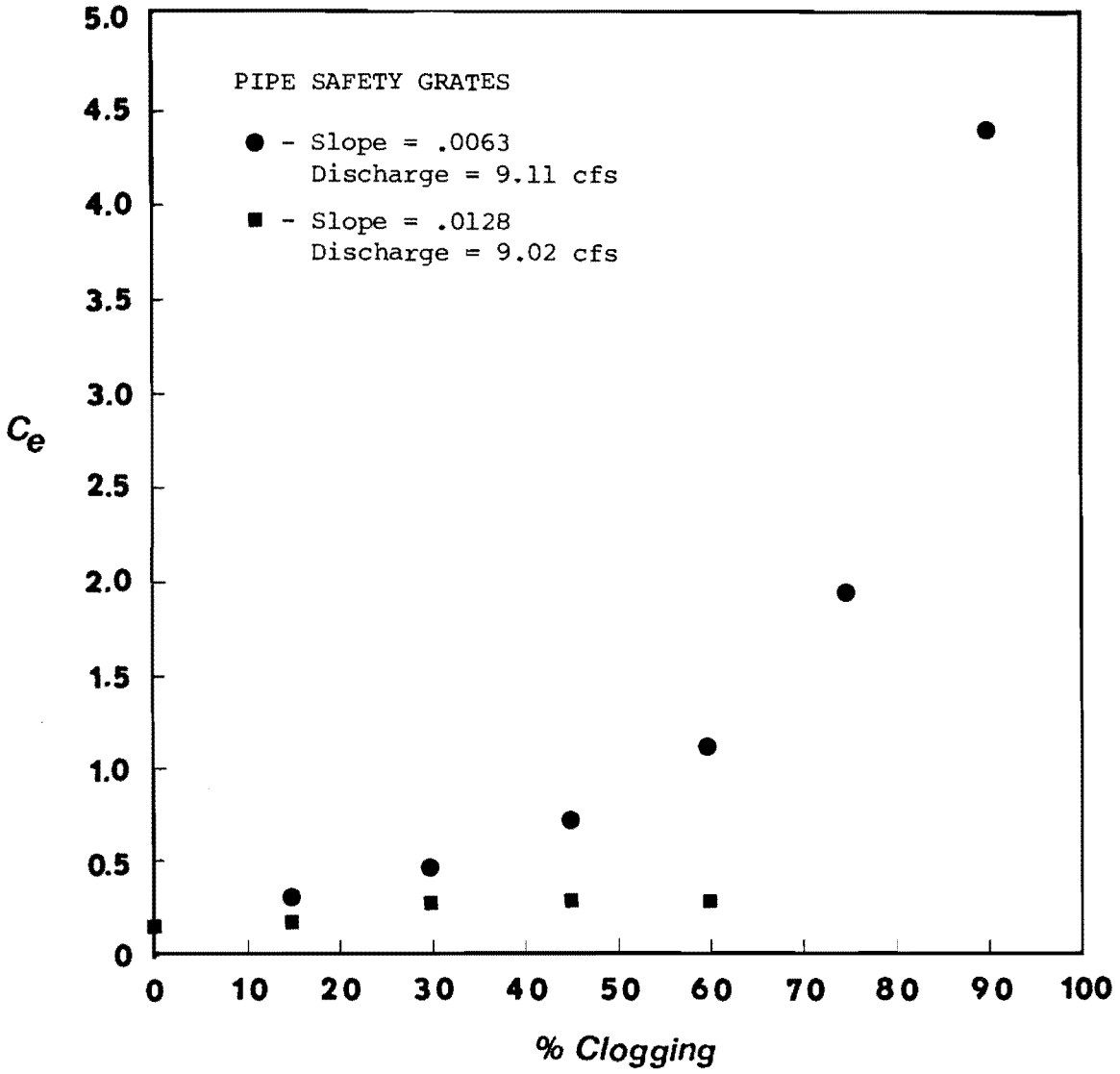


Figure D.26 Entrance Headloss Coefficient vs. Percentage Clogging
($S_o$ = .0063, Q = 9.11 cfs)
($S_o$ = .0128, Q = 9.02 cfs)

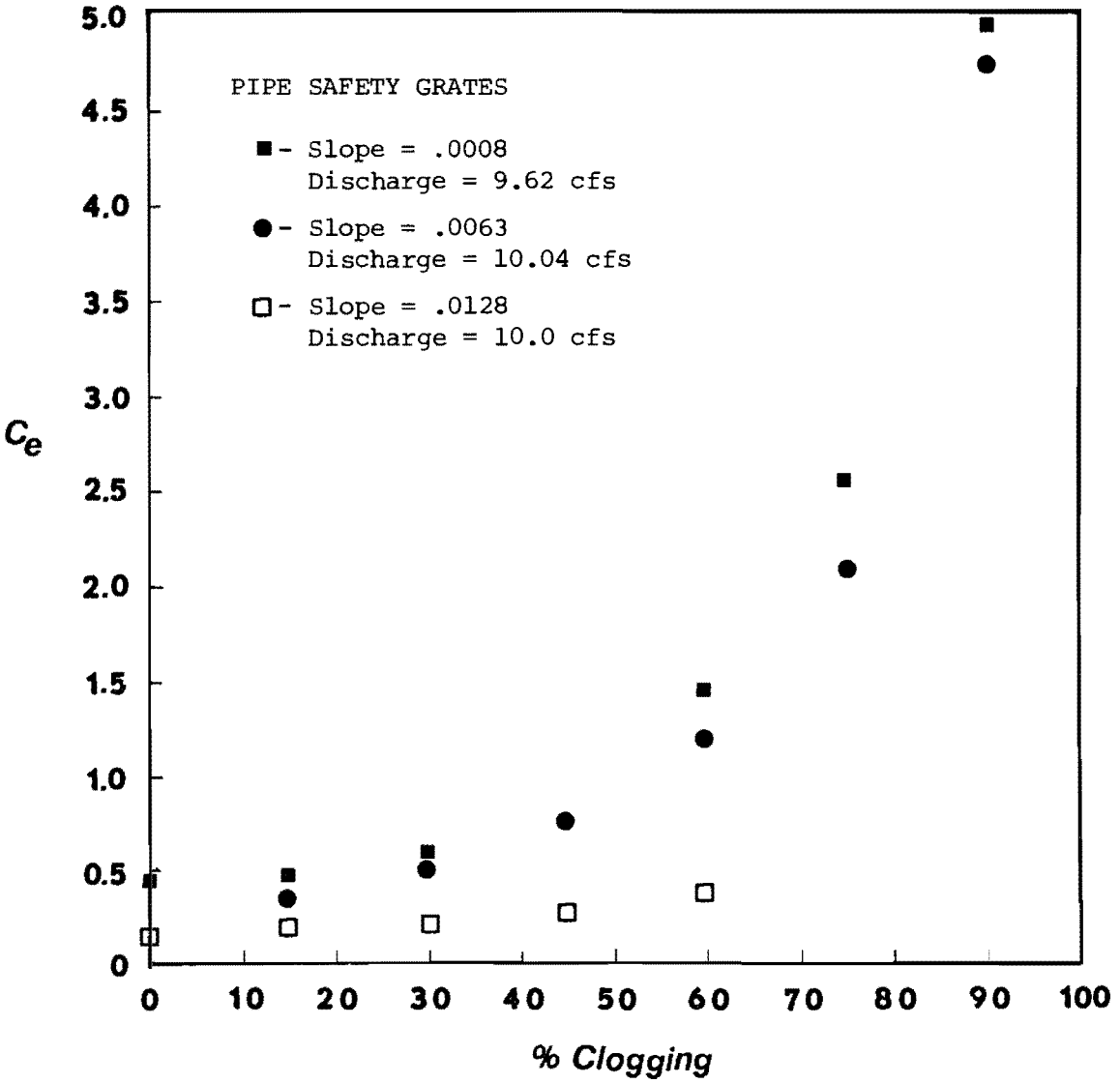


Figure D.27 Entrance Headloss Coefficient vs. Percentage Clogging
($S_o$ = .0008, Q = 9.62 cfs)
($S_o$ = .0063, Q = 10.04 cfs)
($S_o$ = .0128, Q = 10.0 cfs)

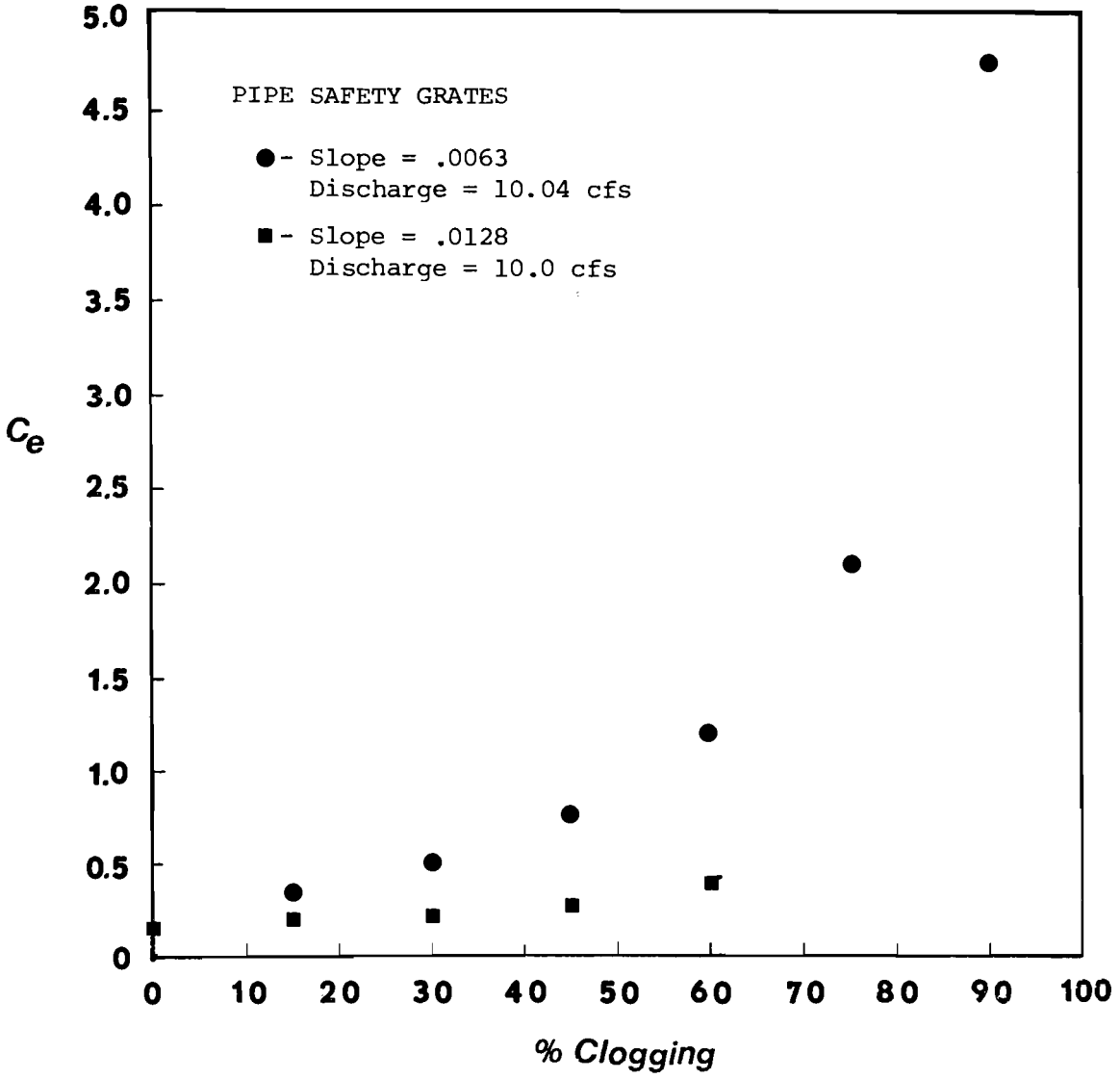


Figure D.28 Entrance Headloss Coefficient vs. Percentage Clogging
($S_o$ = .0063, Q = 10.04 cfs)
($S_o$ = .0128, Q = 10.0 cfs)

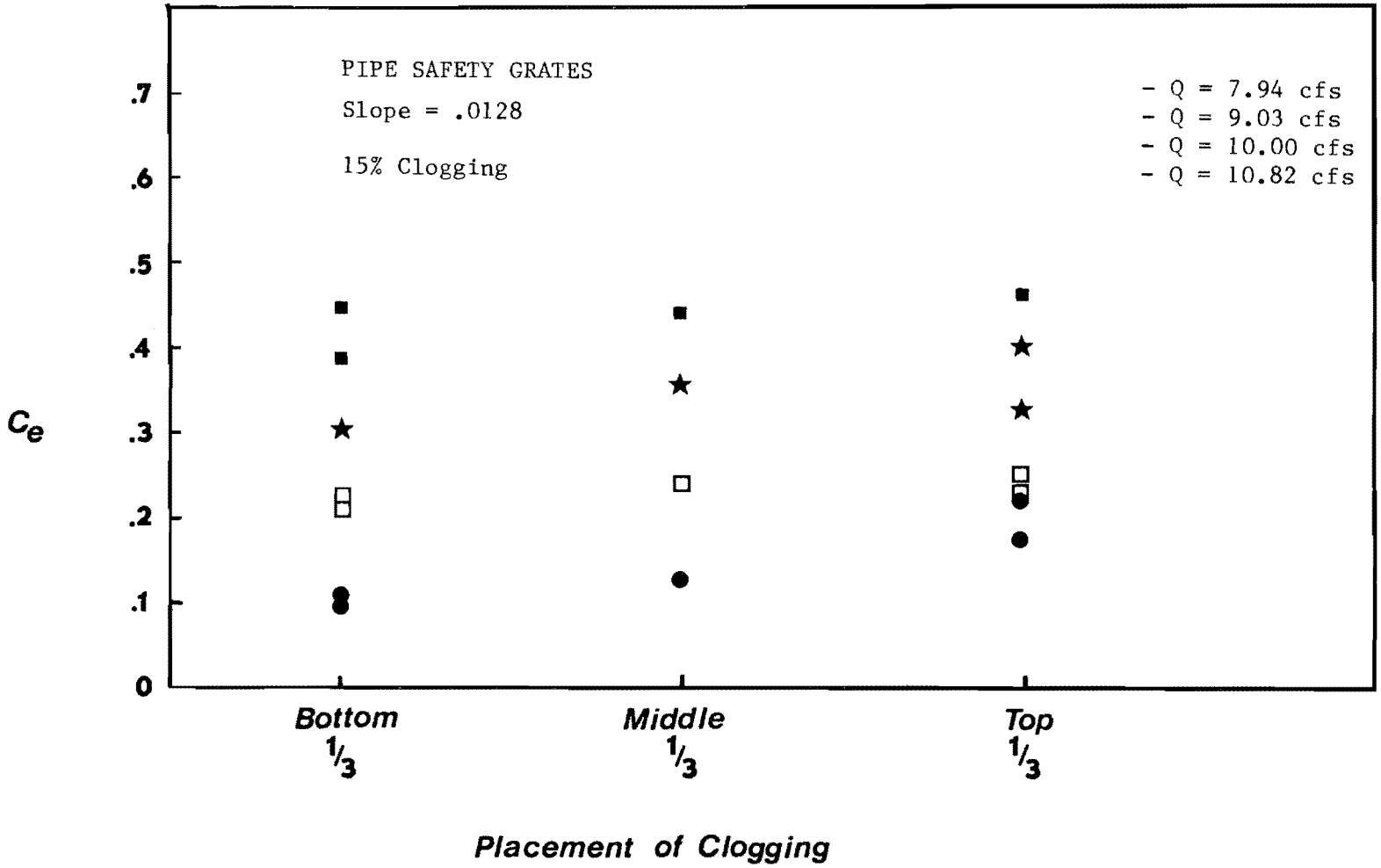


Figure D.29 Entrance Headloss Coefficient vs. Placement of Clogging
$S_o$ = .0128, 15% Clogging

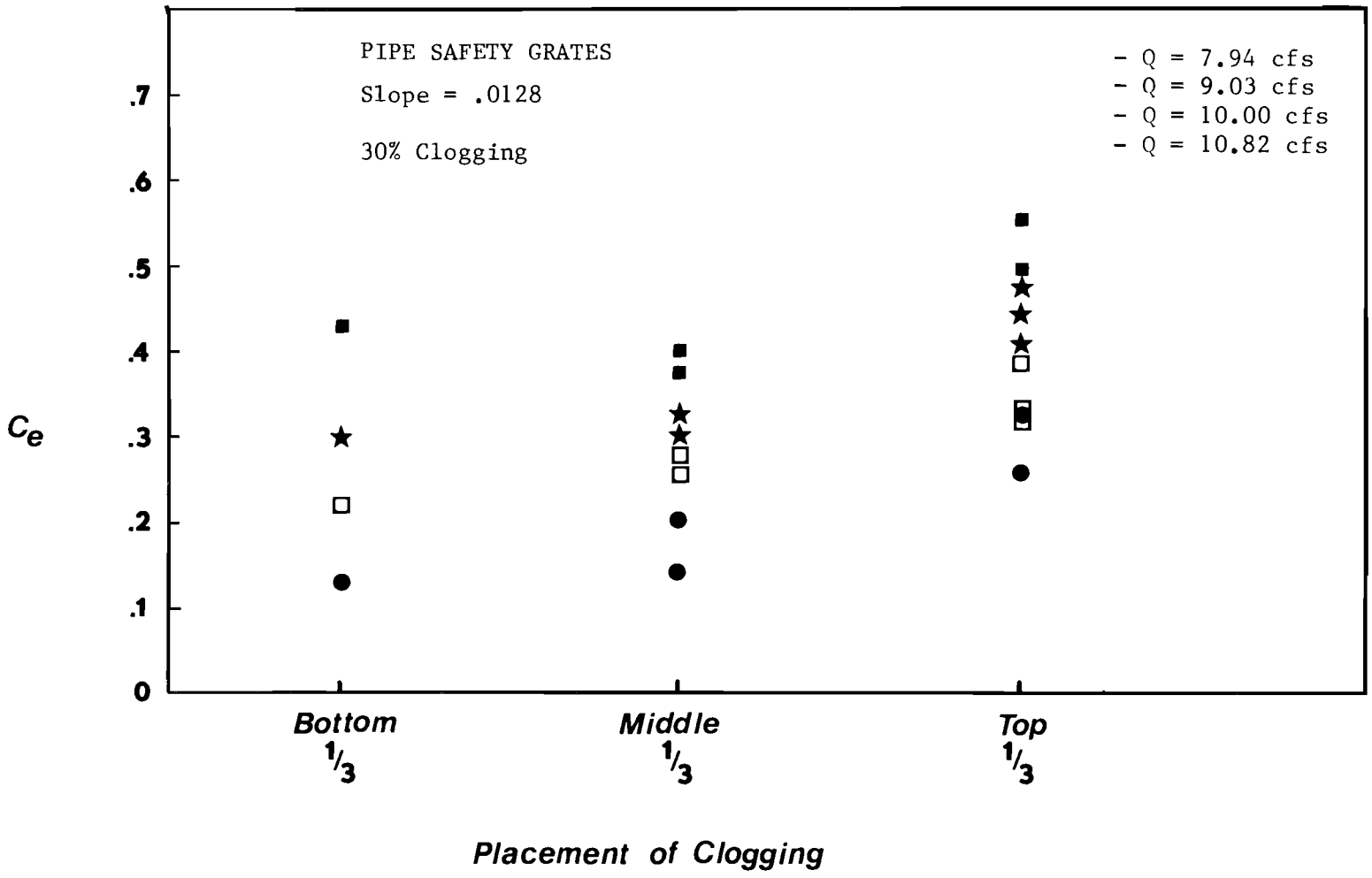


Figure D.30 Entrance Headloss Coefficient vs. Placement of Clogging
$S_o$ = .0128, 30% Clogging

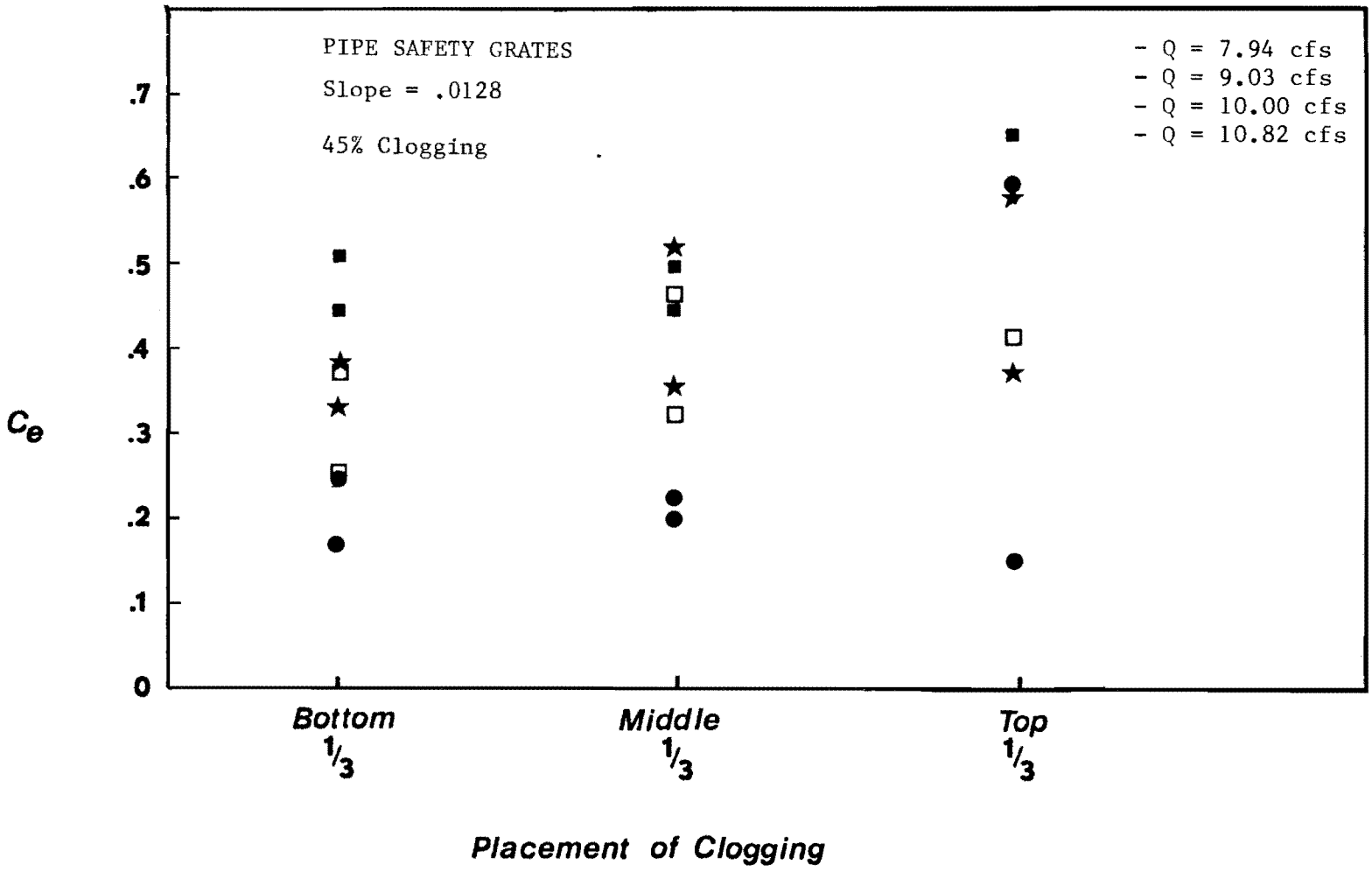


Figure B.31 Entrance Headloss Coefficient vs. Placement of Clogging
$S_o$ = .0128, 45% Clogging

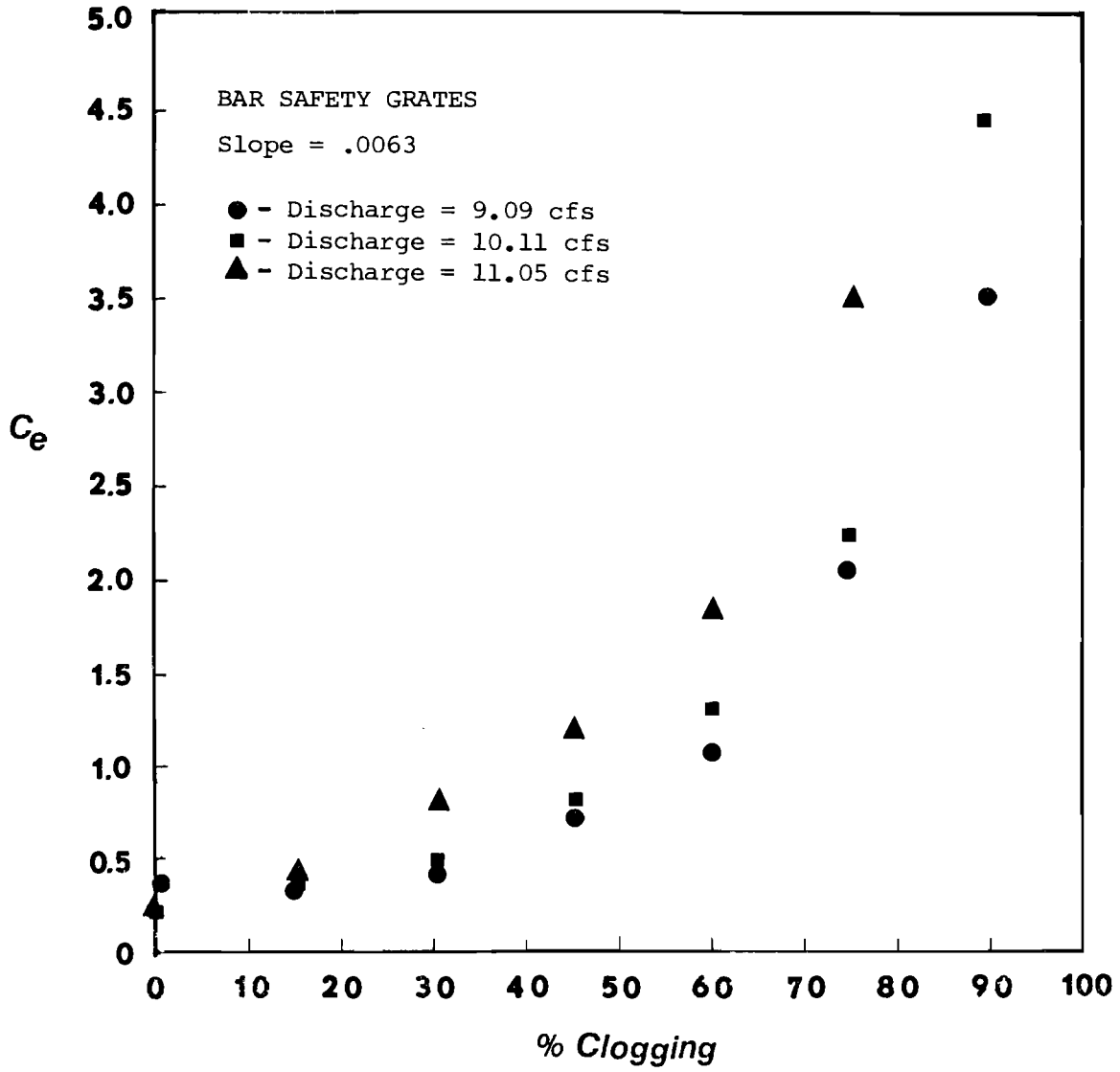


Figure D.32 Entrance Headloss Coefficient vs. Percentage Clogging ($S_o$ = .0063, Q = 9.09 cfs, Q = 10.11, Q = 11.05 cfs)

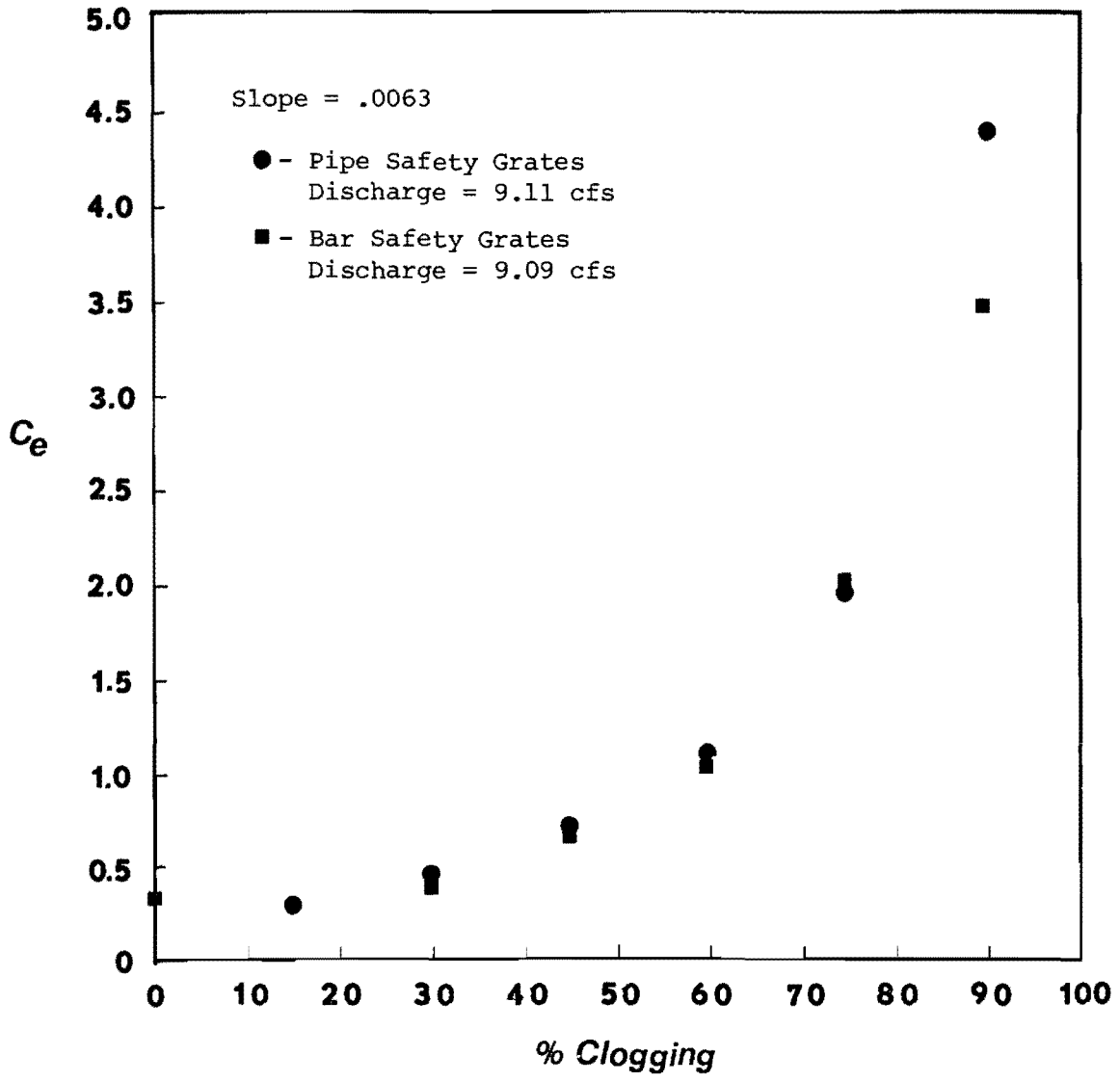


Figure D.33 Entrance Headloss Coefficient vs. Percentage Clogging
Pipe Safety Grates ($S_o$ = .0063, Q = 9.11 cfs)
Bar Safety Grates ($S_o$ = .0063, Q = 9.09 cfs)

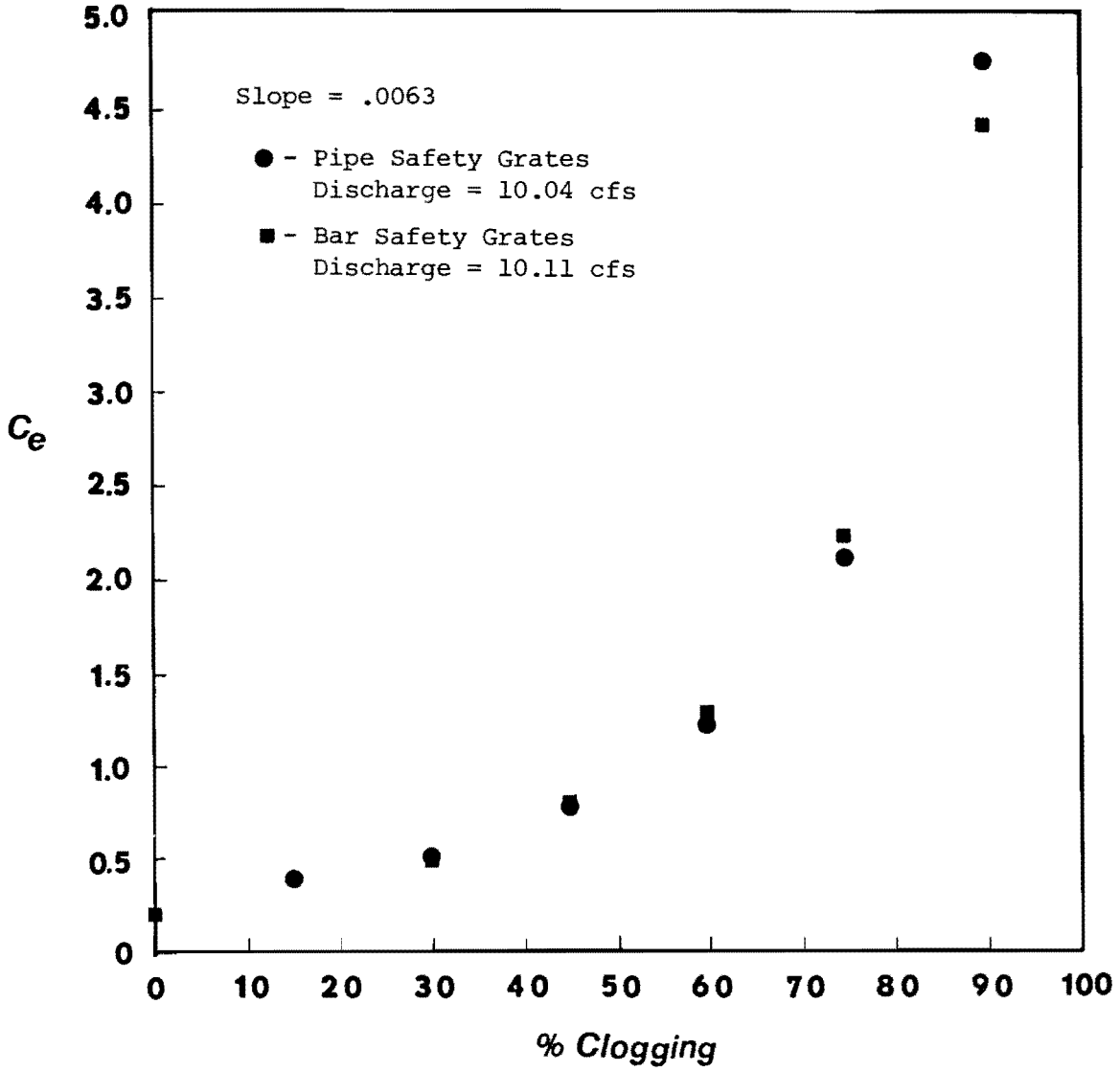


Figure D.34 Entrance Headloss Coefficient vs. Percentage Clogging
Pipe Safety Grates ($S_o$ = .0063, Q = 10.04 cfs)
Bar Safety Grates ($S_o$ = .0063, Q = 10.11 cfs)

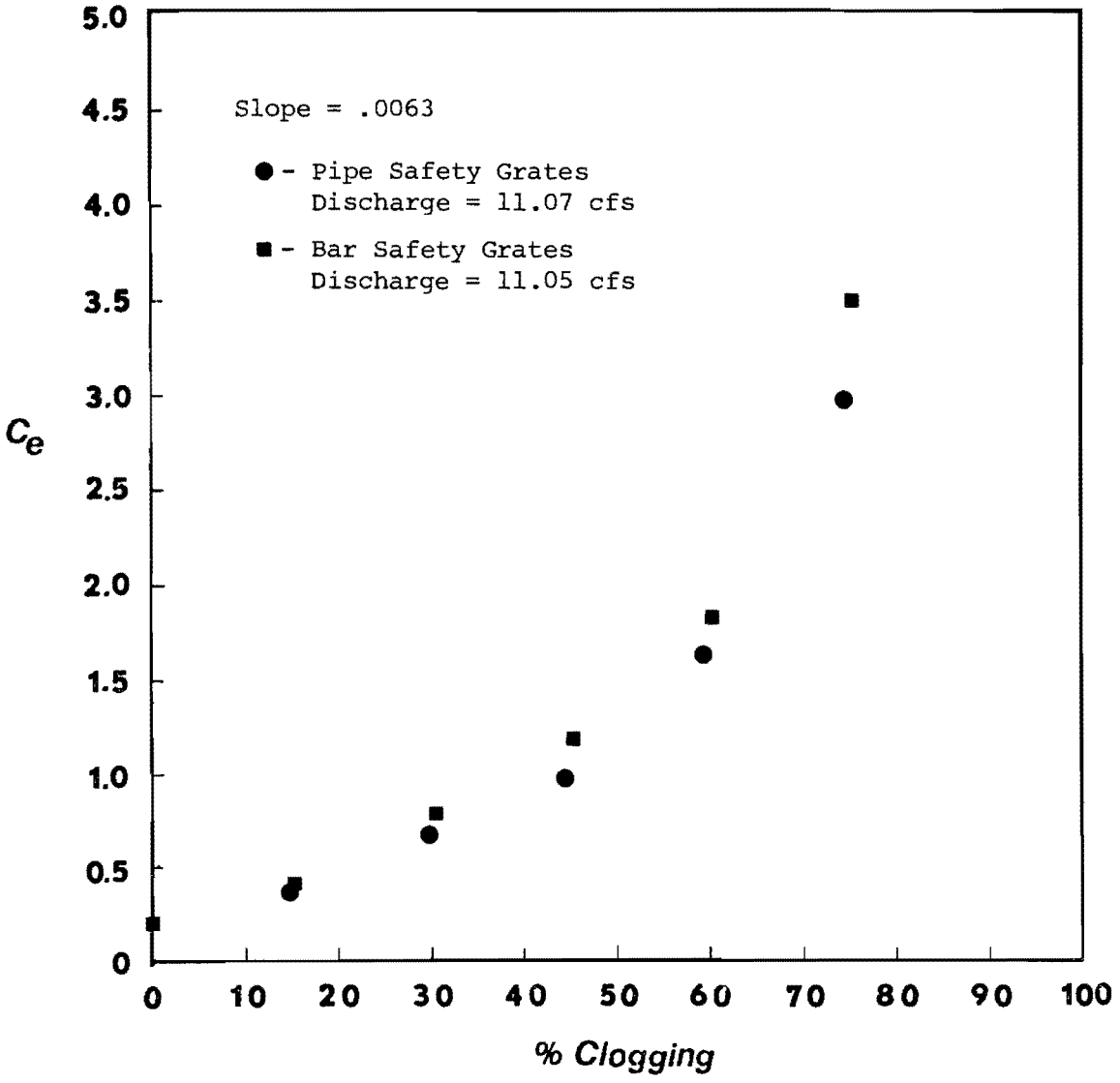


Figure D.35 Entrance Headloss Coefficient vs. Percentage Clogging
Pipe Safety Grates ($S_o$ = .0063, Q = 11.07 cfs)
Bar Safety Grates ($S_o$ = .0063, Q = 11.05 cfs)

# APPENDIX E

## Graphical Results For Pipe Culverts

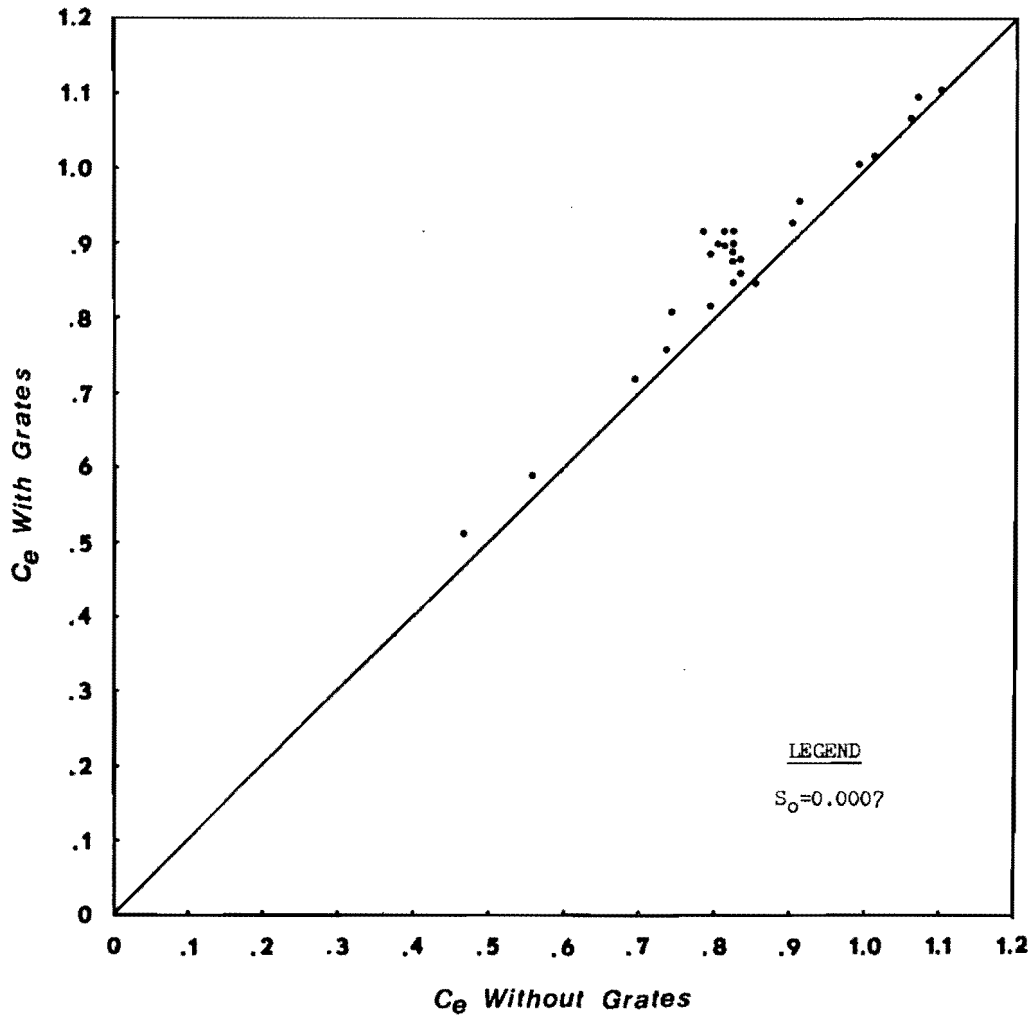


Figure E.1 Comparison of Entrance Headloss Coefficients With and Without Safety Grates
Slope = 0.0007

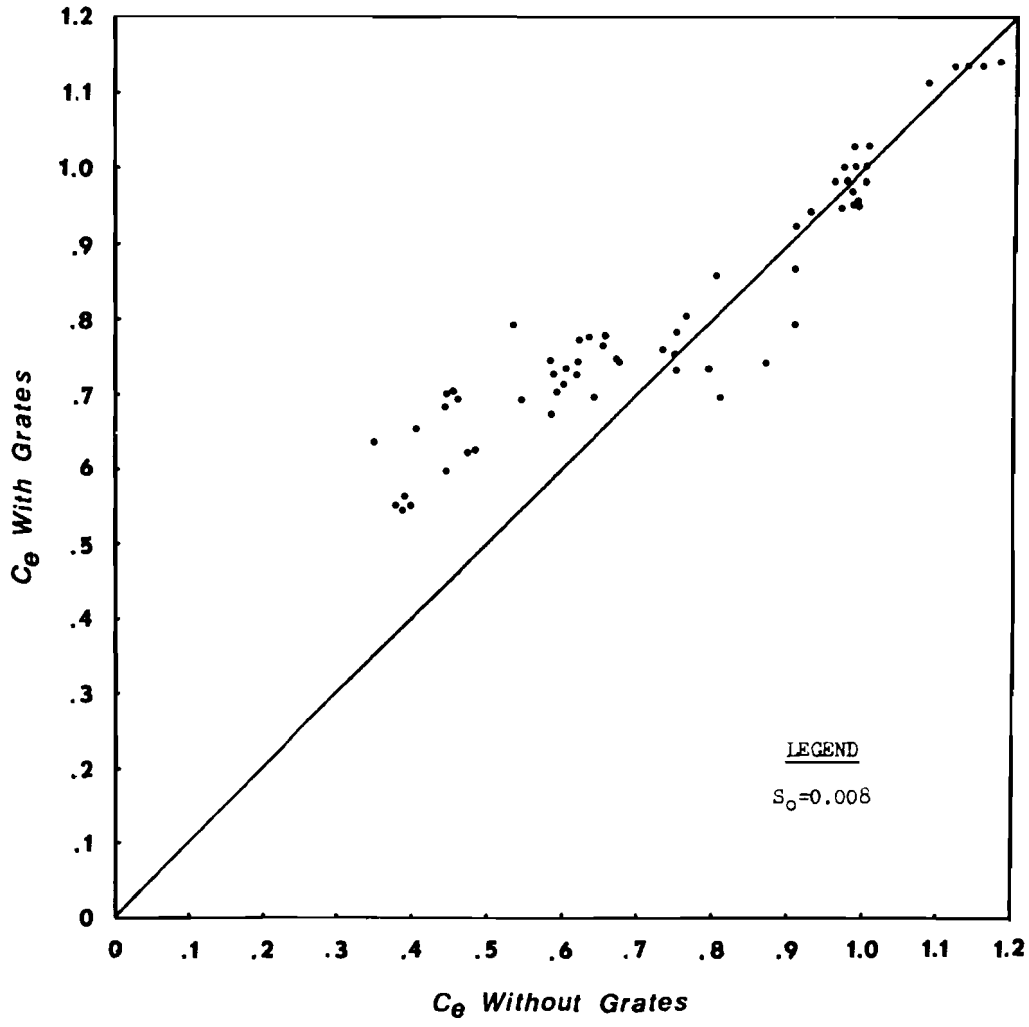


Figure E.2 Comparison of Entrance Headloss Coefficients With and Without Safety Grates Slope = 0.008

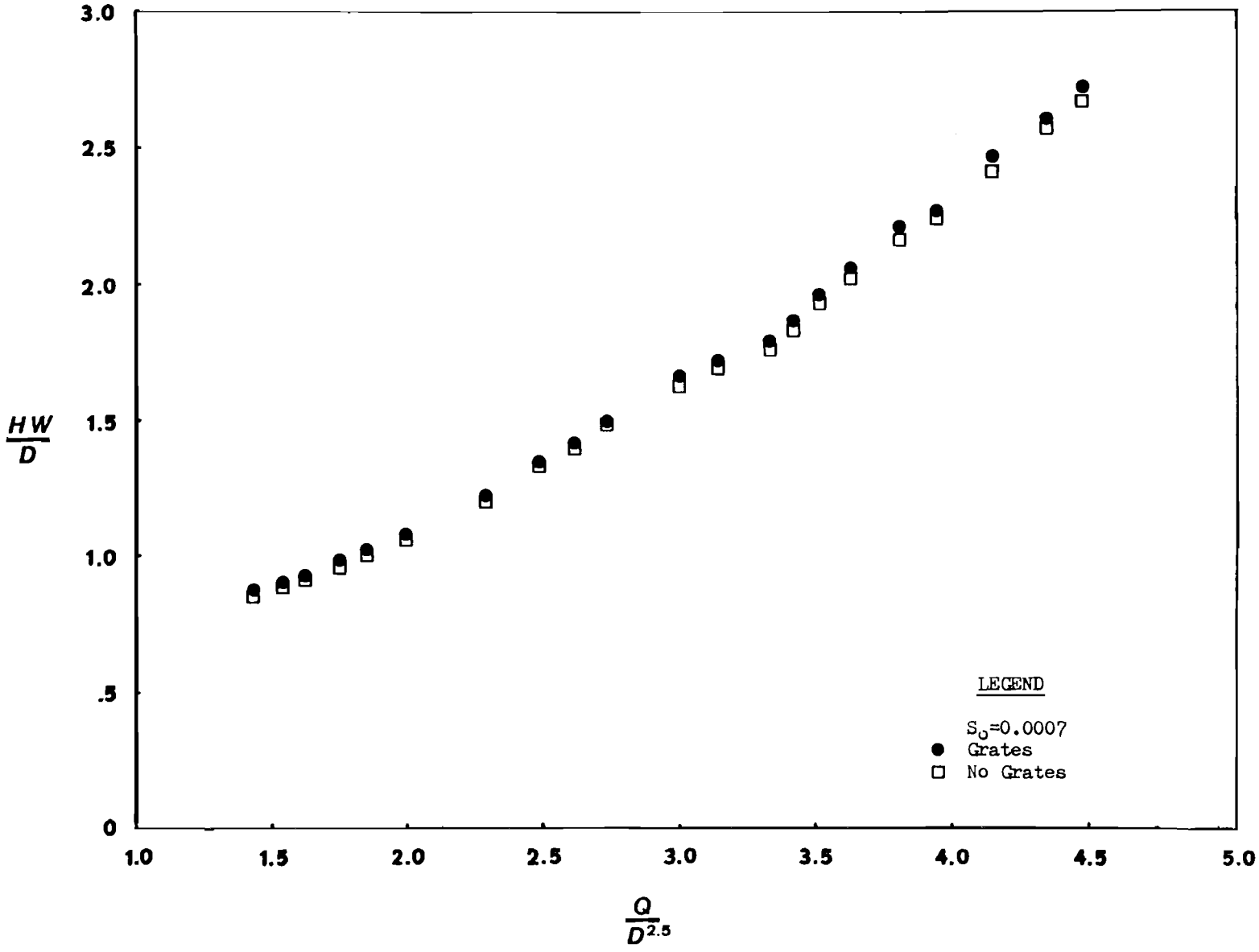


Figure E.3 Headwater Vs. Discharge With and Without Grates
Slope = 0.0007

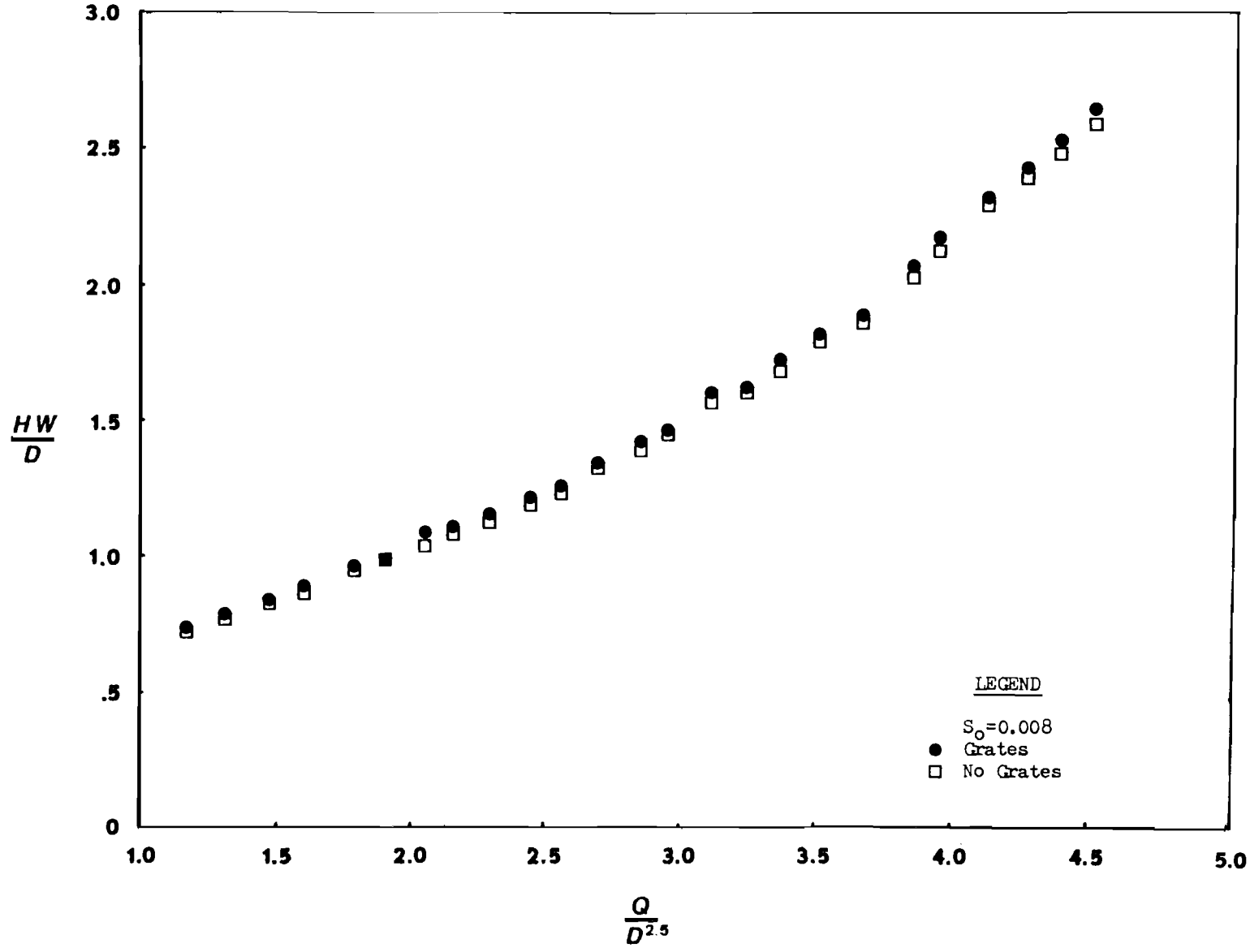


Figure E.4 Headwater Vs. Discharge With and Without Grates
Slope = 0.008

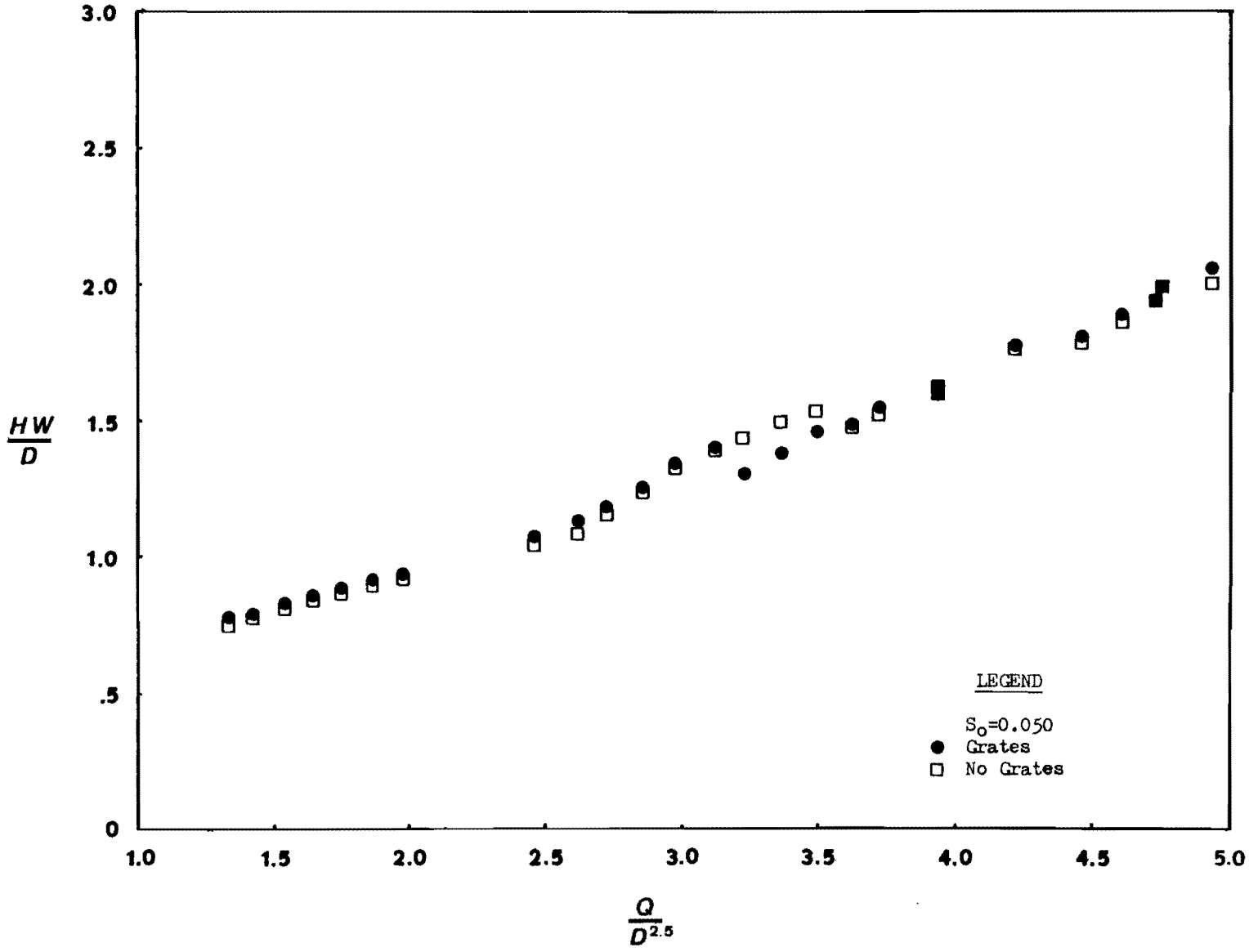


Figure E.5 Headwater Vs. Discharge With and Without Grates
Slope = 0.50

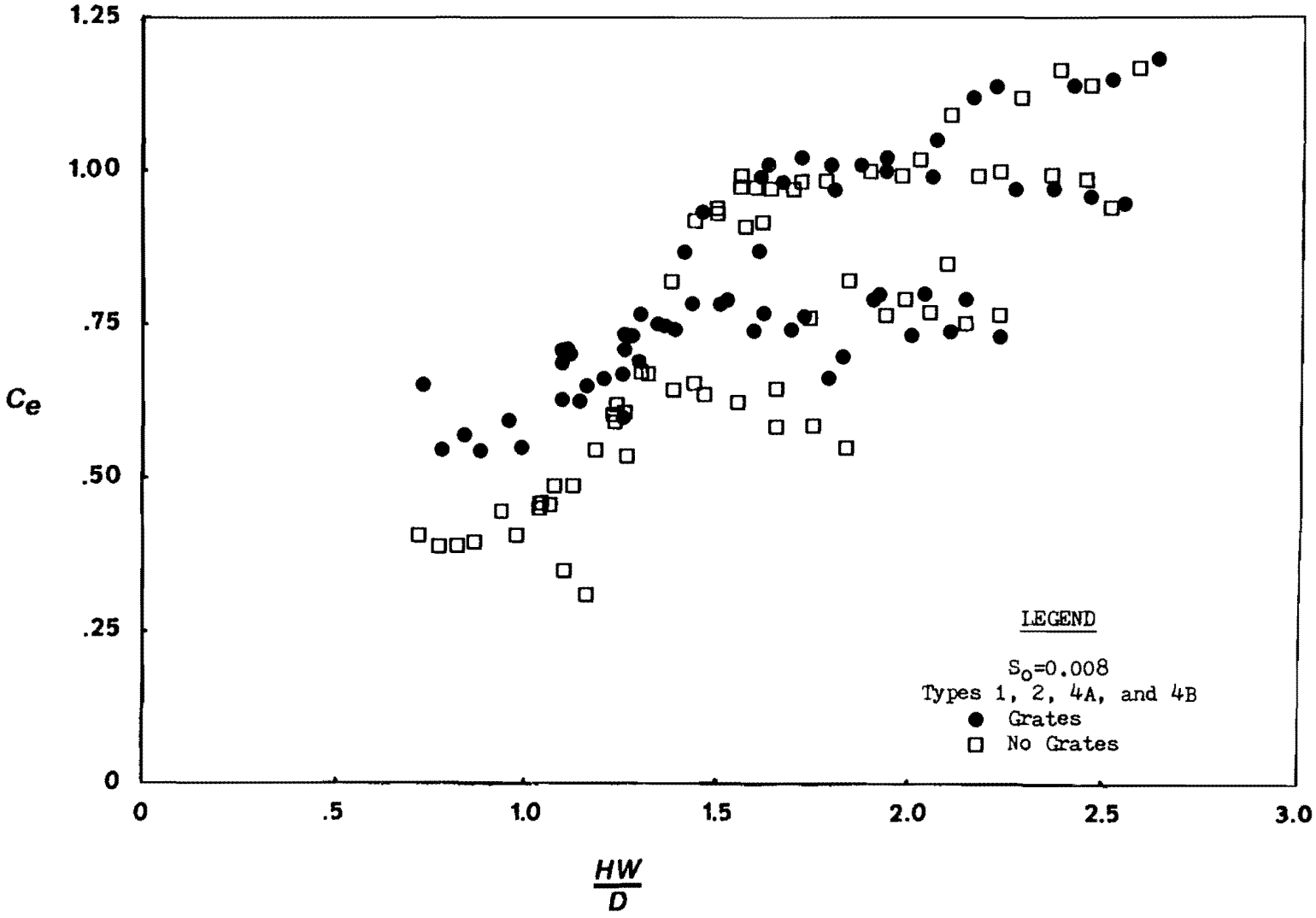


Figure E.6 Entrance Headloss Coefficient Vs. Headwater Types 1, 2, 4A and 4B With and Without Grates, Slope = 0.0008

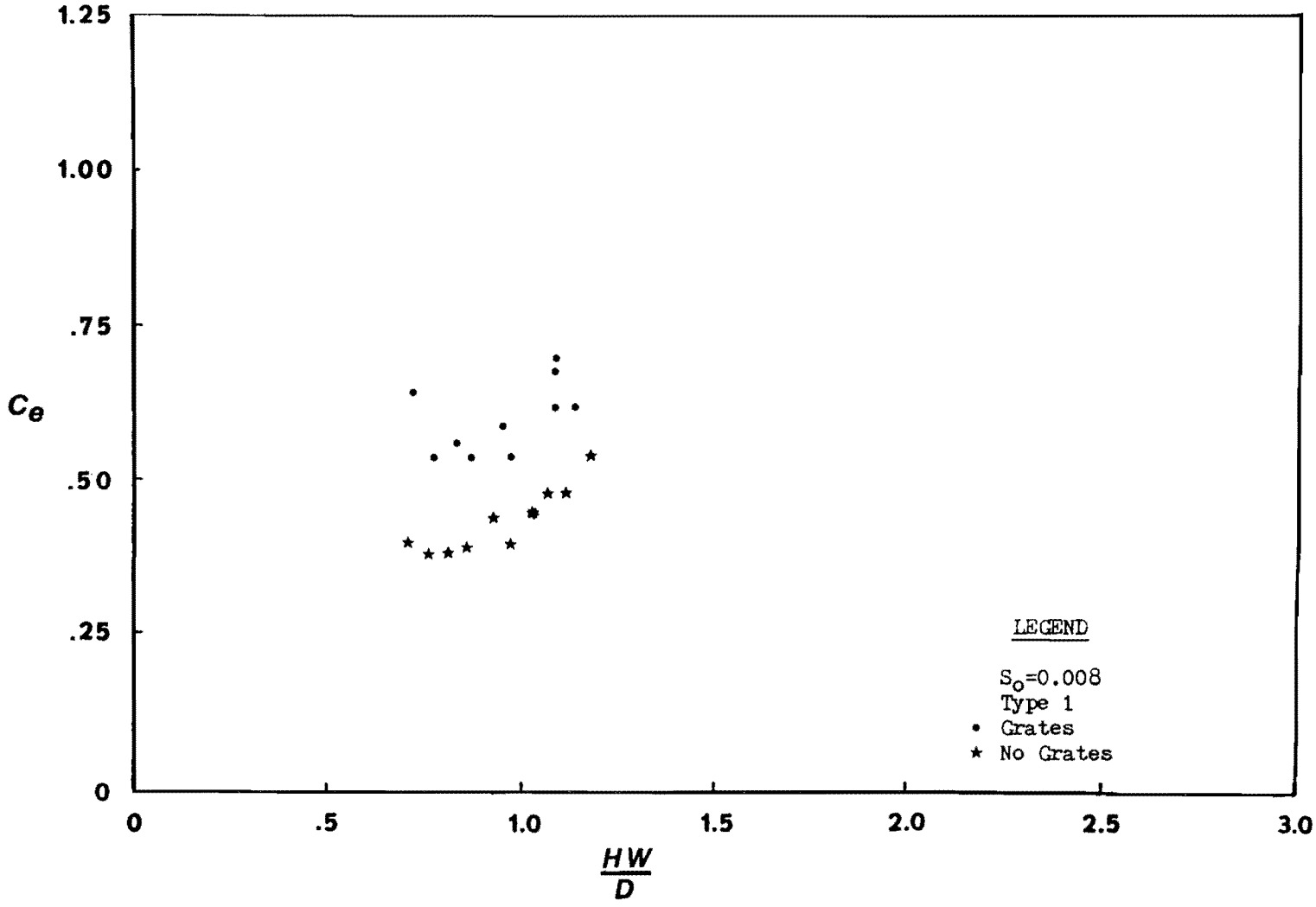


Figure E.7 Entrance Headloss Coefficient Vs. Headwater
Type 1 With and Without Grates,
Slope = 0.0008

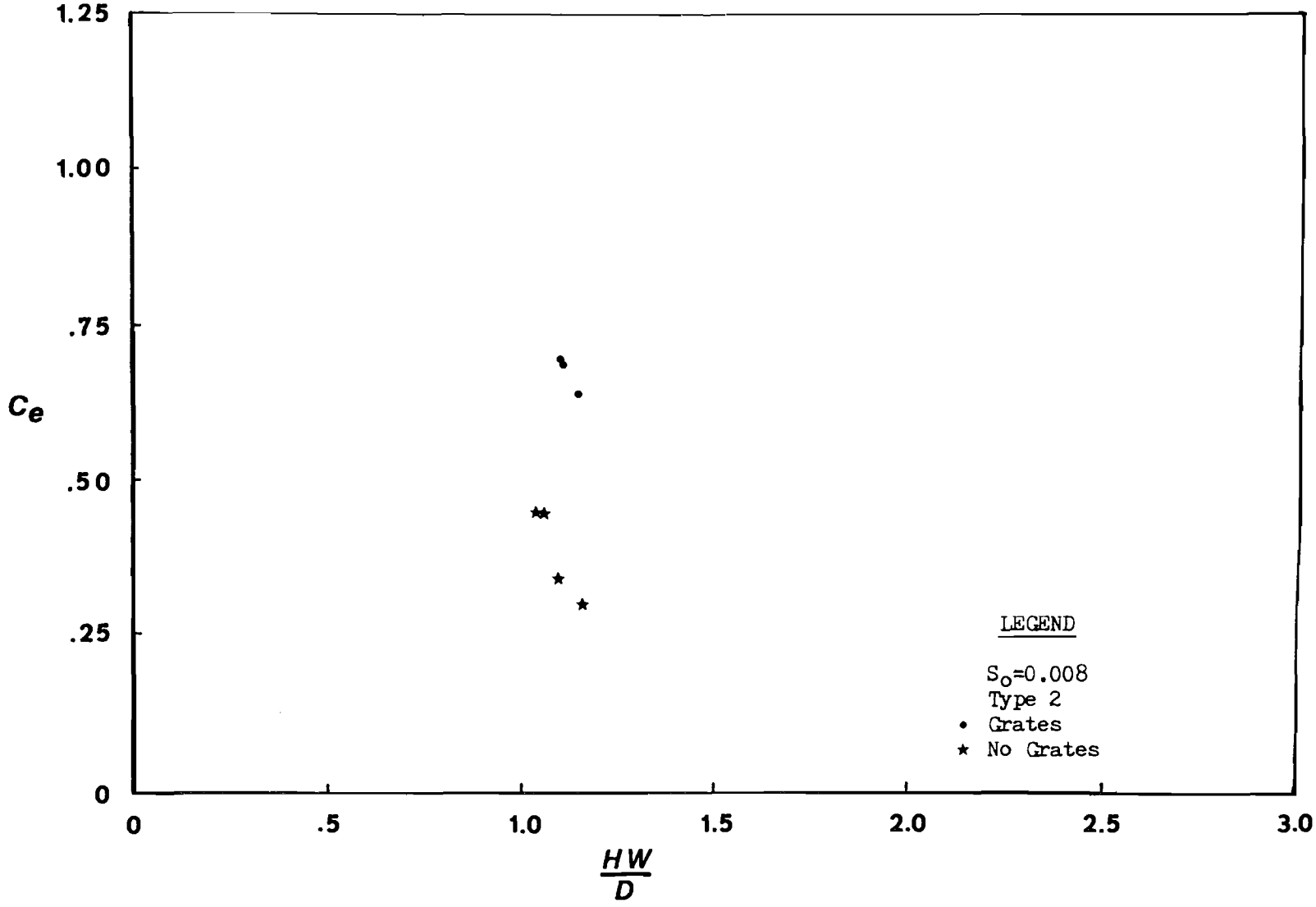


Figure E.8 Entrance Headloss Coefficient Vs. Headwater
Type 2 With and Without Grates,
Slope = 0.0008

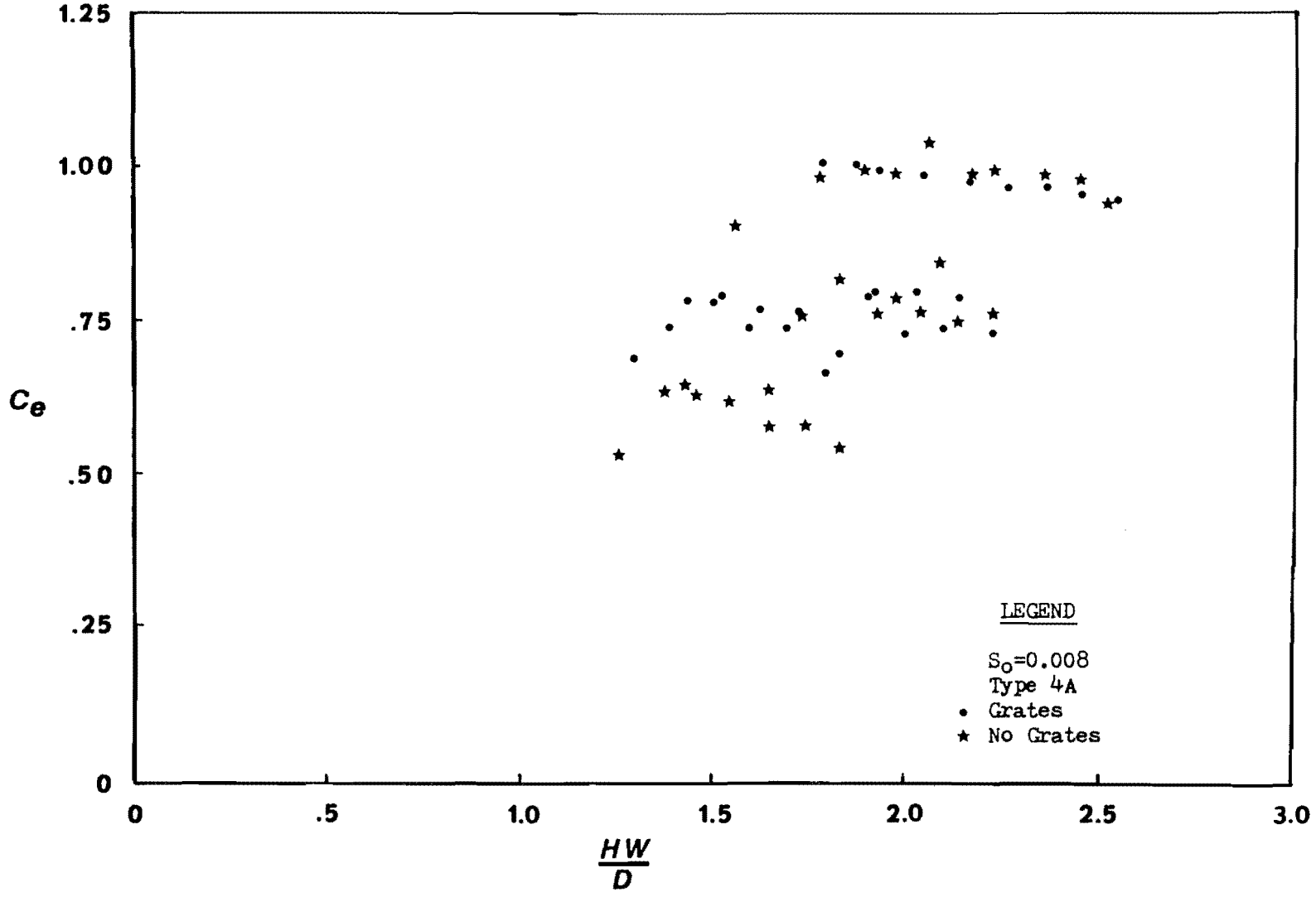


Figure E.9 Entrance Headloss Coefficient Vs. Headwater Type 4A With and Without Grates, Slope = 0.008

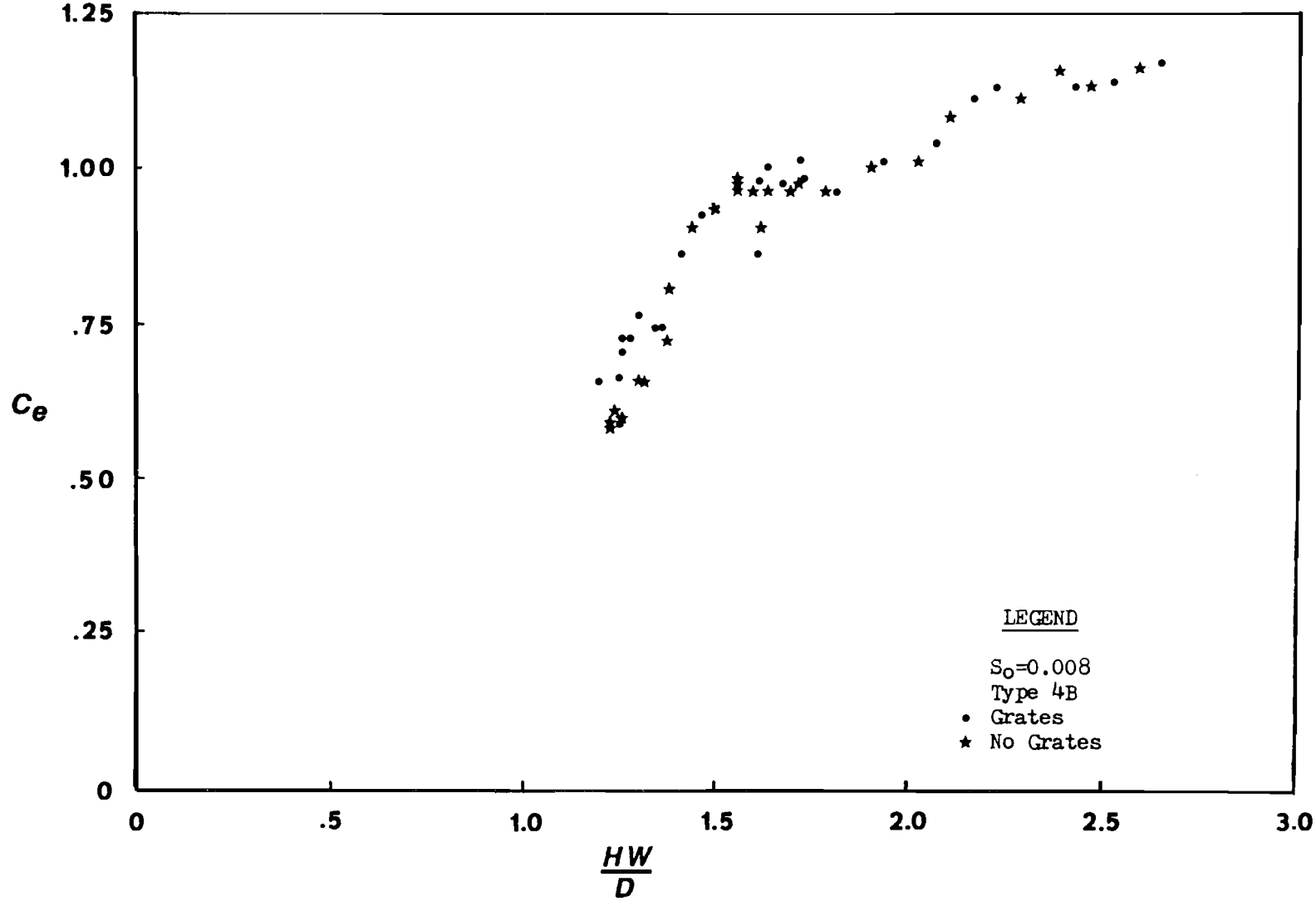


Figure E.10 Entrance Headloss Coefficient Vs. Headwater
Type 4B With and Without Grates,
Slope = 0.008

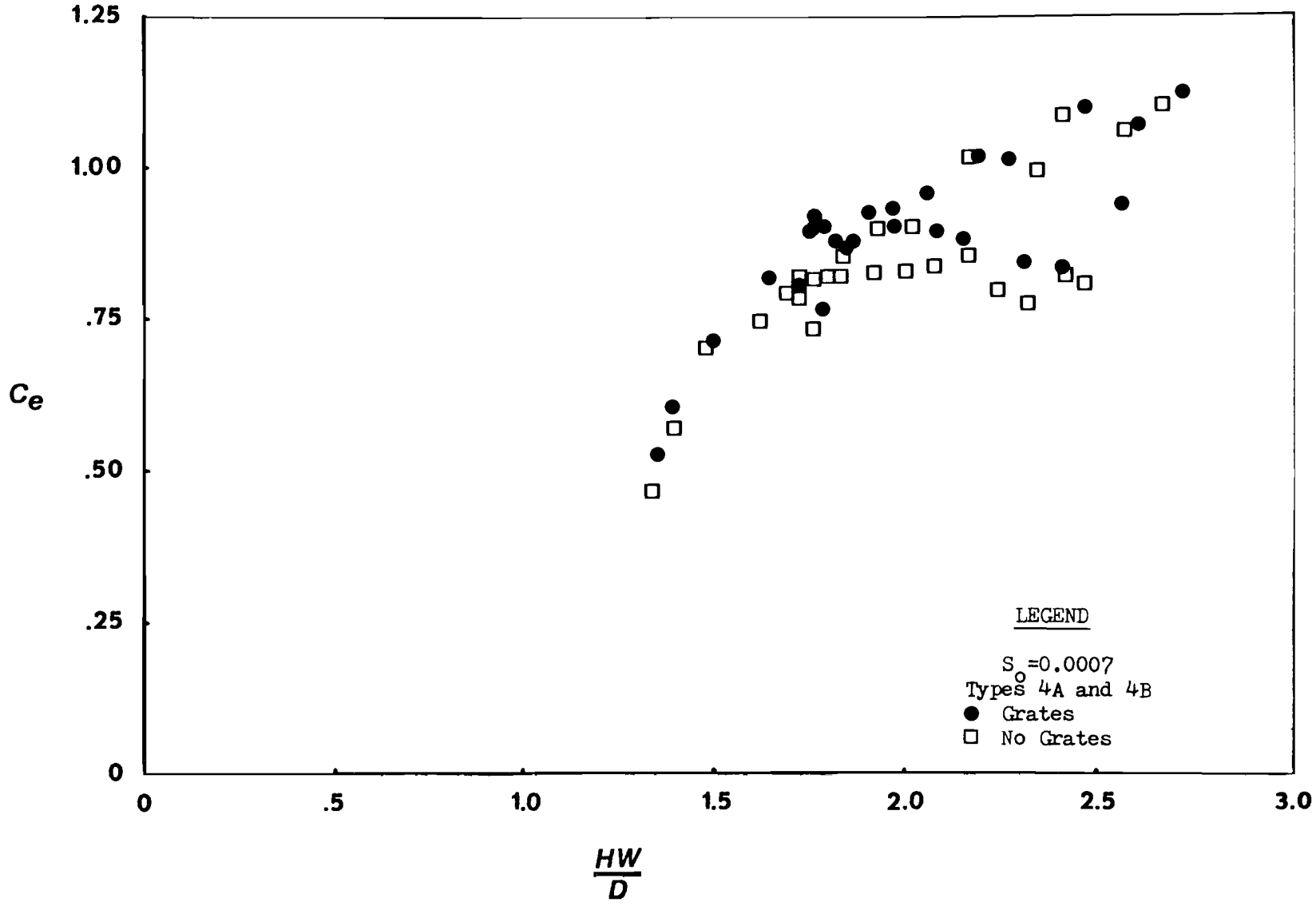


Figure E.11 Entrance Headloss Coefficient Vs. Headwater Types 4A and 4B With and Without Grates, Slope = 0.0007

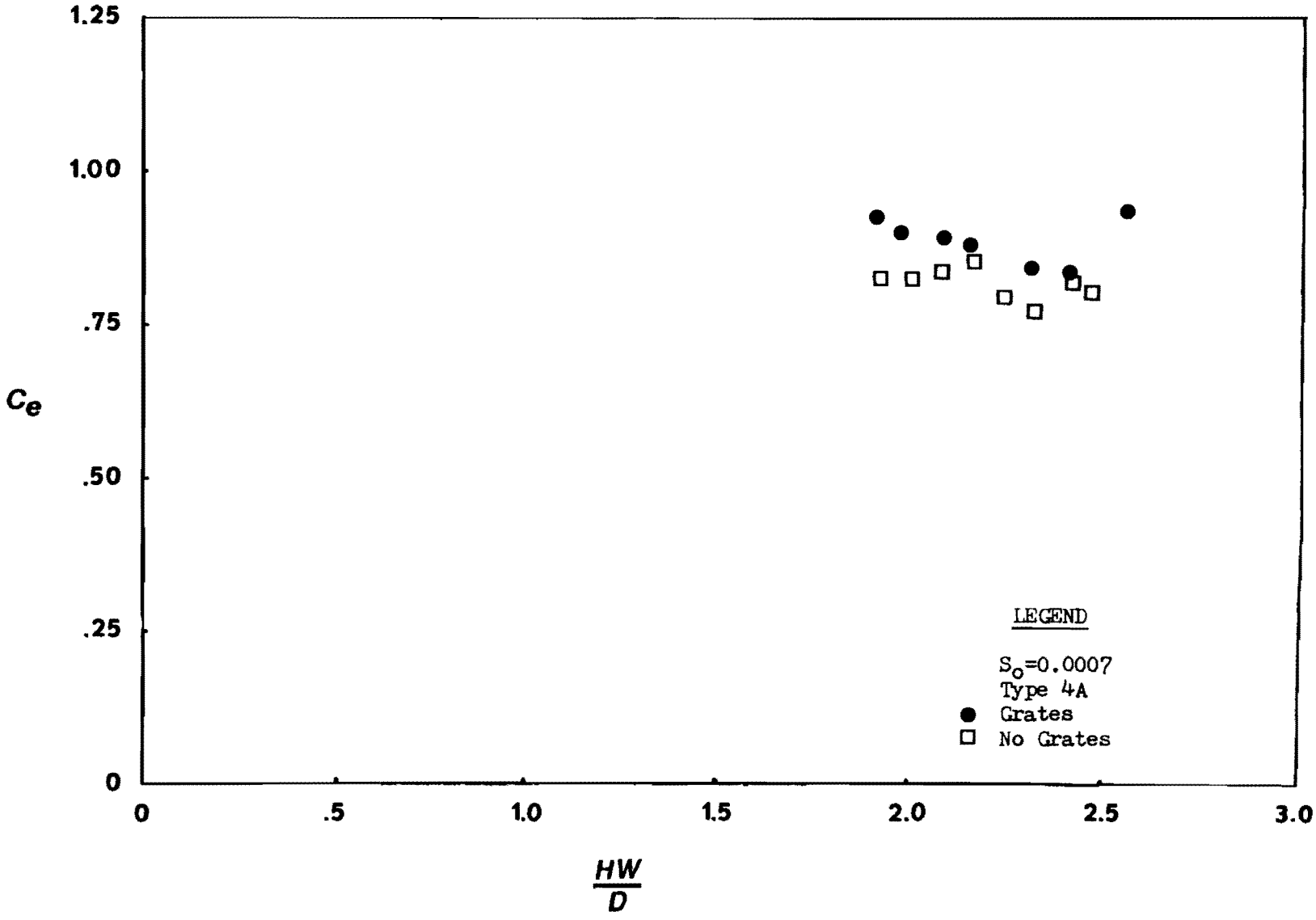


Figure E.12 Entrance Headloss Coefficient Vs. Headwater
Type 4A With and Without Grates,
Slope = 0.0007

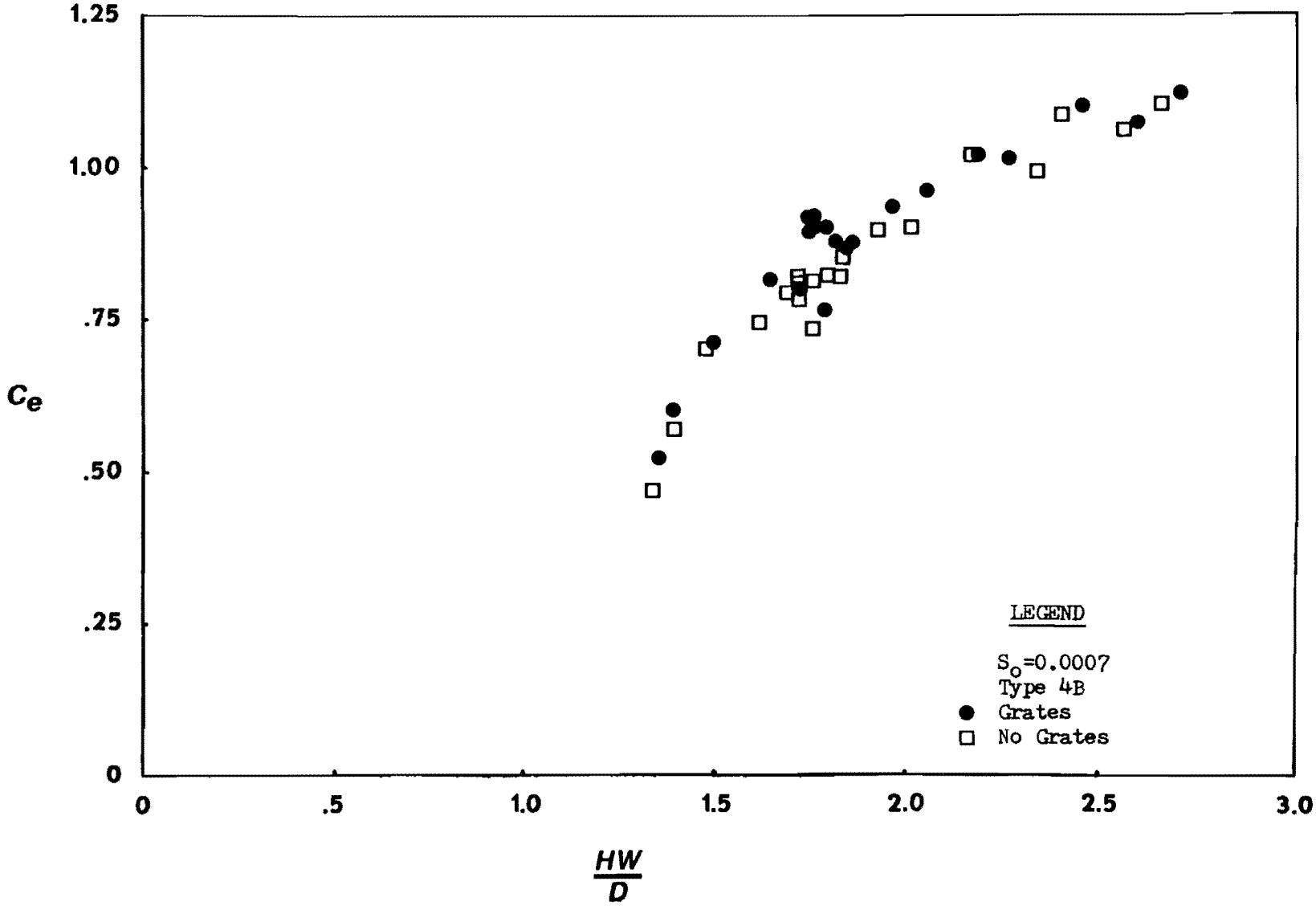


Figure E.13 Entrance Headloss Coefficient Vs. Headwater Type 4B With and Without Grates, Slope = 0.0007

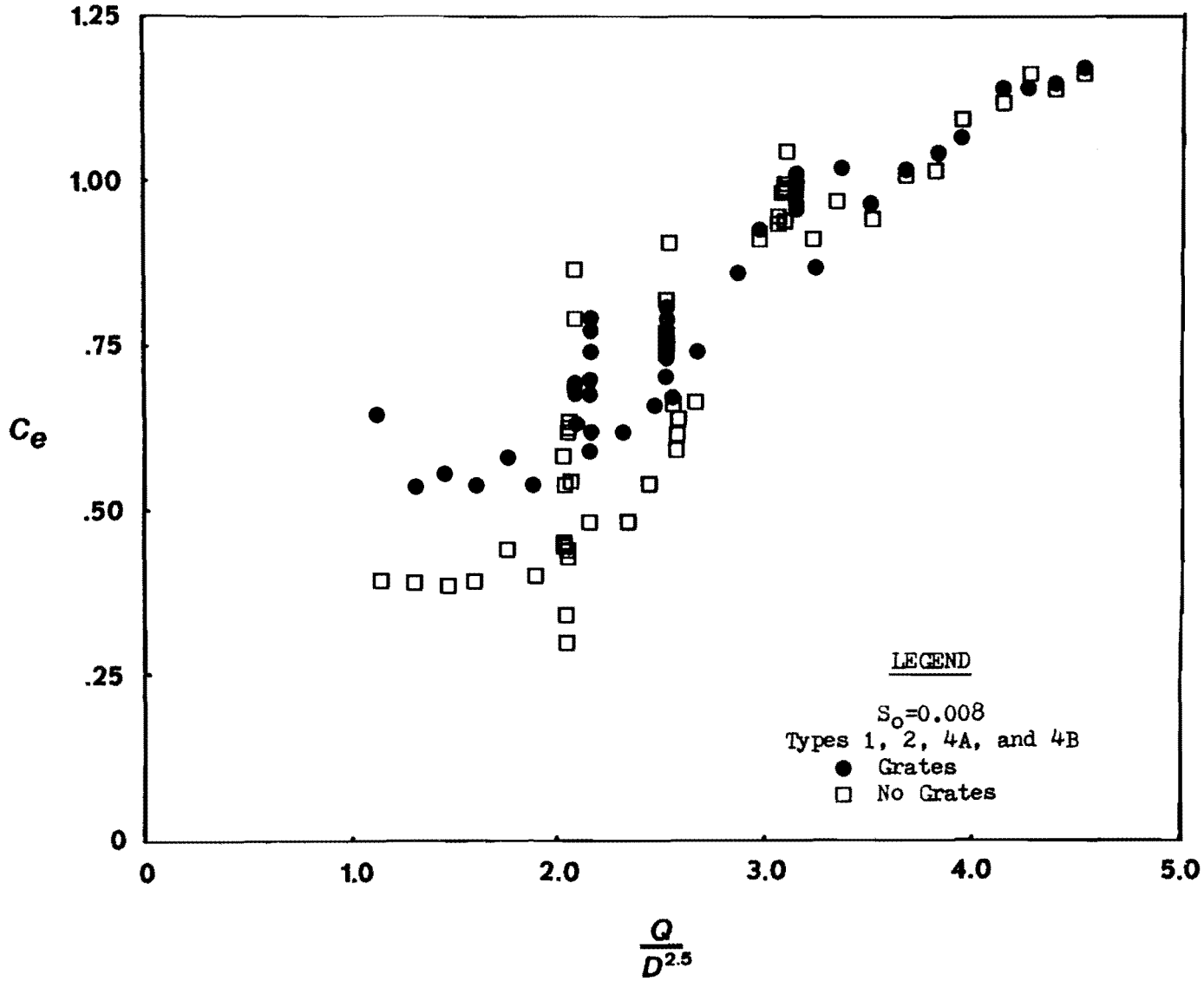


Figure E.14 Entrance Headloss Coefficient Vs. Discharge
Types 1, 2, 4A and 4B With and Without Grates
Slope = 0.008

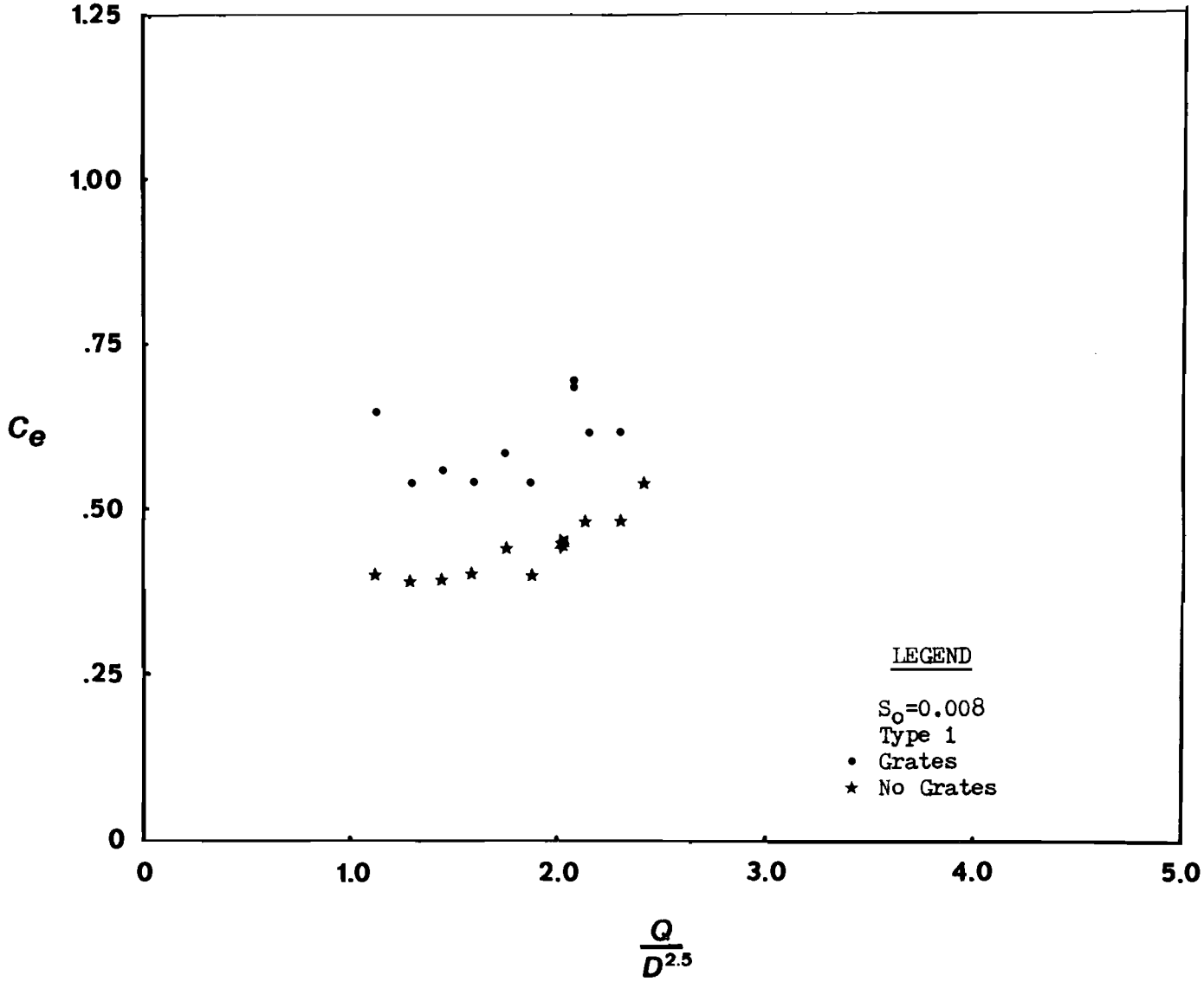


Figure E.15 Entrance Headloss Coefficient Vs. Discharge Type 1 With and Without Grates, Slope = 0.008

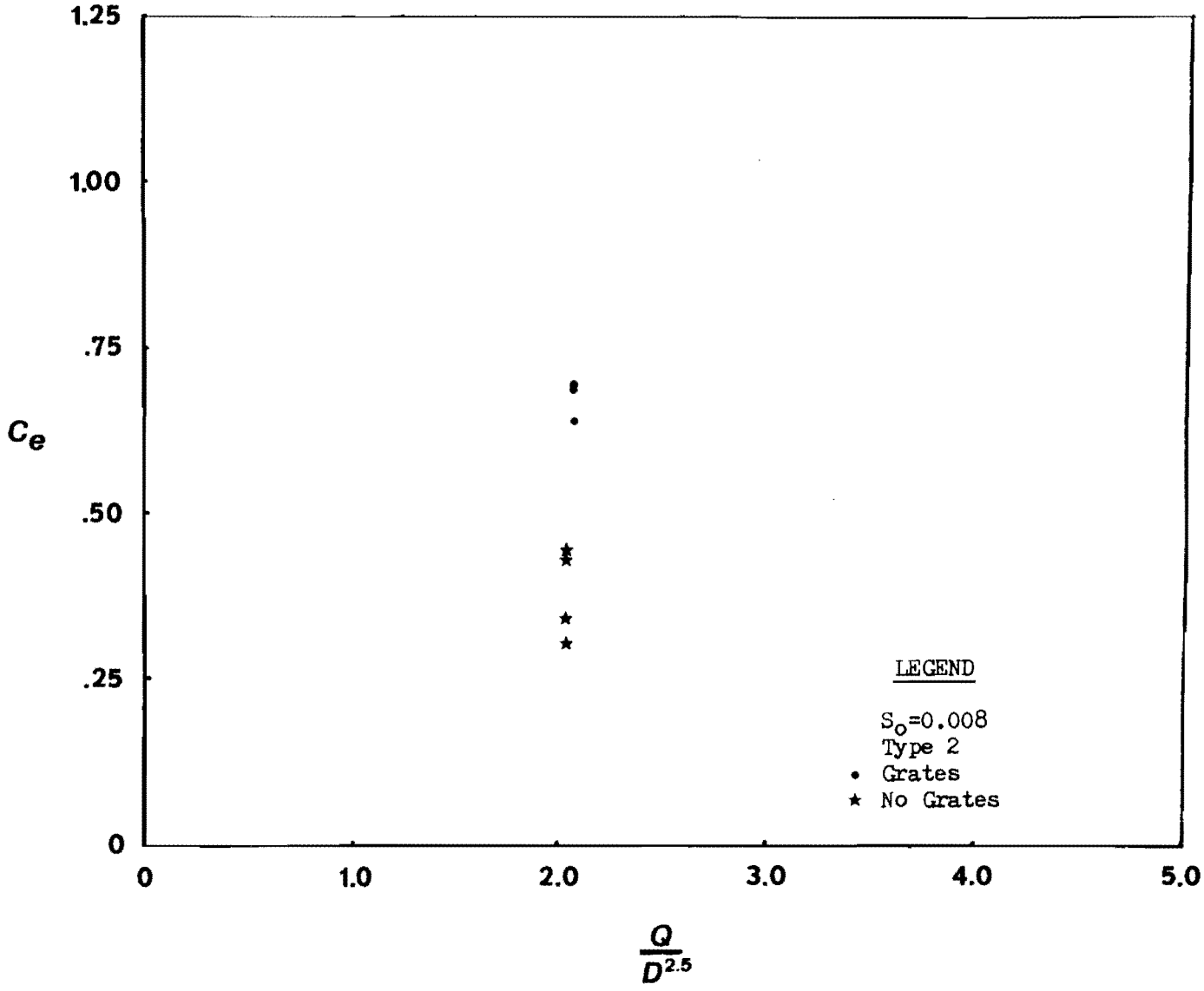


Figure E.16 Entrance Headloss Coefficient Vs. Discharge Type 2 With and Without Grates, Slope = 0.008

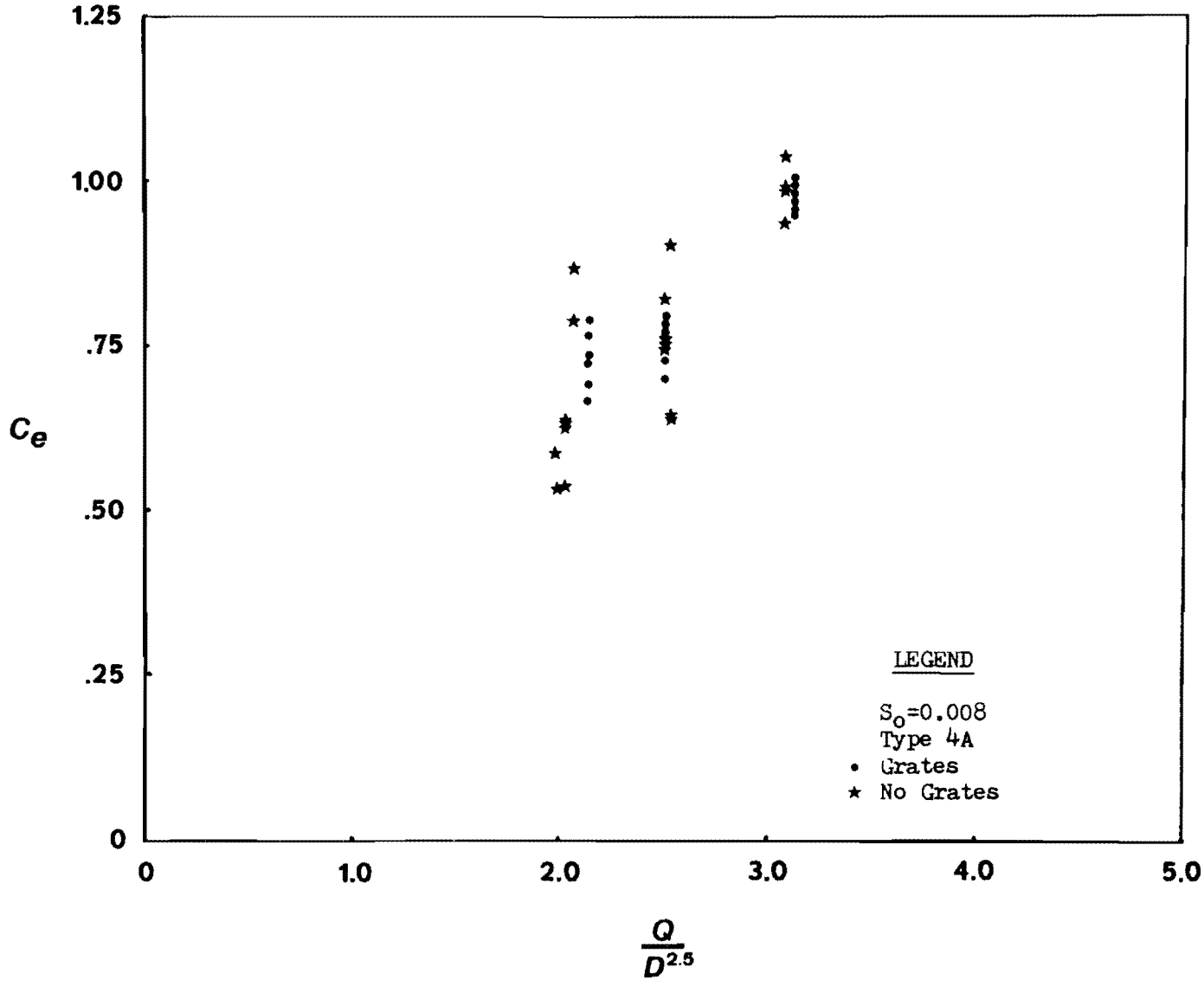


Figure E.17 Entrance Headloss Coefficient Vs. Discharge Type 4A With and Without Grates, Slope = 0.008

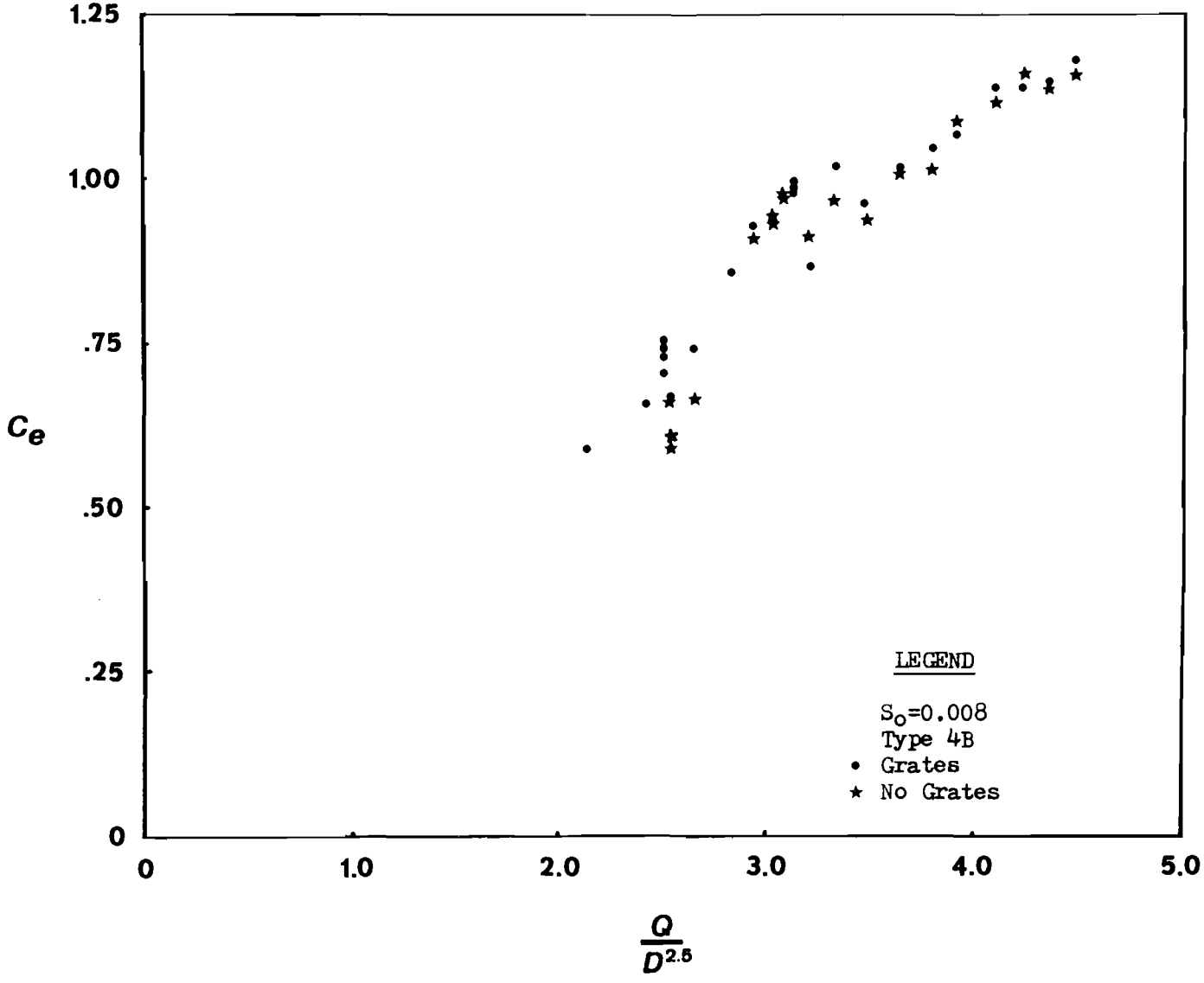


Figure E.18 Entrance Headloss Coefficient Vs. Discharge Type 4B With and Without Grates, Slope = 0.008

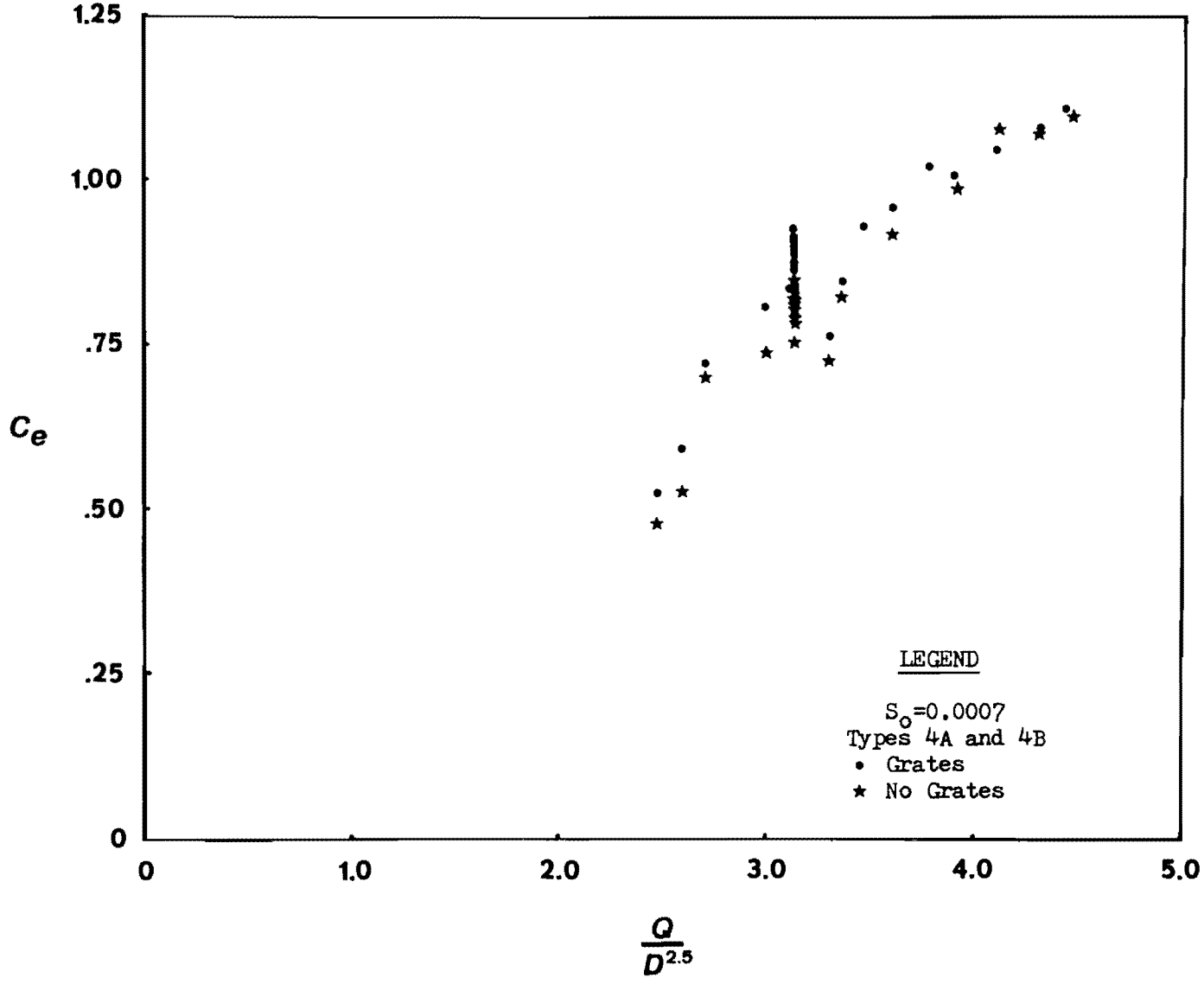


Figure E.19 Entrance Headloss Coefficient Vs. Discharge Types 4A and 4B With and Without Grates, Slope = 0.0007

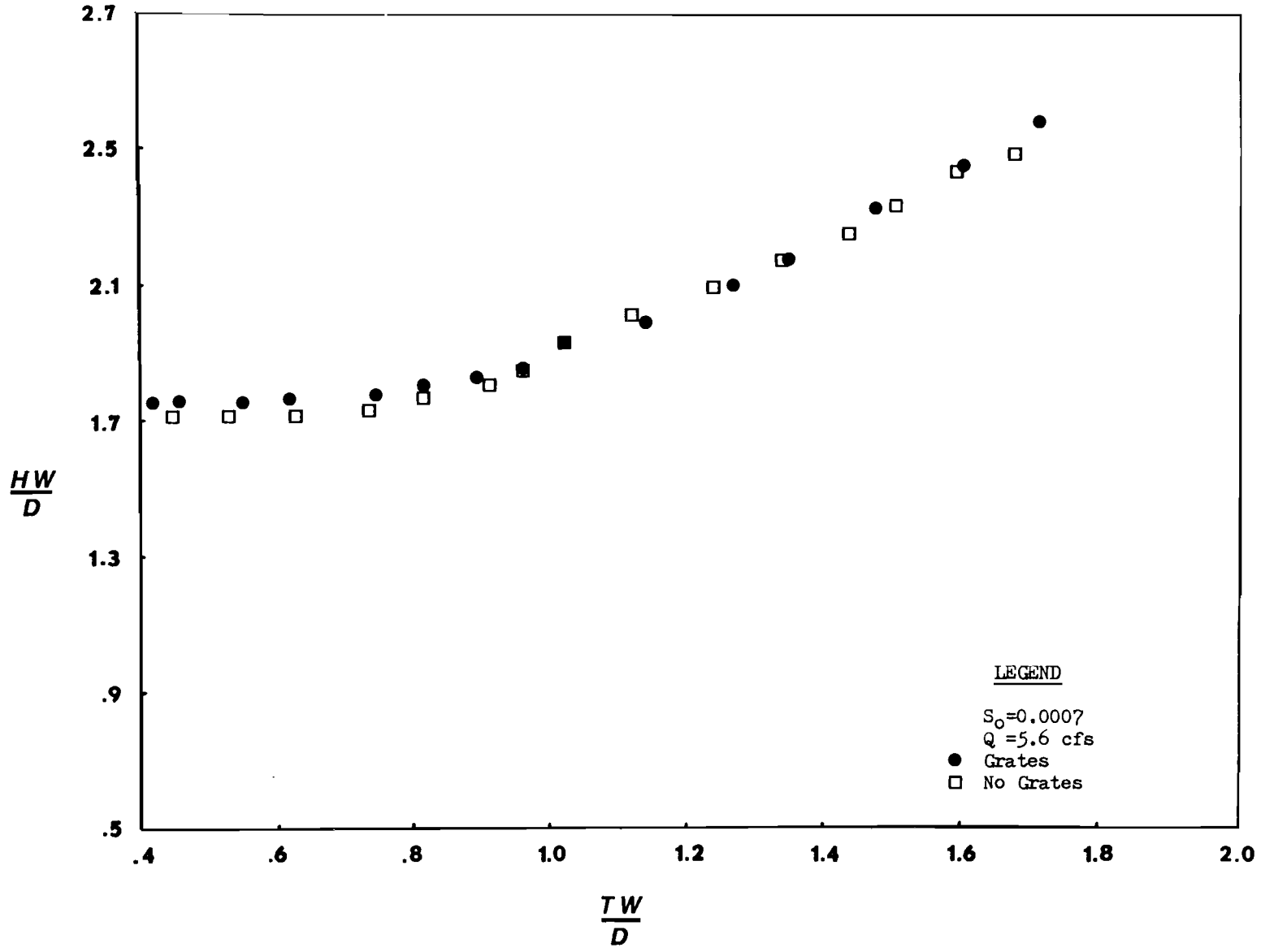


Figure E.20 Headwater Vs. Tailwater, Grates and No Grates
Slope = 0.0007, Q = 5.6 cfs

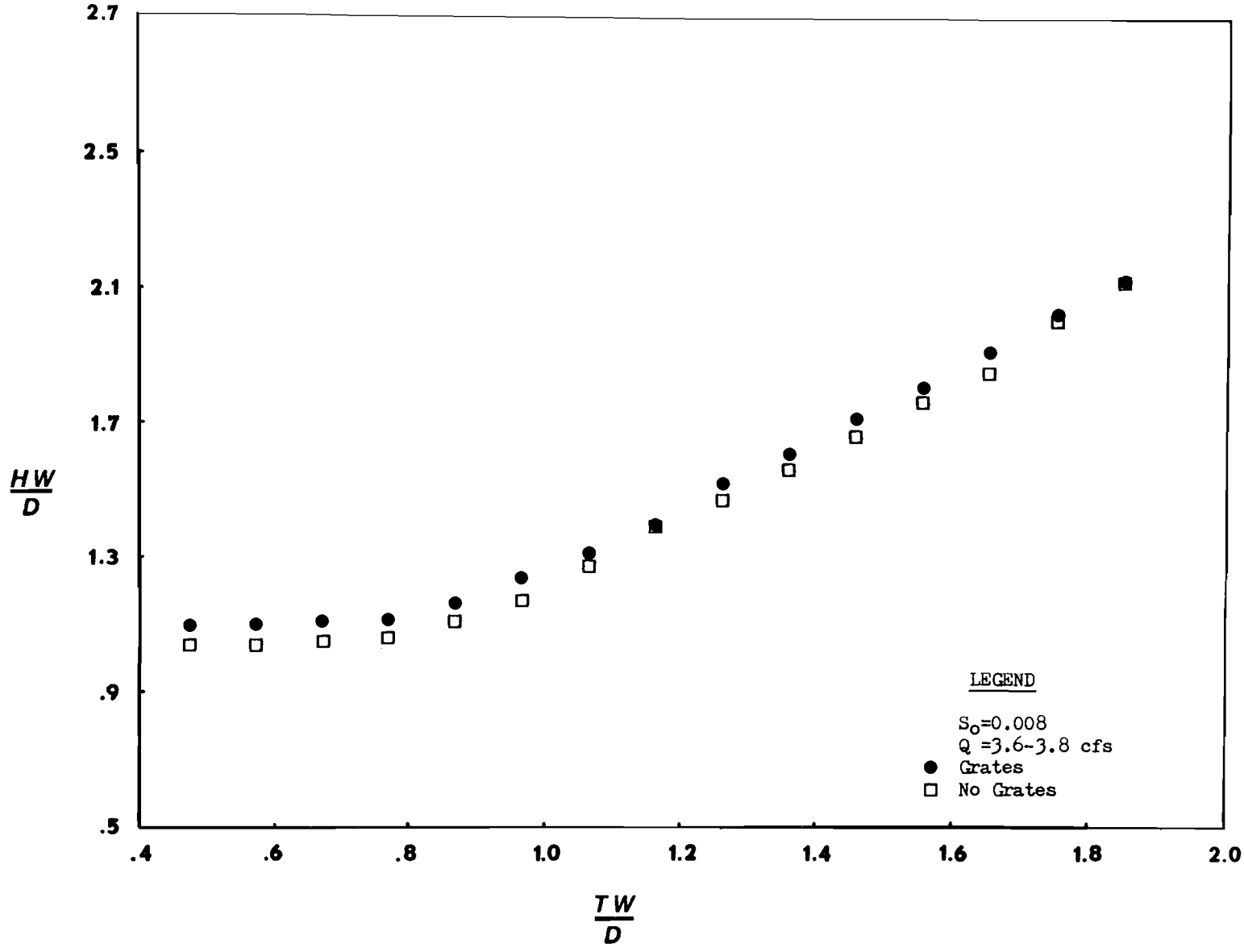


Figure E.21 Headwater Vs. Tailwater, Grates and No Grates
Slope = 0.008, Q = 3.6-3.8 cfs

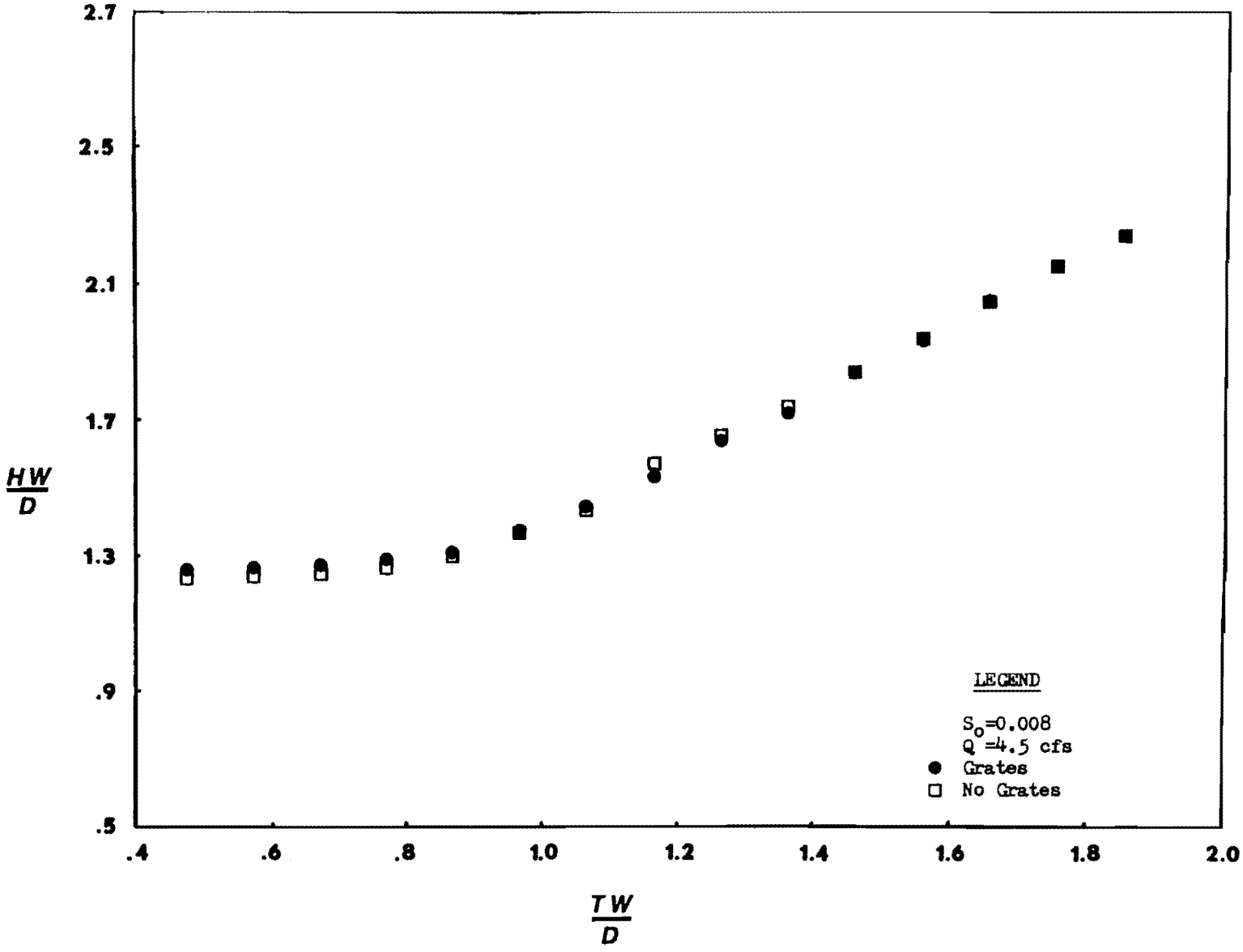


Figure E.22 Headwater Vs. Tailwater, Grates and No Grates
Slope = 0.008, Q = 4.5 cfs

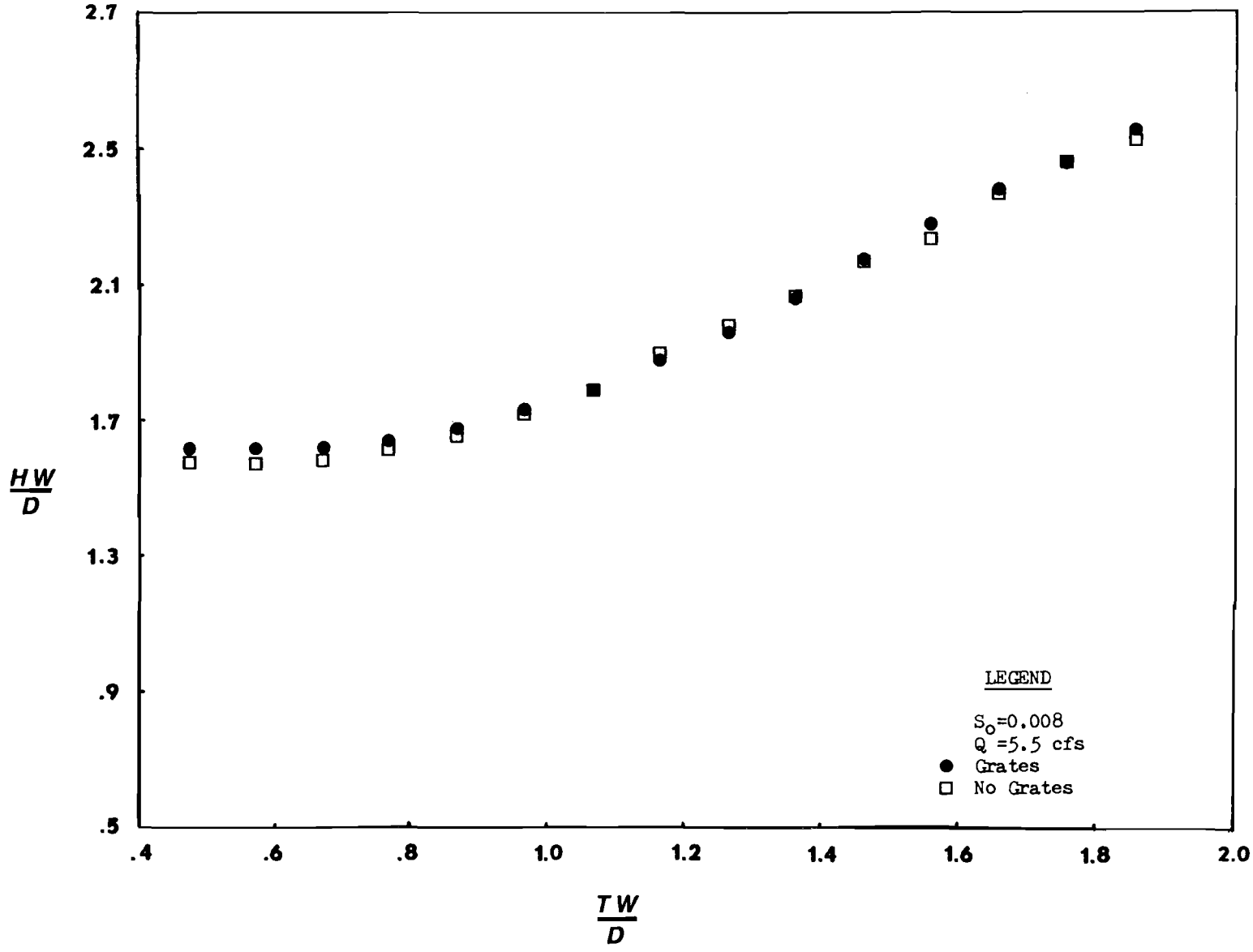


Figure E.23 Headwater Vs. Tailwater, Grates and No Grates
Slope = 0.008, Q = 5.6 cfs

# APPENDIX F

## Data From Culvert Experiments

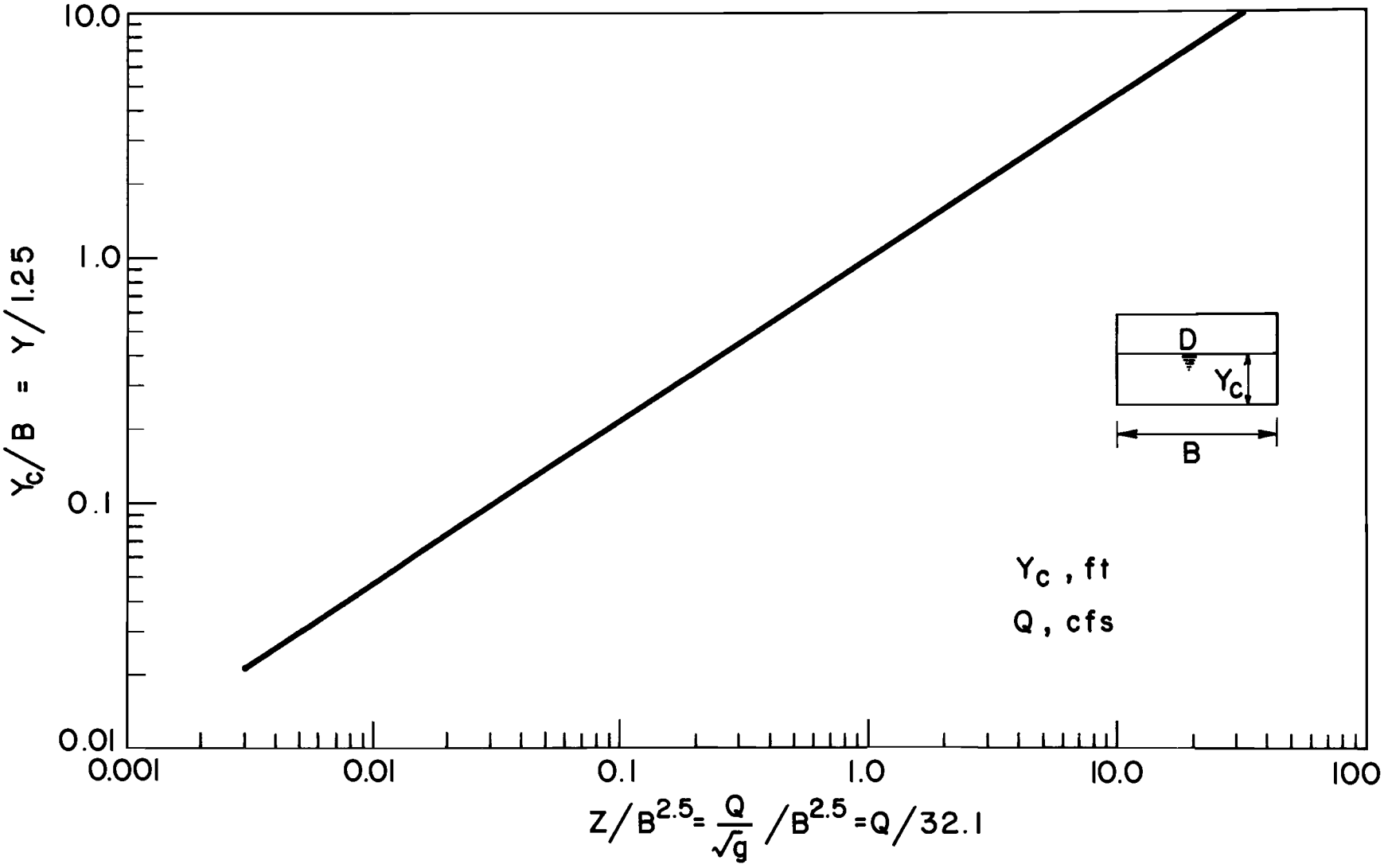


Figure F.1 Curve for Determining Critical Depth ($Y_c$) in Box Culvert

Table F.1 Data, Type 1, No Grates

D = 1.25 ft, B = 2 ft

| $C_e$ | $\frac{HW}{D}$ | $\frac{Q}{BD^{1.5}}$ | $\frac{TW}{D}$ | $S_o$ |
|---|---|---|---|---|
| .00236 | .76500 | 1.86483 | 0.00000 | .00130 |
| .19881 | 1.14348 | 3.28285 | 0.00000 | .00130 |
| .25970 | 1.17748 | 3.39876 | 0.00000 | .00130 |
| .02823 | .81588 | 2.03462 | 0.00000 | .00130 |
| .10059 | .92268 | 2.41140 | 0.00000 | .00130 |
| .09203 | .95788 | 2.57847 | 0.00000 | .00130 |
| .19507 | 1.00308 | 3.03974 | 0.00000 | .00130 |
| .22182 | .91640 | 2.28158 | 0.00000 | .00080 |
| .22491 | .98320 | 2.55520 | 0.00000 | .00080 |
| .25856 | 1.00[illegible] | 2.76113 | 0.00000 | .00080 |
| .26840 | 1.00480 | 2.90538 | 0.00000 | .00080 |
| .09733 | .59120 | 1.18755 | 0.00000 | .00080 |
| .13080 | .64320 | 1.33437 | 0.00000 | .00080 |
| .17305 | .70680 | 1.54043 | 0.00000 | .00080 |
| .19192 | .77120 | 1.77152 | 0.00000 | .00080 |
| .13645 | .83360 | 1.99171 | 0.00000 | .00080 |
| .21195 | .89280 | 2.19822 | 0.00000 | .00080 |
| .22965 | 1.12600 | 3.15117 | 0.00000 | .00080 |
| .20244 | .89680 | 2.23144 | 0.00000 | .00080 |
| .26574 | .98120 | 2.28374 | 0.00000 | .00080 |
| .26452 | 1.00440 | 2.90538 | 0.00000 | .00080 |
| .19797 | .53480 | 1.12472 | 0.00000 | .00630 |
| .29684 | .64200 | 1.32176 | 0.00000 | .00630 |
| .39845 | .67[illegible] | 1.49163 | 0.00000 | .00630 |
| .37899 | .72880 | 1.68992 | 0.00000 | .00630 |
| .15014 | .76160 | 1.89629 | 0.00000 | .00630 |
| .17936 | .82200 | 2.11040 | 0.00000 | .00630 |
| .15089 | .87600 | 2.33210 | 0.00000 | .00630 |
| .20996 | .95[illegible] | 2.56141 | 0.00000 | .00630 |
| .16201 | .99360 | 2.79696 | 0.00000 | .00630 |
| .16667 | 1.00520 | 3.03974 | 0.00000 | .00630 |
| .23203 | 1.12760 | 3.28917 | 0.00000 | .00630 |
| .11791 | .82360 | 2.16516 | 0.00000 | .00630 |
| .15200 | 1.00480 | 2.90538 | 0.00000 | .00630 |
| .13475 | 1.01240 | 2.90538 | 0.00000 | .00630 |
| .21563 | 1.17160 | 3.45477 | 0.00000 | .00630 |

Table F.2 Data, Type 2, Pipe Grates

| $C_e$ | $\frac{HW}{D}$ | $\frac{Q}{BD^{1.5}}$ | $\frac{TW}{D}$ | $S_o$ |
|---|---|---|---|---|
| .00230 | .76500 | 1.86483 | 0.00000 | .00130 |
| .07530 | 1.12260 | 3.28285 | 0.00000 | .00130 |
| .21620 | 1.17740 | 3.39076 | 0.00000 | .00130 |
| .04581 | .81820 | 2.03462 | 0.00000 | .00130 |
| .09277 | .92220 | 2.21140 | 0.00000 | .00130 |
| .10865 | .95820 | 2.57847 | 0.00000 | .00130 |
| .12593 | .95860 | 2.57847 | .52833 | .00130 |
| .16440 | .95820 | 2.57847 | .52833 | .00130 |
| .10674 | .95860 | 2.57847 | .55333 | .00130 |
| .22096 | 1.00780 | 3.03974 | 0.00000 | .00130 |
| .11875 | .89400 | 2.19822 | .38720 | .00080 |
| .21549 | .91640 | 2.28158 | 0.00000 | .00080 |
| .22154 | .98280 | 2.55520 | 0.00000 | .00080 |
| .26318 | 1.00160 | 2.76113 | 0.00000 | .00080 |
| .30249 | 1.00820 | 2.93538 | 0.00000 | .00080 |
| .09733 | .59120 | 1.18755 | 0.00000 | .00080 |
| .14761 | .64480 | 1.33437 | 0.00000 | .00080 |
| .15066 | .70560 | 1.54043 | 0.00000 | .00080 |
| .12676 | .77280 | 1.77152 | 0.00000 | .00080 |
| .15204 | .83560 | 1.99171 | 0.00000 | .00080 |
| .24195 | .89280 | 2.19822 | 0.00000 | .00080 |
| .36910 | 1.00920 | 2.93538 | 0.00000 | .00080 |
| .27149 | 1.00560 | 2.93538 | .57953 | .00080 |
| .17224 | .53280 | 1.12472 | 0.00000 | .00630 |
| .29684 | .60240 | 1.30176 | 0.00000 | .00630 |
| .36751 | .66240 | 1.49163 | 0.00000 | .00630 |
| .36639 | .72680 | 1.68992 | 0.00000 | .00630 |
| .18306 | .76520 | 1.89629 | 0.00000 | .00630 |
| .18330 | .82280 | 2.11044 | 0.00000 | .00630 |
| .16811 | .87800 | 2.33210 | 0.00000 | .00630 |
| .21373 | .95080 | 2.56101 | 0.00000 | .00630 |
| .17612 | .99680 | 2.79696 | 0.00000 | .00630 |
| .18241 | 1.05360 | 3.03974 | 0.00000 | .00630 |
| .24453 | 1.12880 | 3.29917 | 0.00000 | .00630 |
| .12671 | .82440 | 2.16516 | 0.00000 | .00630 |
| .15200 | 1.01480 | 2.90538 | .54973 | .00630 |
| .12454 | 1.01000 | 2.90538 | .54973 | .00630 |
| .21563 | 1.17160 | 3.45477 | .54973 | .00630 |
| .21563 | 1.17160 | 3.45477 | .64973 | .00630 |

Table F.3 Data, Type 1, Bar Grates

| $C_e$ | $\frac{HW}{D}$ | $\frac{Q}{BD^{1.5}}$ | $\frac{TW}{D}$ | $S_o$ |
|---|---|---|---|---|
| .06921 | .66324 | 1.45297 | 0.00000 | .00080 |
| .23451 | .75688 | 1.64960 | 0.00000 | .00080 |
| .13948 | .79769 | 1.85439 | 0.00000 | .00080 |
| .15200 | .84848 | 2.06780 | 0.00000 | .00080 |
| .11486 | .88280 | 2.28718 | 0.00000 | .00080 |
| .21283 | .96488 | 2.51466 | 0.00009 | .00080 |
| .28689 | 1.03440 | 2.73732 | 0.00000 | .00080 |
| .32823 | 1.10720 | 2.99065 | 0.00000 | .00080 |
| .45291 | 1.19460 | 3.23876 | 0.00400 | .00080 |
| .35093 | 1.09120 | 2.89932 | 0.00000 | .00080 |
| .30316 | 1.08560 | 2.89932 | .57053 | .00080 |
| .27489 | .93760 | 2.31522 | 0.00000 | .00080 |
| .24240 | .67160 | 1.43377 | 0.00000 | .00080 |
| .10332 | .59680 | 1.33437 | 0.00000 | .00630 |
| .15650 | .66320 | 1.54533 | 0.00000 | .00630 |
| .18792 | .72560 | 1.75612 | 0.00000 | .00630 |
| .16488 | .77840 | 1.96585 | 0.00000 | .00630 |
| .23032 | .85240 | 2.18167 | 0.00009 | .00630 |
| .22443 | .90920 | 2.40571 | 0.00000 | .00630 |
| .20821 | .96360 | 2.63693 | 0.00000 | .00630 |
| .26250 | 1.03240 | 2.87512 | 0.00000 | .00630 |
| .31595 | 1.10720 | 3.12008 | 0.00000 | .00630 |
| .27561 | 1.18920 | 3.35898 | 0.00000 | .00630 |
| .22636 | 1.02800 | 2.90538 | .54973 | .00630 |
| .17045 | .89240 | 2.19822 | 0.00000 | .00630 |
| .22636 | 1.02800 | 2.90538 | 0.00000 | .00630 |

Table F.4 Data, Type 2, No Grates

| $C_e$ | $\frac{HW}{D}$ | $\frac{Q}{BD^{1.5}}$ | $\frac{TW}{D}$ | $S_o$ |
|---|---|---|---|---|
| .24984 | 1.14268 | 3.28285 | .85333 | .00130 |
| .26893 | 1.17468 | 3.34618 | .82000 | .00130 |
| .11363 | .91948 | 2.41148 | .58667 | .00130 |
| .22482 | 1.09948 | 3.03974 | .88667 | .00130 |
| .26071 | .90120 | 2.20374 | .57053 | .00080 |
| .24238 | .90328 | 2.20374 | .67053 | .00080 |
| .26449 | .94440 | 2.20374 | .77053 | .00080 |
| .32907 | 1.00440 | 2.20374 | .87053 | .00080 |
| .52221 | 1.11600 | 2.20374 | .98720 | .00080 |
| .27149 | 1.08560 | 2.90538 | .67053 | .00080 |
| .27228 | 1.08560 | 2.90538 | .77053 | .00080 |
| .31897 | 1.14520 | 2.90538 | .87053 | .00080 |
| .28844 | 1.15080 | 2.90538 | .97053 | .00080 |
| .26071 | .91120 | 2.20374 | .57053 | .00080 |
| .24238 | .90328 | 2.20374 | .67053 | .00080 |
| .26449 | .90440 | 2.20374 | .77053 | .00080 |
| .32907 | 1.00440 | 2.20374 | .87053 | .00080 |
| .52221 | 1.11600 | 2.20374 | .98720 | .00080 |
| .27149 | 1.08560 | 2.90538 | .67053 | .00080 |
| .27228 | 1.08560 | 2.90538 | .77053 | .00080 |
| .31897 | 1.14520 | 2.90538 | .87053 | .00080 |
| .28844 | 1.15080 | 2.90538 | .97053 | .00080 |
| .09430 | .83240 | 2.19822 | .56640 | .00630 |
| .12193 | .83280 | 2.19822 | .66640 | .00630 |
| .12193 | .83280 | 2.19822 | .74973 | .00630 |
| .18669 | .84480 | 2.19822 | .84973 | .00630 |
| .20542 | .85840 | 2.19822 | .94973 | .00630 |
| .12866 | 1.02280 | 2.95040 | .96640 | .00630 |
| .13475 | 1.01240 | 2.90538 | .64973 | .00630 |
| .13475 | 1.01280 | 2.90538 | .74973 | .00630 |
| .13475 | 1.01280 | 2.90538 | .84973 | .00630 |
| .14355 | 1.01440 | 2.90538 | .84973 | .00630 |
| .17691 | 1.01440 | 2.90538 | .94973 | .00630 |

Table F.5 Data, Type 2, Pipe Grates

| $C_e$ | $\frac{HW}{D}$ | $\frac{Q}{BD^{1.5}}$ | $\frac{TW}{D}$ | $S_o$ |
|---|---|---|---|---|
| .20838 | 1.14588 | 3.28285 | .85333 | .00130 |
| .26170 | 1.17468 | 3.34618 | .80333 | .00130 |
| .32726 | .87428 | 2.83462 | .77833 | .00130 |
| .07381 | .91548 | 2.41140 | .60333 | .00130 |
| .24190 | 1.09988 | 3.03974 | .88667 | .00130 |
| .48605 | 1.00528 | 2.19822 | .97053 | .00080 |
| .19532 | .90724 | 2.19822 | .58724 | .00080 |
| .27981 | 1.05724 | 2.23144 | .93720 | .00080 |
| .22749 | .95528 | 2.23144 | .80387 | .00080 |
| .19465 | .91768 | 2.23144 | .72887 | .00080 |
| .26071 | .90120 | 2.28374 | .57053 | .00080 |
| .24238 | .98328 | 2.28374 | .67053 | .00080 |
| .26449 | .94448 | 2.28374 | .77053 | .00080 |
| .32997 | 1.00448 | 2.28374 | .87053 | .00080 |
| .38963 | 1.11448 | 2.28374 | .98720 | .00080 |
| .27149 | 1.00568 | 2.9 538 | .67053 | .00080 |
| .27228 | 1.00568 | 2.9 538 | .77053 | .00080 |
| .31897 | 1.10528 | 2.94538 | .87053 | .00080 |
| .28844 | 1.15088 | 2.94538 | .97053 | .00080 |
| .13671 | .82768 | 2.16516 | .53387 | .00630 |
| .13671 | .82768 | 2.16516 | .64973 | .00630 |
| .13015 | .82768 | 2.16516 | .74973 | .00630 |
| .23351 | .83448 | 2.16516 | .84973 | .00630 |
| .40724 | .92128 | 2.16516 | .94973 | .00630 |
| .15208 | 1.01488 | 2.94538 | .64973 | .00630 |
| .15208 | 1.01488 | 2.94538 | .74973 | .00630 |
| .15208 | 1.01488 | 2.94538 | .84973 | .00630 |
| .14583 | 1.01328 | 2.94538 | .93307 | .00630 |
| .13475 | 1.01248 | 2.94538 | .64973 | .00630 |
| .13475 | 1.01248 | 2.94538 | .74973 | .00630 |
| .13475 | 1.01248 | 2.94538 | .84973 | .00630 |
| .21563 | 1.17168 | 3.45477 | .74973 | .00630 |
| .21563 | 1.17168 | 3.45477 | .84973 | .00630 |
| .21563 | 1.17168 | 3.45477 | .94973 | .00630 |

Table F.6 Data, Type 2, Bar Grates

| $C_e$ | $\frac{HW}{D}$ | $\frac{Q}{BD^{1.5}}$ | $\frac{TW}{D}$ | $S_o$ |
|---|---|---|---|---|
| .36548 | 1.09640 | 2.89932 | .86220 | .00080 |
| .30316 | 1.08560 | 2.89932 | .78720 | .00080 |
| .30316 | 1.08560 | 2.89932 | .67053 | .00080 |
| .46473 | 1.15680 | 2.89932 | .96220 | .00080 |
| .28874 | .93800 | 2.31522 | .56220 | .00080 |
| .33451 | .93820 | 2.31522 | .67053 | .00080 |
| .30688 | .94720 | 2.31522 | .75387 | .00080 |
| .39303 | .98720 | 2.31522 | .83720 | .00080 |
| .50196 | 1.04640 | 2.31522 | .98720 | .00080 |
| .36862 | .72520 | 1.43377 | .57053 | .00080 |
| .52681 | .77260 | 1.43377 | .67053 | .00080 |
| .59044 | .79720 | 1.43377 | .77053 | .00080 |
| .81383 | .87380 | 1.43377 | .87053 | .00080 |
| .82784 | 1.02460 | 1.43377 | .97053 | .00080 |
| .23639 | .72460 | 1.43377 | .57053 | .00080 |
| .35799 | .74640 | 1.43377 | .65387 | .00080 |
| .17045 | .80240 | 2.19822 | .54973 | .00630 |
| .17045 | .80240 | 2.19822 | .64973 | .00630 |
| .17045 | .80240 | 2.19822 | .74973 | .00630 |
| .23184 | .85240 | 2.19822 | .84973 | .00630 |
| .15078 | .91080 | 2.19822 | .94973 | .00630 |
| .22636 | 1.02800 | 2.98538 | .64973 | .00630 |
| .22636 | 1.02800 | 2.98538 | .74973 | .00630 |
| .22636 | 1.02800 | 2.98538 | .84973 | .00630 |
| .23145 | 1.02840 | 2.98538 | .94973 | .00630 |

Table F.7 Data, Type 3A, No Grates

| $C_e$ | $\frac{HW}{D}$ | $\frac{Q}{BD^{1.5}}$ | $\frac{TW}{D}$ | $S_o$ |
|---|---|---|---|---|
| .8086 | .884[illegible] | 2.42851 | [illegible] | .01280 |
| .7949 | .866[illegible] | 2.37731 | [illegible] | .01280 |
| .0894 | .53240 | 1.18305 | 0.00000 | .01280 |
| .10840 | .91880 | 2.56682 | 0.00000 | .01280 |
| .15544 | 1.34630 | 3.67539 | 0.00000 | .01280 |
| .14083 | 1.08560 | 3.20738 | 0.00000 | .01280 |
| .16277 | 1.1212[illegible] | 3.31447 | [illegible] | .01280 |
| .04854 | .73[illegible] | 1.88454 | [illegible] | .01280 |
| .03124 | .61363 | 1.49163 | 0.00000 | .01280 |
| .03784 | .69[illegible] | 1.77152 | 0.00000 | .01280 |
| .10514 | 1.47[illegible] | 4.[illegible]4853 | 0.00000 | .01280 |
| .12542 | 1.[illegible] | 2.92966 | 0.00000 | .01280 |
| .05514 | .79411 | 2.12681 | 0.00000 | .01280 |
| .19753 | 1.54632 | 4.19154 | 0.00000 | .01280 |
| .09371 | .96183 | 2.67222 | 0.00000 | .01280 |
| .11166 | 1.[illegible]443 | 3.85380 | [illegible] | .01280 |
| .09568 | 1.[illegible]96[illegible] | 2.98453 | [illegible] | .01280 |
| .06210 | .52161 | 1.13398 | 0.00000 | .01080 |
| .14779 | .59443 | 1.31570 | [illegible] | .01080 |
| .02944 | .62563 | 1.56621 | [illegible] | .01080 |
| .08769 | .[illegible]924[illegible] | 1.7[illegible]512 | [illegible] | .01080 |
| .12658 | .75[illegible]6 | 1.91289 | [illegible] | .01080 |
| .09694 | .8[illegible]40[illegible] | 2.12681 | [illegible] | .01080 |
| .11271 | .8[illegible]8[illegible] | 2.34942 | [illegible] | .01080 |
| .15605 | .93529 | 2.57847 | 0.00000 | .01080 |
| .18752 | .99720 | 2.[illegible]1493 | [illegible] | .01080 |
| .21298 | 1.[illegible]6488 | 3.[illegible]5822 | [illegible] | .01080 |
| .16669 | 1.11[illegible] | 3.[illegible]3814 | [illegible] | .01080 |
| .15539 | 1.25922 | 3.56451 | 0.00000 | .01080 |
| .14263 | 1.39[illegible]4[illegible] | 3.82719 | [illegible] | .01080 |
| .16750 | 1.55128 | 4.18469 | [illegible] | .01080 |
| .19421 | .47680 | .93645 | 0.00000 | .01080 |
| .14982 | .8372[illegible] | 2.19822 | [illegible] | .01080 |
| .18508 | 1.[illegible]1368 | 2.90538 | [illegible] | .01080 |
| .20421 | 1.17328 | 3.45477 | [illegible] | .01080 |
| .18646 | 1.52643 | 4.22583 | [illegible] | .01080 |

Table F.8 Data, Type 3A, Pipe Grates

| $C_e$ | $\frac{HW}{D}$ | $\frac{Q}{BD^{1.5}}$ | $\frac{TW}{D}$ | $S_o$ |
|---|---|---|---|---|
| .6127 | .87763 | 2.42851 | .92944 | .01280 |
| .8725 | .86843 | 2.37731 | .89438 | .01280 |
| .1473 | .53368 | 1.18305 | .00000 | .01280 |
| .9126 | .91400 | 2.56682 | .00000 | .01280 |
| .9158 | 1.33683 | 3.67539 | .77770 | .01280 |
| .6439 | 1.08924 | 3.23738 | .00000 | .01280 |
| .5721 | 1.12764 | 3.31447 | .00000 | .01280 |
| .6986 | .73427 | 1.98354 | .00000 | .01280 |
| .2668 | .61483 | 1.69163 | .00000 | .01280 |
| .3784 | .69923 | 1.77152 | .00000 | .01280 |
| .0808 | 1.15166 | 4.04853 | .00000 | .01280 |
| .6241 | .99800 | 2.92966 | .00000 | .01280 |
| .5266 | .79600 | 2.12681 | .00000 | .01280 |
| .9556 | 1.53623 | 4.19154 | .00000 | .01280 |
| .0653 | .96562 | 2.67222 | .00000 | .01280 |
| .4395 | 1.37528 | 3.85380 | .00000 | .01280 |
| .2544 | 1.21348 | 2.98453 | .00000 | .01280 |
| .6446 | .52200 | 1.13398 | .00000 | .01480 |
| .5197 | .59520 | 1.31579 | .00000 | .01480 |
| .3313 | .62600 | 1.50621 | .00000 | .01480 |
| .2168 | .69563 | 1.78512 | .00000 | .01480 |
| .3666 | .75840 | 1.91249 | .00000 | .01480 |
| .1955 | .81700 | 2.12681 | .00000 | .01480 |
| .2447 | .86522 | 2.34952 | .00000 | .01480 |
| .6459 | .93400 | 2.57847 | .00000 | .01480 |
| .9683 | .99720 | 2.81493 | .00000 | .01480 |
| .2224 | 1.06180 | 3.05822 | .00000 | .01480 |
| .7451 | 1.12200 | 3.30814 | .00000 | .01480 |
| .9341 | 1.24400 | 3.56451 | .00000 | .01480 |
| .5343 | 1.34760 | 3.82719 | .00000 | .01480 |
| .2443 | 1.51800 | 4.18469 | .00000 | .01480 |
| .2617 | .47841 | .93645 | .00000 | .01480 |

Table F.9 Data, Type 3A, Bar Grates

| $C_e$ | $\frac{HW}{D}$ | $\frac{Q}{BD^{1.5}}$ | $\frac{TW}{D}$ | $S_o$ |
|---|---|---|---|---|
| .16332 | .59680 | 1.33437 | .00000 | .00630 |
| .15650 | .66320 | 1.54533 | .00000 | .00630 |
| .18792 | .72560 | 1.75612 | .00000 | .00630 |
| .16488 | .77840 | 1.96505 | .00000 | .00630 |
| .23032 | .85240 | 2.18167 | .00000 | .00630 |
| .22843 | .90920 | 2.40571 | .00000 | .00630 |
| .29821 | .96360 | 2.63693 | .00000 | .00630 |
| .26250 | 1.03240 | 2.87512 | .00000 | .00630 |
| .31595 | 1.10720 | 3.12008 | .00000 | .00630 |
| .27561 | 1.18920 | 3.35893 | .00000 | .00630 |
| .25343 | 1.37840 | 3.67539 | .00000 | .00630 |
| .24684 | 1.45480 | 3.88714 | .00000 | .00630 |
| .29583 | 1.58480 | 4.17101 | .00000 | .00630 |
| .08259 | .51080 | 1.16751 | .00000 | .01080 |
| .13408 | .58320 | 1.28787 | .00000 | .01080 |
| .12320 | .63760 | 1.47709 | .00000 | .01080 |
| .13433 | .69320 | 1.67476 | .00000 | .01080 |
| .16287 | .75480 | 1.88854 | .00000 | .01080 |
| .14293 | .80840 | 2.09412 | .00000 | .01080 |
| .13672 | .86840 | 2.31522 | .00000 | .01080 |
| .17955 | .92880 | 2.54369 | .00000 | .01080 |
| .18549 | .98040 | 2.77752 | .00000 | .01080 |
| .22631 | 1.04040 | 3.02130 | .00000 | .01080 |
| .21574 | 1.10880 | 3.27623 | .00000 | .01080 |
| .19477 | 1.25760 | 3.52565 | .00000 | .01080 |
| .17489 | 1.37960 | 3.78739 | .00000 | .01080 |
| .23512 | 1.49960 | 3.98776 | .00000 | .01080 |
| .22956 | 1.55240 | 4.22524 | .00000 | .01080 |

Table F.10 Data, Type 4A, No Grates

| $C_e$ | $\frac{HW}{D}$ | $\frac{Q}{BD^{1.5}}$ | $\frac{TW}{D}$ | $S_o$ |
|---|---|---|---|---|
| .80546 | 1.53320 | 3.92729 | 1.17053 | .00080 |
| .80715 | 1.66160 | 3.92729 | 1.27053 | .00080 |
| .82727 | 1.77840 | 3.92729 | 1.37053 | .00080 |
| .85734 | 1.84960 | 3.92729 | 1.45387 | .00080 |
| .88369 | 1.93280 | 3.92729 | 1.55387 | .00080 |
| .89242 | 2.05400 | 3.92729 | 1.65387 | .00080 |
| .88400 | 2.22200 | 3.92729 | 1.78720 | .00080 |
| .89581 | 2.29280 | 3.92729 | 1.87053 | .00080 |
| .47458 | 1.19200 | 2.20374 | 1.07053 | .00080 |
| .68675 | 1.29600 | 2.20374 | 1.18720 | .00080 |
| .95727 | 1.42840 | 2.20374 | 1.32853 | .00080 |
| .88894 | 1.48320 | 2.20374 | 1.39587 | .00080 |
| .75059 | 1.59080 | 2.20374 | 1.53720 | .00080 |
| .61799 | 1.67680 | 2.20374 | 1.55387 | .00080 |
| .95215 | 1.77400 | 2.20374 | 1.65387 | .00080 |
| .83548 | 1.91320 | 2.20374 | 1.77853 | .00080 |
| .55941 | 1.28520 | 2.90538 | 1.07053 | .00080 |
| .51652 | 1.33960 | 2.90538 | 1.17053 | .00080 |
| .66328 | 1.45280 | 2.90538 | 1.27053 | .00080 |
| .67244 | 1.58280 | 2.90538 | 1.37053 | .00080 |
| .67854 | 1.67880 | 2.90538 | 1.47053 | .00080 |
| .86775 | 1.74360 | 2.90538 | 1.57053 | .00080 |
| .88993 | 1.87600 | 2.90538 | 1.67053 | .00080 |
| .67542 | 1.99240 | 2.90538 | 1.77053 | .00080 |
| .83276 | 1.48560 | 3.92729 | 1.08720 | .00080 |
| .36521 | 1.02320 | 2.19822 | 1.04973 | .00630 |
| .38131 | 1.08280 | 2.19822 | 1.14973 | .00630 |
| .57775 | 1.20280 | 2.19822 | 1.24973 | .00630 |
| .49276 | 1.36840 | 2.19822 | 1.34973 | .00630 |
| .27410 | 1.41960 | 2.19822 | 1.44973 | .00630 |
| .64191 | 1.52160 | 2.19822 | 1.54973 | .00630 |
| .78061 | 1.62240 | 2.19822 | 1.64973 | .00630 |
| .49800 | 1.66680 | 2.19822 | 1.74973 | .00630 |
| .28611 | 1.58880 | 4.22583 | 1.04973 | .00630 |
| .64712 | 1.47560 | 4.22583 | 1.13307 | .00630 |
| .89122 | 1.52480 | 4.22583 | 1.23307 | .00630 |
| .79025 | 1.63680 | 4.22583 | 1.34973 | .00630 |
| .82775 | 1.71520 | 4.22583 | 1.39973 | .00630 |
| .76859 | 1.79280 | 4.22583 | 1.49973 | .00630 |
| .83922 | 1.91840 | 4.22583 | 1.61640 | .00630 |
| .79011 | 2.05080 | 4.22583 | 1.73307 | .00630 |
| .28760 | 1.07960 | 2.95400 | 1.04973 | .00630 |
| .76226 | 1.25120 | 2.95400 | 1.14973 | .00630 |
| .33727 | 1.26760 | 2.95400 | 1.24973 | .00630 |
| .49964 | 1.38160 | 2.95400 | 1.34973 | .00630 |
| .38230 | 1.48080 | 2.95400 | 1.44973 | .00630 |
| .69743 | 1.61640 | 2.95400 | 1.54973 | .00630 |
| .62941 | 1.72520 | 2.95400 | 1.64973 | .00630 |
| .66495 | 1.78480 | 2.95400 | 1.74973 | .00630 |

Table F.10 Data, Type 4A, No Grates

| $C_e$ | $\frac{HW}{D}$ | $\frac{Q}{BD^{1.5}}$ | $\frac{TW}{D}$ | $S_o$ |
|---|---|---|---|---|
| .17832 | 1.20[illegible] | 3.45477 | 1.04973 | .00630 |
| .56866 | 1.26120 | 3.45477 | 1.14973 | .00630 |
| .69708 | 1.38040 | 3.45477 | 1.24973 | .00630 |
| .65535 | 1.47120 | 3.45477 | 1.34973 | .00630 |
| .74180 | 1.58720 | 3.45477 | 1.44973 | .00630 |
| .62517 | 1.66760 | 3.45477 | 1.54973 | .00630 |
| .77634 | 1.79760 | 3.45477 | 1.64973 | .00630 |
| .67920 | 1.86760 | 3.45477 | 1.74973 | .00630 |
| .21896 | 1.00000 | 2.90538 | 1.04973 | .00630 |
| .60462 | 1.26920 | 2.19822 | 1.30413 | .01080 |
| .59395 | 1.37240 | 2.19822 | 1.40413 | .01080 |
| .56197 | 1.49000 | 2.19822 | 1.50413 | .01080 |
| .59794 | 1.34640 | 2.90659 | 1.30413 | .01080 |
| .61618 | 1.45180 | 2.90659 | 1.40413 | .01080 |
| .94549 | 1.62240 | 2.90659 | 1.50413 | .01080 |
| .80832 | 1.66600 | 2.90659 | 1.60413 | .01080 |
| .72824 | 1.47400 | 3.41632 | 1.30413 | .01080 |
| .78802 | 1.55520 | 3.39714 | 1.40413 | .01080 |
| .85772 | 1.66720 | 3.38438 | 1.50413 | .01080 |
| .77005 | 1.78160 | 3.38438 | 1.60413 | .01080 |
| .86450 | 1.87440 | 3.38438 | 1.70413 | .01080 |
| .87799 | 1.96480 | 3.38438 | 1.80413 | .01080 |
| .79350 | 1.63560 | 4.17101 | 1.30413 | .01080 |
| .77827 | 1.72920 | 4.17101 | 1.40413 | .01080 |
| .93716 | 1.82680 | 4.10962 | 1.50413 | .01080 |
| .88988 | 1.93440 | 4.10962 | 1.60413 | .01080 |
| .87632 | 2.01260 | 3.85380 | 1.62833 | .00130 |
| .67694 | 1.66920 | 4.00798 | 1.28667 | .00130 |
| .79469 | 2.14920 | 4.15531 | 1.72833 | .00130 |
| .78136 | 1.87260 | 4.21210 | 1.44500 | .00130 |
| .43419 | 1.75620 | 1.77666 | 1.71200 | .00130 |
| .50993 | 1.59220 | 3.20112 | 1.38667 | .00130 |
| .62936 | 1.83300 | 3.42912 | 1.59500 | .00130 |
| .68016 | 1.70980 | 3.33349 | 1.51167 | .00130 |
| .40118 | 2.00260 | 1.90911 | 1.98667 | .00130 |
| .56799 | 1.76620 | 2.36598 | 1.60333 | .00130 |
| .55160 | 1.80380 | 2.54360 | 1.75333 | .00130 |
| .55266 | 1.54020 | 3.00903 | 1.37000 | .00130 |
| .78422 | 1.77640 | 2.39433 | 1.92053 | .01280 |
| .56860 | 1.39280 | 2.34962 | 1.55387 | .01280 |
| .50995 | 1.33520 | 1.16066 | 1.58720 | .01280 |
| .44370 | 1.27640 | 2.55520 | 1.42053 | .01280 |
| .72586 | 1.57360 | 3.67539 | 1.53720 | .01280 |
| .15430 | 1.12120 | 3.31447 | 1.55387 | .01280 |
| .71265 | 1.51800 | 3.27023 | 1.55387 | .01280 |
| .81824 | 1.74880 | 1.79728 | 1.95387 | .01280 |
| .63025 | 1.61920 | 1.70512 | 1.83720 | .01280 |
| .83220 | 1.87200 | 3.98776 | 1.74553 | .01280 |
| .56283 | 1.39960 | 2.89932 | 1.46220 | .01280 |
| .76837 | 1.97600 | 4.19154 | 1.80387 | .01280 |
| .85353 | 2.02240 | 2.65456 | 2.12053 | .01280 |

Table F.11 Data, Type 4A, Pipe Grates

| $C_e$ | $\frac{HW}{D}$ | $\frac{Q}{BD^{1.5}}$ | $\frac{TW}{D}$ | $S_o$ |
|---|---|---|---|---|
| .76182 | 1.95.28 | 3.[illegible]538[illegible] | 1.62835 | .00130 |
| .65288 | 1.62228 | 4.[illegible]4798 | 1.28667 | .00130 |
| .48287 | 2.88868 | 4.45531 | 1.72833 | .00130 |
| .78410 | 1.87148 | 4.21214 | 1.46167 | .00130 |
| .22989 | 1.75628 | 1.77066 | 1.71167 | .00130 |
| .58805 | 1.64308 | 3.28112 | 1.39588 | .00130 |
| .55518 | 1.83348 | 3.42912 | 1.58667 | .00130 |
| .48754 | 1.73468 | 3.33349 | 1.52988 | .00130 |
| .00156 | 2.04268 | 1.94911 | 1.98667 | .00130 |
| .56799 | 1.70628 | 2.36598 | 1.64333 | .00130 |
| .55168 | 1.88388 | 2.54368 | 1.75333 | .00130 |
| .32126 | 1.53188 | 3.00993 | 1.37488 | .00130 |
| .57245 | 1.22488 | 2.19822 | 1.07453 | .00080 |
| .23678 | 1.25368 | 2.19822 | 1.17453 | .00080 |
| .58862 | 1.37648 | 2.19822 | 1.27453 | .00080 |
| .53531 | 1.47638 | 2.19822 | 1.37453 | .00080 |
| .81785 | 1.61728 | 2.19822 | 1.47453 | .00080 |
| .12282 | 1.74488 | 2.19822 | 1.57453 | .00080 |
| .74855 | 1.84488 | 2.19822 | 1.67453 | .00080 |
| .62861 | 1.89688 | 2.19822 | 1.77453 | .00080 |
| .42879 | 2.04628 | 2.19822 | 1.87453 | .00080 |
| .67393 | 2.09848 | 2.19822 | 1.97453 | .00080 |
| .46776 | 1.21128 | 2.93538 | 1.04387 | .00080 |
| .49837 | 1.32128 | 2.93538 | 1.14387 | .00080 |
| .66927 | 1.54768 | 2.93538 | 1.17453 | .00080 |
| .61714 | 1.44288 | 2.93538 | 1.25387 | .00080 |
| .88628 | 1.58288 | 2.93538 | 1.37453 | .00080 |
| .86477 | 1.68728 | 2.93538 | 1.47453 | .00080 |
| .86888 | 1.75968 | 2.93538 | 1.55387 | .00080 |
| .78844 | 1.87528 | 2.93538 | 1.67453 | .00080 |
| .67821 | 2.02488 | 2.93538 | 1.78728 | .00080 |
| .62942 | 2.06248 | 2.93538 | 1.85387 | .00080 |
| .55515 | 1.39968 | 3.73454 | 1.47453 | .00080 |
| .52922 | 1.53888 | 3.73454 | 1.18728 | .00080 |
| .59959 | 1.58528 | 3.73454 | 1.26228 | .00080 |
| .61795 | 1.71128 | 3.73454 | 1.36228 | .00080 |
| .77246 | 1.78568 | 3.59858 | 1.45387 | .00080 |
| .74246 | 1.94168 | 3.59858 | 1.60387 | .00080 |
| .76239 | 1.99768 | 3.59858 | 1.66228 | .00080 |
| .75247 | 2.09368 | 3.59858 | 1.75387 | .00080 |
| .75237 | 2.22268 | 3.59858 | 1.88728 | .00080 |
| .81243 | 2.32168 | 3.59858 | 1.95387 | .00080 |
| .68774 | 2.85298 | 4.22583 | 1.58728 | .00080 |
| .71668 | 2.11688 | 4.22583 | 1.67853 | .00080 |
| .47281 | 2.25688 | 4.22583 | 1.77953 | .00080 |
| .83779 | 1.72248 | 4.22583 | 1.27853 | .00080 |
| .86667 | 1.84848 | 4.22583 | 1.37453 | .00080 |
| .75116 | 1.95848 | 4.22583 | 1.47053 | .00080 |
| .84637 | 1.58488 | 4.22583 | 1.07053 | .00080 |
| .75858 | 1.65648 | 4.22583 | 1.17453 | .00080 |
| .80548 | 1.53328 | 3.92729 | 1.17053 | .00080 |
| .80715 | 1.66168 | 3.92729 | 1.27053 | .00080 |
| .82727 | 1.77848 | 3.92729 | 1.37053 | .00080 |
| .84734 | 1.84968 | 3.92729 | 1.45387 | .00080 |

Table F.11 Data, Type 4A, Pipe Grates

| $C_e$ | $\frac{HW}{D}$ | $\frac{Q}{BD^{1.5}}$ | $\frac{TW}{D}$ | $S_o$ |
|---|---|---|---|---|
| .89242 | 2,05400 | 3,92729 | 1,65387 | .00080 |
| .88400 | 2,02200 | 3,92729 | 1,78720 | .00080 |
| .89581 | 2,09280 | 3,92729 | 1,87453 | .00080 |
| .87458 | 1,99200 | 2,20374 | 1,87453 | .00080 |
| .88675 | 1,99600 | 2,20374 | 1,18720 | .00080 |
| .95727 | 1,92840 | 2,20374 | 1,32853 | .00080 |
| .80894 | 1,98320 | 2,20374 | 1,39587 | .00080 |
| .75959 | 1,59680 | 2,20374 | 1,53720 | .00080 |
| .61799 | 1,67680 | 2,20374 | 1,55387 | .00080 |
| .95215 | 1,77400 | 2,20374 | 1,65387 | .00080 |
| .83548 | 1,91320 | 2,20374 | 1,77853 | .00080 |
| .55941 | 1,28520 | 2,90538 | 1,47853 | .00080 |
| .51652 | 1,33960 | 2,90538 | 1,17853 | .00080 |
| .66328 | 1,45280 | 2,90538 | 1,27853 | .00080 |
| .67244 | 1,50320 | 2,90538 | 1,37453 | .00080 |
| .67854 | 1,67880 | 2,90538 | 1,47853 | .00080 |
| .86775 | 1,74360 | 2,90538 | 1,57453 | .00080 |
| .80993 | 1,87600 | 2,90538 | 1,67453 | .00080 |
| .67542 | 1,99200 | 2,90538 | 1,77853 | .00080 |
| .93748 | 1,51880 | 3,92729 | 1,07853 | .00080 |
| .83226 | 1,48560 | 3,92729 | 1,48720 | .00080 |
| .98374 | 1,98320 | 2,16516 | 1,03387 | .00630 |
| .89681 | 1,98320 | 2,16516 | 1,13387 | .00630 |
| .84576 | 1,22440 | 2,19822 | 1,24973 | .00630 |
| .37815 | 1,35720 | 2,19822 | 1,34973 | .00630 |
| .28447 | 1,39680 | 2,19822 | 1,44973 | .00630 |
| .59395 | 1,49800 | 2,19822 | 1,54973 | .00630 |
| .64193 | 1,60560 | 2,19822 | 1,64973 | .00630 |
| .58329 | 1,72920 | 2,19822 | 1,74973 | .00630 |
| .20416 | 1,10720 | 2,90538 | 1,06640 | .00630 |
| .53894 | 1,19920 | 2,90538 | 1,16640 | .00630 |
| .48293 | 1,28080 | 2,90538 | 1,24973 | .00630 |
| .54758 | 1,35800 | 2,90538 | 1,33387 | .00630 |
| .56552 | 1,47160 | 2,90538 | 1,43387 | .00630 |
| .55936 | 1,62880 | 2,90538 | 1,57473 | .00630 |
| .72726 | 1,72480 | 2,90538 | 1,64973 | .00630 |
| .65897 | 1,80280 | 2,90538 | 1,74973 | .00630 |
| .57652 | 1,54720 | 4,22583 | 1,14973 | .00630 |
| .66905 | 1,57720 | 4,22583 | 1,24973 | .00630 |
| .76418 | 1,67360 | 4,22583 | 1,34973 | .00630 |
| .81433 | 1,78640 | 4,22583 | 1,44973 | .00630 |
| .79159 | 1,85720 | 4,22583 | 1,54973 | .00630 |
| .68772 | 1,94840 | 4,22583 | 1,64973 | .00630 |
| .78870 | 2,06440 | 4,22583 | 1,74973 | .00630 |
| .22957 | 1,18880 | 3,45477 | 1,03387 | .00630 |
| .56727 | 1,26640 | 3,45477 | 1,13387 | .00630 |
| .51271 | 1,35080 | 3,45477 | 1,23387 | .00630 |
| .59924 | 1,45680 | 3,45477 | 1,33387 | .00630 |
| .63377 | 1,56720 | 3,45477 | 1,43387 | .00630 |
| .68341 | 1,72040 | 3,45477 | 1,58387 | .00630 |
| .75464 | 1,82960 | 3,45477 | 1,66643 | .00630 |

Table F.11 Data, Type 4A, Pipe Grates

| $C_e$ | $\frac{HW}{D}$ | $\frac{Q}{BD^{1.5}}$ | $\frac{TW}{D}$ | $S_o$ |
|---|---|---|---|---|
| .67[illegible] | 1.892[illegible] | 3.45477 | 1.74973 | .[illegible] |
| .[illegible]5637 | 1.2976[illegible] | 2.19822 | 1.30413 | .[illegible] |
| .66859 | 1.37[illegible] | 2.19822 | 1.40413 | .[illegible] |
| .73789 | 1.4872[illegible] | 2.19822 | 1.50413 | .[illegible] |
| .84976 | 1.59368 | 2.19822 | 1.60413 | .01080 |
| .67384 | 1.6044[illegible] | 2.19822 | 1.70413 | .01080 |
| .65794 | 1.7892[illegible] | 2.19822 | 1.80413 | .01080 |
| .61435 | 1.3564[illegible] | 2.98538 | 1.30413 | .01080 |
| .66[illegible]8 | 1.4724[illegible] | 2.9[illegible]538 | 1.40413 | .01080 |
| .74856 | 1.5686[illegible] | 2.98538 | 1.50413 | .01080 |
| .73347 | 1.674[illegible] | 2.98538 | 1.60413 | .01080 |
| .7[illegible]890 | 1.77[illegible] | 2.98538 | 1.70413 | .01080 |
| .47687 | 1.8664[illegible] | 2.98538 | 1.80413 | .01080 |
| .66184 | 1.4668[illegible] | 3.45477 | 1.30413 | .01080 |
| .64253 | 1.5632[illegible] | 3.45477 | 1.40413 | .01080 |
| .71867 | 1.6572[illegible] | 3.45477 | 1.5[illegible]413 | .01080 |
| .68353 | 1.7588[illegible] | 3.45477 | 1.60413 | .01080 |
| .64026 | 1.8458[illegible] | 3.45477 | 1.70413 | .01080 |
| .62299 | 1.9636[illegible] | 3.45477 | 1.80413 | .01080 |
| .85551 | 1.6416[illegible] | 4.22583 | 1.30413 | .01080 |
| .74[illegible]4 | 1.7[illegible]41 | 4.22583 | 1.4[illegible]413 | .01080 |
| .79741 | 1.8272[illegible] | 4.22583 | 1.52413 | .01080 |
| .78[illegible]1[illegible] | 1.95[illegible]4[illegible] | 4.22583 | 1.60413 | .01080 |

Table F.12 Data, Type 4A, Bar Grates

| $C_e$ | $\frac{HW}{D}$ | $\frac{Q}{BD^{1.5}}$ | $\frac{TW}{D}$ | $S_o$ |
|---|---|---|---|---|
| 1,[illegible] | 1,[illegible] | 3,92729 | 1,05387 | ,00000 |
| ,92743 | 1,61200 | 3,92729 | 1,17887 | ,00000 |
| ,89233 | 1,67000 | 3,92729 | 1,27053 | ,00000 |
| ,94086 | 1,79760 | 3,92729 | 1,37053 | ,00000 |
| ,91748 | 1,92000 | 3,92729 | 1,47053 | ,00000 |
| ,84225 | 2,04000 | 3,92729 | 1,58720 | ,00000 |
| ,89397 | 2,09800 | 3,92729 | 1,67053 | ,00000 |
| ,94577 | 2,25400 | 3,92729 | 1,77053 | ,00000 |
| ,58126 | 1,29520 | 2,89932 | 1,08720 | ,00000 |
| ,58125 | 1,39520 | 2,89932 | 1,18720 | ,00000 |
| ,65173 | 1,50040 | 2,89932 | 1,28720 | ,00000 |
| ,72847 | 1,58040 | 2,89932 | 1,35387 | ,00000 |
| ,73142 | 1,67400 | 2,89932 | 1,45387 | ,00000 |
| ,66093 | 1,78160 | 2,89932 | 1,56220 | ,00000 |
| ,71618 | 1,97680 | 2,89932 | 1,75387 | ,00000 |
| ,92142 | 2,20360 | 2,89932 | 1,97053 | ,00000 |
| ,49440 | 1,23120 | 2,31522 | 1,08720 | ,00000 |
| ,63403 | 1,28680 | 2,31522 | 1,15387 | ,00000 |
| ,79768 | 1,40040 | 2,31522 | 1,25387 | ,00000 |
| ,66767 | 1,52960 | 2,31522 | 1,38720 | ,00000 |
| ,79735 | 1,63840 | 2,31522 | 1,48720 | ,00000 |
| ,66758 | 1,74360 | 2,31522 | 1,58720 | ,00000 |
| ,74438 | 1,91600 | 2,31522 | 1,77053 | ,00000 |
| 1,87609 | 2,14160 | 2,31522 | 1,97053 | ,00000 |
| ,27299 | 1,06840 | 2,19822 | 1,14973 | ,00630 |
| ,31674 | 1,12520 | 2,19822 | 1,24973 | ,00630 |
| ,38072 | 1,29000 | 2,19822 | 1,34973 | ,00630 |
| ,59395 | 1,39400 | 2,19822 | 1,44973 | ,00630 |
| ,60985 | 1,49720 | 2,19822 | 1,54973 | ,00630 |
| ,96159 | 1,65960 | 2,19822 | 1,64973 | ,00630 |
| ,44469 | 1,68680 | 2,19822 | 1,74973 | ,00630 |
| ,66201 | 1,45720 | 4,22583 | 1,14973 | ,00630 |
| ,58359 | 1,63760 | 4,22583 | 1,24973 | ,00630 |
| ,84776 | 1,72080 | 4,22583 | 1,34973 | ,00630 |
| ,85078 | 1,79160 | 4,22583 | 1,44973 | ,00630 |
| ,84640 | 1,88440 | 4,22583 | 1,54973 | ,00630 |
| ,75268 | 1,97240 | 4,22583 | 1,64973 | ,00630 |
| ,79449 | 2,08880 | 4,22583 | 1,74973 | ,00630 |
| ,64943 | 1,26760 | 3,45477 | 1,14973 | ,00630 |
| ,71159 | 1,39360 | 3,45477 | 1,24973 | ,00630 |
| ,71378 | 1,49200 | 3,45477 | 1,34973 | ,00630 |
| ,73089 | 1,62920 | 3,45477 | 1,44973 | ,00630 |
| ,69648 | 1,78280 | 3,45477 | 1,54973 | ,00630 |
| ,62985 | 1,78640 | 3,45477 | 1,64973 | ,00630 |
| ,66619 | 1,98320 | 3,45477 | 1,74973 | ,00630 |
| ,61421 | 1,21200 | 2,90538 | 1,14973 | ,00630 |
| ,56247 | 1,31120 | 2,90538 | 1,24973 | ,00630 |
| ,78906 | 1,42040 | 2,90538 | 1,34973 | ,00630 |
| ,72432 | 1,50240 | 2,90538 | 1,44973 | ,00630 |
| ,83113 | 1,63640 | 2,90538 | 1,54973 | ,00630 |
| ,42373 | 1,09920 | 2,90538 | 1,64973 | ,00630 |

Table F.12 Data, Type 4A, Bar Grates

| $C_e$ | $\frac{HW}{D}$ | $\frac{Q}{BD^{1.5}}$ | $\frac{TW}{D}$ | $S_o$ |
|---|---|---|---|---|
| .75472 | 1.84040 | 2.96538 | 1.74973 | .00630 |
| .21318 | 1.58880 | 4.28089 | 1.14973 | .00630 |
| .61754 | 1.63640 | 4.28089 | 1.24973 | .00630 |
| .81753 | 1.69560 | 4.28089 | 1.36640 | .00630 |
| .85689 | 1.78680 | 4.28089 | 1.44973 | .00630 |
| .81201 | 1.90800 | 4.28089 | 1.58307 | .00630 |
| .82458 | 2.09760 | 4.28089 | 1.65800 | .00630 |
| .87662 | 2.11400 | 4.28089 | 1.74173 | .00630 |
| .74836 | 1.29400 | 2.19822 | 1.30413 | .01080 |
| .53524 | 1.37800 | 2.19822 | 1.40413 | .01080 |
| .87135 | 1.49120 | 2.19822 | 1.50413 | .01080 |
| .76987 | 1.57760 | 2.19822 | 1.60413 | .01080 |
| .34322 | 1.69160 | 2.19822 | 1.70413 | .01080 |
| .85536 | 1.81200 | 2.19822 | 1.80413 | .01080 |
| .64757 | 1.28840 | 2.19822 | 1.30413 | .01080 |
| .45536 | 1.39000 | 2.19822 | 1.40413 | .01080 |
| .72434 | 1.49280 | 2.96538 | 1.30413 | .01080 |
| .81655 | 1.48600 | 2.86305 | 1.40413 | .01080 |
| .79141 | 1.58080 | 2.86305 | 1.50413 | .01080 |
| .88881 | 1.69520 | 2.86305 | 1.60413 | .01080 |
| .78998 | 1.78280 | 2.83896 | 1.70413 | .01080 |
| .73565 | 1.88000 | 2.83896 | 1.80413 | .01080 |
| .84460 | 1.48640 | 3.37163 | 1.30413 | .01080 |
| .82438 | 1.59360 | 3.33349 | 1.40413 | .01080 |
| .92882 | 1.69160 | 3.33349 | 1.50413 | .01080 |
| 1.00063 | 1.77320 | 3.33349 | 1.60413 | .01080 |
| .84297 | 1.87280 | 3.33349 | 1.70413 | .01080 |
| .85452 | 1.97480 | 3.33349 | 1.80413 | .01080 |
| .87681 | 1.66360 | 4.22583 | 1.30413 | .01080 |
| .79885 | 1.74360 | 4.22583 | 1.40413 | .01080 |
| .82049 | 1.86560 | 4.22583 | 1.50413 | .01080 |
| .77283 | 1.93840 | 4.22583 | 1.60413 | .01080 |

Table F.13 Data, Type 4B, No Grates

| $C_e$ | $\frac{HW}{D}$ | $\frac{Q}{BD^{1.5}}$ | $\frac{TW}{D}$ | $S_o$ |
|---|---|---|---|---|
| .61703 | 1.38348 | 3.94741 | 0.00000 | .00130 |
| .33966 | 1.22188 | 3.51273 | 0.00000 | .00130 |
| .47977 | 1.36348 | 4.08798 | 0.00000 | .00130 |
| .68801 | 1.47748 | 4.26719 | 0.00000 | .00130 |
| .50524 | 1.42068 | 4.19154 | .00000 | .00130 |
| .33961 | 1.21748 | 3.49982 | 0.00000 | .00130 |
| .39250 | 1.21688 | 3.39714 | 0.00000 | .00080 |
| .23730 | 1.33888 | 3.67539 | 0.00000 | .00080 |
| .64757 | 1.39160 | 3.91389 | 0.00000 | .00080 |
| .26343 | 1.56960 | 4.15734 | .00000 | .00080 |
| .27399 | 1.57560 | 4.22583 | 0.00000 | .00080 |
| .46489 | 1.24360 | 3.44194 | 0.00000 | .00080 |
| .74966 | 1.41560 | 3.92729 | 0.00000 | .00080 |
| .71861 | 1.41160 | 3.92729 | .87053 | .00080 |
| .72544 | 1.41160 | 3.92729 | .97053 | .00080 |
| .71861 | 1.41160 | 3.92729 | .57053 | .00080 |
| .71861 | 1.41160 | 3.92729 | .67053 | .00080 |
| .71861 | 1.41160 | 3.92729 | .77053 | .00080 |
| .15362 | 1.25080 | 3.54506 | 0.00000 | .00630 |
| .20972 | 1.39960 | 3.76094 | 0.00000 | .00630 |
| .22668 | 1.49648 | 3.96757 | 0.00000 | .00630 |
| .21329 | 1.54360 | 4.08922 | 0.00000 | .00630 |
| .23863 | 1.55360 | 4.22583 | 0.00000 | .00630 |
| .23683 | 1.36520 | 3.67539 | 0.00000 | .00630 |
| .21789 | 1.45240 | 3.88714 | 0.00000 | .00630 |
| .27797 | 1.58480 | 4.17101 | 0.00000 | .00630 |
| .23440 | 1.58720 | 4.22583 | 0.00000 | .00630 |
| .20915 | 1.23480 | 3.45477 | 0.00000 | .00630 |
| .23440 | 1.58720 | 4.22583 | .54973 | .00630 |
| .23440 | 1.58720 | 4.22583 | .64973 | .00630 |
| .23471 | 1.60760 | 4.22583 | .74973 | .00630 |
| .24502 | 1.59620 | 4.22583 | .84973 | .00630 |
| .22361 | 1.59600 | 4.22583 | .94973 | .00630 |
| .20915 | 1.24480 | 3.45477 | .54973 | .00630 |
| .20915 | 1.24480 | 3.45477 | .64973 | .00630 |
| .20915 | 1.24480 | 3.45477 | .74973 | .00630 |
| .20915 | 1.24480 | 3.45477 | .84973 | .00630 |
| .20915 | 1.24480 | 3.45477 | .94973 | .00630 |
| .50156 | 1.25560 | 3.49337 | 0.00000 | .00080 |
| .23751 | 1.37480 | 3.73454 | 0.00003 | .00080 |
| .25017 | 1.50880 | 4.00124 | 0.00000 | .00080 |
| .25409 | 1.57840 | 4.19154 | 0.00000 | .00080 |

Table F.14 Data, Type 4B, Pipe Grates

| $C_e$ | $\frac{HW}{D}$ | $\frac{Q}{BD^{1.5}}$ | $\frac{TW}{D}$ | $S_o$ |
|---|---|---|---|---|
| .54185 | 1.36428 | 3.94741 | .00000 | .00130 |
| .56095 | 1.36708 | 3.93399 | .92000 | .00130 |
| .34992 | 1.22188 | 3.51273 | .00000 | .00130 |
| .46747 | 1.35988 | 4.00798 | .00000 | .00130 |
| .48106 | 1.35988 | 4.00798 | .92000 | .00130 |
| .59328 | 1.44868 | 4.26718 | .80333 | .00130 |
| .65387 | 1.46708 | 4.26718 | .00000 | .00130 |
| .53160 | 1.41468 | 4.19154 | .75333 | .00130 |
| .55255 | 1.42068 | 4.19154 | .00000 | .00130 |
| .39114 | 1.22468 | 3.49982 | .00000 | .00130 |
| .33111 | 1.21988 | 3.49982 | .80333 | .00130 |
| .38398 | 1.22488 | 3.39714 | .00000 | .00080 |
| .24893 | 1.33088 | 3.67539 | .00000 | .00080 |
| .61763 | 1.38963 | 3.91389 | .20000 | .00080 |
| .32343 | 1.55160 | 4.15734 | .00000 | .00080 |
| .32189 | 1.57963 | 4.22583 | .00000 | .00080 |
| .74292 | 1.51688 | 4.22583 | .97053 | .00080 |
| .57822 | 1.34088 | 3.74114 | .88720 | .00080 |
| .59096 | 1.34888 | 3.74114 | .82453 | .00080 |
| .59250 | 1.34288 | 3.74114 | .00000 | .00080 |
| .80840 | 1.49360 | 4.19154 | .92053 | .00080 |
| .75082 | 1.47760 | 4.19154 | .80387 | .00080 |
| .74234 | 1.47769 | 4.19154 | .70387 | .00080 |
| .47678 | 1.24880 | 3.44194 | .00000 | .00080 |
| .82173 | 1.43488 | 3.92729 | .00000 | .00080 |
| .82127 | 1.43288 | 3.92729 | .57053 | .00080 |
| .82127 | 1.43288 | 3.92729 | .67053 | .00080 |
| .82127 | 1.43288 | 3.92729 | .77053 | .00080 |
| .82598 | 1.43488 | 3.92729 | .87053 | .00080 |
| .71861 | 1.41168 | 3.92729 | .87053 | .00080 |
| .72544 | 1.41168 | 3.92729 | .97053 | .00080 |
| .71861 | 1.41168 | 3.92729 | .57053 | .00080 |
| .71861 | 1.41168 | 3.92729 | .67053 | .00080 |
| .71861 | 1.41168 | 3.92729 | .77053 | .00080 |
| .24584 | 1.27488 | 3.54586 | .00000 | .00630 |
| .26595 | 1.37888 | 3.76494 | .00000 | .00630 |
| .25541 | 1.47128 | 3.96757 | .00000 | .00630 |
| .26591 | 1.51728 | 4.08922 | .00000 | .00630 |
| .23863 | 1.55368 | 4.22583 | .00000 | .00630 |
| .25938 | 1.55248 | 4.22583 | .53307 | .00630 |
| .24267 | 1.55408 | 4.22583 | .66648 | .00630 |
| .23863 | 1.55368 | 4.22583 | .74973 | .00630 |
| .23863 | 1.55368 | 4.22583 | .84973 | .00630 |
| .23863 | 1.55368 | 4.22583 | .94973 | .00630 |

Table F.15 Data, Type 4B, Bar Grates

| $C_e$ | $\frac{HW}{D}$ | $\frac{Q}{BD^{1.5}}$ | $\frac{TW}{D}$ | $S_o$ |
|---|---|---|---|---|
| .27398 | 1.29160 | 3.49337 | 0.00000 | .00080 |
| .24937 | 1.39560 | 3.73454 | 0.00000 | .00080 |
| .28589 | 1.51760 | 4.00124 | 0.00000 | .00080 |
| .31517 | 1.58960 | 4.19154 | 0.00000 | .00080 |
| .25343 | 1.37840 | 3.67539 | 0.00000 | .00630 |
| .24684 | 1.45080 | 3.88714 | 0.00000 | .00630 |
| .29503 | 1.58480 | 4.17101 | 0.00000 | .00630 |
| .57723 | 1.43960 | 4.22583 | .54973 | .00630 |
| .57384 | 1.43960 | 4.22583 | .64973 | .00630 |
| .57228 | 1.43960 | 4.22583 | .74973 | .00630 |
| .57228 | 1.43960 | 4.22583 | .84973 | .00630 |
| .57362 | 1.43960 | 4.22583 | .94973 | .00630 |
| .21964 | 1.21760 | 3.45477 | .54973 | .00630 |
| .21964 | 1.21760 | 3.45477 | .64973 | .00630 |
| .22161 | 1.21280 | 3.45477 | .74973 | .00630 |
| .22161 | 1.21280 | 3.45477 | .84973 | .00630 |
| .22391 | 1.21280 | 3.45477 | .94973 | .00630 |
| .20120 | 1.60680 | 4.28089 | .54973 | .00630 |
| .22475 | 1.60680 | 4.28089 | .63347 | .00630 |
| .28885 | 1.60680 | 4.28089 | .74973 | .00630 |
| .24832 | 1.60680 | 4.28089 | .81640 | .00630 |
| .24183 | 1.60680 | 4.28089 | .94973 | .00630 |
| .57628 | 1.43960 | 4.22583 | 0.00000 | .00630 |
| .21964 | 1.21760 | 3.45477 | 0.00000 | .00630 |
| .24832 | 1.60680 | 4.28089 | 0.00000 | .00630 |

# APPENDIX G

## Data From Pipe Culver Experiments

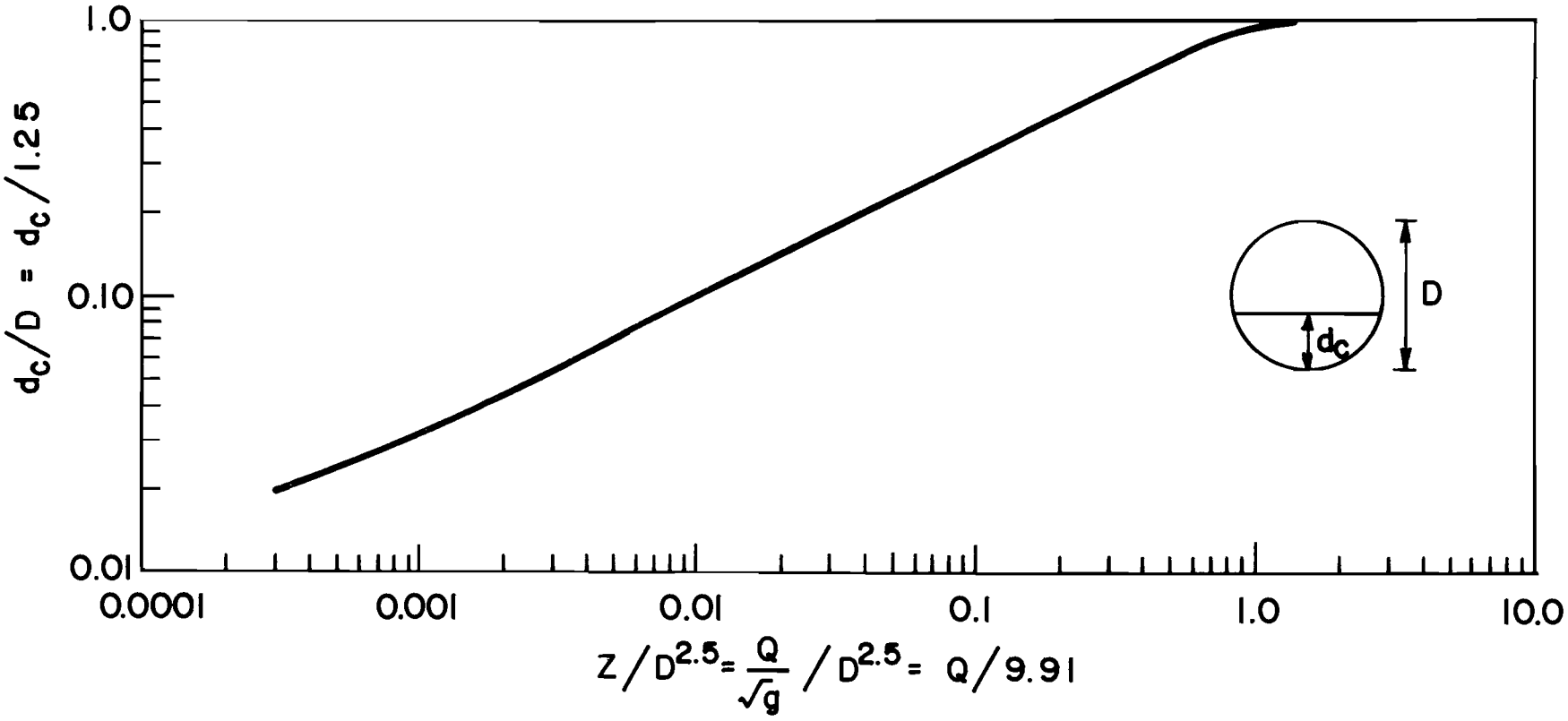


Figure G.1 Curve for Determining Critical Depth ($d_c$) in Pipe Culvert

Table G.1 Data for Pipe Culvert, Outlet Control, No Grates

| $C_e$ | $\frac{HW}{D}$ | $\frac{Q}{D^{2.5}}$ | $\frac{TW}{D}$ | $S_o$ |
|---|---|---|---|---|
| .47079 | 1.35529 | 2.50443 | 0.00000 | .00067 |
| .56778 | 1.41128 | 2.62332 | 0.00000 | .00067 |
| .70756 | 1.49528 | 2.74445 | 0.00000 | .00067 |
| .74843 | 1.64489 | 3.00248 | 0.00000 | .00067 |
| .80450 | 1.71498 | 3.15264 | 0.00000 | .00067 |
| .73566 | 1.78443 | 3.35959 | 0.00000 | .00067 |
| .83487 | 1.85489 | 3.41164 | 0.00000 | .00067 |
| .91260 | 1.95463 | 3.52599 | 0.00000 | .00067 |
| .91728 | 2.04688 | 3.65948 | 0.00000 | .00067 |
| 1.02190 | 2.19 | 3.80 | 0.00000 | .00067 |
| .99681 | 2.27 | 3.96813 | 0.00000 | .00067 |
| 1.08451 | 2.40 | 4.17223 | 0.00000 | .00067 |
| 1.07872 | 2.59563 | 4.37422 | 0.00000 | .00067 |
| 1.10727 | 2.74 | 4.49430 | 0.00000 | .00067 |
| .82743 | 1.78 | 3.17819 | 0.00000 | .00067 |
| .83383 | 1.73 | 3.17819 | .31533 | .00067 |
| .82755 | 1.77 | 3.17819 | .38200 | .00067 |
| .85118 | 1.73 | 3.17819 | .44867 | .00067 |
| .79418 | 1.77 | 3.17819 | .53200 | .00067 |
| .82113 | 1.73 | 3.17819 | .63200 | .00067 |
| .81454 | 1.75 | 3.17819 | .74067 | .00067 |
| .82391 | 1.77960 | 3.17819 | .82400 | .00067 |
| .83232 | 1.82243 | 3.17819 | .91533 | .00067 |
| .83725 | 1.86 | 3.17819 | .97100 | .00067 |
| .82988 | 1.94 | 3.17819 | 1.03200 | .00067 |
| .83133 | 2.02 | 3.17819 | 1.13200 | .00067 |
| .83894 | 2.11 | 3.17819 | 1.24867 | .00067 |
| .86326 | 2.19 | 3.17819 | 1.34867 | .00067 |
| .80471 | 2.27 | 3.17819 | 1.44867 | .00067 |
| .77569 | 2.34 | 3.17819 | 1.51533 | .00067 |
| .81189 | 2.40 | 3.17819 | 1.69967 | .00067 |
| .81975 | 2.45 | 3.17819 | 1.61533 | .00067 |
| .48870 | .72 | 1.15400 | 0.00000 | .00780 |
| .39456 | .77 | 1.31605 | 0.00000 | .00780 |
| .38654 | .83 | 1.47842 | 0.00000 | .00780 |
| .39898 | .87 | 1.63596 | 0.00000 | .00780 |
| .44852 | .95 | 1.79315 | 0.00000 | .00780 |
| .48792 | .98 | 1.91449 | 0.00000 | .00780 |
| .45617 | 1.04 | 2.06 | 0.00000 | .00780 |
| .46251 | 1.04 | 2.06 | .47533 | .00780 |
| .44795 | 1.05 | 2.06 | .57533 | .00780 |
| .44520 | 1.05 | 2.06 | .67533 | .00780 |
| .44477 | 1.07 | 2.06 | .77533 | .00780 |
| .34971 | 1.12 | 2.06 | .87533 | .00780 |
| .38961 | 1.17 | 2.06 | .97533 | .00780 |
| .53789 | 1.28 | 2.06 | 1.07533 | .00780 |
| .65375 | 1.39 | 2.06 | 1.17533 | .00780 |
| .63808 | 1.47 | 2.06 | 1.27533 | .00780 |
| .62981 | 1.57 | 2.06 | 1.37533 | .00780 |
| .58650 | 1.66 | 2.02374 | 1.47533 | .00780 |
| .59190 | 1.76 | 2.02374 | 1.57533 | .00780 |
| .54455 | 1.86 | 2.02374 | 1.67533 | .00780 |

Table G.1 Data for Pipe Culvert, Outlet Control, No Grates

| $C_e$ | $\frac{HW}{D}$ | $\frac{Q}{D^{2.5}}$ | $\frac{TW}{D}$ | $S_o$ |
|---|---|---|---|---|
| .79596 | 2.01484 | 2.11258 | 1.77533 | .00780 |
| .88348 | 2.11842 | 2.11258 | 1.87533 | .00780 |
| .48796 | 1.09368 | 2.17251 | .00000 | .00780 |
| .48725 | 1.13769 | 2.30937 | .04000 | .00780 |
| .55218 | 1.19844 | 2.45683 | .09000 | .00780 |
| .60266 | 1.25122 | 2.58335 | .00000 | .00780 |
| .59143 | 1.25208 | 2.58335 | .00000 | .00780 |
| .59143 | 1.25214 | 2.58335 | .47533 | .00780 |
| .59984 | 1.25247 | 2.58335 | .57533 | .00780 |
| .62191 | 1.25960 | 2.58335 | .67533 | .00780 |
| .61349 | 1.27883 | 2.58335 | .77533 | .00780 |
| .66811 | 1.31928 | 2.58335 | .87533 | .00780 |
| .74236 | 1.39449 | 2.58335 | .97533 | .00780 |
| .65859 | 1.48364 | 2.58335 | 1.07533 | .00780 |
| .92472 | 1.58884 | 2.58335 | 1.17533 | .00780 |
| .65498 | 1.67360 | 2.58335 | 1.27533 | .00780 |
| .76563 | 1.75855 | 2.55152 | 1.37533 | .00780 |
| .82796 | 1.86099 | 2.55152 | 1.47533 | .00780 |
| .77481 | 1.95968 | 2.55152 | 1.57533 | .00780 |
| .77295 | 2.07129 | 2.55152 | 1.67533 | .00780 |
| .75677 | 2.16761 | 2.55152 | 1.77533 | .00780 |
| .76563 | 2.26292 | 2.55152 | 1.87533 | .00780 |
| .67778 | 1.33767 | 2.71197 | .00000 | .00780 |
| .81759 | 1.39888 | 2.88391 | .00000 | .00780 |
| .91685 | 1.46881 | 2.97537 | .00000 | .00780 |
| .94133 | 1.52180 | 3.09314 | .00000 | .00780 |
| .94692 | 1.52681 | 3.09314 | .47533 | .00780 |
| .94958 | 1.52251 | 3.09314 | .57533 | .00780 |
| .99494 | 1.58642 | 3.13557 | .00000 | .00780 |
| .99494 | 1.58642 | 3.13557 | .47533 | .00780 |
| .98396 | 1.59128 | 3.13557 | .57533 | .00780 |
| .99454 | 1.63363 | 3.13557 | .67533 | .00780 |
| .98235 | 1.62562 | 3.13557 | .77533 | .00780 |
| .98871 | 1.66529 | 3.13557 | .87533 | .00780 |
| .99136 | 1.74986 | 3.13557 | .97533 | .00780 |
| .99462 | 1.83529 | 3.13557 | 1.07533 | .00780 |
| 1.00956 | 1.92124 | 3.13557 | 1.17533 | .00780 |
| .99651 | 1.99683 | 3.13557 | 1.27533 | .00780 |
| 1.00994 | 2.08529 | 3.13557 | 1.37533 | .00780 |
| 1.00178 | 2.19886 | 3.13557 | 1.47533 | .00780 |
| 1.01013 | 2.26482 | 3.13557 | 1.57533 | .00780 |
| 1.00481 | 2.39128 | 3.13557 | 1.67533 | .00780 |
| .98921 | 2.48284 | 3.13557 | 1.77533 | .00780 |
| .94778 | 2.55360 | 3.13557 | 1.87533 | .00780 |
| .91815 | 1.62329 | 3.27264 | .00000 | .00780 |
| .98208 | 1.72960 | 3.38543 | .00000 | .00780 |
| .98261 | 1.81129 | 3.54369 | .00000 | .00780 |
| 1.02536 | 1.93288 | 3.78435 | .00000 | .00780 |
| 1.03268 | 2.04600 | 3.87649 | .00000 | .00780 |
| 1.10325 | 2.15160 | 3.97733 | .00000 | .00780 |
| 1.13469 | 2.31888 | 4.17223 | .00000 | .00780 |
| 1.17431 | 2.42480 | 4.31334 | .00000 | .00780 |
| 1.15274 | 2.54000 | 4.42734 | .00000 | .00780 |
| 1.17387 | 2.62882 | 4.56159 | .00000 | .00780 |

Table G.2 Data for Pipe Culvert, Outlet Control, Pipe Grates

| $C_e$ | $\frac{HW}{D}$ | $\frac{Q}{D^{2.5}}$ | $\frac{TW}{D}$ | $S_o$ |
|---|---|---|---|---|
| .52566 | 1.37208 | 2.54483 | .00000 | .00067 |
| .60531 | 1.42833 | 2.62332 | .00000 | .00067 |
| .73391 | 1.51260 | 2.74445 | .00000 | .00067 |
| .81989 | 1.66608 | 3.00288 | .00000 | .00067 |
| .83486 | 1.74520 | 3.15268 | .00000 | .00067 |
| .76767 | 1.81483 | 3.35059 | .00000 | .00067 |
| .86319 | 1.88364 | 3.41164 | .00000 | .00067 |
| .93774 | 1.99[illegible] | 3.52599 | .00030 | .00067 |
| .96688 | 2.[illegible]128 | 3.65948 | .00083 | .00067 |
| 1.02788 | 2.22488 | 3.88283 | .00430 | .00067 |
| 1.01535 | 2.3[illegible]4 | 3.96813 | .00000 | .00067 |
| 1.1[illegible]27 | 2.48[illegible] | 4.17223 | .00078 | .00067 |
| 1.08262 | 2.[illegible]332 | 4.37022 | .00000 | .00067 |
| 1.12263 | 2.74[illegible] | 4.49430 | .00000 | .00067 |
| .89783 | 1.774[illegible] | 3.[illegible]7819 | .00000 | .00067 |
| .89783 | 1.774[illegible] | 3.17819 | .01533 | .00067 |
| .89783 | 1.774[illegible] | 3.17819 | .06533 | .00067 |
| .92982 | 1.774[illegible] | 3.17819 | .54867 | .00067 |
| .93046 | 1.7756[illegible] | 3.17819 | .61533 | .00067 |
| .90808 | 1.7856[illegible] | 3.17819 | .74867 | .00067 |
| .90877 | 1.8[illegible]8[illegible] | 3.17819 | .81533 | .00067 |
| .88723 | 1.8[illegible]4[illegible] | 3.17819 | .89867 | .00067 |
| .87387 | 1.8728[illegible] | 3.17819 | .96533 | .00067 |
| .93133 | 1.9264[illegible] | 3.17819 | 1.032[illegible] | .00067 |
| .9[illegible]852 | 1.9992[illegible] | 3.17819 | 1.14867 | .00067 |
| .9[illegible]223 | 2.1[illegible]6[illegible] | 3.17819 | 1.28233 | .00067 |
| .88666 | 2.18682 | 3.17819 | 1.35733 | .00067 |
| .84945 | 2.3372[illegible] | 3.17819 | 1.49867 | .00067 |
| .83764 | 2.4624[illegible] | 3.17819 | 1.61533 | .00067 |
| .93838 | 2.5876[illegible] | 3.17819 | 1.73200 | .00067 |
| .66319 | .7836[illegible] | 1.15400 | .00000 | .00780 |
| .55279 | .7938[illegible] | 1.31605 | .00083 | .00780 |
| .58933 | .8528[illegible] | 1.47842 | .00000 | .00780 |
| .55242 | .8948[illegible] | 1.66596 | .00000 | .00780 |
| .6[illegible]168 | .9716[illegible] | 1.79315 | .00000 | .00780 |
| .55267 | 1.[illegible]32[illegible] | 1.91449 | .00000 | .00780 |
| .71269 | 1.1116[illegible] | 2.11258 | .00000 | .00780 |
| .71269 | 1.1116[illegible] | 2.11258 | .47533 | .00780 |
| .69[illegible]32 | 1.1116[illegible] | 2.11258 | .57533 | .00780 |
| .7[illegible]632 | 1.1176[illegible] | 2.11258 | .67533 | .00780 |
| .72135 | 1.1316[illegible] | 2.11258 | .77533 | .00780 |
| .64879 | 1.1728[illegible] | 2.11258 | .87533 | .00780 |
| .59825 | 1.2492[illegible] | 2.17251 | .97533 | .00780 |
| .69808 | 1.3176[illegible] | 2.17251 | 1.07533 | .00780 |
| .74541 | 1.4148[illegible] | 2.17251 | 1.17533 | .00780 |
| .77955 | 1.5316[illegible] | 2.17251 | 1.27533 | .00780 |
| .74988 | 1.6188[illegible] | 2.17251 | 1.37533 | .00780 |
| .74706 | 1.7188[illegible] | 2.17251 | 1.47533 | .00780 |
| .67855 | 1.8236[illegible] | 2.17251 | 1.57533 | .00780 |
| .80262 | 1.9272[illegible] | 2.17251 | 1.67533 | .00780 |
| .74439 | 2.0292[illegible] | 2.17251 | 1.77533 | .00780 |
| .75344 | 2.1344[illegible] | 2.17251 | 1.87533 | .00780 |

Table G.2 Data for Pipe Culvert, Outlet Control, Pipe Grates

| $C_e$ | $\frac{HW}{D}$ | $\frac{Q}{D^{2.5}}$ | $\frac{TW}{D}$ | $S_o$ |
|---|---|---|---|---|
| .63216 | 1.11699 | 2.17251 | 0.00000 | .00780 |
| .65485 | 1.15849 | 2.30937 | 0.00000 | .00780 |
| .66737 | 1.21929 | 2.45683 | 0.00000 | .00780 |
| .68442 | 1.27089 | 2.58335 | 0.00000 | .00780 |
| .70340 | 1.27699 | 2.55152 | 0.00000 | .00780 |
| .71662 | 1.28889 | 2.55152 | .47533 | .00780 |
| .72437 | 1.28889 | 2.55152 | .57533 | .00780 |
| .73353 | 1.27689 | 2.55152 | .67533 | .00780 |
| .74173 | 1.29569 | 2.55152 | .77533 | .00780 |
| .77969 | 1.31569 | 2.55152 | .87533 | .00780 |
| .76888 | 1.38329 | 2.55152 | .97533 | .00780 |
| .78687 | 1.46249 | 2.55152 | 1.07533 | .00780 |
| .80247 | 1.55449 | 2.55152 | 1.17533 | .00780 |
| .77787 | 1.65489 | 2.55152 | 1.27533 | .00780 |
| .76690 | 1.74289 | 2.55152 | 1.37533 | .00780 |
| .75786 | 1.86209 | 2.55152 | 1.47533 | .00780 |
| .85559 | 1.95169 | 2.55152 | 1.57533 | .00780 |
| .81332 | 2.06569 | 2.55152 | 1.67533 | .00780 |
| .79523 | 2.17449 | 2.55152 | 1.77533 | .00780 |
| .74122 | 2.25889 | 2.55152 | 1.87533 | .00780 |
| .75986 | 1.35649 | 2.71197 | 0.00000 | .00780 |
| .87 69 | 1.43129 | 2.88391 | 0.00000 | .00780 |
| .94326 | 1.48169 | 2.97537 | 0.00000 | .00780 |
| .99573 | 1.63289 | 3.17819 | 0.00000 | .00780 |
| .99573 | 1.63289 | 3.17819 | .47533 | .00780 |
| .99573 | 1.63289 | 3.17819 | .57533 | .00780 |
| 1.00293 | 1.63169 | 3.17819 | .67533 | .00780 |
| 1.01577 | 1.65289 | 3.17819 | .77533 | .00780 |
| .98927 | 1.69289 | 3.17819 | .87533 | .00780 |
| .99937 | 1.75369 | 3.17819 | .97533 | .00780 |
| 1.01601 | 1.85969 | 3.17819 | 1.07533 | .00780 |
| 1.01932 | 1.89289 | 3.17819 | 1.17533 | .00780 |
| 1.00815 | 1.99769 | 3.17819 | 1.27533 | .00780 |
| 1.00447 | 2.08889 | 3.17819 | 1.37533 | .00780 |
| .98619 | 2.20329 | 3.17819 | 1.47533 | .00780 |
| .98337 | 2.29929 | 3.17819 | 1.57533 | .00780 |
| .98372 | 2.39529 | 3.17819 | 1.67533 | .00780 |
| .96551 | 2.48889 | 3.17819 | 1.77533 | .00780 |
| .95943 | 2.57889 | 3.17819 | 1.87533 | .00780 |
| .89382 | 1.63409 | 3.27264 | 0.00000 | .00780 |
| 1.02679 | 1.70409 | 3.38543 | 0.00000 | .00780 |
| .98111 | 1.83289 | 3.54369 | 0.00000 | .00780 |
| 1.02827 | 1.95649 | 3.70435 | 0.00000 | .00780 |
| 1.06200 | 2.08649 | 3.87649 | 0.00000 | .00780 |
| 1.13857 | 2.19889 | 3.97733 | 0.00000 | .00780 |
| 1.15291 | 2.30889 | 4.17223 | 0.00000 | .00780 |
| 1.14947 | 2.44969 | 4.31334 | 0.00000 | .00780 |
| 1.15894 | 2.55369 | 4.42734 | 0.00000 | .00780 |
| 1.19133 | 2.67409 | 4.56159 | 0.00000 | .00780 |

Table G.3 Data For Pipe Culvert, Inlet Control, No Grates

| $C_e$ | $\frac{HW}{D}$ | $\frac{Q}{D^{2.5}}$ | $\frac{TW}{D}$ | $S_o$ |
|---|---|---|---|---|
| .27496 | .76[illegible] | 1.33520 | 0.00000 | .05000 |
| .29618 | .78680 | 1.42577 | 0.00000 | .05000 |
| .30072 | .81560 | 1.53839 | 0.00000 | .05000 |
| .29310 | .84667 | 1.64696 | 0.00000 | .05000 |
| .29398 | .87320 | 1.76499 | 0.00000 | .05000 |
| .28071 | .90520 | 1.87136 | 0.00000 | .05000 |
| .28004 | .92560 | 1.99441 | 0.00000 | .05000 |
| .27296 | 1.[illegible]536[illegible] | 2.11900 | 0.00000 | .05000 |
| .26749 | 1.[illegible]824[illegible] | 2.63134 | 0.00000 | .05000 |
| .31951 | 1.16720 | 2.72008 | 0.00000 | .05000 |
| .38434 | 1.25240 | 2.87564 | 0.00000 | .05000 |
| .46898 | 1.33080 | 2.99210 | 0.00000 | .05000 |
| .48285 | 1.38880 | 3.13557 | 0.00000 | .05000 |
| .50350 | 1.44720 | 3.26401 | 0.00000 | .05000 |
| .50424 | 1.51480 | 3.37671 | 0.00000 | .05000 |
| .51405 | 1.55360 | 3.51715 | 0.00000 | .05000 |
| .59230 | 1.48560 | 3.65053 | 0.00000 | .05000 |
| .61606 | 1.54280 | 3.74940 | 0.00000 | .05000 |
| .59770 | 1.62360 | 3.95893 | 0.00000 | .05000 |
| .61343 | 1.61320 | 3.95893 | 0.00000 | .05000 |
| .63857 | 1.63640 | 3.95893 | 0.00000 | .05000 |
| .72196 | 1.78160 | 4.27556 | 0.00000 | .05000 |
| .36157 | 1.8[illegible]52[illegible] | 4.5[illegible]389 | 0.00000 | .05000 |
| .41840 | 1.88[illegible]40 | 4.63891 | 0.00000 | .05000 |
| .43888 | 1.94880 | 4.75569 | 0.00000 | .05000 |
| .40319 | 2.[illegible]0040 | 4.78564 | 0.00000 | .05000 |
| .28996 | 2.[illegible]0280 | 4.97228 | 0.00000 | .05000 |
| .33449 | 2.13160 | 5.[illegible]7179 | 0.00000 | .05000 |
| .26948 | 2.20680 | 5.18231 | 0.00000 | .05000 |
| .41865 | 2.31720 | 5.29302 | 0.00000 | .05000 |
| .86938 | 2.59720 | 5.48659 | 0.00000 | .05000 |

Table G.4 Data For Pipe Culvert, Inlet Control, Pipe Grates

| $C_e$ | $\frac{HW}{D}$ | $\frac{Q}{D^{2.5}}$ | $\frac{TW}{D}$ | $S_o$ |
|---|---|---|---|---|
| .37462 | .77[illegible] | 1.33524 | 0.00000 | .05000 |
| .37643 | .79888 | 1.42577 | 0.00000 | .05000 |
| .38349 | .82926 | 1.53839 | 0.00000 | .05000 |
| .39068 | .86040 | 1.64696 | 0.00000 | .05000 |
| .39584 | .89003 | 1.76499 | 0.00000 | .05000 |
| .39259 | .92[illegible] | 1.87134 | 0.[illegible] | .05000 |
| .33295 | .94324 | 1.99041 | 0.00000 | .05000 |
| .32376 | 1.00772 | 2.44980 | 0.00000 | .05000 |
| .30968 | 1.12848 | 2.63134 | 0.00000 | .05000 |
| .37027 | 1.19[illegible] | 2.72088 | 0.00000 | .05000 |
| .41522 | 1.26[illegible] | 2.87564 | 0.00000 | .05000 |
| .53665 | 1.33142 | 2.99210 | 0.00000 | .05000 |
| .54942 | 1.37[illegible] | 3.13557 | 0.00000 | .05000 |
| .49780 | 1.32363 | 3.26481 | 0.00000 | .05000 |
| .57968 | 1.38769 | 3.37671 | 0.00000 | .05000 |
| .62631 | 1.44323 | 3.51715 | 0.00000 | .05000 |
| .64594 | 1.54[illegible] | 3.65953 | 0.00000 | .05000 |
| .68214 | 1.56648 | 3.74940 | 0.00000 | .05000 |
| .55820 | 1.62[illegible] | 3.95893 | 0.00000 | .05000 |
| .69784 | 1.63640 | 3.95893 | 0.00000 | .05000 |
| .75103 | 1.79443 | 4.27556 | 0.00000 | .05000 |
| .37241 | 1.82[illegible] | 4.54389 | 0.00000 | .05000 |
| .40556 | 1.94443 | 4.63891 | 0.00000 | .05000 |
| .34035 | 1.95[illegible] | 4.75569 | 0.00000 | .05000 |
| .33167 | 2.[illegible] | 4.78584 | 0.00000 | .05000 |
| .35657 | 2.46920 | 4.97228 | 0.00000 | .05000 |
| .19034 | 2.12848 | 5.07179 | 0.00000 | .05000 |
| .39511 | 2.23529 | 5.18281 | 0.00000 | .05000 |
| .33680 | 2.36124 | 5.29302 | 0.00000 | .05000 |
| 1.[illegible]1543 | 2.[illegible] | 5.48659 | 0.[illegible] | .05000 |